Establishment of a Split-Combine Cell-SELEX method for Identification of Nucleobase-Modified Aptamers with Specific Binding to Androgen-independent Prostate Cancer Cells

Dissertation

zur
Erlangung des Doktorgrades (Dr. rer. nat.)
der
Mathematisch-Naturwissenschaftlichen Fakultät
der
Rheinischen Friedrich-Wilhelms-Universität Bonn
vorgelegt von

Moujab Choukeife

aus

Damascus, Syria

Bonn 2023

Angefertigt mit Genehmigung der Mathematisch-Naturwissenschaftlichen Fakultät der Rheinischen Friedrich-Wilhelms-Universität Bonn

1. Gutachter: Prof. Dr. Günter Mayer

2. Gutachter: Prof. Dr. Dirk Menche

Tag der Promotion: 29.08.2023

Erscheinungsjahr: 2023

Parts of this thesis have been published in:

Choukeife, M., Jonczyk, A., & Mayer, G. (2022). Implementation of Emulsion PCR for Amplification of Click-Modified DNA During SELEX. In *Nucleic Acid Aptamers: Selection, Characterization, and Application* (pp. 39-44). New York, NY: Springer US. DOI: 10.1007/978-1-0716-2695-5_3.

Martínez-Roque, M. A., Franco-Urquijo, P. A., García-Velásquez, V. M., **Choukeife, M**., Mayer, G., Molina-Ramírez, S. R., ... & Alvarez-Salas, L. M. (2022). DNA aptamer selection for SARS-CoV-2 spike glycoprotein detection. *Analytical Biochemistry*, *645*, 114633. DOI: 10.1016/j.ab.2022.114633.

Abstract

Prostate cancer is the most commonly diagnosed malignancy and the second leading cause of cancer-related mortality in men in the United States. Current therapies, such as chemotherapy, radiotherapy, and photothermal therapy, lack specificity and can cause serious side effects. To address this issue, targeted therapy has gained attention, with antibody-mediated therapy being a mainstay due to its highly specific properties. However, the high cost of production and immunogenicity limit its clinical application. Aptamer-based targeted therapeutics offer several advantages over antibody therapies and have been explored as a potential solution. Aptamers are low molecular ligands, consisting of single-stranded DNA or RNA that can fold into a three-dimensional structure, allowing them to bind with high affinity to specific targets. Aptamers show significant potential in therapeutics and diagnostics, but their ability to interact with a target is limited by the chemical diversity of natural nucleobases. To overcome this challenge, functional groups can be added to the nucleobases to increase chemical diversity. Split-combine SELEX is a technique that enables screening of multiple modifications to the target of interest in a single selection, resulting in the enrichment of nucleobase-modified aptamers with different modifications or the most suitable modification for the selected target. This study introduces a novel approach called split-combine cell SELEX, which utilizes this technology and implemented in the cell-SELEX method to select nucleobase-modified aptamers against prostate cancer cells. Through this method, a new class of clickmers was discovered, which showed the ability to recognize prostate cancer cells with different modifications. It was observed that each modification had a unique impact on the clickmers' binding properties towards prostate cancer cells. Additionally, the S1 aptamer was found to be able to recognize breast cancer cells (MCF-7) when modified with a cyclic-RGD (cRGD), while other modifications (Imidazole) did not produce the same results. Overall, these findings provide insight into the potential of nucleobase modified aptamers and their diverse binding properties towards cancer cells.

Zusammenfassung

Prostatakrebs ist die häufigste diagnostizierte Krebserkrankung und die zweithäufigste Todesursache im Zusammenhang mit Krebs bei Männern in den Vereinigten Staaten. Aktuelle Therapien wie Chemotherapie, Strahlentherapie und photothermische Therapie sind nicht spezifisch genug und können schwerwiegende Nebenwirkungen verursachen. Um dieses Problem zu lösen, hat die zielgerichtete Therapie aufgrund ihrer hochspezifischen Eigenschaften Aufmerksamkeit erlangt, wobei die Antikörper-vermittelte Therapie aufgrund ihrer hochspezifischen Eigenschaften eine feste Größe darstellt. Die hohen Herstellungskosten und die Immunogenität begrenzen jedoch ihre klinische Anwendung. Aptamer-basierte zielgerichtete Therapeutika bieten mehrere Vorteile gegenüber Antikörpertherapien und wurden als potenzielle Lösung erforscht. Aptamere sind niedermolekulare Liganden, bestehend aus einzelsträngiger DNA oder RNA, die sich zu einer dreidimensionalen Struktur falten können, wodurch sie mit hoher Affinität an spezifische Zielmoleküle binden können. Aptamere zeigen ein erhebliches Potenzial in der Therapie und Diagnostik, ihre Fähigkeit zur Interaktion mit einem Ziel ist jedoch durch die chemische Diversität natürlicher Nukleobasen begrenzt. Um diese Herausforderung zu überwinden, können funktionelle Gruppen zu den Nukleobasen hinzugefügt werden, um die chemische Diversität zu erhöhen. Die Split-Combine-SELEX-Technik ermöglicht die Untersuchung mehrerer Modifikationen des Zielmoleküls in einer einzigen Selektion, was zur Anreicherung von Nukleobasen-modifizierten Aptameren mit verschiedenen Modifikationen oder der am besten geeigneten Modifikation für das ausgewählte Ziel führt. In dieser Studie wird ein neuartiger Ansatz namens Split-Combine-Zell-SELEX vorgestellt, der diese Technologie nutzt und im Zell-SELEX-Verfahren implementiert wurde, um Nukleobasen-modifizierte Aptamere gegen Prostatakrebszellen auszuwählen. Durch diese Methode wurde eine neue Klasse von Clickmeren entdeckt, die die Fähigkeit zeigten, Prostatakrebszellen mit unterschiedlichen Modifikationen zu erkennen. Es wurde beobachtet, dass jede Modifikation einen einzigartigen Einfluss auf die Bindungseigenschaften der Clickmeren gegenüber Prostatakrebszellen hatte. Darüber hinaus wurde festgestellt, dass das S1-Aptamer in der Lage war, Brustkrebszellen (MCF-7) zu erkennen, wenn es mit einem cyclischen RGD (cRGD) modifiziert wurde, während andere Modifikationen (Imidazol) nicht dieselben Ergebnisse erzielten. Insgesamt geben diese Erkenntnisse Einblick in das Potenzial von Nukleobasen-modifizierten Aptameren und ihre vielfältigen Bindungseigenschaften gegenüber Krebszellen.

List of content

List of Figures

List of Tables

Abbreviations

BSA	bovine serum albumin
C3-GFP	cycle3-green fluorescent protein
CaCl2	calcium chloride
DAPI	4',6-diamidino-2-phenylindole
ddH2O	distilled water
DNA	deoxyribonucleic acid
dNTP	deoxyribonucleoside triphosphate
e.g.	exempli gratia (for example)
EDTA	ethylenediaminetetraacetic acid
EdU	5-ethynyl-2'-deoxyuridine
RPMI	Roswell Park Memorial Institute
DMEM	Dulbecco"s modified Eagle medium
EdUTP	5-ethynyl-5'-O-triphosphate-2'-deoxyuridine
EtOH	ethanol
FACS	fluorescence-activated cell sorting
g	gram
HEK293	human embryonic kidney 293 cells
HPLC	high-performance liquid chromatography
KD	dissociation constant
L	liter
LC-MS	liquid chromatography-mass spectrometry
M	molar
MFI	mean fluorescence intensity
MgCl2	magnesium chloride
NaCl	sodium chloride
NaOAc	sodium acetate
NMR	nuclear magnetic resonance spectroscopy
NTC	nucleotideno template control of PCR reactions
DPBS	phosphate-buffered saline
PCR	polymerase chain reaction
pH	negative decade logarithm of the hydrogen ion concentration
PNK	polynucleotide kinase
rpm	rounds per minute
SD	standard deviation
sec	second
SELEX	systematic evolution of ligands by exponential enrichment
TBE	Tris-Borate-EDTA buffer
THPTA	Tris(4-(3-hydroxy-propyl)-[1,2,3]triazol-1-ylmethyl)amine
UV	ultraviolet
V	volt
DHPLC	denaturing high-performance liquid chromatography
NGS	Next Generation Sequencing
SOMAmers	Slow-off-rate modified aptamers

CuAAC	copper (I)-catalyzed Huisgen 1,3-dipolar cycloaddition
PSMA	Prostate-specific membrane antigen
5-dUI	5-iododeoxyuridine
dDs	7-(2-thienyl)imidazo[4,5-b]pyridine
dPx	2-nitro-4-propynylpyrrole
AEGIS	Artificially Expanded Genetic Information Systems
CTC	circulating tumor cells
Ctrl 2	Control DNA sequence 2
DAPI	4‘,6-diamidino-2-phenylindole
WGA	Wheat germ agglutinin
PAGE	Polyacrylamide gel electrophoresis
ACN	acetonitrile
dZ	6-amino-5-nitro-3-(1-β-D-2-deoxyribofuranosyl)-2(1H)-pyridone
FDA	Food and Drug Administration
MgCl2	magnesium chloride
TEA	triethylamine
TEMED	N,N,N’,N’-tetramethylethylenediamine
DMSO	Dimethylsulfoxide
APS	Ammoniumperoxodisulfate
SDS	Sodium dodecylsulfate

1 INTRODUCTION

1.1 Aptamer

Aptamers have developed tremendously in the last three decades [1]. Generally, aptamers are short single-stranded DNA or RNA oligonucleotides capable of folding into defined three-dimensional structures and binding with high affinity and specificity to target molecules [2] [3] [4]. Due to their small size, ease of chemical synthesis, stability, and flexibility in design, aptamers are widely used in cancer imaging and therapy [5] [6], as well as in other areas such as disease diagnosis [7], food safety, and environmental toxicity detection [8]. Furthermore, they can be chemically modified to enhance stability or target specificity [9]. Therefore, Aptamers have many advantages and are used as drug delivery tools, diagnostic tools, biosensors, and potential therapeutics [10]. One aptamer (Macugen/Pegaptanib sodium) is currently used for treating neovascular age-related macular degeneration [11], and several others are in clinical trials for various applications such as cancer therapy and coagulation [12] [13] [14] [15] [16].

1.2 Identification of aptamer

The conventional method for identifying aptamers is called **S**ystematic **E**volution of **L**igands by **EX**ponential enrichment (SELEX). SELEX was first described in 1990 by three groups, including G.E. Joyce in La Jolla, J.W. Szostak in Boston, and L. Gold in Boulder [2] [3] [4]. The conventional SELEX method consists of three primary steps: first, incubation of the starting library with the target molecule of interest. The starting library consists of approximately 10^{15} different sequences of either single-stranded DNA or RNA. These libraries typically contain a random region of around 20-60 nucleotides surrounded by primer binding sites of approximately 20 nucleotides. The second step is partitioning, which separates the bound sequences from the unbound ones. Finally, the bound sequences are eluted and amplified by polymerase chain reaction (PCR) for the next round of selection. After several rounds of selection, the potential aptamers are identified, and their binding kinetics are analyzed using various techniques.

The SELEX methodology has been optimized and developed to directly select diverse targets, such as small molecules [17], proteins [18], viruses [19], bacteria [20] [21], live cells [22], and even tissues [23]. Although proteins are the most commonly targeted molecules in aptamer identification using SELEX [24], obtaining sufficient amounts of high-purity recombinant human proteins with their native conformation is challenging, particularly for transmembrane and intracellular proteins produced using in vitro expression systems [25]. As a result, researchers are exploring an alternative method to select aptamers that can address these issues. One method addressing these issues is the cell-SELEX [26].

1.3 Cell-SELEX

The fundamental steps of cell-SELEX are comparable to those of conventional SELEX, consisting of incubation, partitioning, and amplification, as shown in **Figure 1.1** [26]. The process begins with the synthesis of a high-diversity single-stranded oligonucleotide DNA (ssDNA) or RNA library. The process of cell-SELEX can be illustrated by using the example of an ssDNA library. Initially, the library is incubated with the target cells. The ssDNA sequences that bind to the target cells are released by heating the cell at 95°C and collected through centrifugation after washing. The collected pool is then incubated with control cells to remove any sequences that bind to the common profile of proteins expressed on normal cells, thus enhancing the specificity of the identified aptamer candidates for the target cells. This incubation with control cells can occur before or after the incubation with target cells. After elimination, the unbound ssDNA sequences are amplified using PCR. There are different methods to generate ssDNA after amplification. Aptamer candidates' binding affinity typically increases gradually as the number of selection rounds increases, and the enrichment of the selected pools is evaluated through flow cytometry binding assays. Finally, the enriched pools are subsequently sequenced, And a subset of aptamers is chosen as representatives for further analysis and characterization [27].

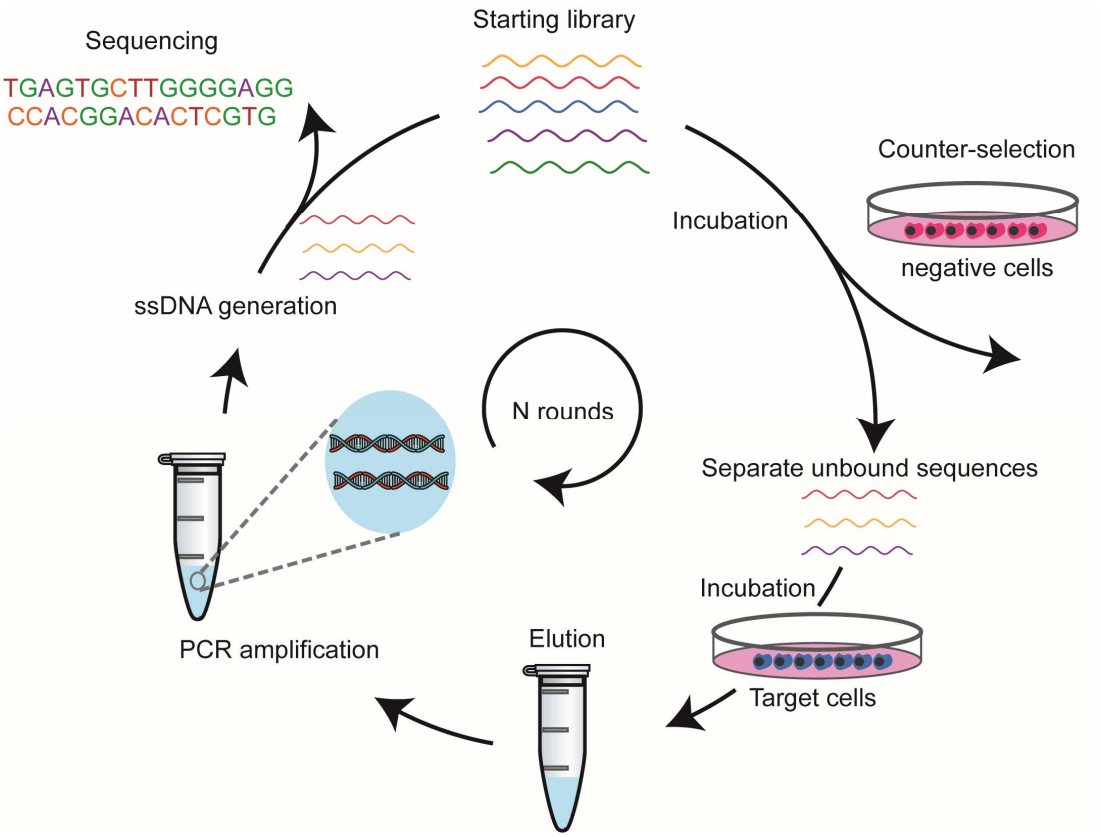

Figure 1.1 cell SELEX.
The ssDNA library was incubated with non-target cells to remove the non-specific binders. The unbound ssDNAs were then incubated with the target cells for positive selection. After washing, the bound ssDNAs were eluted and amplifed by PCR for next-round selection. The evolved ssDNA pool was sequenced to identify individual aptamer sequences after N rounds of enrichment.

The cell-based SELEX methodology (cell-SELEX) was first introduced by Morris and Jensen in 1998 [28], who utilized human red blood cell membranes as a complex mixture target for the purpose of selecting aptamers. This approach offers an *in vitro* protocol for isolating high-affinity aptamers that specifically bind to complex mixtures of potential targets. Unlike other SELEX techniques, cell-SELEX selects aptamers toward whole cells, allowing the molecular targets on the cell surface to maintain their native state and represent their natural folding structures [29]. Over the past two decades, aptamers have been selected using cell-SELEX for a Varios cells and other complex systems, particularly for cancer cells [25].

1.3.1 Advantage and limitations of cell-SELEX

Cell-based screening methods have greatly expanded the potential applications of aptamers by providing a rich source of screening targets[30]. Cell-SELEX has become the preferred method for developing aptamers that can recognize specific biomarkers for cancer cells' diagnostic and therapeutic purposes [31] [32]. Unlike traditional protein-SELEX, which requires prior knowledge of the target proteins, cell-SELEX overcomes the challenges of obtaining purified recombinant membrane proteins and developing aptamers against molecules on the cell surface without prior knowledge of their molecular targets [33]. Membrane proteins are functionally important molecules involved in various biological processes [34]. However, aptamers developed through protein-based SELEX may not be able to selectively recognize and interact with their corresponding targets *in vitro*, leading to the failure of biomedical applications. In contrast, cell-SELEX enables aptamers to bind to the real folded conformation of the targets on living cells, where all molecules on the cell surface are in their native state and maintain their natural folding structures and distribution, with all post-translational modifications intact [35]. Therefore, cell-SELEX eliminates the risk of identified aptamers only binding to purified proteins and not recognizing their native form on living cells [36].

Cell-SELEX has a lot of potential in the biomedical field, but technical limitations still need to be addressed for optimization. One important factor in aptamer selection is the condition of the cells since dead cells in a suspension can lead to non-specific uptake and binding of oligonucleotides, negatively impacting the entire selection process [37]. Various methods have been developed to address this issue to remove dead cells and reduce the likelihood of obtaining non-specific aptamers through cell-SELEX [38]. For example, Raddatz et al [37]. used fluorescence-activated cell-sorting (FACS) to separate aptamers bound to vital suspension cells and collected only those bound to calcein-AM-stained vital cells. Meltem and colleagues [39]. developed a method to remove dead cells from the cell suspension by centrifuging the cells after detachment with EDTA and then isolating the remaining dead cells using dead cell removal microbeads. This optimized method reduced the number of dead cells to 5.2%. These approaches effectively optimized the selection strategies for generating cell-specific aptamers.

In addition, it is recognized that the cell surface has a negative charge, making it challenging to produce nucleic acid aptamers that can bind to it due to repulsion between the DNA polyanion and the cell surface [40]. This poses a significant challenge to the development of nucleic acid aptamers that can effectively bind to the cell surface. Additionally, target cells cannot be fixed in order to avoid covering membrane proteins, resulting in low separation efficiency between binding complexes and unbound nucleic acids[41]. Despite these limitations, efforts are being made to optimize cell-SELEX technology and overcome these challenges[38]. A number of factors need to be considered when designing a new method for cell-SELEX

1.3.1.1 Library design

To design an oligonucleotide library for SELEX, three factors must be considered: the length of the random sequence region, the chemistry of the pool, and the utility of constant regions [42]. Aptamers can be either RNA or ssDNA, and while the original SELEX report used a randomized RNA pool, subsequent studies have favored DNA due to its greater stability, lower cost, and ease of production [43]. However, RNA offers greater diversity in fold due to the 2'OH group. Both RNA and DNA aptamers have demonstrated similar specificity and binding abilities. The length of the random region in the library is typically between 20 to 60 bp, and modified nucleotides can be added to broaden the range of possible sequences and potentially enhance *in vivo* stability or nuclease resistance [44, 45]. The design of conserved primer regions is also critical to avoid nonspecific PCR products, and software such as Integrated DNA Technologies can assist in proper primer design by considering factors such as annealing temperature, G-C content, and avoidance of primer heterodimers and self-dimers [46].

1.3.1.2 Amplification method during the selection

SELEX is the primary method for obtaining aptamers, but the efficiency of conventional PCR amplification of random DNA sequence libraries can be limited by low product yield and high by-product formation [47]. By-products can appear as early as the fifth cycle of PCR and can convert products completely into by-products after a maximum level of products has been reached, resulting in the loss of specific and high-affinity aptamers and eventually selection failure [48]. One proposed mechanism for this conversion is product-product hybridization [49] [50]. Emulsion PCR (ePCR) can overcome these limitations by partitioning the reaction mixture into droplets containing only one template to prevent product-product hybridization [51] [52]. Two protocols for emulsifying PCR mixtures have been developed [53] [54]. Optimization of ePCR parameters, such as starting template concentration, annealing temperature, primer concentration, and polymerase concentration, is important for emulsion stability, and the initial target concentration is the most significant parameter [47] [50]. BSA is added to the PCR mixture to protect polymerase inactivation at the aqueous/organic interface, and its concentration should be optimized for each PCR and emulsification protocol [47].

1.3.1.3 Generation of ssDNA

Various methods have been reported to generate single-stranded DNA (ssDNA) from double-stranded PCR products for proper separation [55]. These methods include asymmetric PCR, denaturing high-performance liquid chromatography (DHPLC), lambda exonuclease digestion, size separation using denaturing urea-polyacrylamide gel with unequal primers and chemical modification, and magnetic separation with streptavidin-coated beads [56, 57]. Asymmetric PCR involves using different amounts of forward and reverse primers, producing excess ssDNA in each cycle once the primer in a limiting amount is used up [58]. However, the diversity of ssDNA in the enriched oligonucleotide pools may be reduced due to the unequal molar ratio of the two primers used [46]. The DHPLC method uses biotinylated and normal primers [59]. The former increases hydrophobicity under denaturing conditions, leading to different retention times for the two strands in HPLC, which allows the separation of the ssDNA species from the PCR products. However, this method is costly and requires specific instruments [60]. To regenerate ssDNA, one effective method involves using denaturing urea-PAGE[61]. During the amplification step, a 5′-elongated reverse primer can be used to increase the size of the antisense strands, or the reverse primer can be coupled with PEG or Biotin. After amplification, the product is incubated in an alkaline solution for separation before undergoing denaturing urea-PAGE [57]. This method effectively suppresses the effect of aptamer structure on migration speed, allowing for the separation of sense and antisense strands based on size. The gel can also identify other components, including by-products and mutated sequences. By extracting the desired size band, unwanted products can be removed in each cycle of SELEX [1]. However, this method only recovers about 30% of the total ssDNA and has relatively long incubation times of up to 12 hours [44]. Another method for ssDNA regeneration involves using streptavidin beads along with a 5′-biotinylated reverse primer [44]. The dsDNA is typically attached to beads through the streptavidin-biotin interaction. To obtain the desired ssDNA, the sense strand can be released from the beads by exposing the sample to high temperatures or an alkaline pH. This method is known for its simplicity and relatively fast turnaround time, with a yield of approximately 30% for the ssDNA product. This yield is comparable to the yield achieved through gel-based separation methods [1]. However, there are several notable disadvantages. Firstly, streptavidin beads can be relatively expensive. Secondly, if biotinylated primers are not removed from the beads before ssDNA regeneration, they may take up space and reduce the yield of ssDNA. Thirdly, streptavidin may detach from the beads and interfere with selection in subsequent rounds, especially if heat is utilized for separation the dsDNA. Finally, PCR by-products may contain more than one biotin molecule, causing them to bind more strongly to the beads than regular aptamers. As a result, by-products are likely to carry over to the next cycle of SELEX [46]. In the lambda exonuclease digestion method, a phosphorylated reverse primer is used in amplification, and then lambda exonuclease digests the phosphorylated strand, leaving behind the sense-stranded DNA[62]. This method is simple and highly efficient compared to other methods, yielding approximately 60% [63]. Therefore, it is a suitable choice for cell-

SELEX, where the preparation of high-quality ssDNA is crucial for the successful selection of aptamers [64].

1.3.1.4 Counter-selection

The addition of a counter-selection step to the cell-SELEX protocol greatly enhances the specificity of the selected aptamers by eliminating sequences that bind non-specifically to cells or all cell lines [65]. Typically, this step involves including counter cell lines in the SELEX procedure. The increased specificity of the selected aptamers has important implications for their use in targeted therapy or detection of cancer cell lines [22]. In this study, an additional counter-selection method was employed to further improve the specificity of the selected aptamers. This method, described in **section 5.2.6.1**, is only suitable for selecting nucleobase-modified aptamers and cannot be used in DNA cell-SELEX. This step aims to eliminate sequences that interact with target cells without functional groups in the random region.

1.3.1.5 Sanger sequencing vs. Next Generation Sequencing (NGS)

The conventional method for identifying aptamers is Sanger sequencing, which involves cloning the DNA from an enriched selection cycle, a common approach is to clone the DNA into a plasmid [66]. This involves inserting the DNA fragment into a plasmid vector, which is then transformed into competent bacteria to enable amplification of the DNA. Following transformation, individual bacterial colonies are formed and amplified to produce a large quantity of the plasmid containing the DNA fragment [67]. To obtain the sequence of the cloned DNA, the plasmids are then purified and sequenced using the Sanger sequencing procedure. However, due to the labor-intensive nature of this approach, only 50-100 clones can be sequenced per selection cycle [46, 67, 68]. Therefore, conducting the final SELEX cycle with a high degree of enrichment is crucial to ensure accurate identification of the aptamers. The emergence of next-generation sequencing (NGS) has transformed SELEX technology, allowing for the generation of large sequencing data [69]. NGS has become increasingly popular in the SELEX community over the last decade due to its high sequencing power and reduced costs. An NGS experiment can sequence up to 100 million sequences, enabling a detailed analysis of the selection process and improved identification of aptamers. Even selection cycles with only slight enrichment can be analyzed using NGS [70]. This technology provides various benefits, including higher sequence coverage, verification of library diversity, and sequence information from all selection cycles, which enables tracking the development of individual sequences and their amplification behavior over multiple selection cycles [71, 72]. Moreover, only a small amount of sample preparation is required for sequencing, which typically involves adding sequencing adapters to the oligonucleotides. This is usually achieved through PCR amplification using modified primers. However, it is important to note that this amplification step is a significant source of sequencing bias, and therefore it should be carefully optimized to reduce the impact of bias on the final sequencing results. Moreover, the availability of several NGS analysis programs [73] [74] [75, 76] [77] has provided

benefits for aptamer identification, but correctly interpreting a large amount of bioinformatics data remains a challenge. Further improvements in the NGS analysis technique are required for SELEX.

1.3.1.6 Chemical modifications and special nucleotides

1.3.1.6.1 Nucleobase-modified aptamers

Aptamers are made up of a backbone consisting of (deoxy)ribose-phosphate and four aromatic nucleotides, either A, G, C, T (for DNA) or U (for RNA). In comparison to antibodies, which are constructed from 20 amino acids featuring aromatic, aliphatic, basic, acidic, and polar side chains, the chemical diversity of aptamers is more limited [78]. As a result of this constraint, the success rate of SELEX experiments is restricted, with only about 3 out of 10 proteins subjected to enrichment processes producing aptamers on average [79]. Therefore, methods that expand the chemical diversity of nucleic acids are thought to improve the success rates of SELEX experiments, as they allow for interactions with target molecules that cannot be achieved with a nucleic acid composed solely of canonical nucleotides [80] [81] [82]. These modifications are shown in **Figure 1.2**

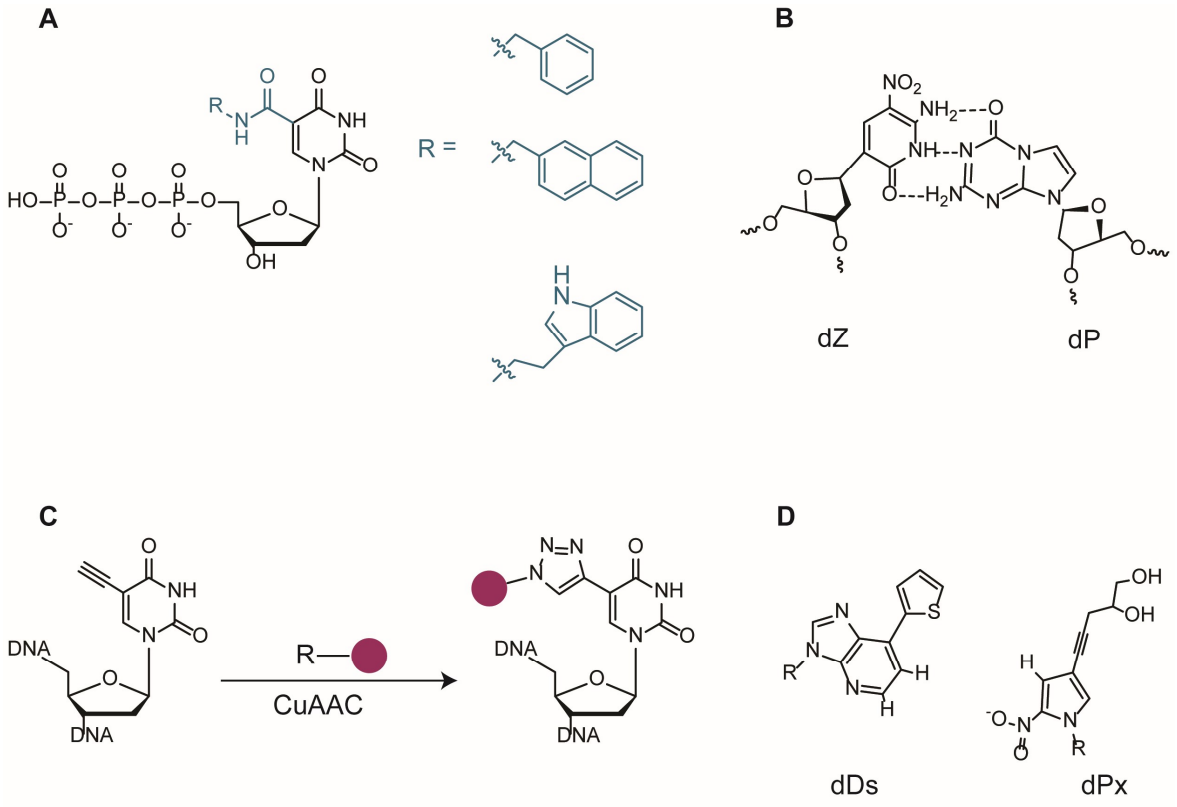

Figure 1.2 Chemical modifications and special nucleotides.
(A) Chemical structures of nucleoside triphosphate analogs modified at the 5-position of uridine triphosphate (dUTP): 5-benzylaminocarbonyl-dU (BndU); 5-naphthylmethylaminocarbonyl-dU (NapdU); and 5-tryptaminocarbonyl-dU (TrpdU). **(C)** Functionalization of EdU in DNA libraries by Cu(I)-catalyzed azide-alkyne cycloaddition (CuAAC) for azide modification. The chemical structures of artificial base pairs used in SELEX. **(B)** The dZ:dP base pair is formed through hydrogen bonds between dP: 2-amino-8-(10-b-D-2-deoxyribofuranosyl)-imidazo[1,2-a]-1,3,5-triazin-4(8H) and dZ: 6-amino-5-nitro-3-(10-b-D-20-deoxyribofur-anosyl)-2(1H)-pyridone. **(D)** Synthetic base pair dDs:dPx is formed via hydrophobic interactions between dDs: 7-(2-thienyl) imidazo[4,5-b] pyridine and dPx:2-nitro-4-propynylpyrrole (Px).

1.3.1.6.1.1. Slow-off-rate modified aptamers (SOMAmers)

Gold and colleagues have created slow-off-rate modified aptamers (SOMAmers) that feature amino acid-like side chains, such as 5-tryptaminocarbonyl-dU (similar to tryptophan) or 5-benzyl aminocarbonyl-dU (similar to phenylalanine), covalently bonded to the C5-position of uridine-triphosphate using an amide bond [79] [83]. These modified triphosphates can be utilized as building blocks in nucleic acid libraries to enrich specific SOMAmers that bind to target proteins. This process has been shown to be more effective than standard nucleic acid libraries, as it can capture target molecules previously missed by the selection process [84] [85]. SOMAmers display affinities to their target molecules in the low nanomolar range, with low off rates matrices [86] [87] [88]. Structural analysis of SOMAmer-target complexes has revealed that the modifications are in direct contact with the cognate protein and that novel nucleic acid structural motifs, such as benzyl zippers, can arise. These examples illustrate that SOMAmers increase chemical diversity and structural diversity when compared to nucleic acids composed solely of canonical nucleobases [78] [85] [89]. Using this technology, Tanaka and his colleague selected aptamers as membrane protein-binding molecules, single-stranded oligonucleotides that exhibit high affinity and specificity for lung cancer cell line (A549) [90]. Using an evolutionary selection approach with a random DNA library containing an uracil derivative with a hydrophobic functional group at the 5-position. Another aptamer was selected by the same group for lung fibroblasts derived from IPF patients (LL97A) cell line with high affinity (Kd = 70 nM) [91]. This aptamer also demonstrated an affinity for other lung fibroblasts, while exhibiting minimal cross-reactivity with epithelial cells. To investigate the aptamer's potential for targeted therapy, they generated an aptamer-monomethyl auristatin F (MMAF) conjugate by hybridizing with complementary DNA linked to MMAF. This conjugate inhibited the proliferation of fibroblasts while appearing non-toxic to non-targeted epithelial cells.

1.3.1.6.1.2. Click SELEX

Click chemistry has emerged as an attractive method to introduce chemical modifications to nucleic acids, and the copper (I)-catalyzed Huisgen 1,3-dipolar cycloaddition (CuAAC) of azides with terminal alkynes has been widely utilized due to its high specificity and efficiency in connecting different molecular entities [92] [93] [94]. This reaction has been incorporated into the SELEX method to enhance the diversity of starting libraries. This approach involves using an alkyne-modified nucleobase, 5-ethynyl-2’-deoxyuridine (EdU), to replace conventional thymidine, followed by click conjugation with small molecules like azido-indole [95] [96]. After target molecule incubation, the selected sequences were PCR-amplified using EdU-modified nucleotide and underwent exonuclease digestion of the 5'-phosphorylated antisense strand. CuAAC was then repeated to reintroduce modifications and enable a new selection round. In 2015, Tolle et al [96]. introduced this method in which a nucleobase-modified aptamer was selected against C3-GFP and modified with azido-indole. The

aptamer's interaction with C3-GFP was found to be dependent on the presence of the indole modification, and no interaction occurred in its absence. The significance of click-SELEX was demonstrated in 2019 by Rosenthal et al., [97] who successfully selected a nucleobase-modified aptamer for THC despite the compound's high hydrophobicity, which had posed a challenge for a long time. The researchers chose benzyl residues for click-SELEX modification based on the receptor-ligand structure of THC in the cannabinoid receptor CB1, which primarily interacts with phenylalanine residues [98]. Following the selection process, a sequence named C11 was identified to bind to THC, but only when it was modified with aromatic residues. In the absence of modification, no binding to THC was observed.

Theoretically, any azide can modify DNA, but it is unclear which type of modification is best for selecting a successful target molecule. However, using Click-SELEX to identify the best modification can be time-consuming and costly because individual selections are required for each modification. A new method called split-combine Click-SELEX has been developed to address this problem [99]. This involves splitting the single-stranded DNA into multiple samples and modifying each sample separately with different azides. The modified DNA samples are then combined and introduced, and selection cycles are conducted. The enriched libraries are compared with the starting library until significant differences in binding assays are detected. The most appropriate azide can then be determined using a deconvolution step for the final binding analysis. Click modification is performed separately on each sample of the enriched library, and two to three selection cycles are conducted using a single azide for each cycle. It is important to analyze the different selection cycles before and after the deconvolution step to assign sequences to azides using NGS. Plückthun and colleagues demonstrated that using C3-GFP as a target facilitated the selection of the appropriate azide for click-modifying DNA. During the first nine selection cycles, the I10 sequence became enriched up to 40%. When single azide selections were conducted using indole, the frequency of I10 increased to almost 70%, while all other single azide selections yielded a frequency close to 0%. Another sequence, F20, had a similar enrichment profile as I10 but was enriched with Benzofuran and depleted with all other azides. Recently, a split-combine procedure was employed to select clickmers for CXCL 9 [100], and two sequences were identified: G125 and I29. I29 showed CXCL 9 binding with an aromatic residue, whereas G125 bound to CXCL 9 when it was unmodified DNA or modified with indole. While this procedure shows great promise and potential, it has not yet been implemented with the cell-SELEX method.

1.3.1.6.1.3. The expansion of genetic alphabet

In addition to adding chemical groups to nucleobases, incorporating novel noncanonical base pairs is another approach to generate modified aptamers with different properties [101] [102].

An artificial base-pair composed of 7-(2-thienyl) imidazo[4,5-b]pyridine (dDs) and 2-nitro-4-propynylpyrrole (dPx) has been developed. Unlike traditional base pairs, which rely on hydrogen bonding, the dDs-dPx pair is based on size and shape complementarity [103]. The ExSELEX genetic alphabet expansion process for the systematic evolution of ligands by exponential enrichment was utilized to achieve this. The effectiveness of the dDs-dPx base pair was demonstrated through selection against two protein targets: VEGF-165 and IFN-γ [103]. The selected aptamers showed a Kd of 0.65 nM and 38 nM, respectively. Additionally, cell-SELEX was performed on three breast cancer cell lines (MCF-7, MDA-231, and T-47D), which resulted in the selection of aptamers that only bound when dDs were present in the aptamer strand [104]. The hydrophobic nature of dDs provided an advantage, as the selected aptamers had over a 100-fold improved affinity compared to conventional DNA aptamers [105]. Overall, the dDs-dPx base pair represents a promising development in the field of artificial base pairs, with potential applications in targeted therapeutics and diagnostics.

The Benner has developed a different approach to genetic alphabet expansion [106], as shown in **Figure 1.2**. In this method, the hydrogen bonding pattern of nucleobases is modified to create analogues that specifically form unique hydrogen bonding interactions [107]. These unnatural base pairs are entirely distinct from the canonical Watson-Crick base pairs. This versatile approach is called **A**rtificially **E**xpanded **G**enetic **I**nformation **S**ystems (AEGIS) and has been utilized to generate highly potent modified aptamers against cell cancer lines, protein targets, and other applications [105] [107] [106].

1.3.2 Application of cell-SELEX

Over the last two decades, aptamers have gained significant interest due to their ability to specifically target molecules, exhibit strong binding affinity, and their potential use in medical applications for the diagnosis and treatment of diseases[108]. The technique of cell-SELEX has advanced the use of aptamers in cancer research by allowing for the development of diagnostic and therapeutic technologies [109]. This method can select aptamers that target specific biomarkers as well as previously unknown biomarkers present on the surface of cancer cells [110].

1.3.2.1 Biomarker discovery

Aptamers are becoming increasingly valuable in the identification of target molecules associated with different cellular states, whether pathogenic or non-pathogenic [111]. This enables identifying new biomolecules with diagnostic and therapeutic relevance, allowing for personalized medical approaches. For instance, aptamers that target specific cell types or subpopulations, such as tumor cells, can be selected and characterized [108] [112] [113]. After single sequence aptamers are generated, the target can be identified using a pull-down assay, followed by SDS-PAGE to isolate protein bands, and then identifying proteins using liquid chromatography/mass spectrometry (LC-MS) [114], as shown in **Figure 1.3**.

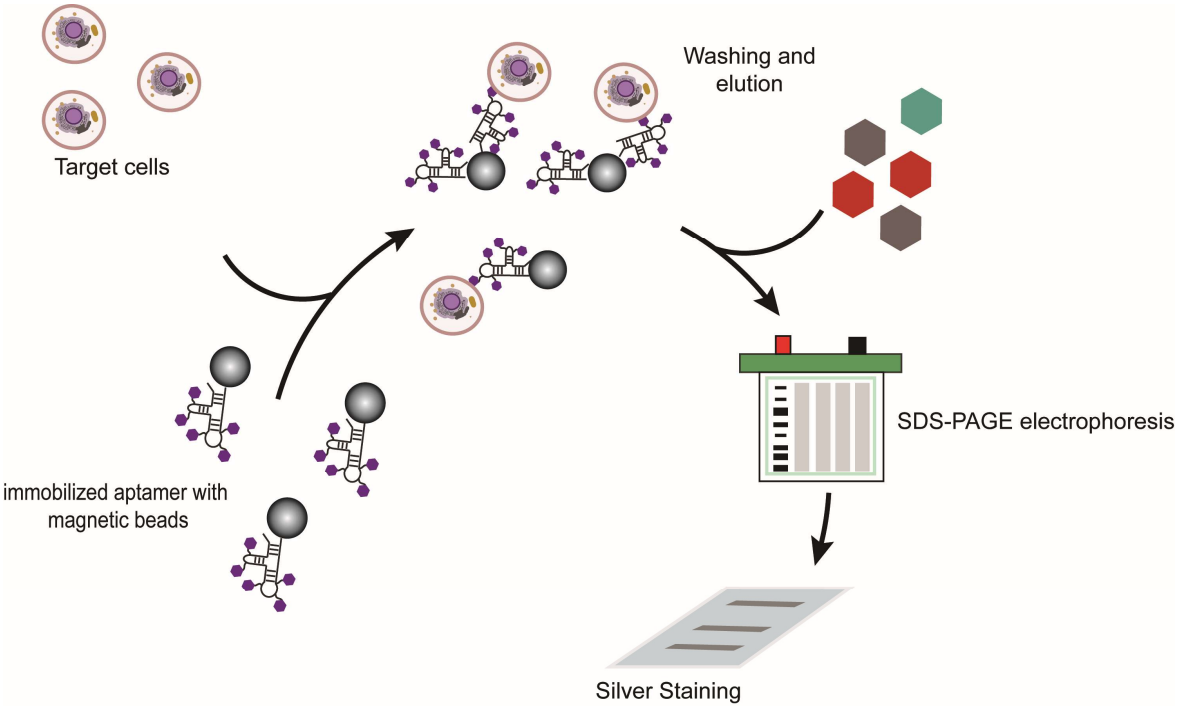

Figure 1.3 Schematic representation of the aptamer-based affinity purification process.
The aptamer is first captured using streptavidin beads, then the target cells are incubated with the coupled aptamer. After cell lysis, the bound fraction is washed and eluted. Finally, the eluted fraction is run on an SDS-PAGE gel and visualized by silver stain to detect the bound protein.

Blank et al [115]. were the first to demonstrate this approach, selecting a DNA aptamer (aptamer III.1) against rat endothelial glioblastoma cells (YPEN-1). They performed a pull-down assay using III.1 aptamer and cell lysates, identifying the protein pigpen as the target of III.1 aptamer through LC-MS analysis. Pigpen is highly expressed in angiogenic microvessels, making it useful for diagnostic or therapeutic purposes. Daniels et al [116]. used cell-Selex to generate DNA aptamers against glioblastoma-derived cell line U251, and its target was identified as Tenascin-C, a protein involved in embryogenesis and oncogenesis. In 2007, Tan's group [32] used the same approach to identify the target DNA aptamer sgc8, which binds with high affinity to T-cell acute lymphoblastic leukemia cells (CCRF-CEM). The molecular target of sgc8 was validated as a cell surface transmembrane protein, protein tyrosine kinase 7 (PTK7), among 25 protein hits identified by MS analysis.

Tan's group used UV-light crosslinking to modify their approach in order to prevent the dissociation of aptamer-protein complexes during isolation, as described in Mallikaratchy's work [31]. They achieved this by substituting several deoxythymidine in the aptamer sequence with 5-iododeoxyuridine (5-dUI) and used this method to identify the putative target of a TD05 DNA aptamer for B-cell human Burkitt's lymphoma cell line (Ramos cell line), which turned out to be a membrane-bound heavy chain (IGHM). However, this substitution may have an impact on the binding ability of the aptamer, so an optimal sequence needed to be selected from a large pool of sequences that had been substituted with 5-dUI at different sites [117]. UV-light crosslinking was not very effective, so Tan's group addressed this by using formaldehyde, a common chemical crosslinker, to crosslink aptamers

to cells. Through this method, they identified the target of the TOV6 aptamer as stress-induced phosphoprotein 1, which has the potential as a biomarker for ovarian cancer, as reported in Van Simaeys' work [118].

1.3.2.2 Using aptamer for cancer diagnosis

Early detection of cancer is critical in improving survival rates and treatment choices [119]. The use of aptamer-based cancer detection systems holds promise for the early and precise detection of cancer, as they are extremely specific and require only small amounts of analytes to generate signals. [120]. In particular, lung cancer is often not detected until it has reached an advanced stage, with five-year survival rates approaching single digits [121]. Li et al developed six DNA aptamers against lung cancer markers using a modified SELEX technique that involved magnetic carboxyl agar beads [122]. During this process, the beads underwent negative selection using clarified serum from healthy individuals, followed by positive selection using serum from lung cancer patients. The six aptamers detected lung cancer in 20 lung cancer patients' serum but not in 20 healthy individuals. In comparison to traditional lung cancer diagnostic methods, this system has a much higher sensitivity, making lung cancer more detectable at an earlier stage. This system was much more sensitive than traditional lung cancer diagnosis methods, making it possible to detect lung cancer earlier [122].

Gynecological cancers are also challenging to diagnose at an early stage [123]. Using an aptamer-based microfluidic system, Tsai et al [124]. captured and detected circulating tumor cells (CTCs), which usually circulate irregularly and are found in low concentrations. In contrast to antibody-based detection, highly specific aptamers allow for the detection of CTCs at a faster rate, with lower false positives.

1.3.2.3 Using aptamer for cancer therapy

By using aptamers as drug payloads or aptamer-functionalized nanoparticles, drugs can be transported to specific sites with better binding properties and reduced off-target toxicity. Prostate-specific membrane antigen (PSMA) is a cell marker found on the surface of prostate cancer cells, and aptamer A10 was identified to detect the extracellular domain of PSMA. Farokhzad et al developed a bioconjugate using RNA aptamers A10 to target docetaxel (Dtxl)-encapsulated nanoparticles to prostate cancer cells with PSMA overexpression [125]. In a nude mouse model, this approach showed significant anti-tumour efficacy and reduced toxicity in vivo [126]. Taghdisi et al. developed a PEG-Apt-Epi complex for the targeted delivery of Epirubicin (Epi) to cancer cells using a PEGylated A10 aptamer [127]. This system was able to specifically deliver and internalize Epi to LNCaP cells, reducing the cytotoxic effects of Epi by targeted delivery. The development of aptamer-functionalized nanoparticles for targeted drug delivery can lead to better diagnosis and treatment of various diseases.

Aptamers possess efficient targeting abilities towards cancer cells and tissues and hold potential as drug delivery vehicles and anti-cancer drugs for cancer therapy. numerous aptamers are currently undergoing clinical evaluation for the treatment of various types of cancers [9]. Among these, AS1411 is the most commonly studied aptamer for cancer therapy. AS1411 is an unmodified 26-mer DNA strand rich in guanosine, which binds to the extracellular domain of nucleolin, a protein over-expressed on the surface of various cancer cells and responsible for cell survival, growth, and proliferation. studies have demonstrated that AS1411 exhibits anti-proliferative activity against numerous cancer cell lines, including prostate, breast, lung, pancreatic, renal cell carcinoma, ovarian, cervical, and colon cancers [128]. However, the exact mechanism of action for AS1411 remains unclear. In 2006, a Phase I clinical study of AS1411 was completed, Having demonstrated its ability to selectively target nucleolin without serious toxicity, it is the first anticancer aptamer drug that has been tested in humans and in its class. Subsequently, a Phase II clinical trial for acute myeloid leukemia showed that AS1411 had therapeutic efficacy. However, the evaluation for renal cell carcinoma in Phase II demonstrated only one patient had a response to treatment out of the 35 patients enrolled and treated [129].

Aptamer-mediated delivery of drugs, including chemotherapy agents like doxorubicin, docetaxel, daunorubicin, and cisplatin, toxins such as gelonin, photodynamic therapy agents, and small interfering RNAs, has been demonstrated [130]. These studies have shown the potential of aptamer-nanoparticle conjugates as effective cancer therapeutics. Aptamer-based delivery can help drugs cross biological barriers, such as epithelial and endothelial barriers, and reach intracellular targets, thereby enhancing the safety and efficacy of therapies. As aptamer selection technologies and nanomedicine continue to advance, aptamer-functionalized nanoparticles are becoming a promising platform for targeted therapeutics. this approach is anticipated that will move from preclinical studies to clinical development for further evaluation and improvement in the ongoing efforts to develop more effective cancer treatments [109].

1.4 Prostate cancer

In 1853 at the London hospital, a surgeon named J. Adam reported the first prostate cancer case and described it as a sporadic disease [131] [132]. Currently, prostate cancer ranks as the most prevalent form of cancer among males. Moreover, prostate cancer is the fifth leading death in men [133]. A multitude of factors are contributing to the substantial rise in incidences of prostate cancer. Until the early 1900s, prostate cancer was not distinguished from other types of urinary obstruction[134]. Additionally, Prostate cancer incidence increases more rapidly with advancing age than any other form of tumor [132]. In the last century, there has been a proportional increase in the number of prostate cancer cases with the rise in life expectancy. Lastly, it appears that the increased incidence of prostate cancer is, in some way, related to the 'Western' lifestyle: Asian populations have lower incidences of prostate cancer than Western populations, and they have an increased incidence in men who have

relocated to Western nations, suggesting the presence of an environmental or dietary influence [135]. With an increase in incidence over the past century, significant progress has been made in the diagnosis and treatment of prostate cancer. A novel era of prostate cancer therapy began when Charles Huggins discovered that metastatic prostate cancer responded to androgen-ablation therapy in the 1940s[136]. To date, androgen ablation remains the most generally effective treatment for prostate cancer with medical castration with oral estrogens [137]. In most cases, prostate cancer is androgen-dependent, meaning it responds to treatment that reduces androgen levels or androgen-depletion therapy. Despite androgen ablation, these tumors eventually become androgen-independent and continue to grow [138].

1.4.1 Androgen-depletion therapy

Huggins was the first to treat prostate cancer with oral systemic estrogen therapy [136]. Huggins was awarded the Nobel Prize in Physiology and Medicine in 1966. This discovery led to more extensive clinical studies. In the 1960s [139], the Veterans Administration Cooperative Urologic Research Group (VACURG) conducted a study considered one of the most influential in this field. This study aimed to compare the effectiveness of treating prostate cancer patients with diethylstilbesterol (DES), an oral estrogen, against ORCHIECTOMY and concluded that DES was equally effective as the former. It became evident that systemic hormonal therapy had two significant problems. According to the VACURG study, lowering serum testosterone levels with oral estrogen is associated with significant cardiovascular and thromboembolic side effects. Furthermore, it became clear that androgen ablation, such as castration or administration of estrogen, did not fully cure patients with advanced prostate cancer [139].

A novel approach was developed between the 1960s and 1980s involving the development of hormone therapies that blocked the production of adrenal androgens or inhibited the interaction of androgens within target tissues. The production of androgen starts from the hypothalamus. The hypothalamus releases luteinizing hormone-releasing hormone (LHRH), which in turn triggers the pituitary gland to produce LH (luteinizing hormone). The LH hormone binds to a receptor on the testicles and activates testosterone production [140]. LHRH agonists were found to cause a temporary increase in serum testosterone levels - referred to as a 'testosterone flare' - associated with pain and obstructive symptoms. It was observed by Schally et al. that chronic administration of LHRH agonists produced inhibitory effects, reducing pituitary receptors for LHRH, resulting in lowered levels of circulating follicle-stimulating hormone (FSH) as well as luteinizing hormone (LH) [141]. Consequently, serum testosterone levels were reduced, leading to decreased tumor growth. Later, numerous synthetic LHRH agonists were developed for clinical use. These included goserelin (Zoladex), leuprolide (Lupron), nafarelin and buserelin [142]. LHRH agonists and DES are both effective treatments for prostate cancer. LHRH agonist treatment carries the same side effects as other treatments

decreasing serum testosterone, including loss of libido, hot flushes and impotence. There is no evidence that these agents cause increased thromboembolic events compared to estrogen therapy [142].

A non-steroidal antiandrogen called flutamide was discovered in the 1970s. It was approved for prostate cancer treatment by the United States Food and Drug Administration (FDA) in 1989. A number of non-steroidal antiandrogens, including bicalutamide and nilutamide, were developed later [132]. They were supposed to have the advantage of not affecting libido or potency as other centrally acting drugs were (cyproterone acetate and LHRH agonists). Later, it became clear that these agents, like cyproterone, crossed the blood-brain barrier, increasing levels of LH released into the bloodstream and testosterone levels. In randomized trials, men with metastatic prostate cancer were compared with those treated with medical or surgical castration based on pure anti-androgen therapy [143]. Even though these drugs are generally well tolerated, they perform worse overall and progression-free survival than other treatments. It is ultimately concluded from these numerous studies that although androgen ablation is an effective palliative treatment for many patients, it is rarely a cure. The results confirm that prostate cancers are composed of heterogeneous collections of androgen-dependent and -independent cells. It is impossible to eliminate androgen-independent cells through androgen-ablative therapy, regardless of how complete or early it is given [144].

1.4.2 Chemotherapy

Chemotherapy is one of the most popular treatment options for cancer and has significantly impacted the outcome of cancer treatment [145]. In 2014, five chemotherapies were approved for the treatment of advanced prostate cancer [146]. A common disadvantage of conventional chemotherapy is its toxicity to healthy tissues and its adverse side effects impairing its overall effectiveness. By minimizing the exposure of healthy tissues to these drugs, the side effects of these drugs are expected to be reduced. In addition, the therapeutic effects will be improved. A targeted drug delivery method using Aptamer-drug conjugates (ApDCs) has been explored to target diseased tissues or cells without affecting healthy tissues [147]. Many aptamers have been selected for this purpose, especially for prostate cancer [148] [149]. However, Aptamers have inherent drawbacks in a wide range of practical applications that often hinder their effectiveness, including the fact that they only have four building blocks (A, G, C, T/U bases), easy degradation by nucleases, rapid renal clearance, poor pharmacokinetic properties, etc. For their performance to be improved in practical (in vivo) applications, a modified nucleobase is required to be incorporated into the aptamer sequence [150]. Multiple modifications can be screened in the split-combine procedure, and the most appropriate modification can be selected. Using this method on a cell such as prostate cancer cells will produce a nucleobase-modified aptamer suitable for the future development of targeted therapies.

2 AIM OF THIS STUDY

The aim of this study is to develop a novel approach for selecting nucleobase-modified aptamers specific to the androgen-independent prostate cancer cell line (PC-3), using a screening method that allows for the simultaneous evaluation of multiple modifications. This method is referred to as split-combine SELEX. Through this methodology, the optimal modifications for targeting the prostate cancer cell line can be identified, and this highly adaptable protocol can be easily implemented for screening aptamers against other cell lines in any laboratory setting. Additionally, this study aims to compare the efficacy of the split-combine cell SELEX method with the commonly used DNA cell-SELEX method in terms of aptamer enrichment and outcome candidates. The selected candidate from both methods will be compared to determine whether the nucleobase-modified aptamer binds better to PC-3 cells than the DNA sequences. Ultimately, the study aims to select a nucleobase-modified aptamer for the prostate cancer cell line and to characterize it for future use in diagnosis or targeted therapy.

3 RESULTS

The results section is divided into six sections: **3.1** pre-selection optimizations. **3.2** DNA SELEX, NGS analysis, and testing of the identified candidates. **3.3** Split-combine cell SELEX, NGS and identification of the candidates **3.4** characterizations of S1 aptamer. **3.5** Optimizing the pull-down assay using two DNA aptamers **3.6** Optimizing pull-down assay for S1 aptamer.

3.1 Pre-selection optimization

3.1.1 Library Design

Previously, click-SELEX was performed with an in-house designed FT2 library, however, this library showed some drawbacks. For instance, the FT-2 library gives a by-product after 22 PCR cycles [151]. In this study, two new libraries were designed that could be used either as a DNA library or as an alkyne-modified library to provide an improved selection of aptamers like the FT2 library but with less by-product formation. These libraries were named M1 and M2 libraries. The original FT2 library GC content in the primer binding sites was 66.7 %. The GC content in the M1 library is 65% with a 20-nucleotide length, and the GC content in the M2 library was 60% with a length of 20 nucleotides. Moreover, M1 and M2 did not have thymidine in the primer binding sites, because it is not recommended to have EdU (5-ethynyl-2'-deoxyuridine) in the primer binding sites of the starting library for click-SELEX, as it may cause steric hindrance during PCR amplification [152]. Furthermore, M1 and M2 contained only 7 EdU in the random region; while the original FT2 library contains 42 nucleotides distributed equally (1:1:1:1) (dA:dG:dC:EdU). **Figure 3.1** is showing M1 and M2 libraries.

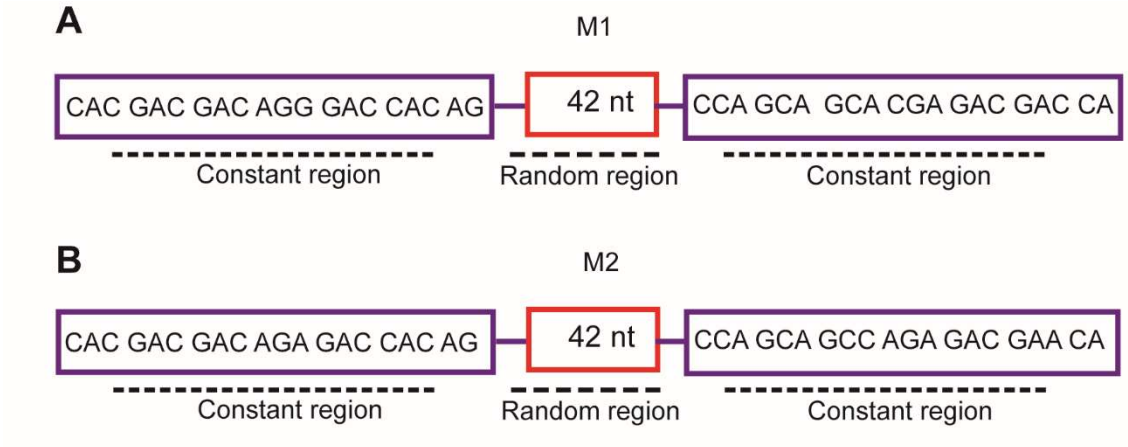

Figure 3.1 M1 and M2 libraries are depicted as schematic representations.
These libraries contain a random region of 42 nucleotides, colored in red, which is bordered by two primer binding sites of 20 nucleotides each, colored in purple. The primer binding sites do not have any thymidine nucleotides.

3.1.2 Amplification of the M1 and M2 library

Before introducing alkyne-modified building blocks, a PCR protocol with canonical DNA libraries must be established [152]. As reported by a previous study, Pwo-polymerase has demonstrated proficient incorporation of alkyne building blocks into DNA[152]. This study used Pwo-polymerase in all PCR reactions before and during selection. Besides this, two gradient PCRs were performed to choose the optimal annealing temperature for both libraries, the first PCR tested the amplification with a 5°C difference starting from 70°C to 45°C, and the second one tested the amplification with a 2°C difference starting from 62°C to 52°C. The optimal annealing temperature for both libraries was 58°C. After selecting the optimal annealing temperature, a simple test was performed to mimic the selection procedure. 5 consecutive PCRs were performed using the product from the previous PCR to know if this library could give any by-products during the selection. For both libraries, there was no by-product observed on the agarose gel. Based on its lower GC content, library M2 was selected for further use in the selection process. **Figure 3.2** illustrates a representative PCR product demonstrating the optimal annealing temperature for both libraries and the successful amplification of the libraries M1 and M2.

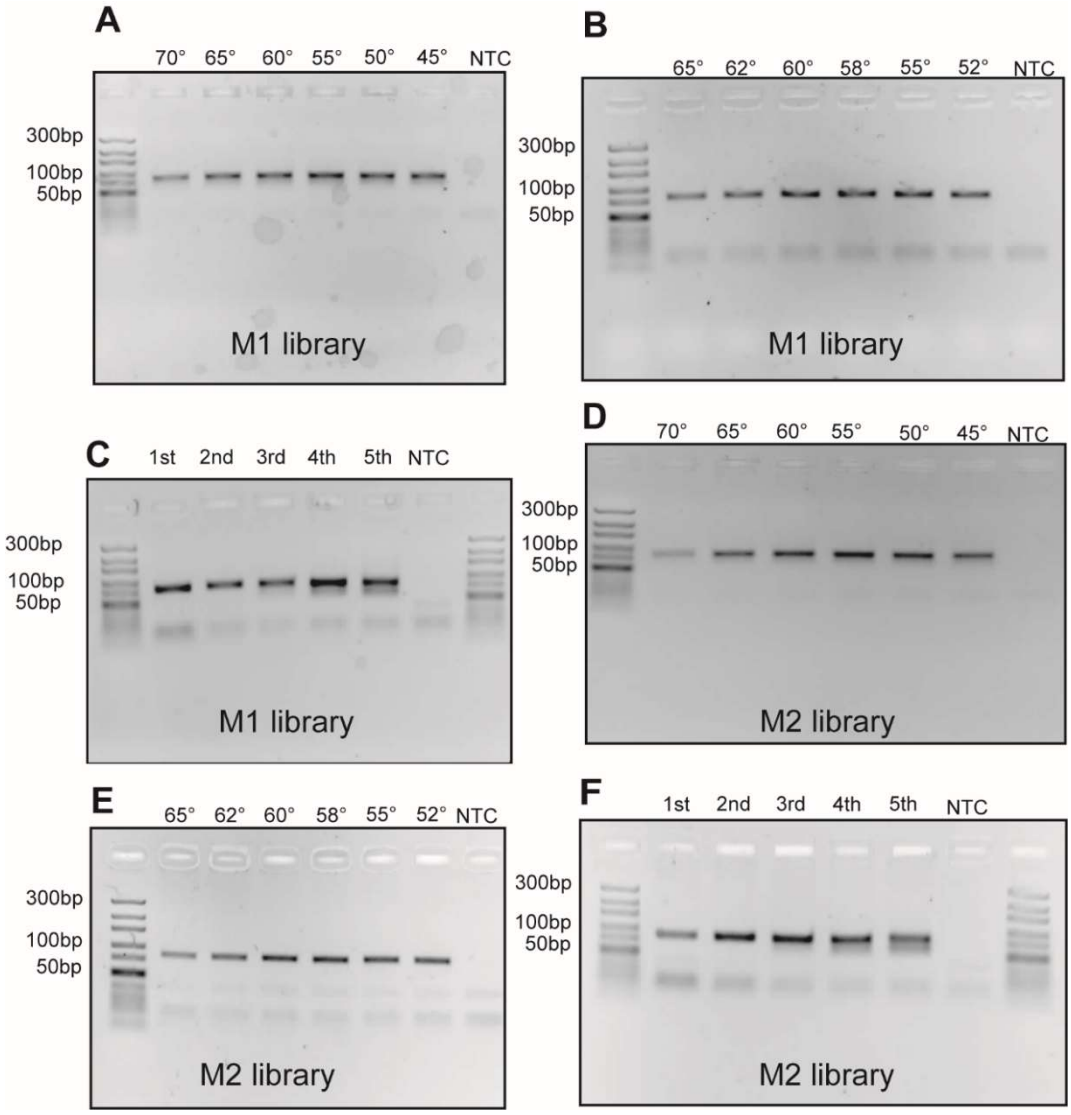

Figure 3.2 Shows the PCR amplification for M1 and M2 libraries using dNTPs.
The gels were stained with Ethidium bromide. To determine the optimal annealing temperature for the M1 library, a gradient PCR was performed, starting from 70°C to 45°C in **(A)** and 65°C to 52°C in **(B)**. The optimal temperature was found to be 58°C. The PCR product for the M1 library obtained at 58°C was reamplified five times using the 10-fold diluted product as a template, as shown in **(C)**. To determine the optimal annealing temperature for the M2 library, a gradient PCR was also performed, starting from 70°C to 45°C in **(D)** and 65°C to 52°C in **(E)**. The optimal temperature was found to be 58°C. The PCR product for the M2 library obtained at 58°C was reamplified five times using the 10-fold diluted product as a template, as shown in **(F)**.

3.1.2 ePCR amplification for the M2 library

Emulsion PCR (ePCR) is used in molecular biology to amplify DNA fragments with a relatively small amount of starting material. In contrast to conventional PCR, emulsion PCR involves suspending DNA templates in droplets surrounded by an oil layer, which is the main difference between them [54]. In general, ePCR can be prepared using two formulas. The difference between these two formulas is the composition of the oil phase and the ratio between the oil phase and the aqueous phase. The first formula's oil phase consists of tween 80, span 80, triton X-100, and mineral oil, and

the ratio between the oil phase to the aqueous phase is 2:1 [54]. ePCR was performed using this formula, and an undefined band beneath the PCR product appeared on the gel, reflecting the emulsion instability, as shown in **Figure 6.1**. Accordingly, to a previous study, the first indicator of breaking the emulsion is to evaluate the PCR product on an agarose gel [47].

The sconed formula's oil phase consists of TEGOSOFT, mineral oil, and ABIL WE 09 with a ratio of oil to aqueous phase of 4:1[54]. The second formula was compared to open PCR under the same conditions using the same amount of the starting library. 50 fmol/100 µl of the M2 library and different amplification cycles were applied to start from 10 to 26 cycles. The M2 library shows no detectable over-amplification using the second formula compared to the open PCR, as shown in **Figure 3.3**. Moreover, the optimized protocol was used to amplify clicked template with imidazole (Im-dU), indole (In-dU), cRGD (cRGD-dU), ethanamine (Ea-dU), or isobutyl (Ib-dU), as shown in **Figure 6.2**. Furthermore, the size of the droplet is another indicator used to evaluate the preparation of the ePCR. For larger droplets, it could contain more than one sequence, leading to the formation of by-products. The droplet size was assessed using laser-scanning microscopy, as shown in **Figure 3.3**. On average, the diameter of the droplet is 7 µm.

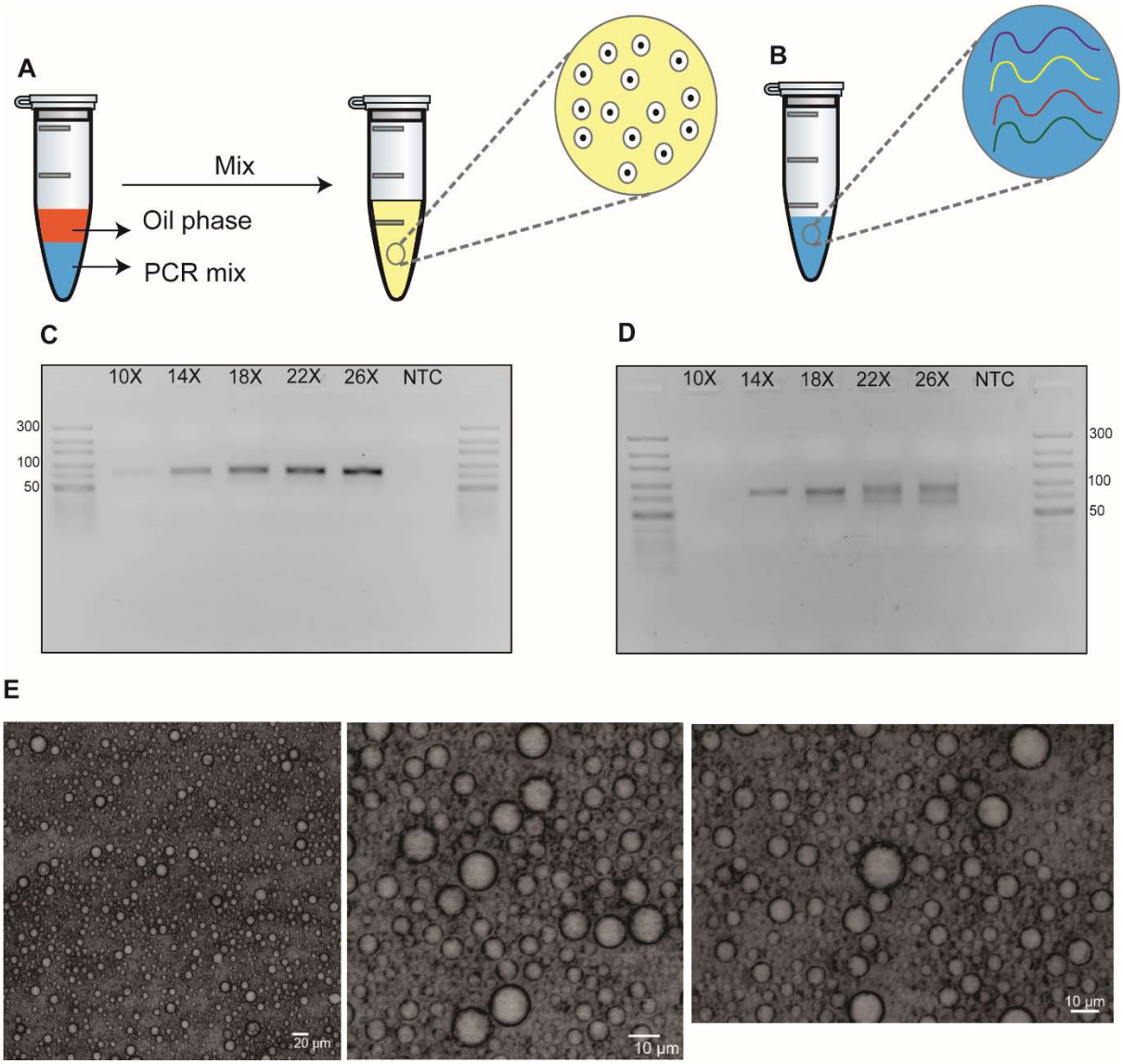

Figure 3.3 Illustrates the comparison between emulsion PCR (ePCR) and conventional PCR.
(A) A diagram shows the preparation of ePCR by mixing the PCR mixture with an oil mixture using a tissue lyzer, creating compartments for the PCR reaction. **(B)** In contrast, conventional PCR is carried out in a single compartment. **(C)** and **(D)** The results of ePCR and conventional PCR were compared by running 4% agarose gels stained with ethidium bromide for 10, 14, 18, 22, and 26 PCR cycles. In conventional PCR, a by-product appears on the 18th cycle, visible as an undefined band beneath the PCR product. **(E)** A phase-contrast image from laser-scanning microscopy shows two independently prepared emulsions, with an average droplet diameter of 7 µm.

3.1.3 Functionalization of M2 library

To ensure optimal results, assessing library functionalization before proceeding with selection is recommended, as stated in 2018 by Pfeiffer et al. [95]. **Section 5.2.4.2** explains how enzymatic digestion is used to isolate individual nucleotides from functionalized and non-functionalized libraries, as HPLC is unable to directly analyze complex DNA mixtures. In this study, the alkyne-modified M2 library was evaluated on HPLC before and after functionalization and after nucleoside digestion. **Figure 3.4** demonstrated clear peaks for dC, dG, dA, EdU, and ketones (KdU), although dT was also visible, possibly due to contamination during solid-phase synthesis. As a control, the FT2 library was

included, analyzed in parallel, and found to be free of thymidine, as shown in **Figure 6.3**. A second batch of the M2 library was synthesized by ELLA-Biotech GmbH and evaluated after nucleoside digestion, including a non-functionalized and functionalized library with indole (In-dU). **Figure 3.4 (C)** showed that the non-functionalized M2 library contained peaks for dC, dG, EdU, ketone (KdU), and dA, and was free of dT as expected. **Figure 3.4 (B)** showed that the functionalized library with indole (In-dU) no longer contained a peak for EdU, but instead had a new peak at 27 minutes retention time indicating the presence of functionalized EdU with indole (In-dU).

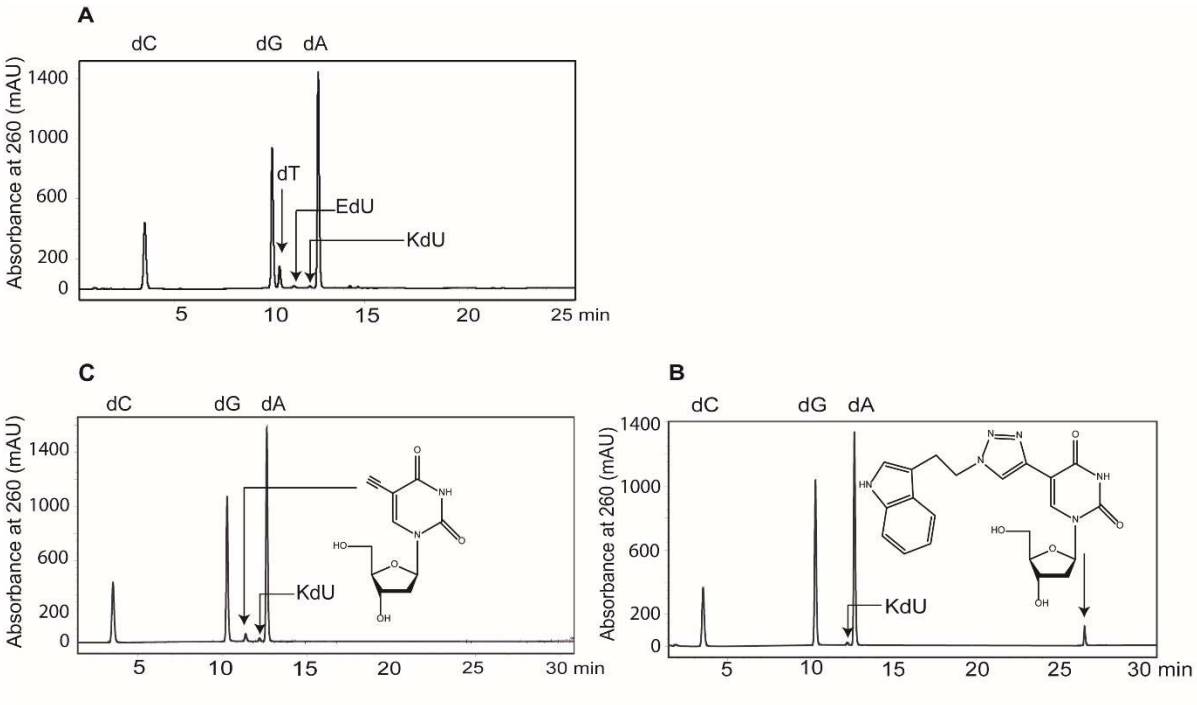

Figure 3.4 Displays the results of the analysis of EdU content in the M2 library and click reactions.
(A) shows the HPLC analysis of the unclicked M2 library after enzymatic nucleoside digestion, revealing the presence of dC, dG, dT, EdU, KdU, and dA. **(B)** shows the HPLC analysis of another batch of the M2 library after nucleoside digestion, with peaks for dC, dG, EdU, KdU, and dA, but no dT as expected. **(C)** shows the HPLC analysis of the clicked M2 library with indole after nucleoside digestion, where the peak of EdU disappears and is replaced with a new peak around 27 minutes, indicating that the EdU has been functionalized.

3.1.4 The initial interaction of clicked M2 library (background binding)

To ensure the effectiveness of the selection process, a background binding determination was performed to assess the initial interaction between the starting library and PC-3 cells. If the initial interaction is high, non-specific binding sequences may interfere with the selection process and decrease its efficiency in subsequent rounds. Moreover, a background binding of less than 1% is considered effective for the selection process [95]. The selection conditions should also be similar to the final application to ensure its efficacy. This study aimed to identify aptamers for targeted delivery in RPMI 1640 culturing medium.

The background binding was expanded to choose the most appropriate azides for the selection. The starting library was clicked with different azides and the background binding was performed using two buffers, DPBS (without divalent cations) and culturing medium (C.M) (with divalent cations). **Figure 3.5** shows that the starting library was clicked with different azides and the background binding was conducted in two buffers - DPBS without divalent cations and culturing medium (C.M) with divalent cations. Comparing the binding interactions of the functionalized starting libraries in these two buffers helped to identify the most appropriate azide for the selection. An azide that showed more binding interaction in the culturing medium than DPBS was considered more suitable for the selection process because the interaction belonged to a well-folded library in the culturing medium and the effect of the azides. However, an azide that showed high binding in both buffers may not be suitable for the selection process as it could be due to non-specific interactions between the azide and the target cells. Out of the 8 azides tested, 5 were selected as the most suitable for the selection process: indole (in-dU), cRGD (cRGD-dU), Ethanamine (Ea-dU), isobutyl (Ib-dU), and imidazole (Im-dU). Furthermore, to evaluate the effect of different competitors on the binding ability of the clicked library with different azides, binding was evaluated using different competitors: 1 mg/ml BSA, 0,1 mg/ml ssDNA, 1:1 (library: clicked competitors), and 1:10 (library: clicked competitors), as shown in **Figure 6.5**. ssDNA was found to reduce the background binding of all clicked libraries and was included in the first selection round.

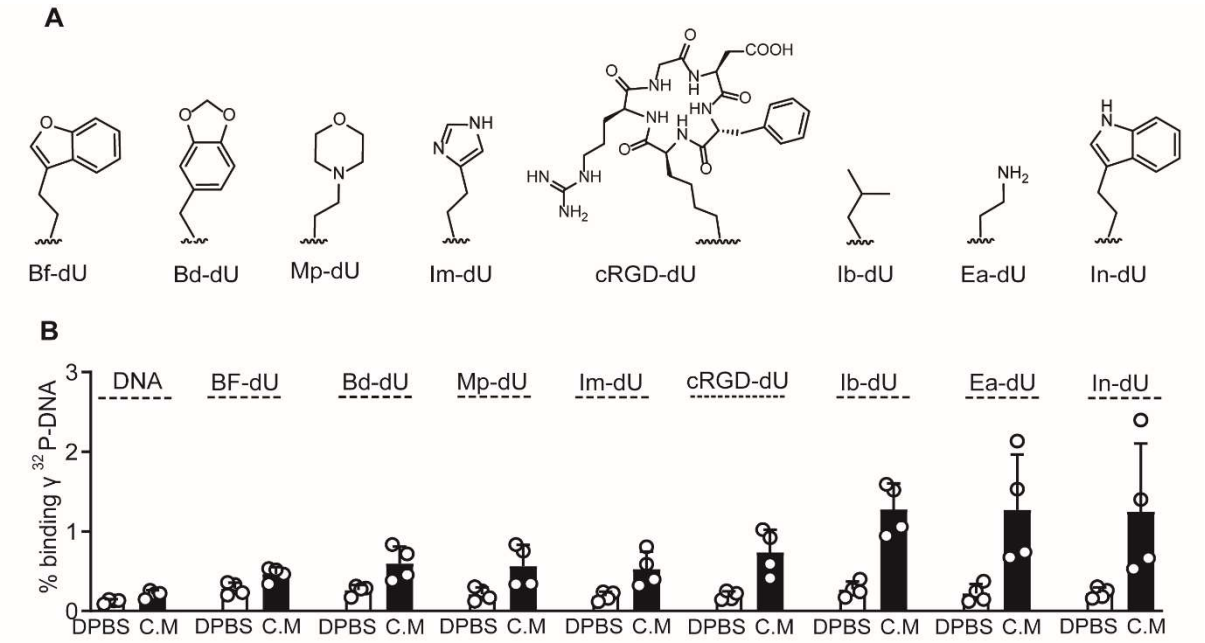

Figure 3.5 The background interaction between the starting library and PC-3 cells.
The chemical structures of the azides used in the background binding against PC-3 cells are illustrated **(A)**. These include 3-(2-azidoethyl) benzofuran (BF-dU), 5-(azidomethyl) benzo[d][1,3] dioxole (Bd-dU), 4-(2-azidoethyl) morpholine (Mp-dU), 4-(2-azidoethyl) -1H-imidazole (Im-dU), cyclic RGD (cRGD), 1-azido-2-methylpropane (Ib-dU), 2-azido-ethanamine (Ea-dU), and 3-(2-azidoethyl)-1H-indole (In-dU). **(B)** The interactions of the functionalized library were compared to the non-functionalized library to determine which azide produced the strongest binding. A 1 pmol of 32P DNA was added to PC-3 cells, and after 45 minutes of incubation, the cells were washed, and the bound fraction was eluted. The ^{32}P DNA was then measured through autoradiography (n=2, duplicated, mean ± SD). The interaction between the starting library and PC-

3 cells in the DPBS buffer was represented by the white bar, while the black bar represented the interaction in culturing medium (RPMI medium).

3.2 DNA SELEX

3.2.1 A test-run of the selection protocol with canonical DNA library

Once all the necessary techniques and materials had been established, as described in the previous sections, the first SELEX was conducted using the DNA M2 library. The method was described in **section 5.2.6.2**. Briefly, the selection process involved incubating 500 pmol of the starting library with PC-3 cells for 45 minutes in RPMI medium supplemented with 10% FCS and 0.01 mg/ml ssDNA. After incubation, the supernatant was collected and incubated again with other PC-3 cells for 1.5 hours. The bound fractions from the cell culture dishes were eluted, followed by phenol-chloroform extraction and RNase A/T1 treatment. The elution was then purified with the Nucleo-Spin®Clean-Up kit (Macherey-Nagel), amplified via ePCR **(see section 5.2.1.4.4)**, and purified again with the same kit **(see section 5.2.2.1)**. PCR product formation was monitored by agarose gel electrophoresis stained with ethidium bromide (22-30 PCR cycles). Single-strand displacement of the double-stranded PCR product was performed as described in **section 5.2.2.5**, and the resulting single-strand DNA was purified with the NucleoSpin®Clean-Up kit (Macherey-Nagel) as well. Approximately 20 pmol of purified single-strand DNA was used for the next SELEX round, with 15 pmol used from Round 9. No by-products were observed on the 4% agarose gel after staining with ethidium bromide for all the rounds, as shown in **Figure 3.6**.

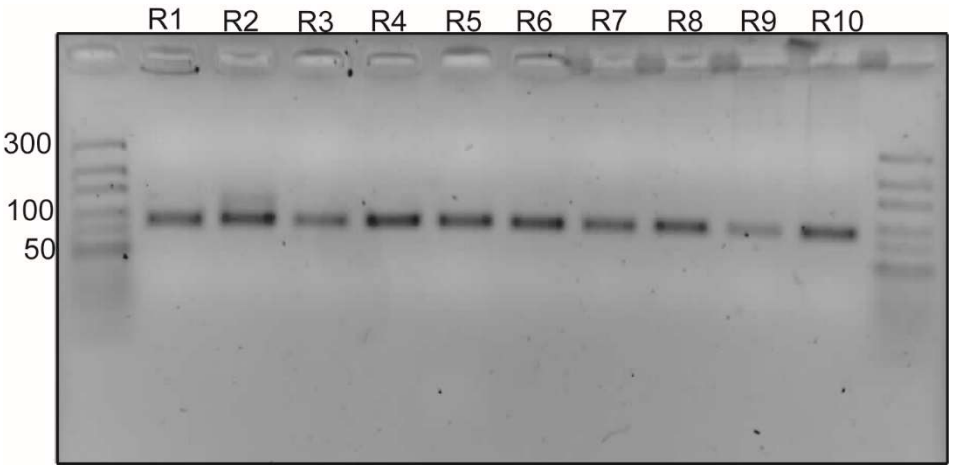

Figure 3.6 Displays the PCR products of the DNA cell SELEX method.
visualized on a 4% agarose gel stained with ethidium bromide. The gel shows the PCR products obtained from all 10 rounds of selection. All rounds produced PCR products of the expected size, without any detected by-products, except for a slight by-product in round 2, which disappeared in subsequent rounds

3.2.2 Next-generation sequencing (NGS) for the Test-run selection

After completing 10 rounds of selection, NGS was used to analyze all the selection cycles. Approximately 10^6 sequences per round were assessed. The starting library had an equal distribution of the

nucleotides dT, dA, dC, and dG, and after 10 rounds, the distribution remained largely unchanged. This might suggest that there was no significant enrichment during the selection process. Another factor considered during the NGS analysis was the number of unique sequences. Almost 100% of the sequences were unique in the first round, but this percentage decreased as the selection progressed. In rounds 6, 7, 9, and 10, the percentages of unique sequences were 86%, 73%, 61%, and 46%, respectively. After 10 rounds of selection, MD1, MD2, MD3, MD4, MD5, MD6, MD7 (family), MD8, and MD9 were slightly enriched. Among these sequences, MD1 had the highest frequency of 0.7% in round 10, as illustrated in **Figure 3.7**

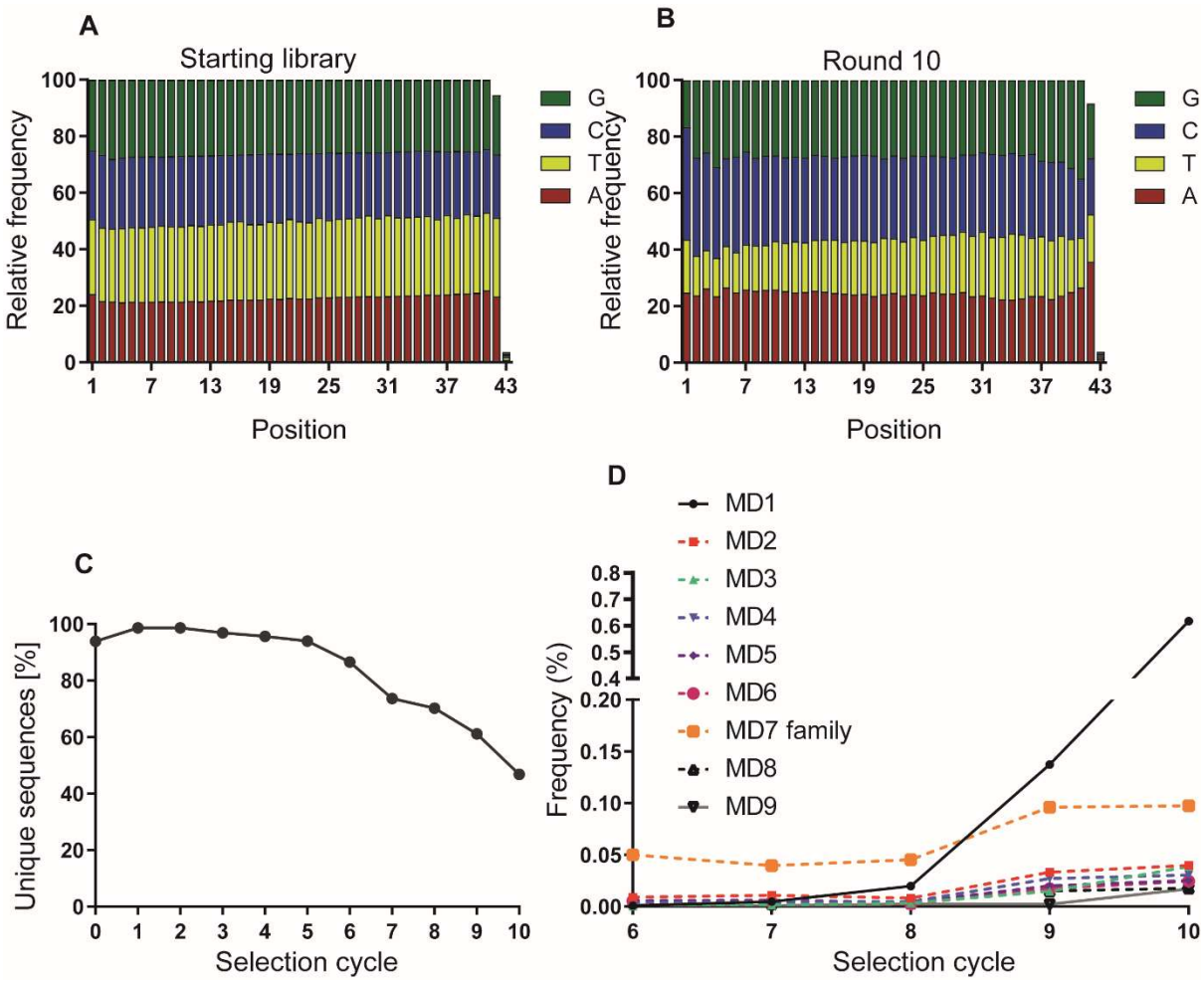

Figure 3.7 Shows the results of the Next Generation Sequencing (NGS) analysis conducted on the Test-run DNA cell-SELEX.
The figure includes four panels. The first panel **(A)** presents the distribution of the four nucleobases (dT, dA, dC, and dG) in the starting M2 library, which is equal across all 42 positions. The second panel **(B)** displays the nucleotide distribution in round 10 of the selection, which shows a slight change in distribution, with a decrease in thymidine and an increase in cytosine and adenine. The third panel **(C)** illustrates the percentage of unique sequences identified in the selection rounds. It shows a gradual decrease in the percentage of unique sequences from nearly 100% in the starting library to 46% in round 10. The fourth panel **(D)** presents the most enriched sequences identified by NGS analysis. MD1 is the most enriched sequence with a frequency of 0.7% in round 10, followed by MD2 to MD9, which are unique sequences except for one family (MD7)

3.2.3 Test the binding of the enriched sequences from the Test-run selection

The binding of MD (1-9) was analyzed by flow cytometry. 100 nM of ATTO 647N labeled aptamers were incubated with PC-3 cells in RPMI medium supplemented with 10% FCS and 0.5 mg/ml ssDNA for 45 min. The starting library labeled with ATTO 647 was used as a negative control. Using flow cytometry, the mean fluorescence intensity (MFI) and percentage of cells bound by the labeled aptamers was measured. **Figure 3.8** shows the relative MFI (aptamer/starting library) and the percentage of cells bound by labeled DNA aptamers. All the sequences exhibited low binding in the range of 5-9% to PC-3 cells, with MD7 being the most effective binder with approximately 9% binding.

A

MD1	TGATGGCGGTTTGACGGTCCGAGCCAAGAGTGGTGAGTTCGA
MD2	AAGCAGAGATTAGGGCCATGTGCCCCAAGTCAAGGGATTAG
MD3	CCTGAGGACAAAACTCTACGAGCGCAACGAGGTTAAAGAGGT
MD4	GAAGAAAAGGGAAGCAATGCTGGACAGCCGGCCAGCTCCTGG
MD5	AGGCACAGCGTAGAGCCAGGCAGCTGCAAATCAAGACATGA
MD6	AGGCAAAGACTGGAGTGCTGTGGCCATAAGCCAAGGAATGA
MD7 family	CCACTCCCCTCTCCCCATCCGCCCGAGACCACAGCCACTCCC
MD8	CAGCAAACGTGGCTATACTAAGAACACTGACAAGTCCGCAAA
MD9	CCACGGACACTCGTGCCTGAACTGAGTGCTTGGGGAGGGCCA

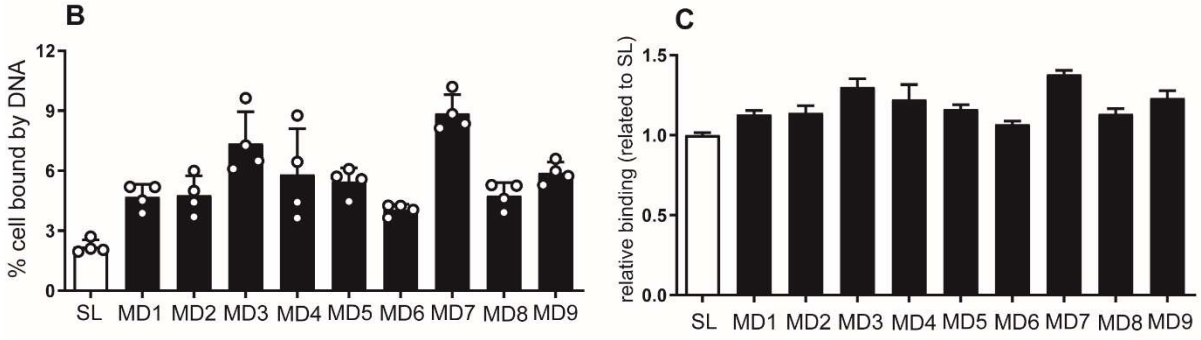

Figure 3.8 Interaction analysis of the DNA sequences and PC-3 cells.
(A) Sequences identified by NGS analysis in the DNA cell-SELEX. These sequences were the most enriched. The primer binding sites were not included. **(B) (C)** Flow cytometer was used to evaluate the interaction between the sequences and PC-3 cells. 100 nM of the labeled sequences with ATTO 647N were incubated with PC-3 cells. After 45 min the cells were washed three times, and the fluorescence was evaluated with a flow cytometer. (n=2, duplicated, mean ± SD). **(B)** the percentage of cells bound by labeled DNA aptamer **(C)** relative binding, MFI (aptamer/starting library).

3.3 Split-combine cell SELEX

3.3.1 Monitoring the click reaction during the selection

During the split-combine cell SELEX, the evaluation of the click reaction was challenging because it required at least 100 pmol of the functionalized library for each clicked-in moiety. Amplifying a large quantity of the SELEX rounds via PCR to test on HPLC/HPLC-MS could result in an increase in non-specific binding, which is difficult to avoid. To address this, a control named the tester EdU was clicked simultaneously with the rounds and evaluated on HPLC-MS. The tester EdU is a 16-nucleotide single-stranded DNA that contains only one EdU (Tester EdU: 5'-GCACTGT-EdU-

CATTCGCG-3'). It was included in all the click reactions during the selection process and was used to evaluate the click reaction for all the azides. As shown in **Figure 6.4**, the tester EdU indicated that click reactions occurred in rounds 1-12, but not in round 11 when indole (In-dU) was used, suggesting an issue with the reaction in round 11. Since indole did not show any signs of enrichment, this reaction was not repeated. **Figure 3.9** presents the HPLC-MS evaluation of clicked and unclicked tester EdU in the first round

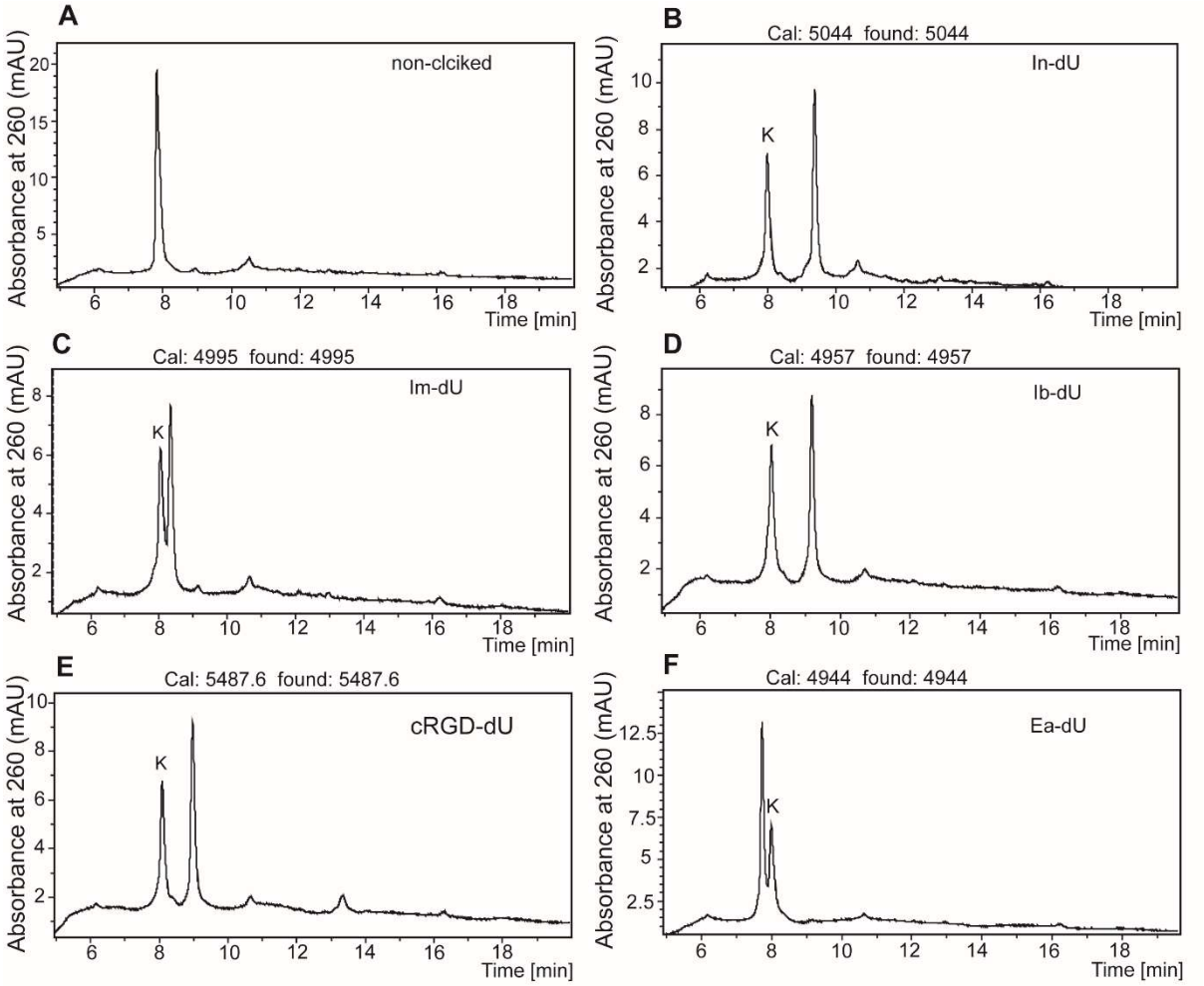

Figure 3.9 Investigation of the click reaction with tester EdU during the split-combine cell SELEX.
(A) HPLC/MS of unclicked tester EdU. K being KdU that cannot be clicked. 10 pmol of clicked tester EdU is analyzed on HPLC/MS after clicking with the chosen azides for the selection: (B) 3-(2-azidoethyl)-1H-indole (In-dU) (C) 4-(2-azidoethyl) -1H-imidazole (Im-dU) (D) 1-azido-2-methylpropane (Ib-dU) (E) cyclic RGD (cRGD) (F) 2-azido-ethanamine (Ea-dU)

3.3.2 Split-combine cell SELEX protocol

The protocol of the split-combine cell SELEX was described in detail in **section 5.2.6.1**. Briefly, the starting library was split into five sub-libraries, these sub-libraries were clicked independently with one of the following azides: imidazole (Im-du), cRGD (cRGD-dU), ethanamine (Ea-dU), isobutyl (Ib-dU), and indole (In-dU). Followed by NucleoSpin®Clean-Up kit (Macherey-Nagel) purification

and then, combining the sub-libraries together. The purpose was to increase the diversity of the starting library. The functionalized library was incubated with PC-3 cells for 45 min and then the supernatant was collected and incubated again with fresh PC-3 cells for 1.5 hours. The bound fraction from both cells was collected, eluted, and purified and ePCR was used to amplify the bound fraction using the protocol described in **section 5.2.1.4.4.** In this study, the main concern was reducing the non-specific binders, and to achieve this, two counter-selection steps were developed. The first counter-selection was to use LNCaP as a negative cell to remove most non-specific binders and the sequences binding to all cell lines. The other counter-selection step was developed for this selection but it can be used for other click-SELEX or split-combine SELEX protocols. The aim of this counter-selection step was to remove the sequences which were binding to PC-3 without the clicked-in moieties. To achieve this, round 1 was amplified using dNTPs, and after purification and digestion, the ssDNA was incubated again with PC-3 cells, and the unbound fraction was collected, as shown in **Figure 5.2.1**.

After nine rounds of selection, the binding of the 9th round and the starting library (St.L) against PC-3 cells was evaluated by flow cytometry. Round 9 and St.L were amplified via ePCR by using ATTO 647N forward primer. And then, the enrichment was tested for each azide separately, As shown in **Figure 3.10** Round 9 showed strong enrichment using: imidazole (Im-dU), ethanamine (Ea-dU) and isobutyl (Ib-dU), weak enrichment using: cRGD (cRGD-dU) and no enrichment using indole (In-dU). Additionally, three more selection rounds, referred to as deconvolution steps, were conducted to increase the copy number of each sequence associated with the corresponding azide. The objective of these rounds was to enhance the selection process. Similar to the previous experiment, the binding capacity of the 12th round was compared to that of the St.L and 9th round using flow cytometry. As shown in **Figure 3.10**, the highest level of enrichment is observed by imidazole azide to PC-3 cells, followed by ethanamine and isobutyl, and the lowest level is observed by cRGD. For indole, there was no sign of enrichment.

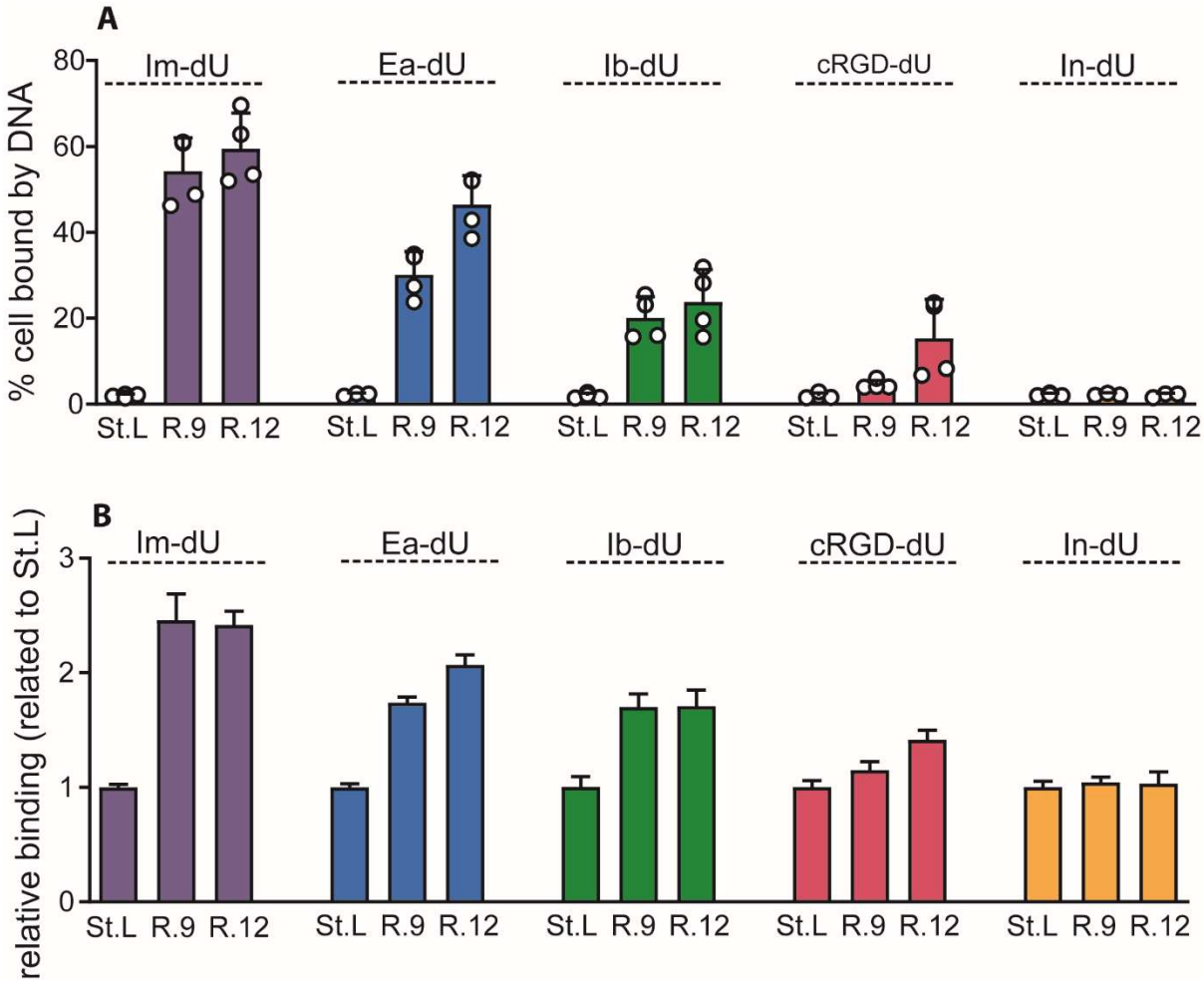

Figure 3.10 Interaction study between the enriched libraries and PC-3 cells.
(A) Interaction assay using 93.1 nM of St.L (starting library), R.9 (round 9) and R.12 (round 12) labeled with Atto 647N. The rounds were clicked with imidazole (Im-dU), ethanamine (Ea-dU), isobutyl (Ib-dU), and cyclic RGD (cRGD-dU) or Indole (indole-dU). A flow cytometer was used to detect fluorescence after incubation with PC-3 cells for 45 minutes. 20 thousand events were measured. (n=2, duplicated, mean ± SD). (A) the percentage of cells bound by labeled clicked libraries (C) relative binding, MFI (clicked enriched library/clicked starting library).

3.3.3 NGS analysis of split-combine cell SELEX

NGS analysis was performed for all the rounds, including the deconvolution step. In total, 25 samples, St.L with 9 rounds during the split-combine cell SELEX and 15 rounds of the deconvolution step. NGS sample preparation was described in **section 5.2.3**. the nucleotide distribution refers to the frequency of occurrence of each of the four nucleotide bases (A, C, G, and T) at each position in the random region. The starting library was expected to have an equal distribution for all the nucleotides. However, after 9 rounds of selection, the nucleotide distribution changed reflecting a potential enrichment of sequences that specifically bind to the target cells. Additionally, the most influential factor is the EdU distribution within the random region. A comparison between the starting library and round 9 shows that the level of EdU decreases in some positions and increases in others. These changes were more apparent after the deconvolution step, as depicted in **Figure 3.11**. Integrating the nucleotide distribution with unique sequences can provide a more comprehensive understanding of

the selection enrichment. The starting library consisted of nearly 100% unique sequences. However, the percentage of unique sequences decreased from 45% in round 9 to approximately 4% in round 12 for all the azides. Prior to the deconvolution step, two families, S1 and S2, were enriched. The frequency of S1 and S2 families remained low until round 8. In round 9, the frequency increased to 11.6% and 0.07% for S1 and S2, respectively. For the S1 family, imidazole (Im-dU) and ethanaime (Ea-dU) were highly enriched (75% and 70%, respectively) while for cRGD (cRGD-dU) and indole (In-dU) showed de-enrichened, and the percentage was reduced to 0.5%. Isobutyl was also enriched, but not to the same degree as imidazole (Im-dU) and ethanaime (Ea-dU). Moreover, there was an increase in the percentage of S1 to 48%. Furthermore, the S2 family is enriched with cRGD (cRGD-dU) to 7.2%, while the S1 family is diminished with cRGD (cRGD-dU). The S2 with indole (In-dU) was increased to 1.12% in round 11 and then de-enriched to 0.48% in round 12, this could be explained due to the failure of the click reaction in round 11, as explained before in **section 3.3.1**, this could be justified. After deconvolution, the S2 was diminished for imidazole (Im-dU) and ethanaime (Ea-dU), all the data with S1 and S2 families were shown in **Figure 3.12**.

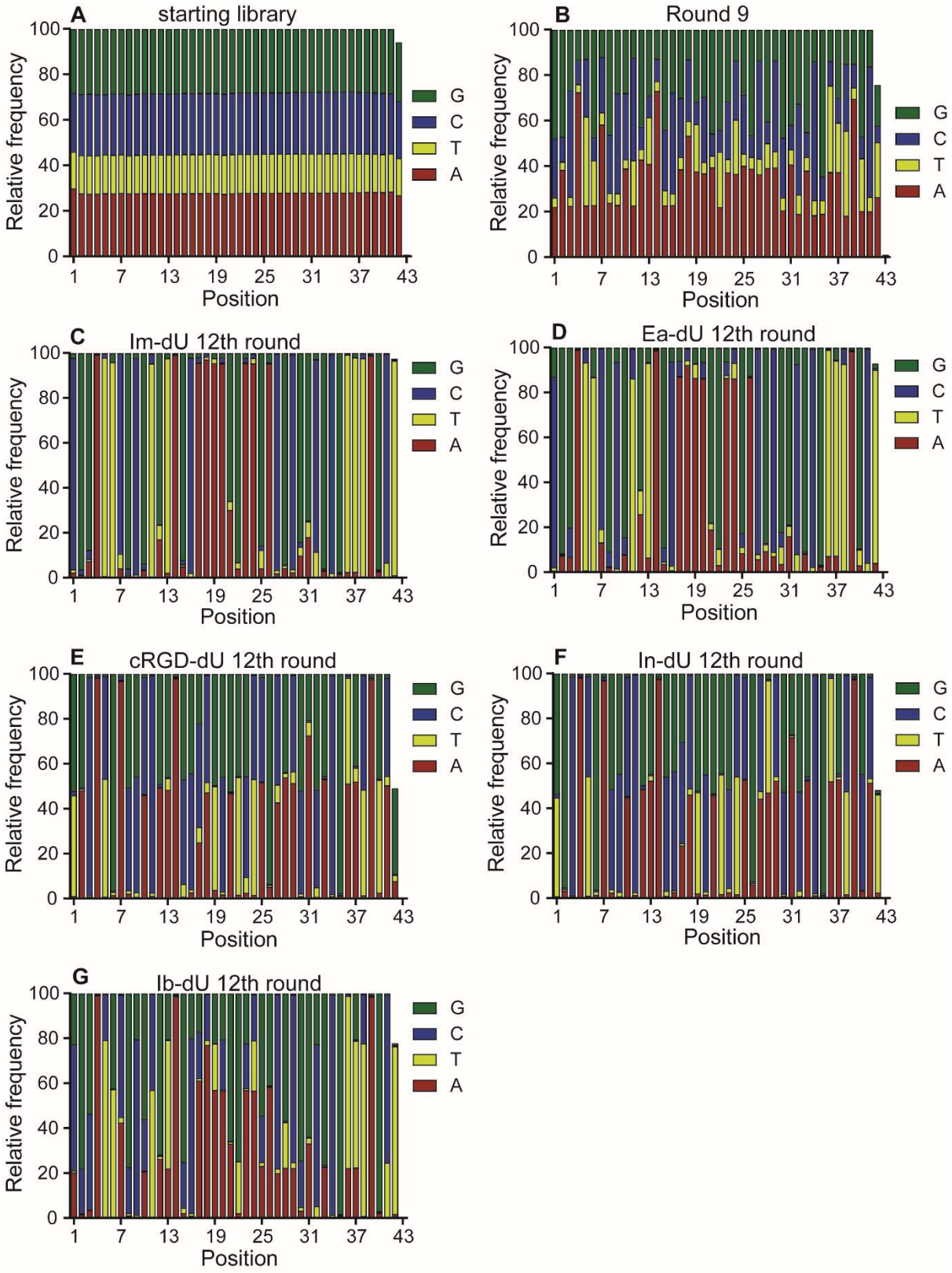

Figure 3.11 Presents the nucleotide distribution for the alkyne-modified starting library, the 9th and 12th rounds of the split-combine cell SELEX.

(A) shows the distribution of nucleotides at different positions in the random region of the alkyne-modified M2 starting library. **(B)** displays the nucleotide distribution for the last round before the deconvolution step in round 9 of the split-combine cell SELEX. **(C-G)** show the nucleotide distribution for round 12 of imidazole (Im-dU), ethanamine (Ea-dU), cyclic RGD (cRGD-dU), indole (In-dU), and isobutyl (Ib-dU), respectively.

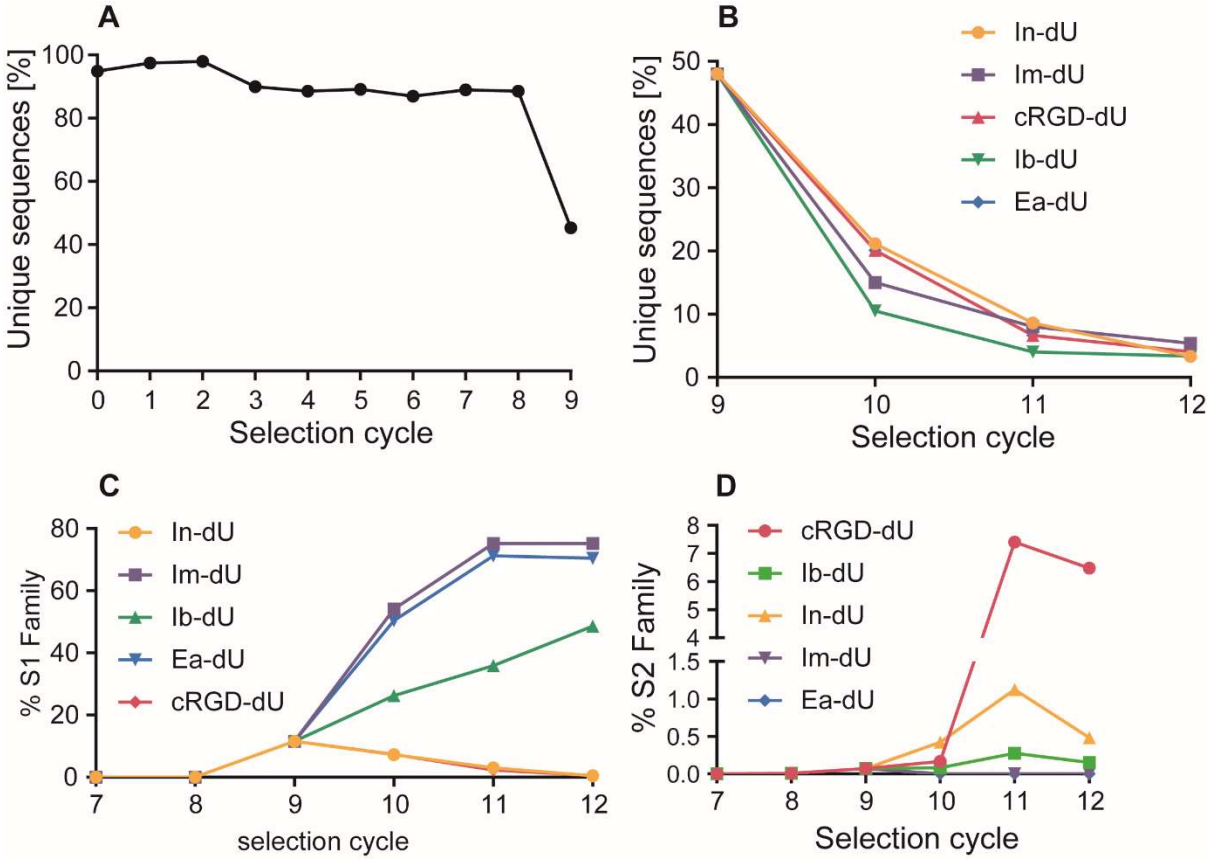

Figure 3.12 The NGS analysis of the split-combine cell SELEX.
(A) shows the analysis of unique sequences in the split-combine cell SELEX, revealing a sudden drop in the percentage of unique sequences from 88% in round 8 to 45% in round 9. **(B)** shows that the percentage of unique sequences dropped to less than 10% with all azides in the deconvolution data. **(C-D)** show the percentage of the S1 and S2 families, respectively, during the last rounds of split-combine cell SELEX and the deconvolution step.

3.3.4 The binding ability of the enriched sequences against PC-3 cells

As a result of the NGS data analysis, two families were identified: S1 and S2. A sequence representing each family was selected. For both sequences, a scramble sequence (SC) was generated. The scramble sequence shared the same primer binding sites; however, the random region was randomized. The scrambled version of S1 or S2 was used as a negative control for any subsequent experiments. S1 and S1 SC were amplified by PCR utilizing ATTO 647N forward primers using the protocol in **section 5.2.1.3.2**. After λ-exonuclease digestion (**Section 5.2.2.5**) and purification (**section 5.2.2.1**), the S1 and its negative control were clicked with imidazole (Im-dU), cRGD(cRGD-dU), ethanamine (Ea-dU), isobutyl (Ib-dU), or indole (In-dU), as described in **section 5.2.4.** After purification (**section 5.2.2.1**), the binding of S1 was evaluated using flow cytometry. As shown in **Figure 3.13**, The non-modified version (E) of the S1 sequence did not show any binding to PC-3 cells. The maximum binding of S1 to PC-3 was observed when S1 was clicked with imidazole (Im-dU). Moreover, S1 showed binding to PC-3 when clicked with ethanamine (Ea-dU), cRGD (cRGD-dU) or isobutyl (Ib-dU) but less than S1 clicked with imidazole. On the other hand, S1 clicked with indole showed a weak interaction with PC-3 cells. To serve as a positive control, the 12th round clicked

with imidazole was included in this experiment. Additionally, the starting library clicked with imidazole was included as a negative control.

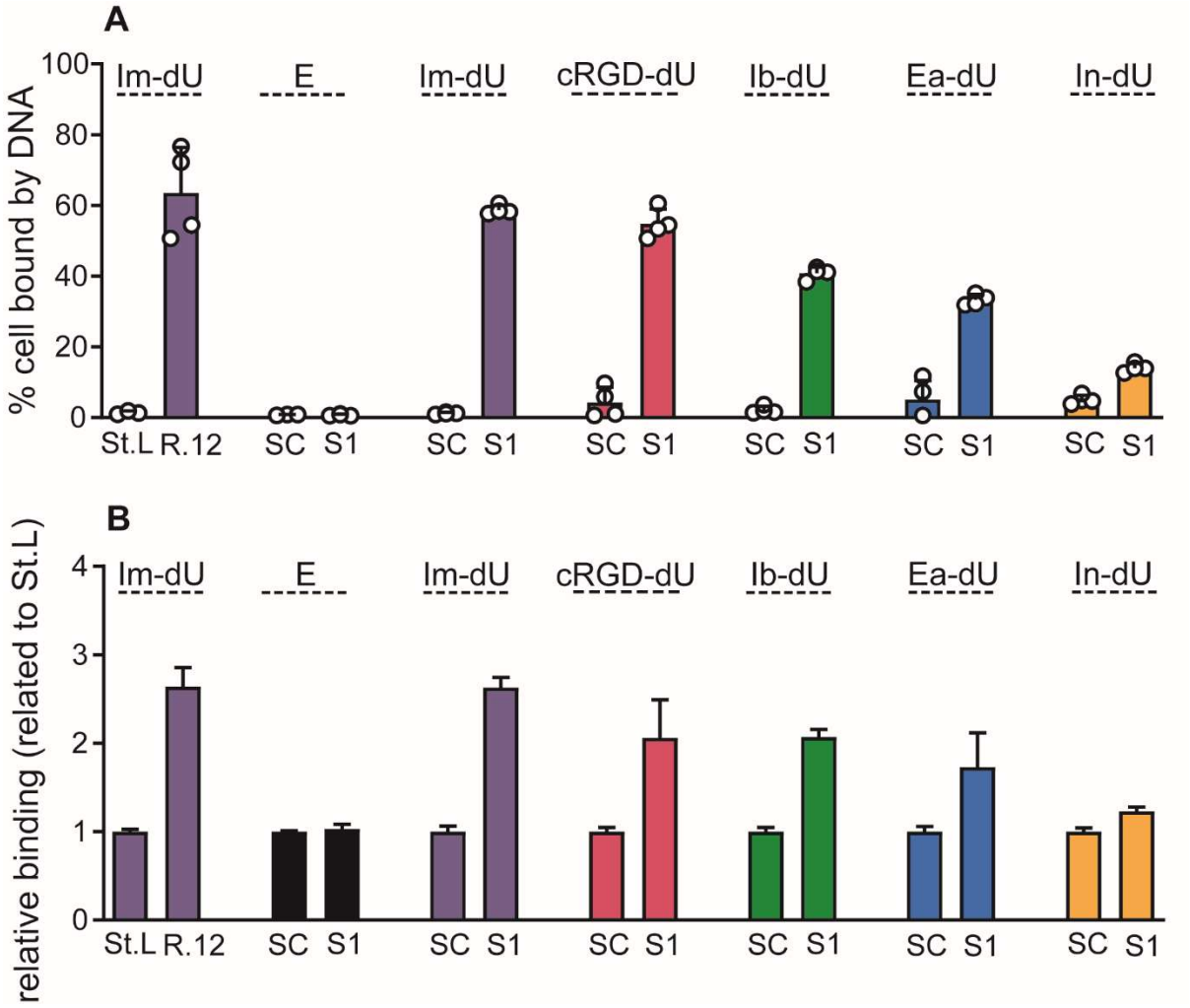

Figure 3.13 The interaction study between the enriched S1 clickmer and PC-3 cells.
The study involved incubating the labeled S1 clickmer (93.1 nM) with PC-3 cells for 45 minutes, and then measuring the fluorescence using flow cytometry. The study was conducted in duplicate (n=2, duplicated, mean ± SD), and 20 thousand events were measured. The S1 clickmer was clicked with imidazole (Im-dU), ethanamine (Ea-dU), isobutyl (Ib-dU), cyclic RGD (cRGD-dU), indole (In-dU), or un-clicked S1 (E). **(A)** shows the percentage of cells bound by the labeled clicked S1, while **(B)** shows the relative binding in terms of MFI (clicked S1/S1 scramble sequence (SC)).

In the case of the S2 sequence, the same steps for amplification, purification, and clicking were followed as for the S1 aptamer. Based on flow cytometry data, S2 exhibited the highest level of binding with indole (In-dU) and cRGD (cRGD-dU), followed by isobutyl (Ib-dU), ethanamine (Ea-dU) and imidazole (Im-dU). It was found that the non-modified version did not bind to PC-3 cells, as depicted in **Figure 3.14**.

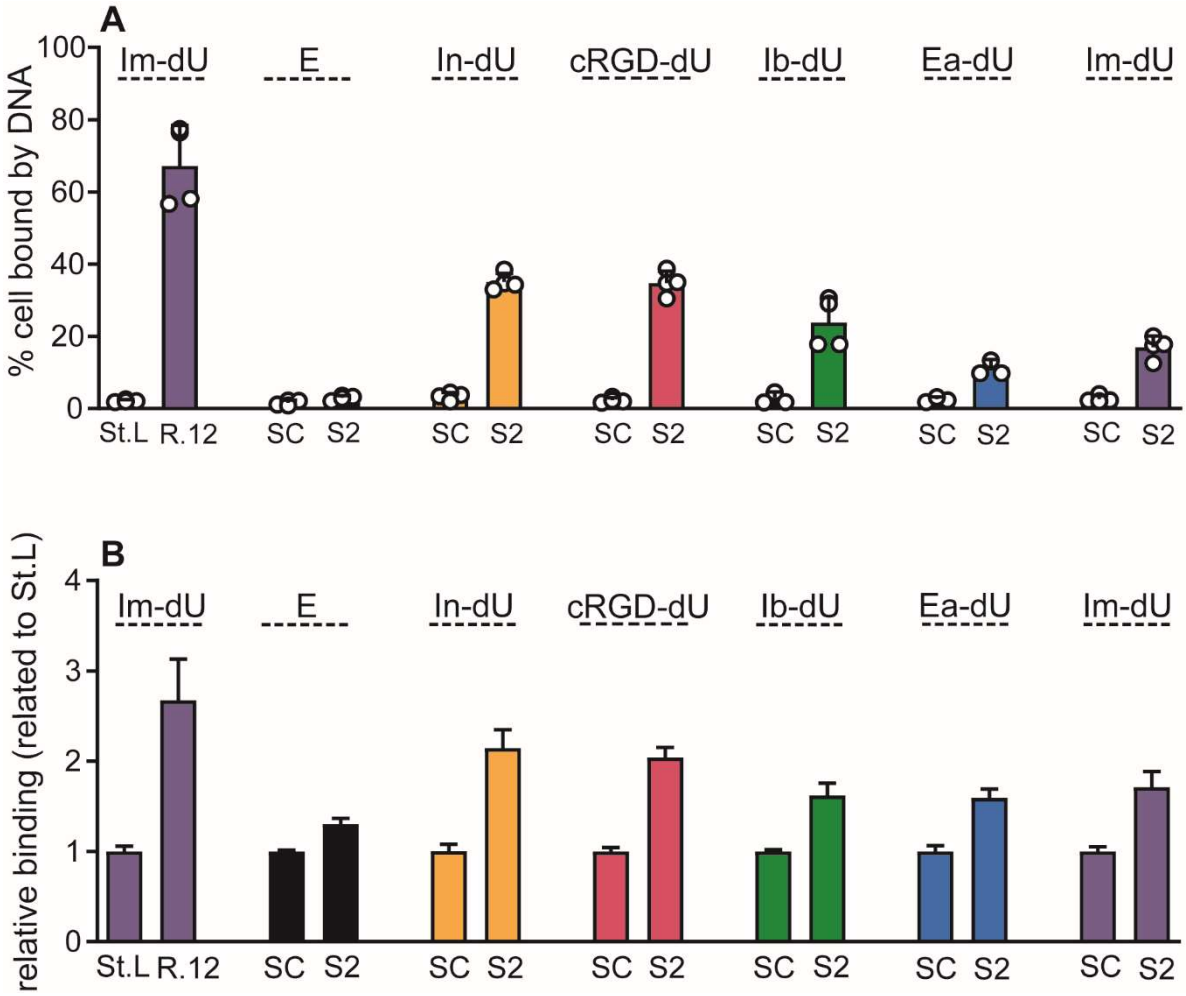

Figure 3.14 The interaction study between the enriched S2 clickmer and PC-3 cells.
The study involved incubating the labeled S2 clickmer (93.1 nM) with PC-3 cells for 45 minutes, and then measuring the fluorescence using flow cytometry. The study was conducted in duplicate (n=2, duplicated, mean ± SD), and 20 thousand events were measured. The S2 clickmer was clicked with imidazole (Im-dU), ethanamine (Ea-dU), isobutyl (Ib-dU), cyclic RGD (cRGD-dU), indole (In-dU), or un-clicked S1 (E). **(A)** shows the percentage of cells bound by the labeled clicked S1, while **(B)** shows the relative binding in terms of MFI (clicked S1/S2 scramble sequence (SC)).

3.4 Characterization of S1 clickmer

3.4.1 Competition assay

Competition assays are commonly used in laboratories to investigate binding interactions between two molecules, typically a receptor and a ligand. In these assays, an unlabeled ligand competes with a labeled ligand for binding to the receptor [153]. In this study, ATTO 647N labeled S1 clicked with imidazole (Im-dU) was used as the labeled ligand and competed with S1 clicked with other moieties, including Indole (In-dU), cRGD (cRGD-dU), isobutyl (Ib-dU), and ethanamine (Ea-dU). The experiment was performed as described in **section 5.2.7.3.1.3**. Briefly, the labeled and the unlabeled version of S1 were incubated with PC-3 at the ratio (1:10) (labeled: unlabeled). After incubation time for 45 min, the cells were washed, and the fluorescence was measured using flow cytometry. As negative controls, SC clicked with Indole (In-dU), cRGD (cRGD-dU), isobutyl (Ib-dU), ethanamine

(Ea-dU), and Imidazole (Im-dU) were included. Moreover, as a positive control, unlabeled S1 clicked with imidazole was incubated with labeled S1 clicked with imidazole. As shown in Figure 3.15, there was no decrease in fluorescence when S1 was incubated with SC. Furthermore, there was no detectable fluorescence when S1 was incubated with unlabeled S1 clicked with imidazole (Im-dU) or Isobutyl (Ib-dU). There was a decrease in the fluorescence when S1 was incubated with S1 clicked with cRGD (cRGD-dU) or ethanamine (Ea-dU).

Using the same method, this experiment was repeated but the labeled S1 was clicked with cRGD (cRGD-dU) and it was competing with unlabeled S1 clicked with Indole (In-dU), imidazole (Im-dU), isobutyl (Ib-dU), and ethanamine (Ea-dU). As shown in **Figure 3.15,** the fluorescence of S1 clicked with cRGD was detectable when it was incubated with all the S1 variants or SC. Furthermore, there was no observable decrease in fluorescence when the labeled S1 clicked with imidazole (Im-dU) was incubated with S1 clicked with isobutyl (Ib-dU), indicating no substantial competition for binding.

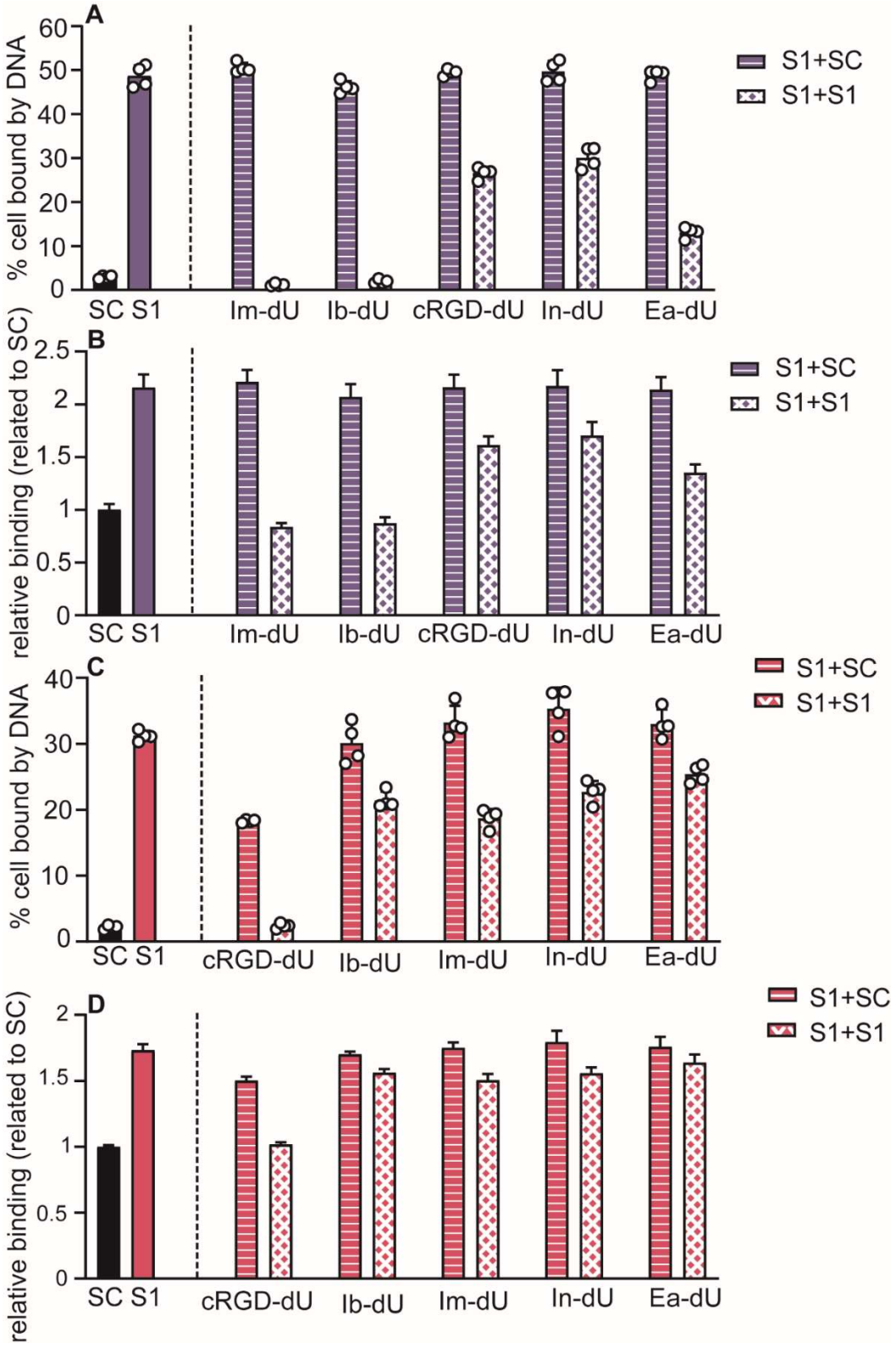

Figure 3.15 The results of a competition assay involving S1 that was clicked with different azides.
The experiment involved mixing labeled S1 clicked with imidazole (Im-dU) with 10 times more unlabeled S1 clicked with cyclic RGD(cRGD-dU), ethanamine (Ea-dU), isobutyl (Ib-dU), and indole (In-dU). The mixture was then incubated with PC-3 cells for 45 minutes, and the fluorescence of the labeled S1 was measured using flow cytometry (n=2, duplicated, mean ± SD). **(A)** shows the percentage of cells bound by S1 labeled and clicked with imidazole, while **(B)** shows the relative binding measured as the MFI of clicked S1 relative to the S1 scramble sequence (SC). The same experiment was repeated using labeled S1 clicked with cyclic RGD (cRGD-dU) (n=2, duplicated, mean ± SD), and **(C)** shows the percentage of cells bound by S1 labeled and clicked with cyclic RGD, while **(D)** shows the relative binding measured as the MFI of clicked S1 relative to the S1 scramble sequence (SC).

3.4.2 Concentration binding of S1 with different clicked azides

The interaction between an aptamer and its target cells can be characterized by the concentration-dependent binding relationship, which describes the correlation between the concentration of the aptamer and its binding affinity to the cell surface.This relationship is critical to understand when using aptamers as targeting agents in various applications, such as drug delivery or imaging[154] [155]. Moreover, the binding interaction can be used to determine the minimum effective concentration of the aptamer required for binding to the target cells, as well as the maximum binding capacity of the target cells [154].

The ATTO 647N labeled S1 aptamer was tested against PC-3 cells with the following azides: imidazole (Im-dU), cRGD (cRGD-dU), ethanamine (Ea-dU), and idole (In-dU) at concentrations of 0.956 nM, 9.56 nM, 23.9 nM, 47.8 nM, 95.7 nM, 191.4 nM, 335 nM, and 478.5 nM, respectively. Binding was evaluated using flow cytometry. In the case of S1 clicked with imidazole, the fluorescence increased with increasing concentrations of the clicked aptamer. In addition, fluorescence was detectable at a low concentration of 0.956 nM. The binding of S1 clicked with indole was weak, and there was no substantial difference between the binding of S1 and its scramble sequence. In the case of S1 clicked with RGD and ethanamine, the aptamer showed binding to PC-3 cells at various concentrations, with a minimum effective concentration of 9.56 nM.

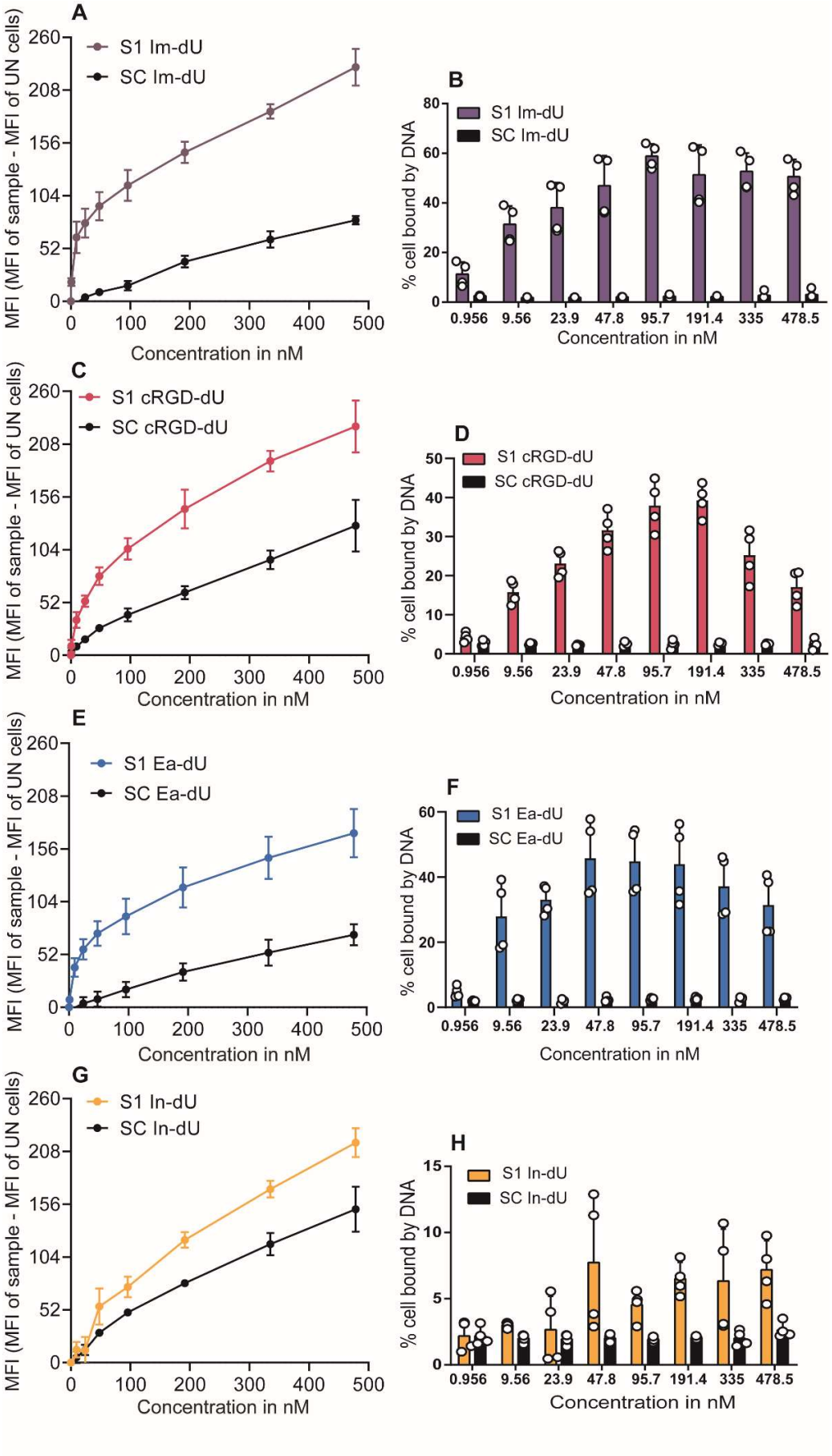

Figure 3.16 The concentration-dependent binding of S1 clickmer clicked with different azides to PC-3 cells.

The experiment involved seeding 30,000 PC-3 cells into 48-well plates, followed by incubation with varying concentrations of clicked S1 or scrambled sequence (S1 SC) clicked with different azides ranging from 0.956 nm to 478.5 nM for 45 minutes. The cells were washed, scraped, and collected, and the fluorescence was measured using flow cytometry (n=2, duplicated, mean ± SD). **(A)** demonstrates the MFI of clicked S1 and its scramble sequence (SC) after being clicked with imidazole, with background MFI subtracted from both measurements. **(B)** shows the percentage of cells bound by S1 labeled and clicked with imidazole (Im-dU). Similarly, **(C-D)** show the MFI and percentage of cells bound by S1 labeled and clicked with cyclic RGD (cRGD-dU), respectively. **(E-F)** show the MFI and percentage of cells bound by S1 labeled and clicked with ethanamine (Ea-dU), respectively. Finally, **(G-H)** show the MFI and percentage of cells bound by S1 labeled and clicked with indole (indole-dU), respectively.

3.4.3 Testing the specificity against different cancer cell lines

Testing the specificity of an aptamer against cells is an initial step in the development and validation of the aptamer as a targeting agent [156]. Furthermore, reducing non-specific binding when testing specificity was an influential factor during the evaluation of specificity. Based on the previous binding interaction data, it was observed that S1 SC, the scrambled sequence of S1, exhibited non-specific binding at a concentration of 95.7 nM (as shown in **Figure 3.16**). Therefore, the concentration of S1 used in this experiment was 48.7 nM. S1 was tested against the following cell lines: MCF-7, HEK 293T, Hep G2, HeLa, H460, and LNCaP. During the specificity test, PC-3 cells were used as a positive control. The specificity of S1 was tested against the following cell lines: MCF-7, H460, HeLa, HEK 293T, and Hep G2. Due to the tendency of LNCaP cells to detach easily, the cells were lost during the binding experiments. Therefore, suspended cells were used in the binding experiment. The S1 clicked with imidazole bound only to PC-3 cells, whereas the S1 clicked with cRGD bound to both PC-3 and MCF-7 cells. The S1 clicked with ethanamine bound to PC-3 and LNCaP cells, as shown in **Figure 3.17**.

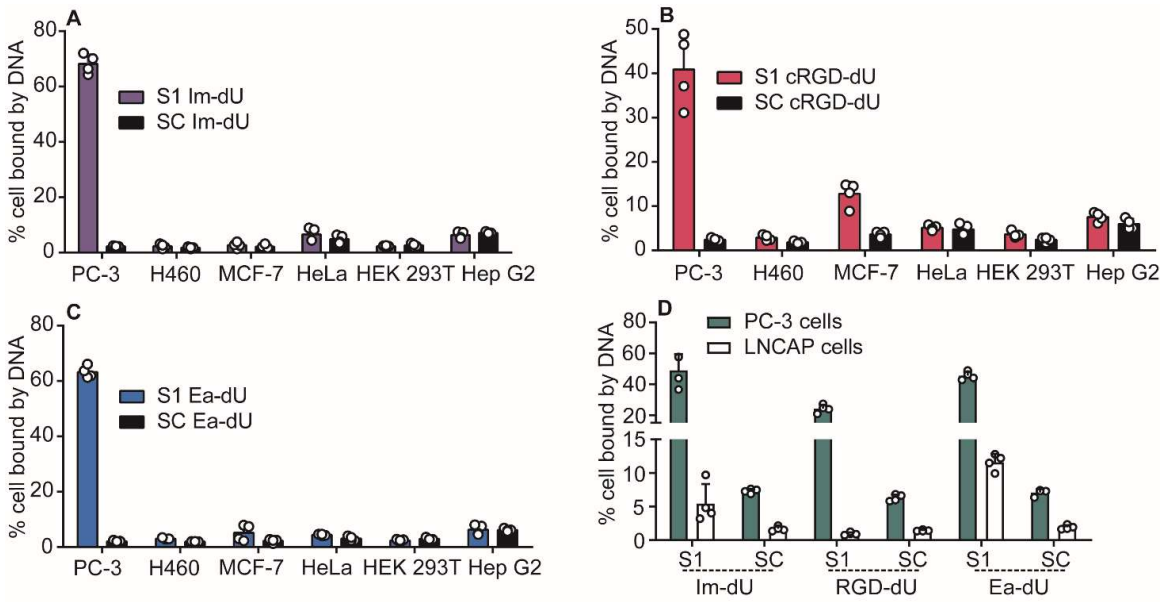

Figure 3.17 The determination of the specificity of clickmer S1 clicked with different azides.
The experiment involved incubating 48.7 nM of labeled S1 clicked with different azides with various cancer cell lines, including H460, MCF-7, HeLa, HEK 293T, and Hep G2, for 45 minutes. After washing and scraping the cells, the fluorescence of the bound S1 clickmer was measured using flow cytometry. The experiment was repeated twice in duplicate. The

figure is divided into four panels. Panel **(A)**, **(B)**, and **(C)** show the percentage of binding of S1 clicked with imidazole (Im-dU), cyclic RGD (cRGD-dU), and ethanamine (Ea-dU), respectively, with different cell lines. Panel **(D)** presents the results of an interaction study between S1 or S1 SC clicked with Im-dU, cRGD-dU, and Ea-dU with PC-3 and LNCaP cells. In this panel, cells were detached and incubated with labeled clickmers, and fluorescence was measured using flow cytometry. The experiment was repeated twice in duplicate, and the panel shows the percentage of binding of S1 clickmer against PC-3 and LNCaP cells.

3.4.4 Internalization study of the clicked S1 against PC-3 and MCF-7 cells

Internalization studies for aptamers against cells are important to evaluate the aptamer's ability to enter the cells and to deliver cargo, such as therapeutic agents or imaging probes, to the intracellular compartment [157]. An internalization study was conducted against PC-3 cells and MCF-7 cells. the method was described in **section 5.2.7.4.1**. Briefly, ATTO 647N S1 clickmer (red) was incubated with PC-3 cells or MCF-7 cells for 45 min. The cells were then washed and fixed using 4% para-formaldehyde. The membrane was stained with WGA 488 (green) and the nuclei was stained with DAPI (blue). During confocal microscopy, images of cells at various depths within the Z-axis were acquired (Z-stacks). **Figure 3.18** illustrates that S1 labeled with imidazole (Im-dU) bound and was internalized by PC-3 cells. Conversely, S1 labeled with cRGD (cRGD-dU) bound and was internalized by both PC-3 and MCF-7 cells.

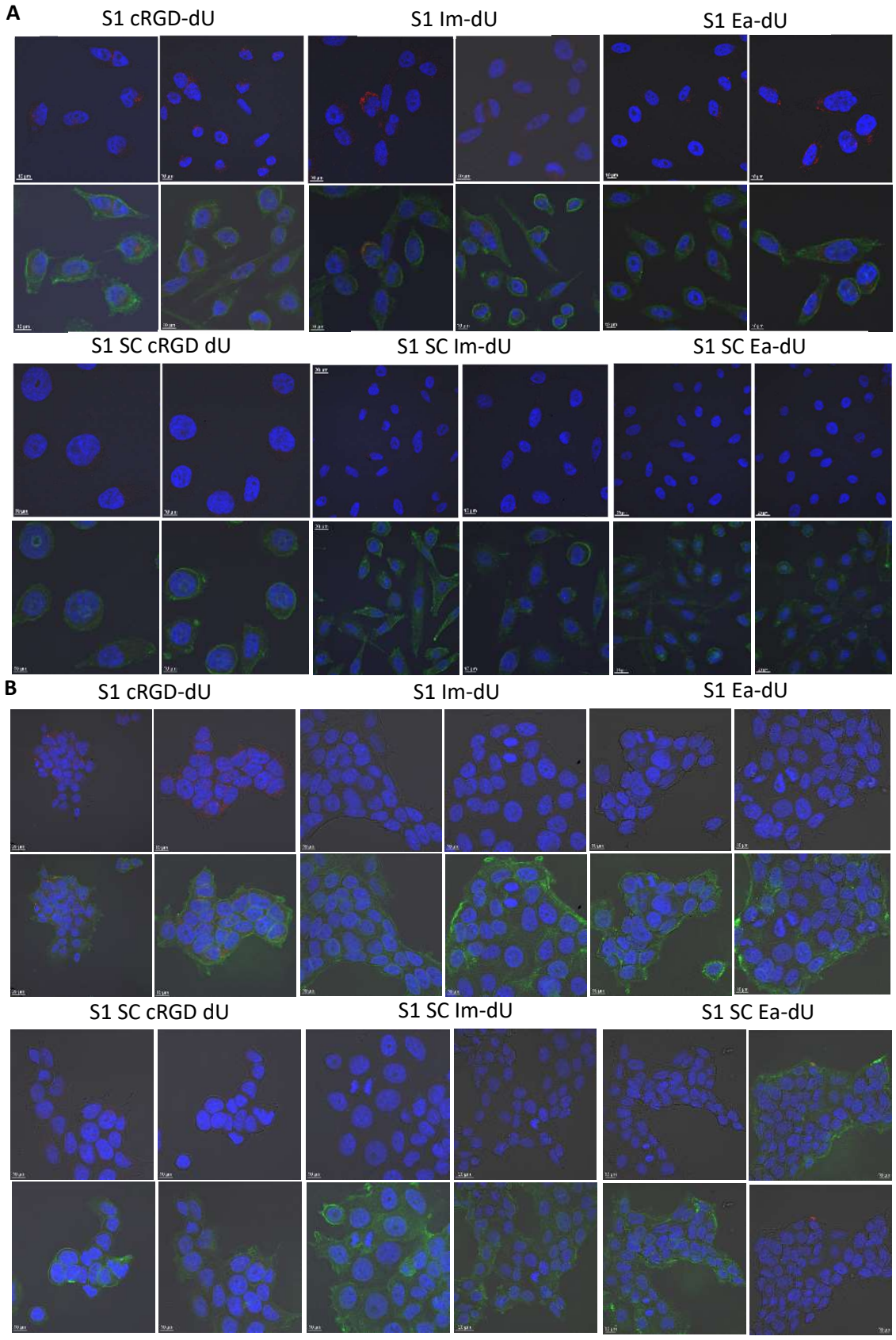

Figure 3.18 The internalization of S1 and S1 SC clicked with different azides was studied.

The PC-3 and MCF-7 cells were incubated with 50 nM of Atto 647N labeled S1 or S1 SC clicked with Im-dU, cRGD-dU, and EA-dU for 45 minutes. After washing the cells three times, they were fixed with 4% paraformaldehyde. The cells were

stained with wheat germ agglutinin conjugated with Alexa 488 (Green) and DAPI (Blue). **(A)** For PC-3 cells (n=3, duplicated) **(B)** For MCF-7 cells (n=2, duplicated)

3.4.5 EdU substitution study

It is expensive to use a clickmer sequence containing eight EdUs for targeted therapies. Therefore, it was necessary to minimize the amount of EdU presented in the sequence in order to reduce the costs for potential targeted therapies. Previous studies have indicated that not all EdUs are required for binding [97] [96]. It is necessary to note that S1 contained eight EdUs in its sequence. In order to verify which EdUs are essential for binding, deoxythymidine has been substituted at each position for EdU. Accordingly, eight variants were designed and their binding capabilities were tested against PC-3 cells. As illustrated in **Figure 3.19**, each EdU position that can be modified by click reaction is highlighted in green. T represents the EdU that has been replaced by dT in the S1 sequence. Moreover, the DNA version of S1 was included in this study and S1 with eight EdUs was used as a positive control. The method was described in **section 5.2.7.3.1.2**. As a brief overview, 47.8 nM of ATTO 647 N clicked S1, and its variants were incubated with PC-3 cells for 45 minutes. After that, the cells were washed three times, and the fluorescence of the bound clickmer was measured using flow cytometry. As a result, the fluorescence was dramatically decreased when EdU was substituted in the positions 11, 13, 36 and 38. Conversely, there was no decrease in the fluorescence with EdU substituted in the positions 5, 6, and 37. Furthermore, the substitution in position 42 had an slightly negative effect in binding but was not similar to the previous position, as shown in **Figure 3.19**. To evaluate the EdU substitution study, it was necessary to test more variants.

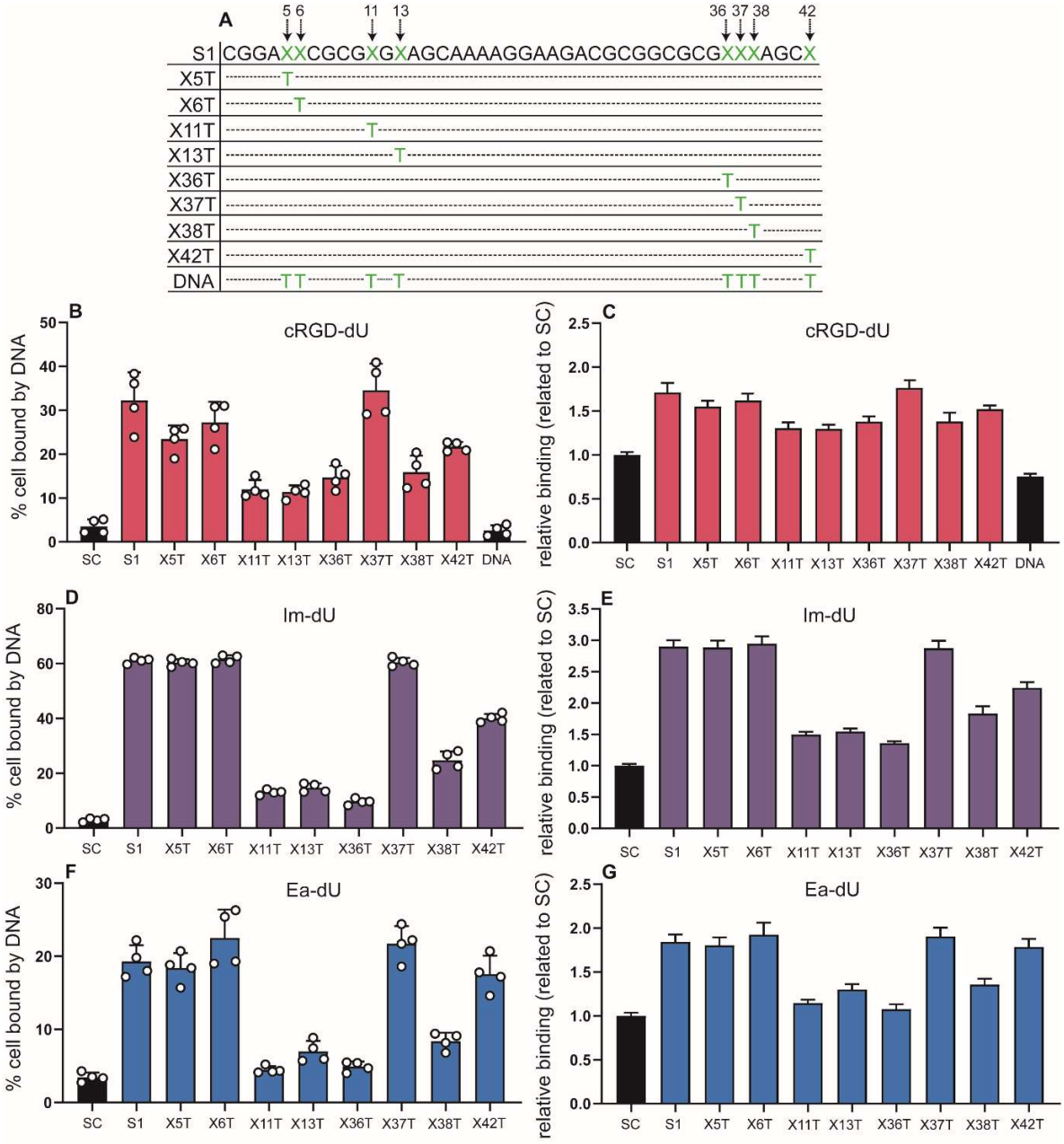

Figure 3.19 The substitution of EdU with Ts for S1 assessment
The diagram in **(A)** shows the eight S1 variants used in this study and the S1 as DNA. To evaluate the interaction of these variants with PC-3 cells, 48.7 nM of Atto 647N 43abelled S1 or the variants were incubated with the cells, washed and scraped, and their fluorescence was measured using flow cytometry. The experiment was performed twice in duplicate, and 20 thousand events were measured. **(B, C, D, E, F, and G)** show the results of the interaction study of S1 variants with PC-3 cells. In **(B-C)**, S1, S1 SC, or variants were clicked with cRGD (cRGD-dU), in **(D-E)**, they were clicked with imidazole (im-dU), and in **(F-G)**, they were clicked with ethanamine (Ea-dU).

Four variants of S1 were designed to confirm the results from the EdU substitution study. S1.5 contained 5 EdUs at positions: 11, 13, 36, 38, and 42. S1.4 had 4 EdUs at places: 11, 13, 36, and 38. S1.3 contained 3 EdUs at positions: 13, 38, and 42. S1.2 contained 2 EdUs at positions: 13 and 38, as shown in **Figure 3.20**. The binding was tested via flow cytometry. The study included S1 with 8 EdUs as a positive control and S1 SC with 8 EdUs as a negative control, both with the exact same concentration and incubation time used in the previous EdU study. S1, S1.5, and S1.4 exhibited

comparable binding behavior to PC-3 cells when attached to imidazole and ethanamine. However, there was a reduction in binding for S1 when it was attached to cRGD, when compared to S1. All the binding data can be found in figure 3.20. The next phase is to shorten the aptamer to the smallest version to lower the expense of the S1 aptamer for future use.

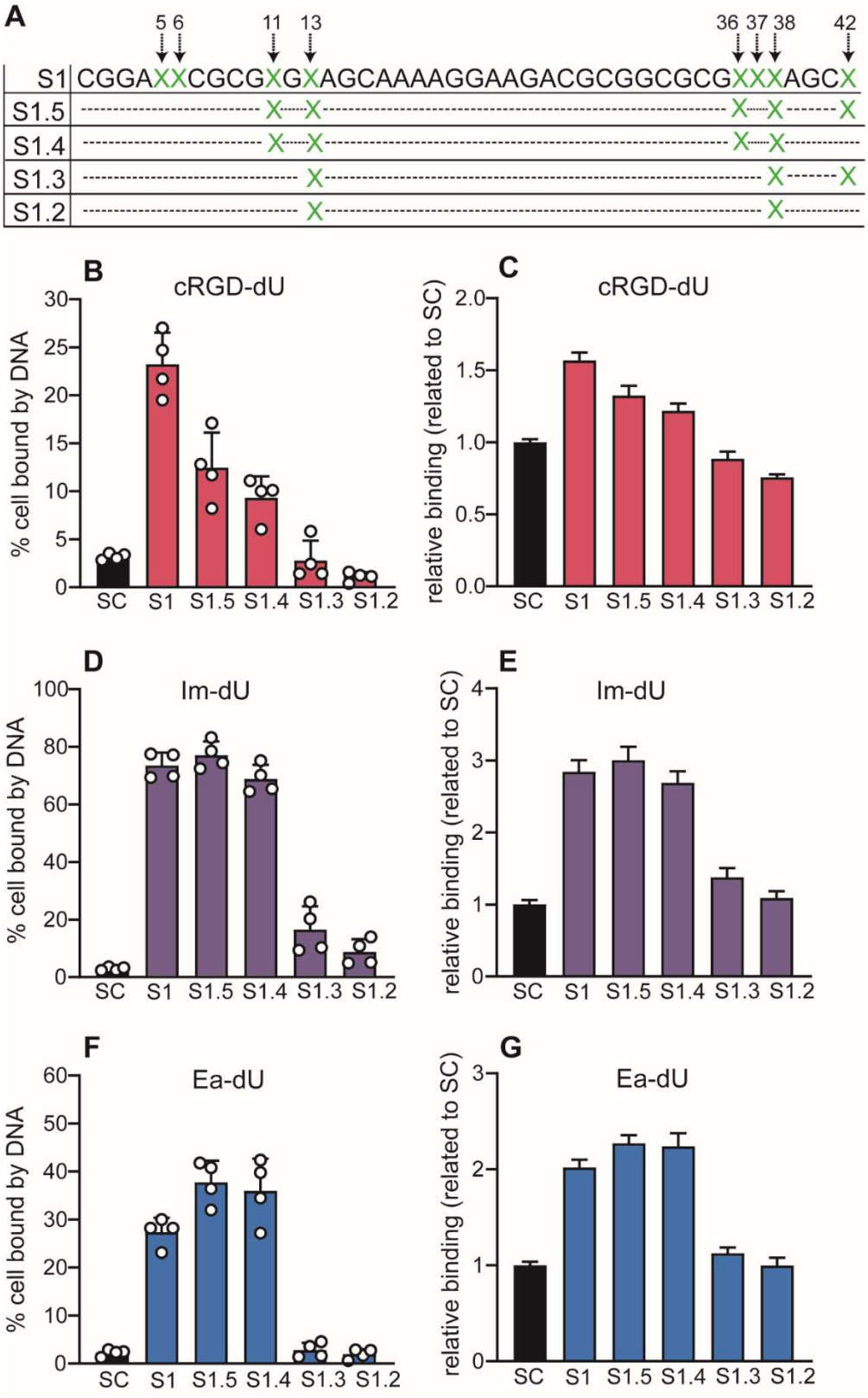

Figure 3.20 Presents an experiment that tested four S1 variants with fewer EdUs (S1.5, S1.4, S1.3, and S1.2) against PC-3 cells.

The diagram in **(A)** shows variants with fewer EdUs. To analyze their interaction with PC-3 cells, 48.7 nM of the labeled S1 or its variants were incubated with the cells, and the fluorescence was assessed using flow cytometry. The experiment was performed twice in duplicate, and 20 thousand events were measured. The interaction analysis results are presented in **(B, C, D, E, F, and G)**. The S1 and its variants in **(B-C)** were clicked with cRGD (cRGD-dU), in **(D-E)** they were clicked with imidazole (Im-dU), and in **(F-G)**, they were clicked with ethanamine (Ea-dU).

3.4.6 Truncation study of S1 clickmer

Truncation of aptamers refers to the removal of one or more nucleotides from the 5' or 3' end of the original aptamer sequence to generate shorter variants. The most effective way to reduce the cost of the S1 aptamer for future applications may be to remove the primer binding sites from the S1 sequence, as there were no EdUs in the primer binding sites, resulting in the creation of S1.42. After that, the secondary structure of the S1.42 was predicted using mfold as shown in **Figure 3.21**. Based on the secondary structure prediction, three more variants were designed; S1.36, which had six nucleotides less than S1.42 from the 5'- end, S1.35, which had one nucleotide less than S1.36 from the 3'-end, and S1.33, which had two additional nucleotides removed from the 5'-end. The binding intensity of the truncated version was evaluated using the protocol in **section 5.2.7.3.1.2.** S1.42 showed a higher binding intensity than the original S1 as shown in **Figure 3.21**. On the other hand, the other version showed a reduced binding intensity compared to the S1 clickmer.

To investigate the efficiency of the click reaction and to confirm the presence of the clicked-in moieties in the S1 sequence, the clicked-in S1, point mutant S1, S1 with a lower amount of EdU, and the truncated version analyzed using MS. It should be noted that the clicked-in azides have a distinct mass, as shown in **Table 3.1** and **Figure 6.13**. For this evaluation, only two types of azides were used: Imidazole (Im-dU) and cRGD (cRGD-dU).

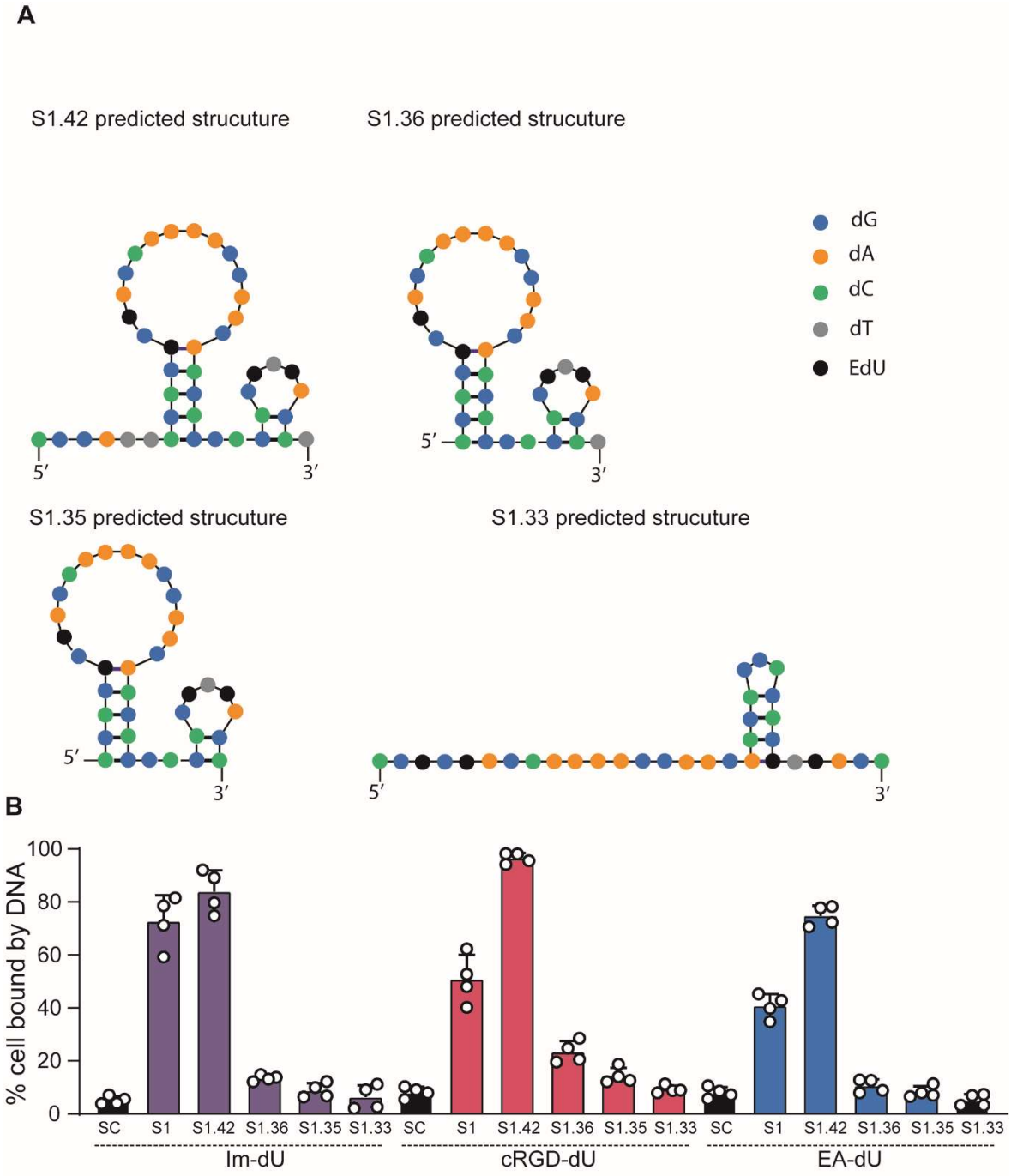

Figure 3.21 The truncation study of S1 clickmer.
The secondary structure prediction of four truncated versions of S1 (S1.42, S1.36, S1.35, and S1.33) is predicted using mfold. **(B)** Four shorter versions of S1 were designed and tested against PC-3 cells. To test their binding ability, PC-3 cells were incubated with 48.7 nM of either labeled S1 or its shorter versions, and the fluorescence was measured using flow cytometry. A total of 20 thousand events were recorded, and the experiments were performed twice in duplicate. The S1 and its truncated versions were clicked with different azides (imidazole (Im-dU), cyclic RGD (cRGD-dU), and ethanamine (Ea-dU)).

Table 3.1 the detected Masses of the S1 clickmer, point mutants, S1 with less EdU content, and truncated version of S1 clickmer.

Aptamer	Non-clicked		Clicked With imidazole (137.14 g/m)		Clicked With cRGD (629,7 g/m)	
	calculated	found	calculated	found	calculated	found
S1 (8 EdU)	26283	26284.24	27380.12	27381.22	31310.6	31337.06
X5T (7 EdU)	26273	26276.94	27232.98	27263.57	30680.9	30690.98
X6T (7 EdU)	26273	26276.94	27232.98	27250.11	30680.9	30698.75
X11T (7 EdU)	26273	26276.94	27232.98	27250,11	30680.9	30698.75
X13T (7 EdU)	26273	26276.94	27232.98	27264,7	30680.9	30682.80
X36T (7 EdU)	26273	26276.94	27232.98	27282.13	30680.9	30681.92
X37T (7 EdU)	26273	26276.94	27232.98	27233.16	30680.9	30696.54
X38T (7 EdU)	26273	26276.94	27232.98	27246.71	30680.9	30684.12
X42T (7 EdU)	26273	26276.94	27232.98	27243.69	30680.9	30679.58
S1.5 (5 EdU)	26253	26255.75	26938.7	26968.04	29401.5	29418.91
S1.4 (4 EdU)	26243	26246.33	26791.56	26793.83	28761.8	28766.40
S1.3 (3 EdU)	26223	26226.22	26497.28	26498.09	27482.4	27482.36
S1.2 (2 EdU)	26233	26243.40	26644.42	26646.82	28122.1	28158.15
S1.42 (4 EdU)	13891	13892.12	14439.56	14441.25	16409.8	16410.86
S1.36 (4 EdU)	12022	12022.54	12570.56	12571.67	14540.8	14541.46
S1.35 (4 EdU)	11718	11718.36	12266.56	12267.32	14236.8	14237.16
S1.33 (4 EdU)	11100	11099.84	11648.56	11648.82	13618.8	13618.96

3.5 Optimizing the pull-down assay using two DNA aptamers.

The pull-down assay was optimized using two DNA aptamers to develop a protocol that can later be used for S1 clickmer. These two aptamers were identified through cell-SELEX targeting BM-DCs [158]. They are known as DC-12 and D-7. They bound strongly to macrophages (J774A.1) as well as monocytes (THP-1) [159]. DNA aptamers were chosen as the optimal candidates for the optimization of the pull-down assay due to their ease of synthesis and cost-effectiveness.

3.5.1 Optimizing pull-down assay using DC-12 aptamer

3.5.1.1 Testing the binding of DC-12 at 4°C

The pull-down assay needs to be performed at 4°C because the enzymes present within the cells can be released into the supernatant during cell lysis, particularly proteases, which can degrade the aptamer's target. At 4°C, the protease activity is minimized, hence the assay can be carried out more effectively.[160]. The binding experiment was described in **section 5.2.7.3.2**. In brief, ATTO 647N labeled DC-12 was incubated with THP-1 cells for 10 minutes, followed by washing steps. The fluorescence was then detected by flow cytometry. To exclude non-specific fluorescence, Control-2 (Ctrl2) was included as a negative control. As shown in **Figure 3.22**. DC-12 had similar binding abilities to THP-1 cells at 4°C as at 37°C.

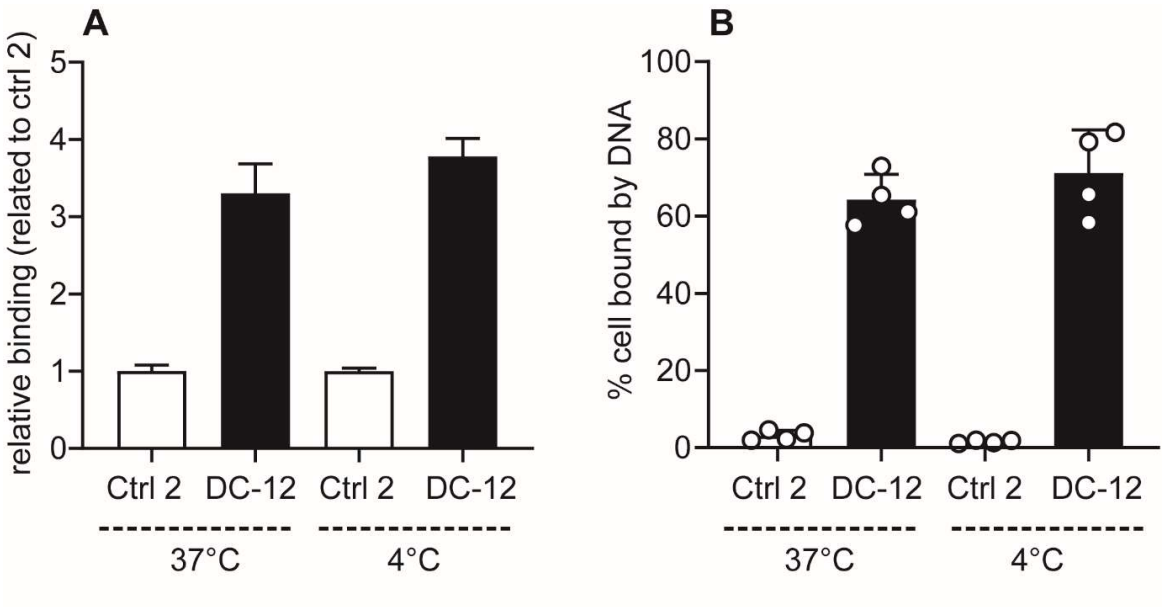

Figure 3.22 Interaction analysis of DC-12 at 37°C and 4°C against THP-1 cells.
250 nM of DC-12 or Ctrl 2 were incubated with THP-1 cells for 10 min. After washing 3 times, the fluorescence of the bound DC-12 or Ctrl 2 was detected by a flow cytometer (n=2, duplicated, mean ± SD). (A) relative binding, MFI (DC-12/Ctrl 2). (B) the percentage of cells bound by DC-12.

3.5.1.2 Binding evaluation of coupled DC-12 with streptavidin

Measuring the binding of the aptamer coupled with beads to THP-1 cells posed a challenge, therefore, streptavidin labelled with Alexa fluor 488 was used as an alternative model to beads. Biotinylated DC-12 has coupled to Alexa fluor 488 streptavidin, and the coupled aptamer was incubated with THP-1 cells. after washing, the fluorescence of the bound aptamer was measured via a flow cytometer. The method was described in **section 5.2.7.3.2.1**. Two negative controls were included in this experiment to evaluate the binding, SC1 (Scramble sequences 1) and SC2 (Scramble sequences 2). SC1 and SC2 were the scrambled sequences designed from DC-12, they had the same primer binding sites, but the variable region was randomized. **Figure 3.23** depicts the strong binding of DC-12 to THP-1 cells, confirming its ability to bind even after coupling with streptavidin.

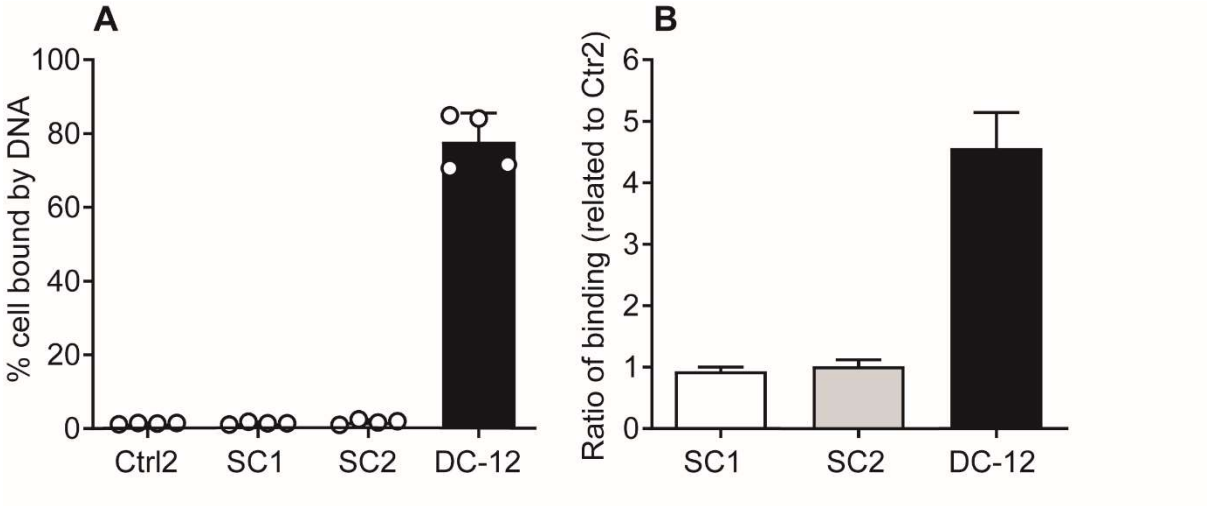

Figure 3.23 Shows the interaction of biotinylated DC-12 coupled with Alexa flour 488 labeled streptavidin. Different negative controls for DC-12 were included in the experiment, DC-12 SC 1 (SC 1), DC-12 SC 2 (SC 2), and a control aptamer (Ctrl 2), was first coupled with Alexa flour 488 labeled Streptavidin at a ratio of 1:1. Then, 250 nM of the coupled aptamers were incubated with THP-1 cells for 10 minutes. After washing the cells three times, the fluorescence of the bound aptamers was detected using flow cytometry (n=2, duplicated, mean ± SD). (A) the percentage of cells bound by DC-12. (B) relative binding, MFI (DC-12/Ctrl 2)

3.5.1.3 Pull-down assay using DC-12 aptamer

As DC-12 aptamers exhibited strong binding affinity towards THP-1 cells, the optimization of the pull-down assay was initiated using this aptamer. The method was described in detail in **section 5.2.8.1.4**. Briefly, the biotinylated DC-12 was first coupled to streptavidin beads, followed by several washing steps to remove the uncoupled aptamer, and then THP-1 cells were added to the coupled aptamer for 30 min. Afterward, several washing steps were conducted to wash the unbound cells. Subsequently, the cells were lysed, and additional washing steps were carried out to eliminate cellular debris and unbound proteins, while retaining the bound fraction for recovery. Finally, the recovered fraction was loaded onto a 10% SDS-PAGE gel, followed by staining with silver stain to visualize the separated proteins. Prior to initiating the pull-down assay, several parameters were evaluated. Firstly, the appropriate number of cells for the assay was determined by isolating membrane proteins from different cell quantities, ranging from 1.8 million to 50 thousand cells, and subjecting them to 10% SDS-PAGE followed by staining with Glutardialdehyde-silver or Blue-silver, as depicted in **Figure 6.12**. Based on the results, the silver stain was selected as the staining method due to its higher sensitivity compared to Blue-silver staining. Additionally, the cell number was determined to be 1.5 million cells for the pull-down assay, and the amount of aptamer used was adjusted accordingly. In the process of pull-down optimization, two types of streptavidin beads were employed: Dynabeads M-280 streptavidin and MagStrep type 3X beads, as illustrated in Figure 3.24. Dynabeads M-280 streptavidin was found more suitable for the pull-down assay. Finally, two elution methods were used during the optimization of the pull-down assay: heat elution (10 min at 95°C) or elution with urea (5 M or 8 M), as shown in **Figure 3.24** and **Figure 6.12**. Moreover, elution with heat was

performed after urea elution to show the non-specific proteins that stick to the beads during the pull-down assay, as shown in **Figure 3.24**. The optimal settings for the DC-12 aptamer were found to be 1.5 million THP-1 cells, 100 pmol of DC-12, and elution with urea. Negative control (Ctrl2) was also included to remove non-specific bands.

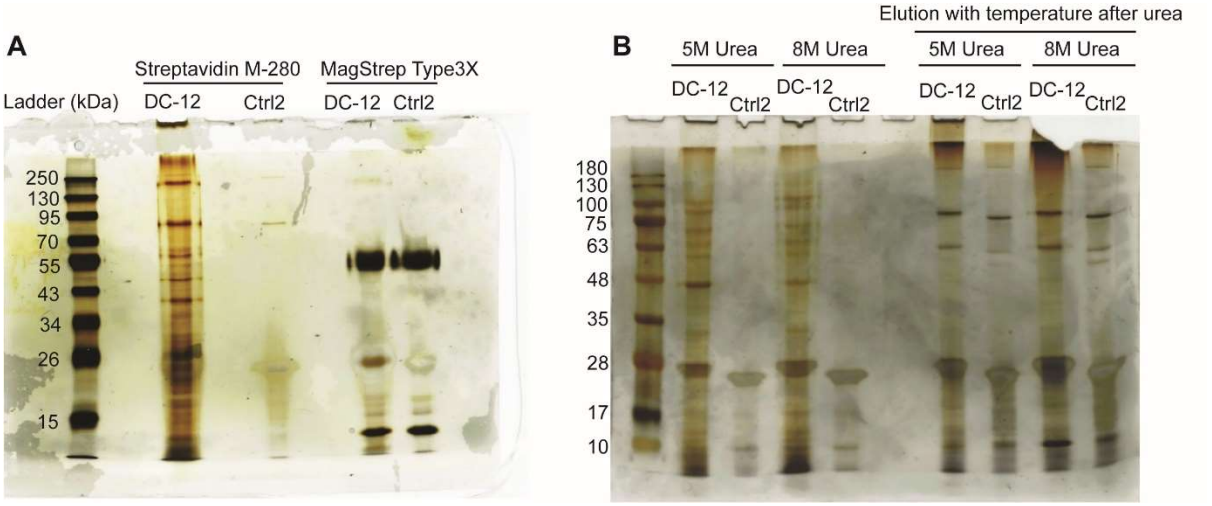

Figure 3.24 Silver stain for 10% SDS-PAGE page of the capture proteins.
(A) The pull-down assay was performed using two different types of beads: Dynabeads M-280 Streptavidin and MagStep Type 3 X beads. Biotinylated DC-12 coupled with the different beads was incubated with 1.5 million THP-1 cells, and after washing and cell lysis, the protein complex was recovered with temperature. The experiment was repeated twice, independent experiments. **(B)** Pull-down assay, 100 Pmol of DC-12 or control 2 was coupled with Dynabeads M-280 Streptavidin, and then the coupled aptamer was incubated with 1.5 million of THP-1 cells after washing and cell lysis. The protein complex was recovered with 5 M or 8 M urea at 37°C. followed by another elution with temperature (10 min at 95°C) (n = 2 independent experiments).

3.5.1.4 Test the interaction between DC-12 and different cell lines

The binding of DC-12 to various cell lines, including Jurkat, Raji, PC-3, and HeLla cells, was assessed to incorporate a control cell line into the pull-down experiment. The experimental approach was explained in **section 5.2.7.3.2.2**. In brief, biotinylated DC-12 has coupled with Alexa Fluor 488 streptavidin and subsequently incubated with the cell lines for a period of 10 minutes. Following washing, the fluorescence of the bound aptamer was measured using a flow cytometer. Negative controls SC1, SC2, and G24A were utilized for Raji and Jurkat cells, respectively. Results depicted

in **Figures 3.25** and **3.26** demonstrate that DC-12 displayed binding to all tested cell lines.

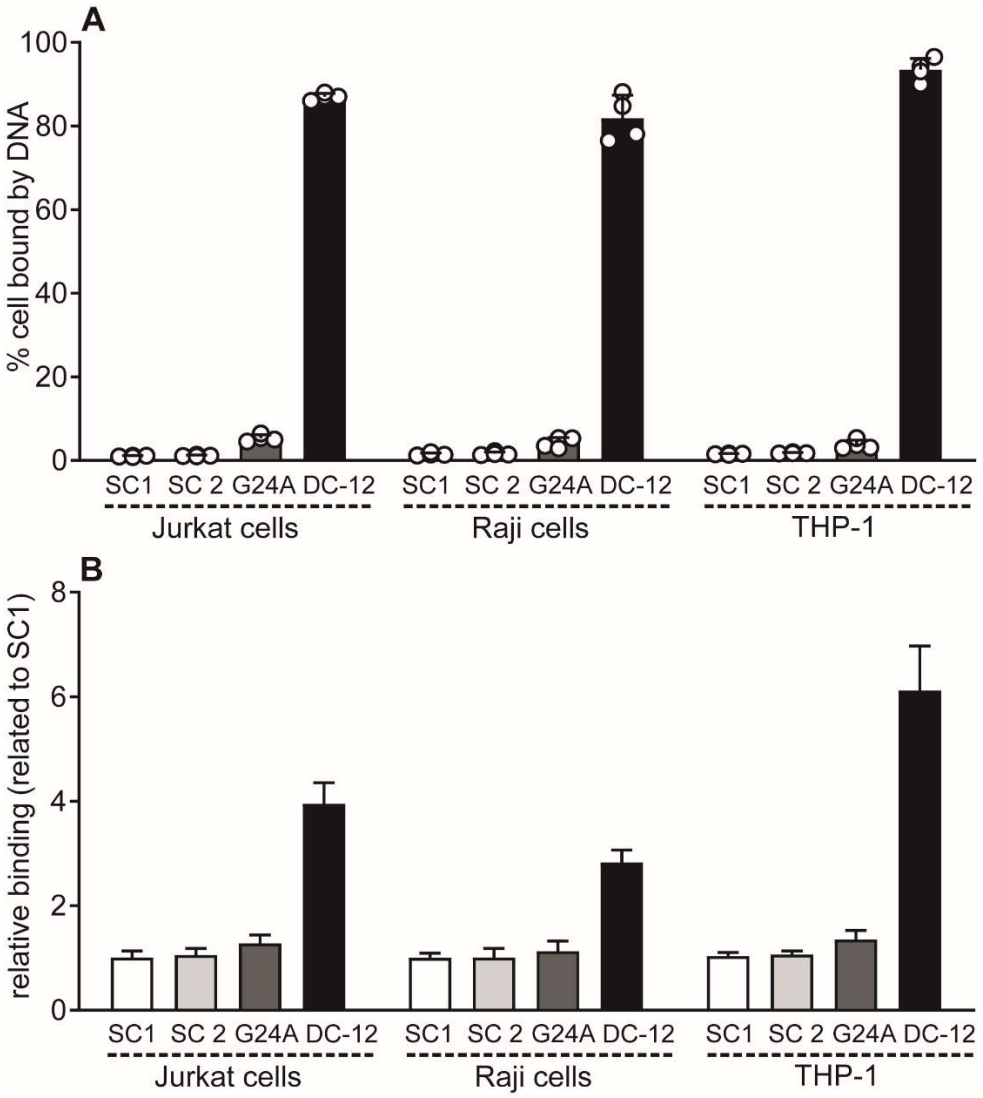

Figure 3.25 Shows the specificity determination of DC-12 with Jukart and Raji cells, with THP-1 cells included as a positive control.
Biotinylated DC-12, DC-12 SC1, DC-12 SC2, and G24A were coupled with 488 labeled streptavidin at a ratio of 1:1. After coupling, 250 nM of the coupled aptamers were incubated with the cells for 10 minutes. The cells were then washed three times, and the fluorescence was measured using FCAS Canto II. The experiment was repeated twice and presented as duplicates and standard deviation (n=2, duplicated, mean ± SD). The percentage of cells bound by DC-12 and the relative binding, as measured by the mean fluorescence intensity (MFI) of DC-12 compared to Ctrl 2, are shown in (A) and (B), respectively.

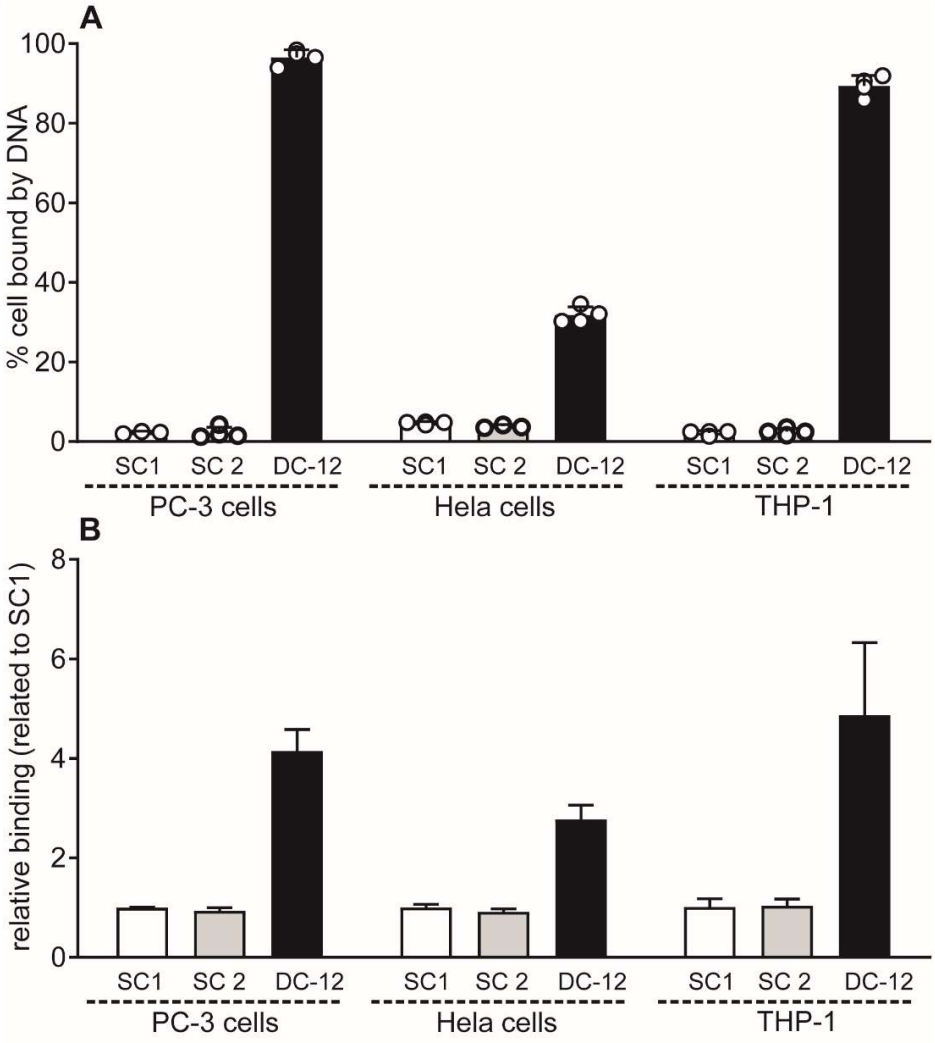

Figure 3.26 Shows the specificity of DC-12 with PC-3 and HeLa cells, and THP-1 cells were used as a positive control. Biotinylated DC-12, DC-12 SC1 (SC1), and DC-12 SC2 (SC2) were coupled with Alexa flour 488 labeled streptavidin at a ratio of 1:1. The coupled aptamers were then incubated with the cells for 10 minutes, washed three times, and the fluorescence was measured using FCAS Canto II. The experiment was duplicated twice, and the mean and standard deviation were calculated. **(A)** shows the percentage of cells bound by DC-12, while **(B)** shows the relative binding, MFI (DC-12/Ctrl 2)

3.5.2 Optimizing pull-down assay using D-7 aptamer

3.5.2.1 Binding of the biotinylated version of D-7

The competition assay between a labeled aptamer and a biotinylated aptamer is a highly specific method employed to investigate the interaction between the two aptamers and the target cell. The labeled and biotinylated aptamer competes for binding to one cell surface target. The protocol was described in **section 5.2.7.3.3.2.** In this study, the biotin was coupled to D-7 with different linkers: C6, C18 at the 5' end and with a C6 linker at 3' end. Furthermore, D-7 was labeled with ATTO 647N, and the competition assay was performed in different ratios, as shown in **Figure 3.27**. As a positive control, non-biotinylated D-7 was included in the experiment and Ctrl 2 was included as a negative control. All D-7 variants were competing with the labeled D-7, as shown in **Figure 3.27.**

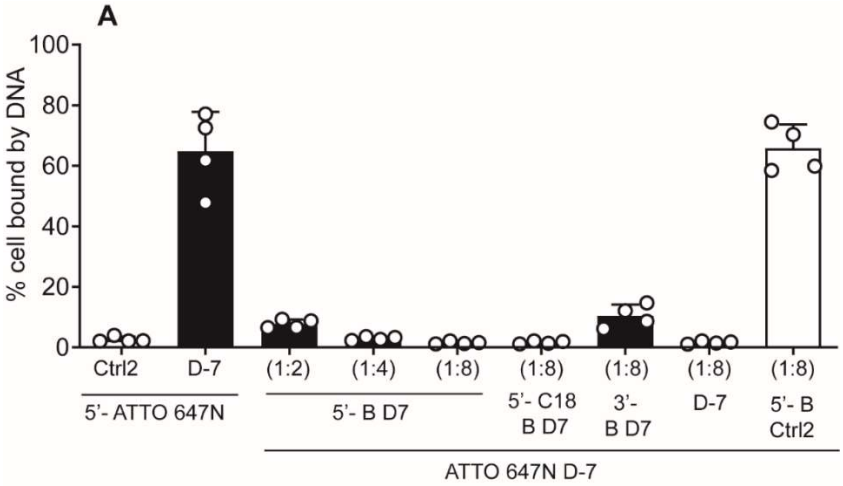

Figure 3.27 Shows the evaluation of the interaction between different biotinylated versions of D-7 and J774A.1 cells. Three types of biotin linkers were used: C6 at the 5' end (5'-B D7), C18 at the 5' end (5'-C18 B D7), and C6 at the 3' end (3'-B D7). The experiment involved incubating 250 nM of ATTO 647n D-7 with J774A.1 cells for 10 minutes, followed by washing and detection of the fluorescence of bound D-7 using FACS Canto II. The biotinylated versions of D-7 were added as competitors to evaluate if there was any competition between the labeled D-7 and biotinylated versions. (5'-B D7) was added in different ratios (1:2, 1:4, 1:8 labeled: biotinylated), whereas (5'-C18 B D7) and (3'-B D7) were used only at a 1:8 ratio. D-7 without linkers or biotin was also included as a positive control, while 5'-biotinylated Ctrl 2 was included as a negative control. The experiment was performed in duplicate (n=2) and mean ± SD were reported.

3.5.2.2 Inhibit the internalization of D-7

D-7 was found to internalize into J774A1 cells, and in order to hinder the internalization, two different internalization inhibitors, namely Dynasore and Genistein, were utilized. Dynasore, a small molecule inhibitor of dynamin, has the capacity to impede the internalization of aptamers through clathrin-mediated endocytosis [161]. Moreover, Genistein can inhibit the internalization of molecules by inhibiting tyrosine kinases involved in endocytosis pathways. Studies have shown that Genistein can inhibit clathrin-mediated endocytosis and caveolae-mediated endocytosis, two mechanisms involved in aptamer internalization [162]. In this study, Dynasore and Genistein were used to inhibit the internalization of D-7 aptamer at different temperatures; 4°C and 37°C. As shown in **Figure 3.28**. the internalization of D-7 was inhibited using Dynasore at 4°C.

A

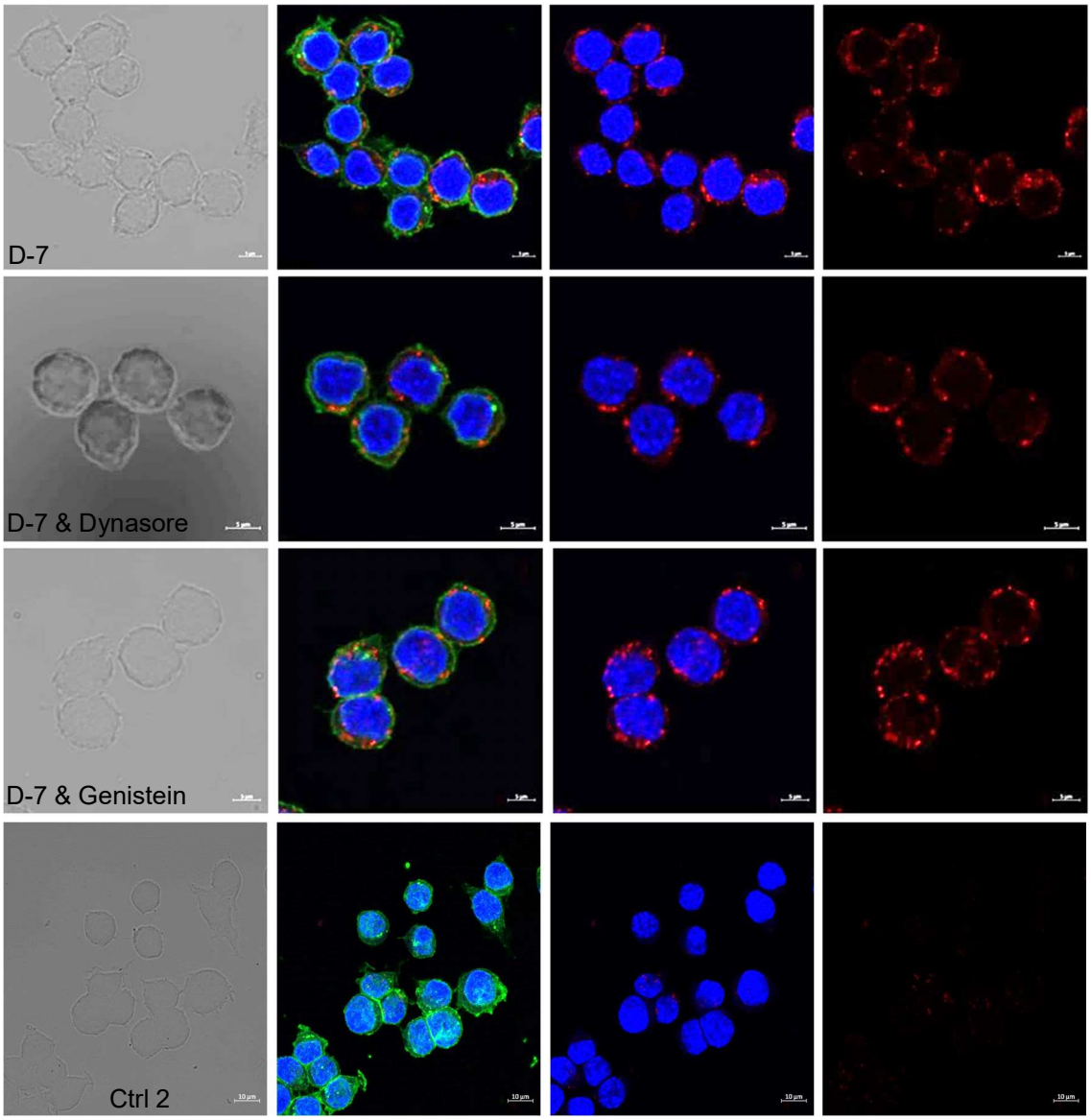

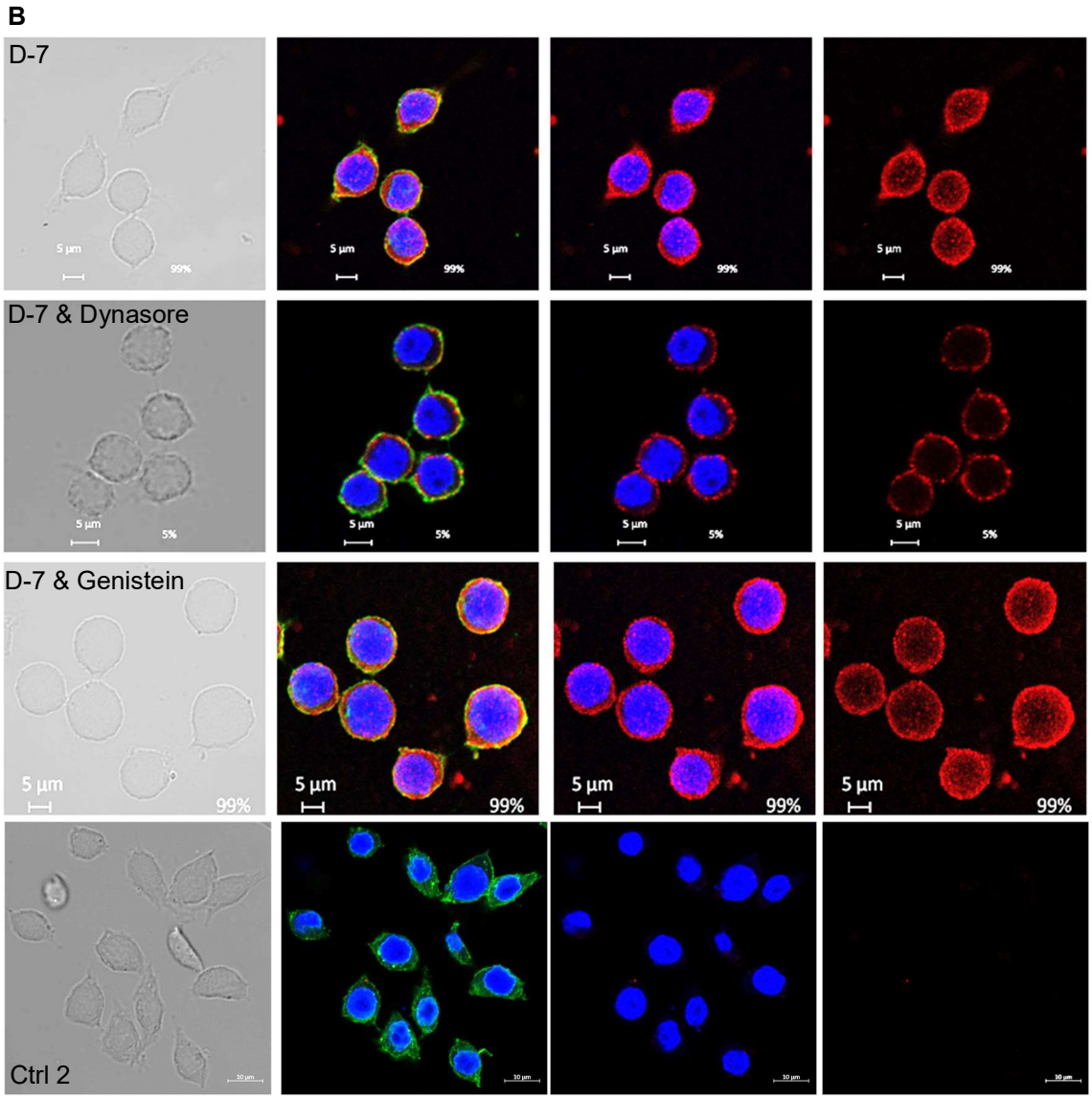

Figure 3.28 Cellular internalization inhibition of D-7 against J774A.1 cells. Figure 3.32. Cellular internalization inhibition of D-7 against J774A.1 cells.
The cells were treated with either 100uM of Dynasore, 160uM Genistein, or washing buffer. After that, they were incubated with 250nM of ATTO 647N D-7 for 10 min at 37°C, followed by fixation and co-staining with the membrane marker wheat germ agglutinin-Alexa Fluor 488 and the nuclear marker DAPI. **(A)** the experiment was performed at 37°C **(B)** the experiment was performed at 4°C. Confocal microscopy was used to evaluate the results, and the percentage of internalization was calculated based on 157 different cells. The results showed that internalization was not inhibited in the presence of dynasore at 37°C, Genistein at 37°C, or 4°C

3.5.2.3 Optimizing pull-down assay using D-7 aptamer

To identify the true target of J774A1 cells, an aptamer-based pull-down assay was employed. The method was described in **section 5.2.8.2**. Briefly, J774A.1 cells were first treated with Dynasore for 30 min, followed by incubation of biotinylated D-7 for 10 min. After that, the cells were washed, detached by scraping and Dynabeads M-280 Streptavidin was added to capture the bound aptamer. Afterward, the cells were lyzed and more washing steps were applied to remove the cell debris and unbound proteins. Finally, the bound fraction was eluted with temperature, loaded on 10% SDS-

PAGE gel, and after electrophoresis, the gel was stained with silver stain. As shown in **Figure 3.29**, there were no bands appeared on the SDS-PAGE gel.

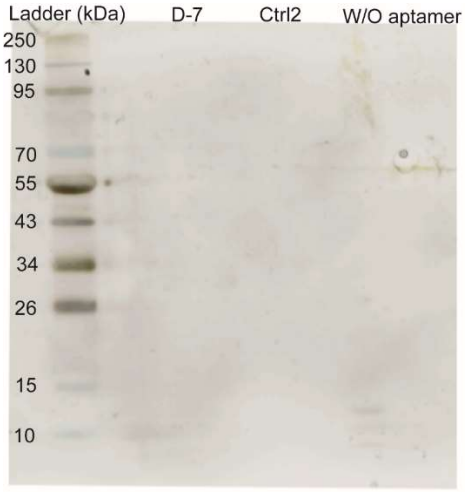

Figure 3.29 Pull-down assay of D-7 with J774A1 cells
The cells were teated with Dynasore at a concentration of 100uM for 30 minutes at a temperature of 4°C. Next, 100pmol of biotinylated D-7 was introduced to the cells for 10 minutes at 4°C. The cells were then scraped and collected, and Streptavidin beads were utilized to capture the attached aptamer. After multiple washes, the attached proteins were eluted by heating the sample. The eluted proteins were separated via electrophoresis on an SDS-PAGE gel, which was then stained with silver stain. This process was repeated twice independently.

3.5.2.4 Binding evaluation of coupled D-7 with labeled Streptavidin

To evaluate the binding of the coupled aptamer with J774A.1 cells, a streptavidin-labeled Alexa Fluor 488 was used as an alternative model to beads. The experimental procedure is described in **section 5.2.7.3.3.1**. First, the biotinylated aptamer was coupled with Alexa Fluor 488 Streptavidin. Next, the coupled aptamer was incubated with J774A.1 cells, followed by washing, and the fluorescence was measured using flow cytometry. However, as depicted in **Figure 3.30**, the coupled aptamer did not bind to the J774A.1 cell.

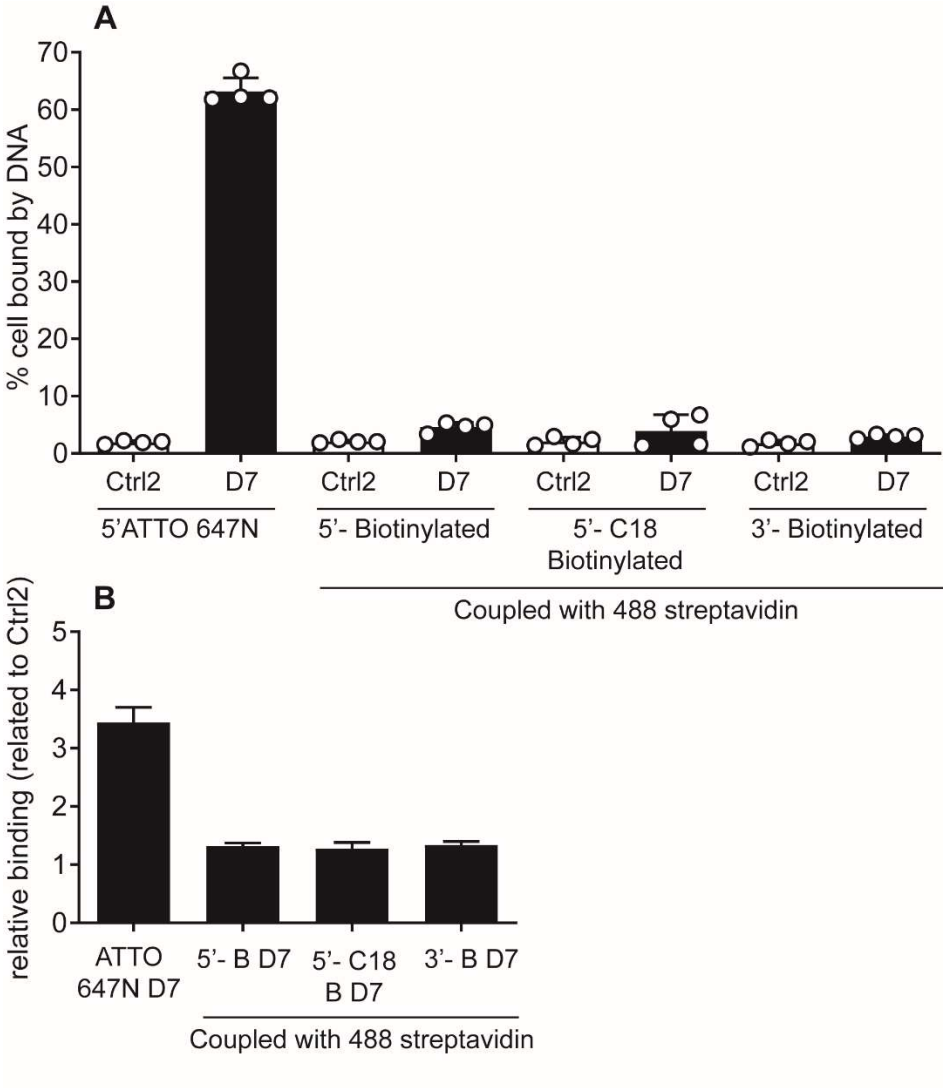

Figure 3.30 Interaction study between coupled D-7 with 488 streptavidin with J774A.1 cells.
Biotinylated D-7 with different linkers C18 or C6 was coupled first with 488 streptavidin for 30 min. After that, the coupled D-7 was incubated with J774A.1 cells for 10 min. Followed by, three washing steps were performed to wash the unbound aptamer and the fluorescence was detected using FCAS Canto II. (n=2, duplicated, mean ± SD). **(A)** the percentage of cells bound by D-7. **(B)** relative binding, MFI (D-7/Ctrl 2).

3.6 Optimizing pull-down assay for S1 aptamer

After performing the first two optimizations on DC-12 and D-7 aptamers (**described in section 3.5**), the optimization of the pull-down assay for S1 clickmer was initiated. Prior to the optimization process, experiments were conducted to evaluate the binding of biotinylated aptamer coupled with labeled streptavidin, as well as binding at 4°C. As the pull-down method utilizing DC-12 demonstrated promising results, this approach was selected for the S1 clickmer.

3.6.1 Binding evaluation of coupled S1 clickmer with labeled Streptavidin

Streptavidin was utilized as a control to evaluate whether the clickmer, once coupled, could still bind to PC-3 cells, or whether the coupling procedure resulted in structural conformational changes in the S1 clickmer. Details regarding the binding experiment are presented in **section 5.2.7.3.1.7**. The findings demonstrated that S1 and S1.4, clicked with imidazole (Im-dU) or cRGD (cRGD-dU), retained the ability to bind to PC-3 cells, while no binding was observed when S1 and S1.4 were clicked with ethanamine (Ea-dU), as illustrated in **Figure 3.31**.

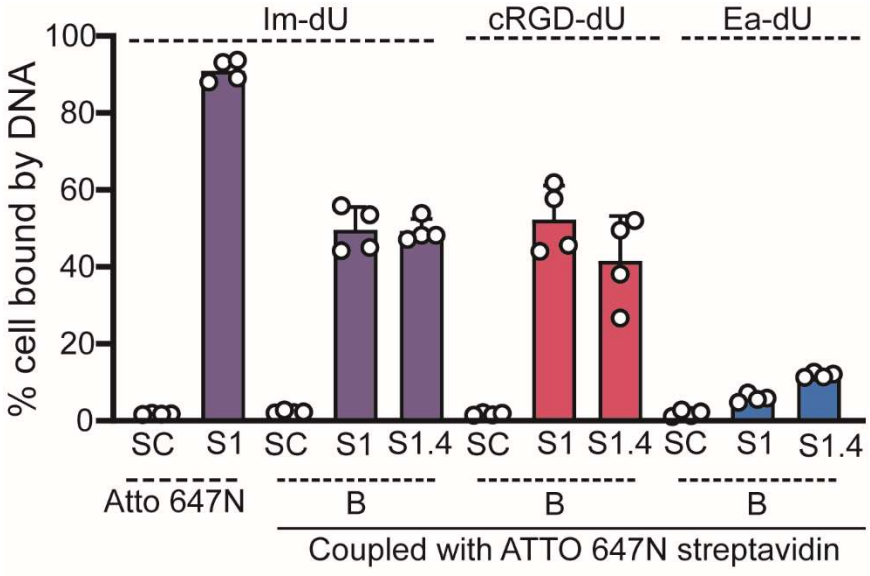

Figure 3.31 An interaction study between S1 clickmer coupled with ATTO 647N streptavidin with PC-3 cells. Biotinylated S1 was clicked with imidazole (Im-dU), cRGD (cRGD-dU), or athanamine (Ea-dU), and then coupled with ATTO 647N streptavidin for 30 minutes. The coupled S1 was then incubated with PC-3 cells for 45 minutes, and after 3 washing steps, the fluorescence was detected using flow cytometry. the percentage of cells bound by S1 is displayed on the graph. SC clicked with imidazole (Im-dU), cRGD (cRGD-dU), or ethanamine (Ea-dU) was included in the experiment as a negative control, while S1 clicked with imidazole (Im-dU) and directly labeled with ATTO 647N was included as a positive control. The experiment was conducted in duplicate (n=2, duplicated, mean ± SD).

3.6.2 Testing the binding of S1 clickmer under 4°C

An experiment was performed at a temperature of 4°C to evaluate the binding of S1 clickmer to PC-3 cells, as outlined in Section 5.2.7.3.1.6. The findings revealed that S1 and its truncated form, S1.42, exhibited binding to PC-3 cells when clicked with imidazole (Im-dU) or cRGD (cRGD-dU). However, S1.33 did not display any binding to PC-3 cells at 4°C, as depicted in **Figure 3.32**. In conclusion, the binding characteristics of S1 and its variants remained unchanged at different temperatures.

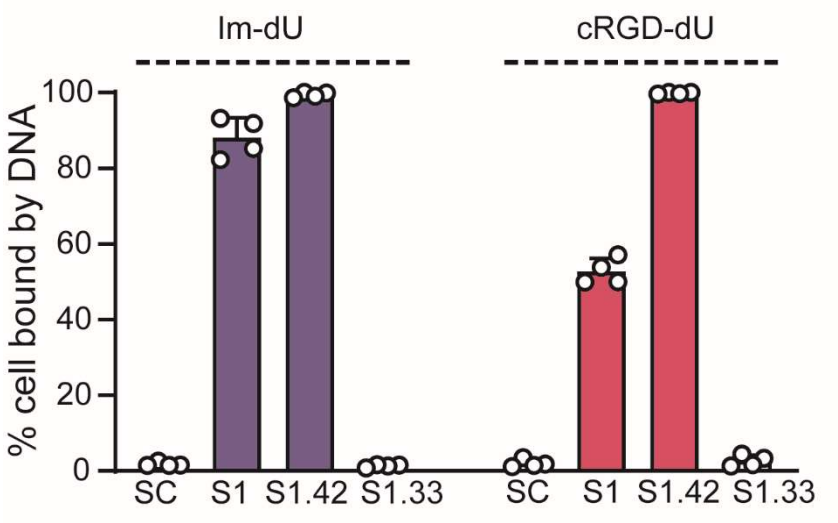

Figure 3.32 Illustrates the analysis of the interaction between S1 clickmer and PC-3 cells at a temperature of 4°C. Four different clickmers, S1, S1.42, S1.33, and SC, each clicked with imidazole or cRGD, were incubated with PC-3 cells for 45 minutes at a concentration of 48.7 nM. After washing the cells three times, the fluorescence of the bound clickmers was measured using flow cytometry. the percentage of cells bound by S1 is displayed on the graph. (n=2, duplicated, mean ± SD).

3.6.3 Optimization of Pull-down assay for S1 clickmer

DC-12 pull-down conditions were used with the following changes for the S1 clickmer pull-down assay; Firstly, 50 pmol of S1 clickmer was used in spite of 100 pmol, since increasing clickmer amounts could lead to more non-specific binding and elution of non-specific proteins. Furthermore, 1 million PC-3 cells were used, and the incubation time was extended to 45 min. Besides this, S1 clicked with ethanamine (Ea-dU) was excluded from the pull-down assay as the coupled clickmer with streptavidin did not bind to PC-3 cells (**see section 3.6.1**). the protocol was described in **section 5.2.8.3**. Accordingly, a pull-down assay was performed using S1 clicked with imidazole (Im-dU) or cRGD (cRGD-dU). As a result, a smear appeared on the gel even with the negative control (SC), as shown in **Figure 3.33 (A-B)**. A smear on the gel after a pull-down assay made identifying the target band challenging. The next step was to compare the eluted fraction from S1 clicked with imidazole (Im-dU) and cRGD (cRGD-dU). Furthermore, MCF-7 was included as negative cells for S1 clicked with imidazole (Im-dU) and other positive cells for S1 clicked with cRGD (cRGD-dU). As shown in **Figure 3.33 (C-F)**, S1 clicked with cRGD (cRGD-dU) showed more smear on gel than S1 clicked with imidazole (Im-dU) for both cell lines. As S1 clicked with imidazole (Im-dU) exhibited less smear, further optimization was conducted using this variant. The optimization process began by utilizing different amounts of S1 clicked with imidazole (Im-dU), specifically 5 pmol and 50 pmol. As shown in **Figure 3.34 (A-B)**, the smear was reduced using less amount of S1 clickmer, especially with the negative cell line (MCF-7). With 5 pmol, various cell amounts were evaluated, including 1 million, 500 thousand, and 100 thousand cells. As a result, using 100 thousand cells the conditions were stringent and only the non-specific bands appeared on the gel. The smear disappeared when

500 thousand cells were utilized, as evidenced in **Figure 3.34 (C-E)**. Moreover, decreasing the incubation time between the coupled clickmer to PC-3 cells could have a beneficial effect to decrease the smear that appeared on the gel after the pull-down assay. Furthermore, the incubation time was reduced to 10 minutes, and various amounts of clickmer (30, 20, and 10 pmol) were tested as shown in **Figure 3.35 (A)**. The results showed that 30 pmol of the clickmer was promising for further optimization. However, when the experiment was repeated with MCF-7 cells included (as shown in **Figure 3.35 B**), no significant difference was observed between S1 clicked with imidazole (Im-dU) and its negative control. Furthermore, the experiment also considered the effect of cell passage on the results. The assay was repeated using cells from both high and low passages, but no difference was observed between S1 and its negative control (SC), as depicted in **Figure 3.35 (C)**. To investigate the effect of varying incubation times on the binding of the coupled aptamer to PC-3 cells, different time points were tested, including 30, 20, and 10 minutes. 30 min showed a smear while 20 min showed less smear on the gel, as shown in **Figure 3.35 (D).** The last pull-down experiment was performed using 20 min, 30 pmol of S1 clickmer clicked with imidazole, and 500 thousand PC-3 and MCF-7 cells. As shown in **Figure 3.35 (E)**, the same bands were observed between S1 clicked with imidazole and its negative control. However, the bands observed with S1 were slightly sharper. The pull-down assay was optimized by testing different cell numbers, clickmer amounts, and incubation times, however, none of these variables produced a sharp positive result. Concludingly, this pull-down assay method might not be suitable for the S1 clickmer.

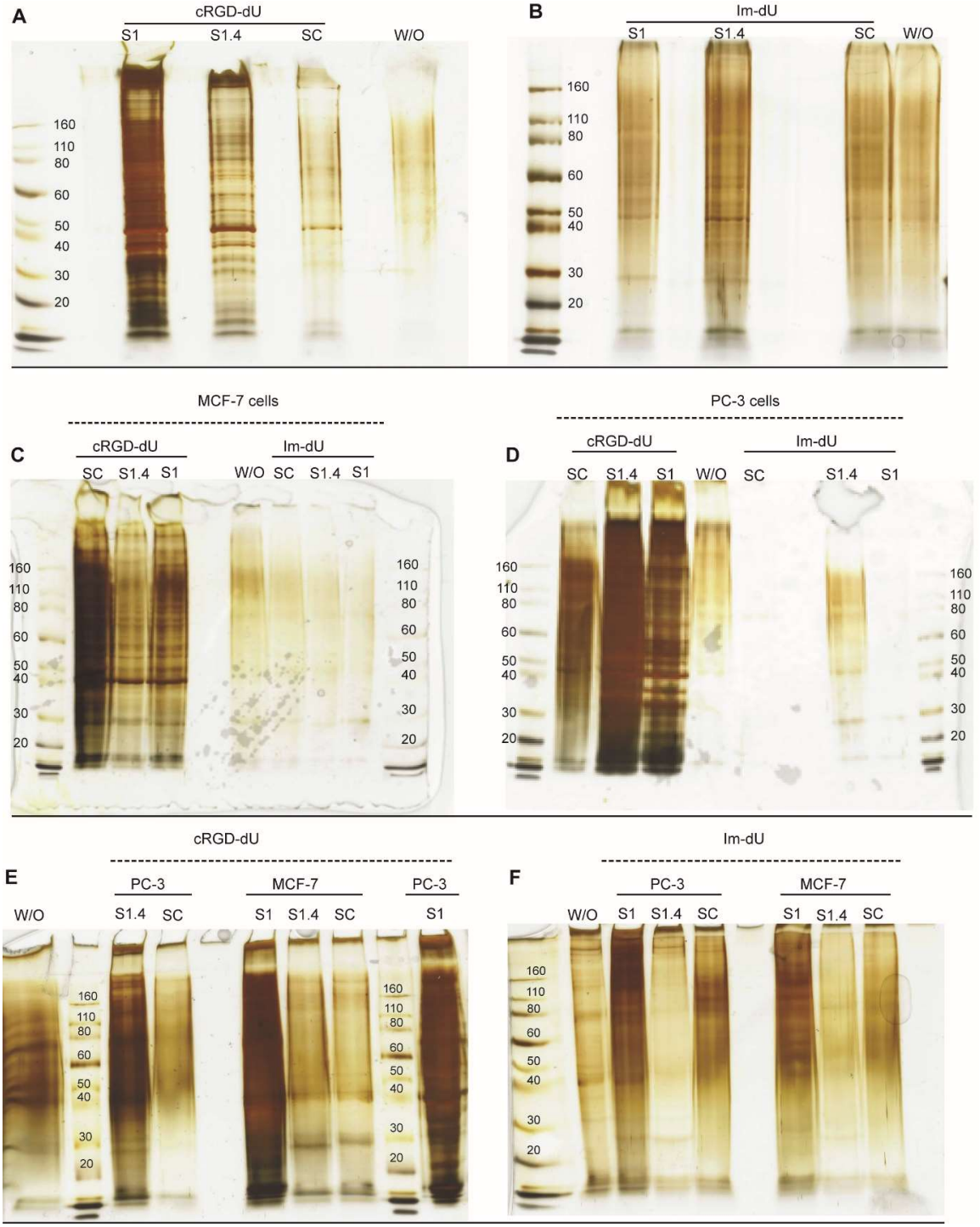

Figure 3.33 Proteins pulled from PC-3 or MCF-7 cells were visualized on an SDS-PAGE gel stained with silver. The aptamers used were S1, S1.4, and S1 SC clickmer clicked with imidazole (Im-dU) or cRGD (cRGD-dU), which were coupled to streptavidin beads. 1 million PC-3 or MCF-7 cells were incubated with the aptamer-bead conjugates for 45 min. After incubation, the cells were washed and lysed with 1% NP-40. By eluting the pulled proteins with urea were separated via electrophoresis on an SDS-PAGE gel and staining the gel with silver, the protein was visualized on SDS-PAGE gel. Different panels show the protein pulled from different cells using different aptamers (S1, S1.4, and S1 SC) clicked with imidazole (Im-dU) or cRGD (cRGD-dU).

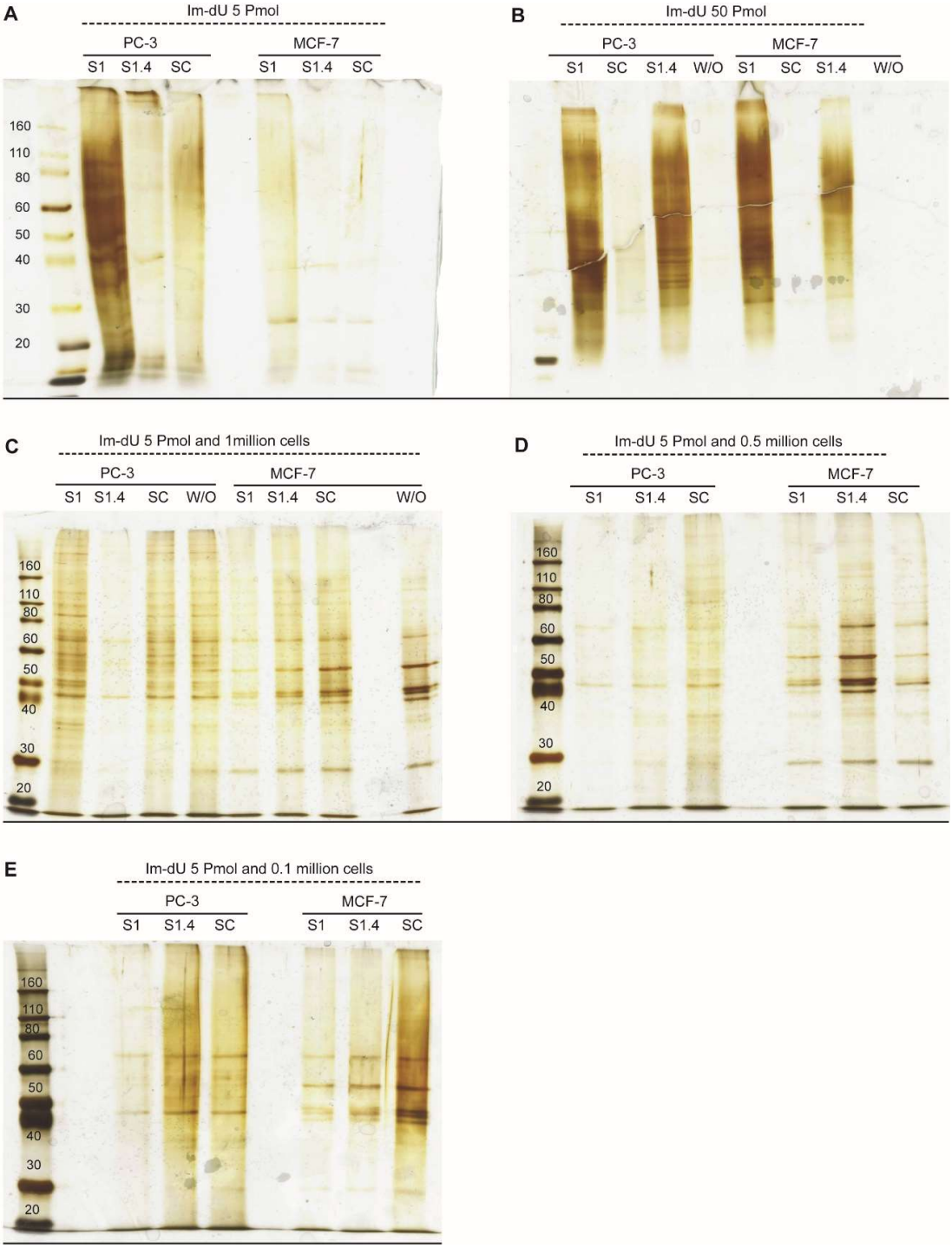

Figure 3.34 Optimization of the pull-down assays by varying the amount of S1 clickmer clicked with imidazole (Im-dU) and the number of cells used in the experiment.
The silver stain was used to visualize proteins pulled from PC-3 or MCF-7 cells. Specifically, **(A)** 5 pmol of S1 clickmer was used with one million cells, **(B)** 50 pmol of S1 clickmer was used with one million cells, **(C)** 5 pmol of S1 clickmer was used with one million cells, **(D)** 5 pmol of S1 clickmer was used with 500 thousand cells, and **(E)** 5 pmol of S1 clickmer was used with 100 thousand cells. After cell lysis and recovery of the pulled protein, the proteins were loaded and separated via electrophoresis on an SDS-PAGE gel and stained with silver stain.

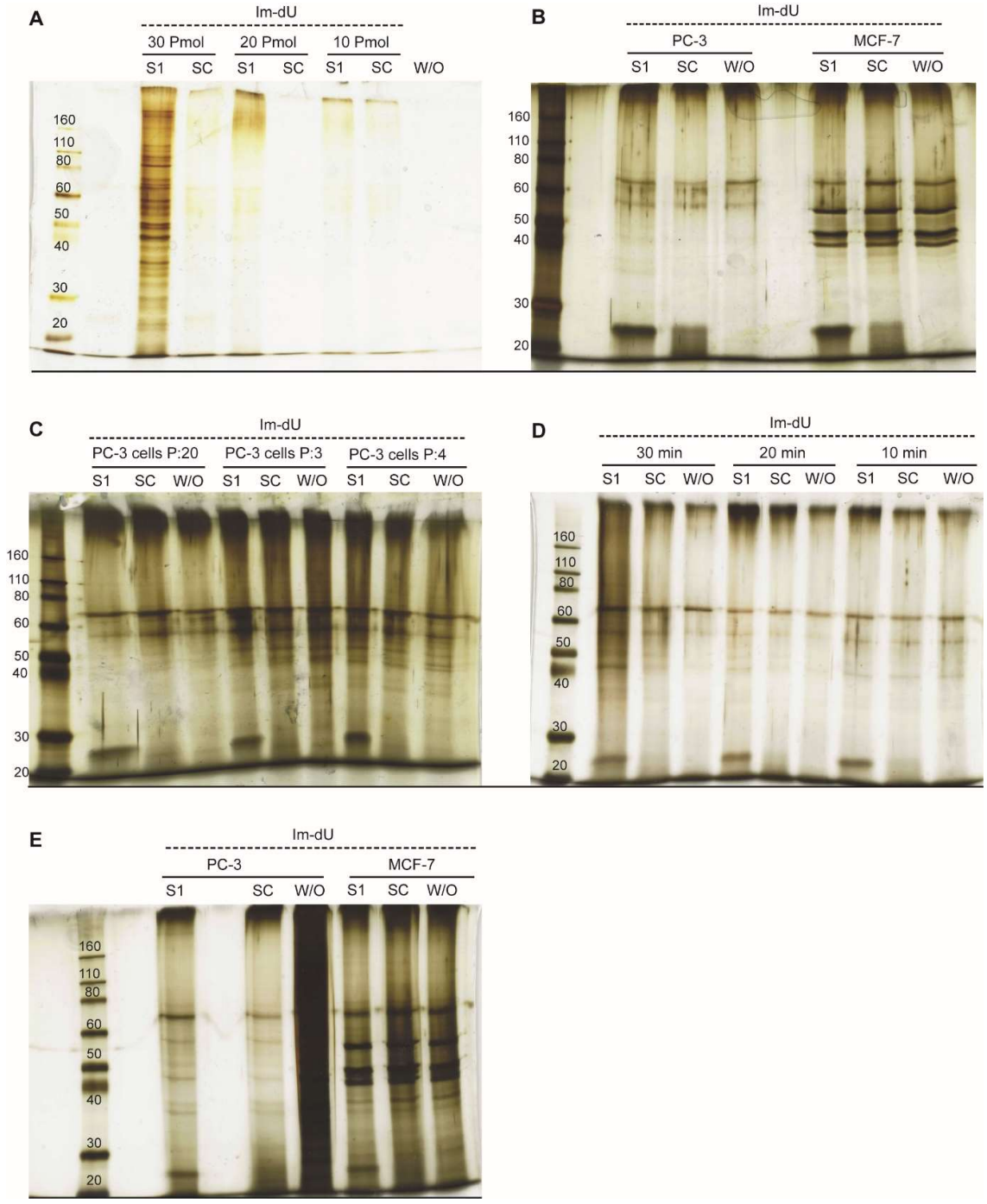

Figure 3.35 Shows the optimization of the pull-down assay by testing various factors.
(A), 30, 20, and 10 pmol of S1 clickmer were incubated with 500 thousand PC-3 cells for 10 minutes. The proteins were then pulled, loaded onto an SDS PAGE gel, and stained with silver stain. **(B)** 30 pmol of S1 clickmer incubated with either 500 thousand PC-3 or MCF-7 cells for 10 minutes, with the same protein pulling, gel loading, and staining process. **(C)** 30 pmol of S1 clickmer incubated with 500 thousand PC-3 cells from different passages, with the same protein pulling, gel loading, and staining process. **(D)** 500 thousand PC-3 cells incubated with 30 pmol of S1 clickmer at different time points (30, 20, and 10 minutes), with the same protein pulling, gel loading, and staining process. Finally, experiment **(E)** used 30 pmol of S1 clickmer incubated either PC-3 cells of MCF-7 for 20 min with the same protein pulling, gel loading and staining process.

4 DISCUSSION

4.1 Library design for split-combine cell SELEX

Standard SELEX libraries consist of 1 random region flanked by 2 primer binding sites. Previous studies have shown that primer binding sites should possess 40-60% GC content [163] [164]. To minimize non-specific primer annealing, three subsequent G or C residues near the 3′-end should be avoided. Likewise, primers with complementary intramolecular or intermolecular sequences should be avoided to minimize the formation of primer dimers [44]. Therefore, the primer binding sites in the M2 library had 60% GC content and were 20 nucleotides long. These primer binding sites were separated by a 42 nucleotides long random region. In addition, complementary primer sequences were avoided using IDT oligo analyzer software. Further, this M2 library was used [165] for the SARS-COV-2 spike protein aptamer selection resulting in the identification of two DNA aptamers [165]. Moreover, this M2 library was utilized for cell-SELEX, which identified some aptamer sequences that showed weak binding to PC-3 cells as shown in **section 5.3**.

To increase the diversity of an aptamer selection, the M2 Library was modified to Alkyne M2 Library, which contains 7 EdU in the random region that can be further modified by click chemistry. Previously, Siegl et al. had designed three different libraries. Three libraries with decreasing numbers of EdU in the random region, containing 9.3, 7, and 5.5 EdU, respectively, were constructed for selection against C3-GFP protein. The success of SELEX, at least for targeting C3-GFP, may be enhanced in some cases by increasing the level of modifications within the library. In contrast, amplification behaviour seems to be improved by reduced alkyne modifications [166]. In conclusion, bearing 7 EdU in the random region was beneficial for both selection and amplification.

To test the quality of alkyne-modified library synthesis, it was critical to evaluate the initial library with HPLC before performing the selection. As demonstrated in **Figure 3.3**, a thymidine contamination was detected in one of the solid-phase synthesized M2 alkyne library batch. This type of error in the synthesis could affect the selection; hence the alkyne-modified library must be verified before selection in addition to the published protocol [95]. It is highly recommended to test the functionality of the initial library by analysis of the unclicked starting library and clicked starting library on HPLC after nucleoside digestion.

The M2 library was initially designed for split-combine cell SELEX selection but was also used in one additional selection in our laboratory. The selection was performed against the SARS-COV-2 spike protein using the M2 library, as described in master thesis from the University of Bonn [200]. This led to the identification of a nucleobase-modified aptamer against the SARS-COV-2 spike protein. In conclusion, this library showed good amplification properties, as shown in **Figure 3.2**. More-

over, aptamers were selected using the M2 DNA library and clickmers (nucleobase-modified aptamers) from the alkyne-modified M2 library. The M2 library has been approved for use in our laboratory for further selection using either click SELEX or split-combine SELEX.

4.2 Implementation of ePCR in the split-combine method

Each enriched DNA library must be amplified correctly during SELEX to ensure the success of aptamer selection. In general, a DNA library with highly diversified sequences is usually used as a starting point for selection. The target-binding sequences within this pool are typically rare and unique, and each sequence should be amplified at the same rate after the target-partition step [167]. Conventional PCR has several drawbacks when used during the selection process. Conventional PCR produces by-products more frequently, but only a few publications address this issue. During conventional PCR, the primary sources of by-products are non-specific primer annealing and primer dimer formation [47, 48, 53]. Moreover, By-products may also be formed from product-product hybridization of the homologous sequences [47, 48, 53]. Aside from the formation of by-products in PCR, the formation of products is biased toward shorter sequences or structurally less stable sequences. These sequences match with the preference of the polymerase (PCR bias) [49] [51]. According to Levay et al., conventional PCR can reduce the diversity of a library by up to 50% within each PCR cycle, which can ultimately result in a loss of important variants and decrease the overall quality of the selected aptamer pool. [52].

A solution to this problem is to separate each sequence of the initial library into a droplet and then perform the amplification within the droplet. This method is known as emulsion PCR (ePCR) [54]. ePCR significantly reduces the PCR bias and by-product formation while preserving library diversity simultaneously [50]. Here, two formulas were used to optimize the ePCR for click SELEX. The difference between the two formulas is the oil phase composition and the ratio between the oil and aqueous phases. This is discussed in **section 3.1.3**. For the first formula, the oil phase in the first formula is based on tween 80, span 80, and mineral oil. The ratio between the oil and aqueous phases is (2:1) (oil phase: aqueous phase) [54]. For the second formula, the oil phase comprises TEGOSOFT, ABIL WE 09, and mineral oil. The ratio between the oil and aqueous phases is (4:1) (oil phase: aqueous phase). During the optimization and implementation of both formulas in the click-SELEX protocol, the first formula is less stable than the second formula. As demonstrated in **Figure 6.1**, the by-product was shown on the 4% gel after amplification of the M2 library. Using the second formula, the by-product disappeared, and one sharp band on the 4% agarose gel was observed, which reflected the PCR product, as shown in **Figure 3.3**. The observation that the first formula is less stable was reported in an article. [50]. After choosing the more stable formula, the amplification of the clicked library with imidazole (Im-dU), indole (In-dU), cyclic RGD (cRGD-dU), ethanamine (Ea-dU) and isobutyl (Ib-dU) was performed. As shown in **Figure 6.2**, amplifying the clicked library

is possible using the second formula. The five clicked libraries showed comparable amplification, and the clicked moiety did not impair the amplification process. This was the first step to implementing the ePCR into the SELEX protocol. The second step for implementation is to perform a click-SELEX using the ePCR. Since using the click-SELEX is expensive, a DNA cell-SELEX was performed first using ePCR; as shown in **Figure 3.6**, no by-product appeared after each ePCR amplification. 10 rounds were performed in this selection. Another two selections were performed using ePCR. The first one is the split-combine cell SELEX that was established herein. Another selection was performed using the split-combine SELEX approach against the SARS-COV-2 spike protein, as described in master thesis from the University of Bonn [200]. In both selections, no by-products appeared on the 4% agarose gel after ePCR amplification. All the amplified rounds for the split-combine cell SELEX are shown in **Figure 6.8**. Moreover, both selections had a strong enrichment after several rounds of selection. In split-combine cell SELEX, a strong enrichment was observed using imidazole (Im-dU), ethanamine (Ea-dU), and isobutyl (Ib-dU), as shown in **Figure 3.10**. Regarding the split-combine SELEX against SARS-COV-2, a strong enrichment appeared using Indole azide (In-dU). Conclusively, the selection of a nucleobase-modified aptamer is possible using ePCR as an amplification method.

4.3 Split-combine cell SELEX

A cell-based SELEX methodology (cell-SELEX), developed by Morris and Jensen [28], was the first method to select aptamers against complex mixtures of potential targets by using human red blood cell membranes as a target. An *in vitro* protocol was developed to isolate high-affinity aptamers specific to complex mixtures of targets. The aptamer is selected against an entire cell surface with cell-SELEX, representing molecular targets' natural folding structure. Additionally, cell-SELEX can be used to discover new biomarkers, particularly on cancer cell surfaces [25]. Even though cell-SELEX holds significant potential for biomedical applications, several technical limitations will need to be addressed. When selecting aptamers, it is crucial to consider the cell condition. Dead cells will take up oligonucleotides non-specifically during selection, resulting in a negative impact outcome. To overcome this problem, a fluorescence-activated cell sorting (FACS) method was developed by Raddatz et al. [37]. Using this technique, fluorescently labelled libraries are incubated with target cells. The separation of aptamer-bound cells is achieved using a FACS device, which is sensitive, efficient, and high-throughput. The bound aptamers are eluted, purified, and amplified for the next step. The selection process can also limit the selection of aptamers that bind non-specifically to target cells due to complex cell surface components. To overcome this problem, counter-selection steps can be added during the selection process to increase the specificity of the selected aptamers[38]. These are the main limitations regarding cell status. Still, for selecting aptamers, the starting library can be

improved to select better aptamers for the target cells. Added unnatural nucleotides to the starting library can enrich sequences that bind to target cells with a higher affinity [107]. Artificially amplified genetic information system (AEGIS) and cell-SELEX were combined for the first time by Sefa et al. [107]. This method is named AEGIS-SELEX. This method identified aptamers that bind to breast cancer cells with high affinity. Adding artificial nucleotides can be performed by incorporating modified nucleobases into the starting library. A study in 2021 selected aptamers bearing an aromatic ring (indole) modification at the 5-position of uracil against A549 lung cancer cells. [90]. The selected aptamers showed superior internalization to A549 cells over unmodified aptamers. Previous studies used only one type of nucleobase modification to select aptamer for the target cells By incorporating multiple modifications into the selection protocol, the success of the selection can be increased. Additionally, multiple modifications can be screened, and the most suitable modification can be chosen. In 2020, a protocol was published for selecting aptamers against C3-GFP using this approach. [99]. The starting library bearing EdUs was split into five equal parts. A click reaction is used to modify each part with one azide, and then it is combined with the other five parts to start the selection process. This method was dubbed split-combine SELEX. In this method, different azides are screened against the target of interest in one selection. Several parameters and controls were considered to implement this protocol in the cells-SELEX protocol—first, testing the success of the click reaction in each round for all the azides. Secondly, non-specific binding during the selection process should be minimized. Thirdly, an appropriate amplification method should be chosen to ensure all sequences have an equal chance of amplification during PCR. The fourth step is to select the most appropriate method for the elution of the bound fraction. In the end, compare the split-combine cell SELEX with DNA cell-SELEX to understand more about the enrichment process and the selected candidates.

Regarding the click reaction, testing the click reaction for the starting library and the subsequent rounds is impossible during selection [95]. To overcome this obstacle, single-strand DNA containing only one EdU was clicked in parallel with the starting library and the subsequent rounds. Using this control, the efficiency of the click reaction was verified by LC-MS during the selection process. The LC-MS data is illustrated in **Figure 6.4** and **Figure 3.9**. This control is further explained in **section 3.3**.

The inclusion of counter-selection is critical in the SELEX protocol, especially in cell-SELEX, to minimize the amount of non-specific binders [27]. Some researchers include more than one cell type in the counter-selection process to reduce non-specific binders and increase the specificity of selected aptamers. For example, Gao and his team [168] conducted a selection against PC-3 cells and used three cell lines (Hela, RWPE-1, and SMMC 7721) in the counter-selection step. The aptamer they selected (Wy-5a) demonstrated high specificity to PC-3 cells. In the split-combine cell SELEX protocol, two counter-selection steps were incorporated to enrich only specific binders. The first step

involved including LNCaP cells as non-target or negative cells to decrease the percentage of non-specific binders. The second type of counter-selection was developed for this protocol. This step removes most sequences that can bind to PC-3 cells without clicked-in moieties. To achieve this, the eluted fraction from round 1 was amplified using dNTPs without including EdUTP. The resulting product was then subjected to digestion and purification to obtain canonical single-stranded DNA. The single-stranded DNA was incubated again with PC-3 cells (target cells), and the unbound fraction was collected and purified for the next step. The SELEX protocol is explained in more detail in **Section 5.2.6.1**.

For the amplification method, ePCR was chosen to amplify the rounds. Using a complex library for selection could give many structural possibilities for the selected sequences. Some sequences could have a complex structure, making them undesired to amplify during PCR. Choosing an amplification method giving all the sequences the same chance to amplify could be beneficial to select better candidates. The implementation of ePCR was discussed in detail in **section 5.2**.

In this study, four extraction methods were examined. The first was centrifugation, the second was phenol-chloroform extraction, the third was NucleoSpin® Clean-Up (Macherey-Nagel), and the fourth was GE Healthcare's G-25 column. To achieve the most effective results, three different methods were combined. First, centrifugation was used to remove debris, phenol-chloroform extraction to remove the proteins, followed by NucleoSpin® Clean-Up kit (Macherey-Nagel) as described in **section 5.2.2.4** data in **Figure 6.7.**

In recent decades, the cell SELEX method has been extensively explored, as mentioned above. The split-combine cell SELEX method was developed to gain a better understanding of the split-combine method. It was compared with other cell SELEX protocols like DNA cell SELEX and an artificial DNA library with only one modification. For a more comprehensive comparison, DNA cell SELEX was conducted similarly to split-combine cell SELEX. For the DNA cell-SELEX, the percentage of unique sequences dropped gradually over the rounds, from almost 100% in the starting library to 46% in round 10, as shown in **figure 3.7**. For the split-combine cell SELEX, the percentage of unique sequences dropped suddenly from 88% in round 8 to 45% in round 9, as shown in **Figure 3.12**. Comparing the first 100 enriched sequences, all the sequences enriched in split-combine cell SELEX belong to families as shown in **table 6.2-6.7**. Contrary to DNA cell SELEX, most enriched sequences are unique, and only one family (MD7) exists, as shown in **Table 6.1**. Split-combine cell SELEX showed more robust enrichment than DNA cell SELEX in fewer selection rounds, which can also be seen in the nucleotide distribution, as shown in **Figure 3.11** and **Figure 3.7**. DNA cell SELEX does not contain any of the top 100 enriched sequences found in split-combine cell SELEX. Enriched sequences from split-combine cell SELEX, S1 and S2 showed stronger binding to PC-3 cells than

the DNA cell SELEX sequences, as shown in **Figure 3.11, Figure 3.12 and Figure 3.8**. The sequences obtained from the DNA cell-SELEX showed weak binding to PC-3 cells, as shown in **Figure 3.8**. On the other hand, the clickmers obtained from the split-combine protocol showed a high binding intensity to PC-3 cells, as shown in **Figure 3.8**.

During the split-combine cell SELEX experiment, a selection was conducted which involved the use of an artificial DNA library for selection [90]. This method utilized 5-((3-indolyl)propionamide-N-allyl)-20-deoxyuridine (Utrp) instead of deoxythymidine. The researchers aimed to select sequences that could be internalized into A549 cells and compared this method to DNA selection. The results showed that the artificial library method yielded a strong enrichment after eight rounds, and the top 10 sequences belonged to families. The use of an artificial library also excluded sequences that did not belong to a family, resulting in selected sequences that demonstrated superior internalization into A549 cells. Similarly, the split-combine cell SELEX method resulted in the enrichment of only two families (S1 and S2), which exhibited higher binding to PC-3 cells compared to the DNA sequences obtained from DNA cell SELEX. Overall, these findings confirm that modifying the starting library by introducing one or more modifications can lead to the selection of sequences that demonstrate a higher binding affinity to target cells.

To gain more insights into the process of enrichment, a comparison was made between split-combine protocols targeting a simple target like a protein and a complex target like cells. In the original split-combine protocol [99], C3-GPF was used as the target, resulting in a strong enrichment after eight rounds of selection. The researchers then selected sequences that demonstrated binding with specific modifications, such as I10, which bound to C3-GFP when it was functionalized with indole but not to other modifications like ethanamine, benzyl, or benzofuran. In contrast, the split-combine cell SELEX protocol resulted in a strong enrichment after nine rounds of selection, and the selected candidates S1 and S2 showed binding to completely different modifications, including imidazole, cyclic RGD, ethanamine, and isobutyl. Furthermore, the binding behavior of the selected candidates from both selections had a different binding behavior.

The split-combine cell SELEX method is a versatile technique that can be employed to target any cell line with different modifications. In this protocol, the starting library was modified using imidazole, ethanaime, cyclic RGD, isobutyl, and indole, but further modifications such as benzofuran, benzyl, or morphaline could also be utilized. The modifications chosen were based on previous experiment (see **section 3.1.4**) and the individual properties of each modification. For instance, cyclic RGD was selected because it can bind to the αvβ3 integrin protein[169]. integrin is a group of 24 transmembrane receptors that play a vital role in connecting cell adhesion and interaction with the extracellular microenvironment to intracellular signaling and cytoskeletal rearrangement. Among the integrins, Integrin αvβ3 is highly expressed in various solid tumors and is specifically targeted due

to its affinity for extracellular matrix proteins containing the arginine-glycine-aspartic (RGD) tripeptide sequence. [169]. Imidazole was also included in the modified library because it can increase the stability of the DNA duplex by forming a hydrogen bond with neighboring GC bases [170]. Indole was chosen because it is the most used modification in most of the nucleobase-modified selections [96, 99, 100] [90]. Furthermore, isobuyl and ethanamine were chosen to expand the diversity of the strating library.

Before expanding this method to other cell lines, several factors need to be considered. Firstly, it is important to determine the appropriate stage to initiate the deconvolution step. In the current study, deconvolution started after achieving strong enrichment, which was based on the split-combine protocol against a simple target. However, it may be more advantageous to begin the deconvolution step before obtaining enrichment against the target cells. This is particularly relevant since it was unexpected to identify an aptamer capable of binding to target cells with multiple modifications during the split-combine cell SELEX. Thus, initiating the deconvolution step earlier could aid in selecting aptamers that bind to target cells with mono-modification. For instance, commencing deconvolution from round 7 may produce different candidates, although in this study, only the best candidates will survive the selection procedure. To put it another way, by using this protocol, weak binders are excluded, and only the best candidates like S1 and S2 are enriched. The second factor to consider is the use of different modifications and repeating the selection procedure against the same cell line to compare the binding behaviour of the selected candidates. Additionally, it may be valuable to use the same modifications on another cancer cell line. Performing these three selections will result in a better understanding of enrichment profile of the split-combine cell SELEX.

Some drawbacks of split-combine cell SELEX include the fact that the bound fraction often requires more PCR cycles to amplify using ePCR. For example, in DNA cell SELEX, up to 30 PCR cycles may be needed to obtain enough material for subsequent rounds of selection. In split-combine cell SELEX, most rounds need another round of ePCR to have enough quantity for the next round, as shown in **Table 5.2.13**. This is one of the reasons making the split-combine procedure time-consuming. The click reaction and purification in each round also make this procedure time-consuming, and above this, after enrichment, more selection rounds are needed to complete the selection procedure. These rounds are called the deconvolution step, and the purpose of these rounds is to increase the copy number of the sequences belonging to each azide. In summary, the split-combine cell SELEX requires more time and effort, but the outcome sequences showed a higher binding ability to PC-3 cells.

4.4 Identification and characterization of the outcome candidates

The NGS analysis of split-combine cell SELEX showed only two primary families named S1 and S2, which was unexpected considering the target was PC-3 cells, a complex target. It was expected

to have at least five families because five azides were used in the selection procedure. However, the two identified aptamer families (S1 and S2) were found to bind to PC-3 cells using different click-in moieties, including aromatic modifications (imidazole (Im-dU) and indole (In-dU)), aliphatic modifications (ethanamine (Ea-dU) and isobutyl (Ib-dU)), and a small peptide cyclic-RGD (cRGD-dU). As shown in figure 3.12, these aptamers showed no binding when they were non-clicked. The first impression was that the interaction between the aptamer and PC-3 cells might be due to the triazole ring formed between the clicked azide and DNA regardless of the clicked-in azides. These results were aligned with the previously observation for selection against simple targets like streptavidin beads. One sequence, P2, was identified against streptavidin beads and showed consistent binding regardless of the clicked-in moiety but showed no binding when it was non-clicked similar to S1 and S2. [99]. However, Plückthun et al. have concluded that it binds irrespective of clicked in moieties. Therefore, a study was conducted to determine whether the selected clickmers (S1 and S2) interact with PC-3 cells independently of the clicked-in moieties or if the moieties play a crucial role in the interaction. The study found that the click moieties were crucial for the interaction. Taken together, S1 was chosen for further experiments as it showed more enrichment compared to S2

S1 clickmer was tested in the competition assay to see if the sequence bound to the same target on PC-3 cells with different moieties or if changing the moieties could change the binding site. PC3 cells were incubated with labeled S1 clicked with imidazole (Im-dU), and 10-fold unlabeled S1 clicked with cRGD, isobutyl, ethanamine, and indole. Subsequently, the fluorescence of the bound S1 was analyzed using flow cytometry. In order to obtain more conclusive results, the labeled S1 sequences were clicked with imidazole without competitors, and unlabeled S1 sequences were clicked with imidazole (Im-dU). According to the theory, the strongest competition would be between S1 clicked with imidazole and itself, but the S1 clicked with isobutyl also showed equal competition. There was less competition among the other variants of S1. This study confirmed that S1 bound to the same target on PC-3 cells when it was clicked with imidazole or isobutyl. However, whether the other variants bind to the same target on PC-3 cells is unclear, as shown in **figure 3.15**. In addition, the same experiment was repeated using labeled S1 clicked with cRGD, as shown in **figure 3.15**. It was found that the other variants were less competitive with S1 when clicked with cRGD. Comparing the imidazole and cRGD competition data, it is clear that isobutyl does compete with imidazole. This was the first indication that the clicked azide might affect the interaction between PC-3 cells and S1 sequences.

The second experiment performed on S1 examined concentration-dependent binding. This experiment was conducted at concentrations ranging from 0.956 to 478.5 nM. The highest binding capacity was obtained when S1 was clicked with imidazole (Im-dU). Moreover, Binding to PC-3 cells was detectable from 0.956 nM, while S1 clicked with cRGD (cRGD-dU) and ethanamine (Ea-dU) from

9.56 nM. When the S1 sequence was clicked with indole (In-dU), there was no concentration-dependent binding, as shown in **figure 3.16**. In this case, it is inaccurate to calculate the Kd for the S1 clicked with imidazole (Im-dU), cRGD (cRGD-dU), and ethanamine (Ea-dU) since the plateau is not reached [171]. This experiment showed another hint that the clicked moieties impacted the binding capability to PC-3 cells.

The third experiment was conducted to test the specificity of the S1 clickmer. Several cancer cell lines were chosen; H460, MCF-7, HeLa, HEK 239T, Hep G2 and LNCaP cells. The S1 clicked with imidazole bound only to PC-3 cells among all tested cell lines. Conversely, S1 clicked with cRGD bound to PC-3 and MCF-7 cells. Additionally, S1 clicked with ethanamine bound to PC-3 and LNCaP cells, as shown in **figure 3.17**. A third hint emerged from this experiment that the clicked-in moieties changed the binding capability of S1 sequences. This finding was confirmed by performing an internalization study using confocal microscopy. S1 clicked with cRGD can bind and internalize PC-3 and MCF-7 significantly. On the other hand, S1 clicked with imidazole showed substantial binding and internalization only in PC-3 cells, as demonstrated in **figure 3.18**. The confocal and flow cytometry data were consistent, with S1 clicked with imidazole exhibiting the highest binding to PC-3 cells. Based on this data, S1 can bind and internalize to PC-3 cells, making it suitable for drug delivery. More studies can be conducted to determine the pathway of internalization. However, the internalization of aptamers is largely dependent on the target receptors' function. Studies have categorized the mechanism of aptamer internalization as either clathrin-dependent or -independent [172, 173] [174] [156]. To investigate the clathrin-dependent pathway, researchers conducted colocalization studies using fluorescently labeled transferrin, as the transferrin receptor's endocytic pathway is well characterized through clathrin-mediated endocytosis [175]. Burkett's lymphoma cell-specific DNA aptamers and anti-protein tyrosine kinase 7 aptamers were found to internalize via clathrin-dependent endocytosis, which was confirmed by fluorescently labeled transferrin [176, 177]. To investigate the clathrin-independent endocytic pathway, most studies used internalization inhibitors. For example, AS1411 aptamers were characterized for their clathrin-independent pathway. G-quadruplex nucleolin DNA aptamers, which selectively bound to nucleolin expressed on cancer plasma membranes, were internalized into cells [178] [179]. To revealed the endocytic pathway of AS1411, DU145 prostate cancer cells were previously treated with cytochalasin D (an actin polymerization inhibitor) and dynasore (a dynamin inhibitor), which found that AS1411 was not internalized through clathrin-mediated endocytosis [180]. However, pretreatment with amiloride (a macropinocytosis inhibitor) significantly reduced the uptake of AS1411 in cancer cells, suggesting that AS1411 was predominantly internalized via micropinocytosis [180]. In another study, the endocytic pathway of AS1411 was investigated in different PC3 prostate cancer cells. The uptake of AS1411 was significantly inhibited by both amiloride and chlorpromazine (a clathrin-mediated endocytosis inhibitor),

suggesting that a mix of clathrin-mediated endocytosis and micropinocytosis were used for the endocytosis of AS1411[181]. However, genistein (a caveolae- and lipid raft-mediated endocytosis inhibitor) had no effect on AS1411 cellular uptake, indicating that caveolae- and lipid raft-mediated endocytosis were not involved in the endocytosis of AS1411[181]. At the end, further studies could be conducted to investigate the endocytosis mechanism of the S1 aptamer in PC-3 cells. The purpose of this study is to determine whether the S1 aptamer internalizes into PC-3 cells through different pathways when it is clicked with different clicked moieties (cRGD-dU, Im-dU, and Ea-dU). Furthermore, these studies could provide valuable insights into the mechanisms underlying aptamer internalization and could have implications for the development of aptamer-based therapeutics.

Concentration-dependent assay, testing the specificity, and internalization study are performed on all selected aptamers against cells to confirm the binding affinity and specificity. These experiments showed that the S1 clickmer bound to PC-3 cells in high specificity and affinity. Moreover, S1 clicked with cRGD bound differently to PC-3 cells than S1 clicked with imidazole or ethanamine. Using these experiments with the competition assay for this type of clickmer, develop a procedure to determine whether the interaction occurs due to the clicked-in moieties or the triazole ring. In the end, a final confirmation of this aptamer's ability to bind to multiple targets with different clicked moieties is the identification of the actual targets on the cell surface. However, the separation and identification of aptamer targets, especially membrane proteins, still face many obstacles; so far, only a limited number of targets of aptamers obtained by cell-SELEX have been identified and validated [182]. This was the first attempt at identifying the target, which is discussed in the **section 5.6.**

4.5 EdU study and truncation

In order to reduce the costs associated with future targeted therapies for prostate cancer, determining which modification sites significantly influence S1 binding to PC-3 cells. A total of eight variants of S1 were synthesized. A thymidine was substituted for an EdU at a certain position in each sequence. The substitution of a thymidine nucleotide with EdU can alter the structure and function of the DNA molecule, depending on the substitution's location and the EdU residue's specific properties. The variants were tested for their ability to bind to PC-3 cells. It is expected that when one EdU modification site is important for binding, the substitution into dT will result in a loss of the binding ability. Positions 11, 13, 36 and 38 are involved in the interaction process based on the reduced binding to PC-3 to less than 10%. As shown in **figure 3.20**, the substitution of thymidine at positions 5, 6, 37, and 42 did not affect the binding. All three modifications, namely imidazole (Im-dU), cyclic-RGD (cRGD-dU), and ethanamine (Ea-dU), exhibited similar binding results. Evaluation using EdU showed that a multi-position modification is crucial for binding. This observation is consistent with

a previous study on the clickmer C12, which was selected against C3-GFP, where modification at positions 23, 24, and 41 was found to be critical for binding [96].

Further confirmation of our conclusion was obtained by testing four additional variations. The variants S1.5, S1.4, S1.3, and S1.2 contain five EdUs, four EdUs, three EdUs, and two EdUs, respectively. S1.5 and S1.4 exhibited similar binding to the clickmer against PC-3 cells with imidazole (Imdu) and ethanamine (Ea-dU). Compared to S1, there is a slight decrease in binding for cRGD. The purpose of designing S1.3, and S1.2 was to use one of them as a point mutant control in the future. Moreover, testing the binding of these two variants will confirm the binding data obtained from the EdUs study. Likely, removing the modifications at positions 11, and 36 will disrupt the structure of clicked S1 with all the modifications. As shown in **figure 3.21**, the binding was almost similar to that obtained with the scramble sequence.

Ellington and Cowperthwaite [183] evaluated more than 2000 previously published aptamers from the aptamer database. According to their analysis, most of the aptamers had secondary structures independent of their primer binding sites [183]. The SELEX procedure itself could probably explain this observation. Sequences that contain highly structured regions at the primer binding sites may impede their own amplification during the PCR process by hindering the annealing of primers. This is because the secondary structures at the primer binding sites can interfere with primer binding, potentially disrupting the amplification process. In the SELEX library, sequences whose random regions do not interact with primers already have a selective advantage. As the SELEX cycle progresses, those sequences are likely to be amplified more readily and dominate later oligonucleotide pools[184]. A click-SELEX may further enunciate this bias. Primer binding sites were built in a way that no modifications could be introduced while modifications were introduced in the random region. We do not know how much click-SELEX's modifications contribute to forming secondary structures. Theoretically, they could create distinct sequences for DNA or RNA that do not exist in conventional sequences. Modifications within the random region might interact to produce unknown DNA structures, as observed in some known SOMAmers. A crystal structure of SOMAmers revealed that modified nucleobases interact with one another and unwind helical DNA structures. Due to the stacking of aromatic modifications with adjacent uridine, zipper-like structures can be found in NGF-SOMAmers, IL-1-SOMAmers, and other SOMAmers [80] [84] [185] [78]. A similar phenomenon may exist for clickmers and click-SELEX libraries. Due to the absence of modifications in the primer binding sites, they cannot participate in similar structures. Therefore, complex structures are presumably excluded from primer binding sites. Truncating the non-essential binding component of an aptamer could enhance specificity, sensitivity, and cost-effectiveness by reducing nonspecific interactions [186]. Vu and colleagues truncated an aptamer selected against platelet-derived growth factor BB (PDGF-BB) [187]. The full-length aptamer has 86 nucleotides and has been truncated to 36 nucleotides. In comparison with the full-length aptamer, the truncated variant has a 150-fold higher

affinity for PDGF-BB. After removing the primer binding sites from the S1 clickmer, S1.42 was obtained. The binding of the truncated variant was similar to S1 clickmer when clicked with imidazole (Im-dU), but demonstrated higher binding with cRGD (cRGD-dU) and ethanamine (Ea-dU). In order to remove all the non-essential nucleotides, more variants were designed based on the Mfold prediction **Figure 3.21**. With all the modifications, the binding was dramatically reduced in these two variants, S1.36, and S1.35. Based on the Mfold structure prediction, a variant of S1.33 was designed. Removing two nucleotides from the 5' end can disrupt the structure. S1.33 was designed to serve as a negative control in the future. However, none of the truncated variants bound PC-3 cells. Therefore, S1.42 is the shortest variant for S1.

4.6 Difficulty in identifying the actual target of S1 clickmer

Cell-SELEX often aims to produce aptamers to target cells of interest [111]. The molecular targets of most of these aptamers are unknown. [38]. A standard methodology for identifying aptamer targets involves isolating the target molecules using the aptamers as affinity ligands, followed by identifying the isolated targets through mass spectrometry (MS) or other means, and finally validating the isolated molecules. In order to identify proteins, biotin-labelled aptamers are incubated with cell lysate, and streptavidin-coated beads are applied to separate the aptamer-protein complex from cell lysate; the proteins are separated by SDS-polyacrylamide gel electrophoresis (SDS-PAGE); finally, the characteristic protein bands are cut off the gel, and then the proteins are analyzed by liquid chromatography-tandem mass spectrometry (LC-MS/MS) [29] [114]. This is the original method; modifications were made by lysis of the cells after coupling the aptamer. Aptamers were sometimes incubated first with cells, and then streptavidin-coated beads were added to capture the aptamer-cells complex. Then, the cells were lysed to separate proteins by SDS-polyacrylamide gel electrophoresis (SDS-PAGE). In this way, the internalization of the aptamer should be inhibited before adding the aptamer to the target cells [11] [188].

However, although more than 700 DNA aptamers generated by cell SELEX were reported, in the past 20 years, less than 30 targets have been identified [182] [38] [111]. The success rate of the aforementioned strategy for protein identification is quite low. This complexity of the strategy results in a low success rate. One of the major reasons is that aptamers usually target membrane proteins. Membrane proteins are highly hydrophobic, poorly soluble in water, and relatively abundant, making them very difficult to isolate. The non-specific interactions with beads and aptamers by interfering components in cells interfere greatly with protein isolation and subsequent MS analysis [182]. Among the non-specific components binding to aptamers are the numerous nucleic acid binding proteins that bind all nucleic acid sequences in cells, as well as components with multiple positive charges (poly-anion) that interact electrostatically with nucleic acid sequences without being specific

[27]. In SDS-PAGE, the sensitivity is not high enough to detect low-abundance protein bands; also, many non-specific protein bands usually interfere with picking the target bands. MS is a highly sensitive technique that generally results in many protein candidates, making it challenging to identify the target protein [189] [190]. Multiple steps are involved, including cell lysis, aptamer binding, aptamer-target complex isolation, SDS-PAGE separation, and MS analysis; if an experiment fails, it is difficult to pinpoint the error [182].

The challenges of conducting a pull-down assay to identify putative targets have been discussed previously. Therefore, initiating the pull-down assay with nucleotide-modified aptamers could pose significant difficulties. In order to gain more insight into the pull-down assay, optimization was carried out on two DNA aptamers that were selected through cell-SELEX. The DC-12 and D-7 aptamers were intensively studied in our laboratory. The aptamers were selected against BM-DCs. Additionally, these two aptamers are bound to J774A1 and THP-1 cells. Moreover, The DC-12 bound to THP-1 cells better than the D-7. The optimization of the pull-down assay started with DC-12 and THP-1 cells. The pull-down assay needs to be optimized by considering several parameters, including the amount of aptamer, beads, elution methods, staining methods, washing steps, and the number of cells. A detailed discussion of these parameters can be found in **section 5.3.1.2**. Briefly, two protein staining methods were compared **(Figure 6.12)**, and a silver stain was chosen. Depending on the staining method, the number of cells and the amount of aptamer were determined accordingly. Two types of beads were used, and the most suitable ones were selected (Dynabeads M-280 streptavidin beads) **(Figure 6.12)**. After testing two elution methods, urea was selected as the most suitable **(Figure 6.12)**. After optimizing the pull-down assay conditions for DC-12, the pull-down assay was conducted, and several bands appeared on the gel. To exclude the non-specific bands, a negative cell line should be included in the experiment [188]. Indeed, Non-specific bands can be excluded from the experiment by including a negative cell line. The binding of DC-12 to four different cell lines was tested, but DC-12 showed high binding to all cell lines. It is not possible to include a negative cell line in this experiment. This aptamer showed binding to all cell lines. Some of these cells are immune cells, while others are cancer cells. The issue of aptamers interacting with common proteins in all cell lines or non-specifically with cells is a common problem encountered in selecting aptamers using cell SELEX [27] [35] [27]. This is one of the main reasons why it is crucial to test the specificity of the selected aptamer before moving on to the application part. This aptamer, however, provided some information for optimizing the pull-down for the S1 clickmer. To recover the bound proteins, we tested some parameters, such as staining, number of cells, beads, and elution method.

Further optimization for pull-down assays was conducted using D-7 aptamer and J774A.1 cells. J774A.1 cells were chosen since D-7 showed higher binding intensity to these cells than THP-1 cells. Furthermore, this method is based on a published method [188]. This method was described in detail in **section 5.2.8.2**. First, inhibit the biotinylated aptamer's internalisation and then capture the bound

aptamer with streptavidin magnetic beads. After washing, the bound cells were lysed, and a series of extra washing steps were applied to remove all the debris from the cells and recover the bound fraction. Finally, the bound fraction was visualized on SDS-PAGE gel. First, Dynasore was used to inhibit the internalization of D-7. Dynasore is an inhibitor of dynamin-dependent endocytosis that affects cells' cholesterol, lipids, and actin [161]. D-7 internalization was significantly reduced after treatment with Dynasore at 4°C. A recent study also showed that Dynasore inhibited the internalization of the C10.36 aptamer into human Burkitt's lymphoma cells [188]. Pull-down assays were performed, but SDS-PAGE gels showed no detectable bands. Instead of continuing the optimization of the pull-down assay, more investigations were performed on the binding of D-7 against J774A.1 cells. Biotinylated D-7 was conjugated with labeled streptavidin beads to mimic streptavidin-aptamer binding. It was found that no fluorescence was detected after coupling with labeled streptavidin, which indicates that D-7's structure has changed. Therefore, this method is unsuitable for identifying the target on the cell surface using D-7 aptamers. Coupling an aptamer to a molecule can induce conformational changes in the aptamer, resulting in changes in its binding affinity or specificity towards the target [191].

Information from both methods with and without inhibiting internalization should be gathered to optimise the aptamer pull-down assay. However, optimization without inhibiting internalization may be easier. Before using this method, it is necessary to perform two binding tests: binding biotinylated clickmer with labeled streptavidin and binding at 4°C. The entire procedure is done at 4°C due to proteases inside the cells. During cell lysis, proteases can digest the target at 37°C [160]. In brief, when S1 clickmer is clicked with imidazole and cRGD, it can bind to PC-3 after coupling with streptavidin, but not when clicked with ethanamine. For this reason, S1 clicked with ethanamine was excluded from the pull-down assay optimization. The pull-down assay was conducted using S1 clicked with imidazole or cRGD against PC-3 and MCF-7 cells. The results of the pull-down assays showed smears on the gels, as illustrated in **Figure 3.33**. These outcomes posed a challenge in identifying the actual target of S1. The SDS PAGE gel showed more smears and eluted proteins when S1 was clicked with cRGD. Due to the fewer smears of S1 clicked with imidazole, optimization began with S1 clicked with imidazole. Different cell numbers, aptamer amounts, and varying incubation times were examined. The pull-down assay initially used 1 million cells, but the number of cells was later reduced to 500 thousand. The amount of S1 used ranged from 50 pmol to 30 pmol. The incubation time for the assay was 45 minutes, followed by a reduction to 20 minutes. Using 500 thousand cells, 30 pmol of aptamer, and 20 minutes of incubation time, the final pull-down assay was performed using PC-3 cells as a positive cell line and MCF-7 cells as a negative cell line. It was not possible to optimize the pull-down assay despite all the investigations. A smear appeared on the SDS-PAGE gel and decreased the amount of aptamer, cells, and increasing washing steps, resulting in no difference between the bound fraction for S1 and the scramble sequence. The main problem was

obtained on the SDS-PAGE gel, probably due to the non-specific binding between the imidazole in the S1 sequence and the intracellular proteins. the elution fraction on the SDS-PAGE gel between S1 and S1.4 was compared, and it was observed that S1.4 had less smear in most of the conditions. This difference was particularly noticeable when comparing the elution fraction of S1 and S1.4 with cyclic RGD (cRGD-dU), where S1.4 consistently showed less smear than S1.

More stringent conditions are recommended to be applied to reduce non-specific proteins' presence. For example, more washing steps are required using a high salt buffer. In high salt buffers, nonspecific interactions between proteins and beads or aptamers can be disrupted, making it easier to isolate specific aptamer-protein interactions [192]. However, high salt buffers may affect most aptamer-protein interactions [193] [194]. A more appropriate method would involve a covalent bond between the aptamer and the target on the cellular surface. Covalent crosslinking of the aptamer with its target can be achieved by replacing some bases with nucleobases that are photo-reactive, such as 5-iodo-2'-deoxyuridine (5dUI) [31]. However, a disadvantage to this method is that the positioning of the substitution requires optimization in order to preserve the affinity of the aptamers for binding [117]. However, the substitution position in the S1 clickmer case can be predicted based on the EdU study. Additionally, it should be noted that the S1 sequence contained eight EdUs, of which four were found to be unnecessary for binding. Specifically, these four EdUs were located at positions 5, 6, 37, and 42. To further investigate the target of S1, creating variants of S1 with replacements using 5-dUI at these positions or other modifications could be explored. Replacement of positions 37 and 42 is highly recommended. The position of 37 is located between two essential EdUs, namely 36 and 38. Therefore, modifying this position would be the most effective approach for this method to work as it is within the binding motif. Alternatively, positions 5 or 6 could be considered as a second option.

4.7 CONCLUSION

The Split-combine protocol has been successfully implemented with the cell-SELEX method, enabling the screening of different functional groups in a single selection for target cells. This innovative technique saves time and effort. In this study, a nucleobase-modified aptamer was selected against PC-3 cells. This aptamer can bind to PC-3 cells using different functional groups. When modified with cyclic RGD, it can bind to both PC-3 and MC-7 cells. When functionalized with imidazole, it binds to PC-3 cells only. Although it was challenging to identify the actual targets for the S1 aptamer, it shows potential for the development of a targeted therapy for prostate cancer. Furthermore, expanding this technology to other cell lines can lead to the selection of similar nucleobase-modified aptamers for other cancer cell types.

5 MATERIAL AND METHODS

5.1 Material

5.1.1 Equipment

Table 5.1 Equipment

NAME	SOURCE
Biometra Personal Cycler	Biometra, model no. T
BD FACSCanto II	BD Biosciences
Genoplex Gel Documentation System	VWR
Tissuelyzer MM200	Retsch
Veriti Thermocycler	Applied Biosystems
Heraeus® HERAcell® CO2 Incubators	Thermo Fisher Scientific
Neubauer Haemocytometry	Marienfeld
Zeiss LSM 710 Confocal Laser Scanning Micro-scope	Zeiss
Agarose Electrophoresis chamber	In-house construction
DynaMag™-2 Magnet	Invitrogen
Water purification system (Barnstead™ Micro-pure™)	Thermo Scientific
Pipettes	Eppendorf
pH meter	Mettler Toledo
Vortex	VWR
Microwave	Bosch
Electrophoresis power supply	Consort
Freezer -80°C	New Brunswick Scientific
Freezer -20°C	Liebherr
Centrifuge	Eppendorf
Heraeus® Herasafe Biosafety Cabinet	Thermo Fisher Scientific
Liquid scintillation counter	PerkinElmer, model no. WinSpectral 1414
PAGE gel equipment	Protean II xi Cell; Bio-Rad
Odyssey blot imager	LI-COR
HPLC 1100 series, C18 Hypersil ODS	Agilent
Phosphorimager FLA-3000	Fujifilm

Radioactive protection shield	Nalgene
Analytical balances	Sartorius
Analytical HPLC system, 1260 Infinity	Agilent

5.1.2 Chemicals

Table 5.2 Chemical

NAME	SOURCE	IDENTIFIER
dNTP-Set 100 mM	Genaxxon	M3015.4100
EdUTP 5.0 µmol 100 mM	Baseclick	BCT-08-L
Pwo DNA-Polymerase	Genaxxon	M3002.1250
RotiPhenol	Roth	0038.1
Lambda exonuclease	ThermoFisher	EN0562
Trypsin/EDTA 0,05%	ThermoFisher	25300054
RPMI 1640 Medium	ThermoFisher	21875091
Ham's F-12 Nutrient Mix	ThermoFisher	11765054
Abil WE 09 MB	Surfachem	ABILWE09MB.11
Tegosoft DEC	Surfachem	TEGOSOFTDEC.07
Macherey-Nagel NTC Buffer	Fisher Scientific	11922312
Dulbecco's phosphate-buffered saline (DPBS)	ThermoFisher	14190-250
Protease Inhibitor Cocktail	Sigma-Aldrich	P8340-1 ml
Cyclo[Arg-Gly-Asp-D-Phe-Lys(Azide)]	Peptides International	RGD-3749-PI
UltraPure ™ salmon sperm DNA solution	ThermoFisher	15632011
BD FACS Flow Sheath Fluid	BD	342003
Albumin (BSA) Fraction V (pH 7.0) for Western blotting	AppliChem	A6588,0100
FACS Shutdown Solution	BD	334224
RPMI 1640 Medium, no phenol red	ThermoFisher	11835030
Atto 647N-Streptavidin	Sigma-Aldrich	94149-1MG
TEMED	Roth	2367,1

Gene Ruler, Ultra Low Range DNA Ladder, 0.5 µg/µl	Fermentas	SM 1212
Dynabeads M-280	Invitrogen	112-06D
Ammoniumperoxodisulfat (APS)	Carl Roth	125141
Agarose Standard (GenAgarose LE)	Genaxxon	M3044.1000
DMEM, high glucose, Gluta-MAX™ supplement	ThermoFisher	61965059
ɣ-32P-ATP	Perkin Elmer	NEG502A
4‘,6-diamidino-2-phenylindole (DAPI)	Sigma-Aldrich	24894213
Wheat Germ Agglutinin, Alexa Fluor™ 488 Conjugate	ThermoFisher	W11261
Mineral oil	Sigma-Aldrich	M55904
RNase A/T1	ThermoFisher	EN0551
Trichloromethane/Chloroform	Carl Roth	3313.1
Ethanol absolute	VWR	20821.310
Sodium Acetate	Th Geyer	127-09-3
Magnesium Chloride Hexahy-drate	Alfa Aesar	7791-18-6
Isoamyl Alcohol	Roth	T870.1
Ethidium bromide solution 10mg/ml	Roth	2218.1
Fetal calf serum (FCS)	Thermo Fisher	A4766801
Acetonitrile	Sigma-Aldrich	270717
Copper(II) sulfate	Sigma-Aldrich	451657
K2HPO4	Fluka	60355
KH2PO4	AppliChem	A36200500
Nuclease S1 with 10× reaction buffer	Life Technologies	18001-016
THPTA	BaseClick	BCMI-006
Tween 20	Roth	9127.2
Urea	Roth	3941.2
Azides	Synthesized at AK Mayer (LIMES)	
Dimethyl sulfoxide (DMSO)	Sigma-Aldrich	472301

HCl	Roth	20252.290
Tris	Roth	77-86-1
Triethylammonium acetate (TEAA)	Sigma Aldrich	69372
Triethylamine (TEA)	Sigma Aldrich	121-44-8
Sodium dodecylsulfate (SDS)	Roth	151-21-3
Flourogel mounting medium	EMS	1798510
Formaldehyde	Fluka	ICS045
Bromophenol blue	Merk	108122
NaOH	Sigma-Aldrich	1310-73-2
Boric acid	AppliChem	131015.1211
Span 80	Sigma-Aldrich	1338-43-8
Triton X-100	Merk	9036-19-5
MagStrep Type 3 X beads	Iba	2-4090-002
Acetic acid glacial	Merk	1.00063.2500
G-250 Coomassie	Thermo Fisher	20279
Methanol	Merk	106009
Phosphoric acid	Carl Roth	7664-38-2
PSMF	Carl Roth	329-98-6

5.1.3 Consumables

Table 5.3 Consumables

NAME	SOURCE	IDENTIFIER
TC-Flasche T75, Standard	Sarstedt	833911
SafeSeal Micro Tube 2 ml, PP	Sarstedt	72695500
Amicon 3K 0.5 ml	Merck Millipore	UFC500324
Streifen PCR-Gefäße und Deckel, 0,2 ml	VWR	731-0433
FACS Round Bottom Tubes 12 x 75 mm	VWR	734-0442
Serologische Pipette 10 mL	Sarstedt	86.1254.001
Serologische Pipette 5 mL	Sarstedt	86.1253.001

cell scraper S, L=24cm	TTP	99002
Falcon Tube, 15 ml	Sarstedt	62554502
TC-Platte 24 Well,Cell+,F	Sarstedt	833922300
serologische Pipetten, 25 ml	Sarstedt	86.1685.001
Cell culture flask, T-75, surface: Suspension	Sarstedt	83.3911.500
Serologische Pipette 50 mL	Sarstedt	861689001
TC-Platte 48 Well,Cell,F	Sarstedt	83.3923.005

5.1.4 Buffer

Table 5.4 Buffer

Buffer	Composition
10x TBE buffer	890 mM Tris/HCl 890 mM boric acid 20 mM Na2EDTA, pH 8.0
6x DNA loading dye	60% (v/v) glycerol 10 mM Tris/HCl 0.03% (w/v) Xylencyanol 60 mM Na2EDTA, pH 8.0
5x SDS Running buffer	15.1 g/l Tris 72 g/l glycine 5 g/l SDS pH 8.2 (do not titrate)
10 x PAA loading buffer	60 % formamide 5 % SDS 0.25 mM EDTA bromphenol blue
0.1 M phosphate buffer	61.5 mM K2HPO4 38.5 mM KH2PO4, pH 7.4
4 x Laemmli buffer	150 mM Tris pH 6.8 30 % glycerol 12 % SDS 15 % β-mercaptoethanol bromophenol blue
homogenization buffer	300 mM Sucrose 5 mM Tris-HCl pH 7.4 0.1 mM EDTA 1 mM PMSF
storage buffer	5 mM Tris-HCl, pH 7.4 1 mM PMSF
Blue silver staining	
fixing solution	50% (v/v) Ethanol 2% (v/v) Phosphoric acid
silver-impregnating solution	10% (v/v) Phosphoric acid 10% (v/v) Ammonium sulfate 0.12% (w/v) G-250 Coomassie 20% (v/v) Methanol

Glutaraldehde-silver stain	
fixing solution	40% (v/v) Ethanol 10% (v/v) Acetic acid
sensitizing solution	6.8% (v/v) Sodium acetate 0.125% (v/v) Glutaraldehyde 0.2% (w/v) Sodium thiosulfate
silver impregnating solution	0.015% (v/v) Formaldehyde 0.25% (w/v) Silver nitrate
developing solution	3% (w/v) Sodium carbonate 0.008% (v/v) Formaldehyde
stopping solution	1.5% (w/v) EDTA
DC-12 and D-7 pull down assay	
cell lysis buffer	DPBS, 1mM MgCl2, 1% NP40, 0.1% protease inhibitor cocktail
washing buffer II	DPBS, 1mM MgCl2, 0.05% protease inhibitor cocktail, 1mM PMSF
S1 pull-down assay	
cell lysis buffer	RPMI medium without FCS or phenol red 1%NP-40, 10 mg/ml PSMF

5.1.5 Kits

Table 5.5 Kits

NAME	SOURCE	IDENTIFIER
Macherey-Nagel™ NucleoSpin™ Gel and PCR Clean-up Kit	Fisher Scientific	11992242
TruSeq DNA PCR-Free Sample Preparation Kit LT	Illumina	20015962
ProteoSilver™ Silver Stain Kit	Sigma-Aldrich	PROTSIL1-1KT
MicroSpin™ G-25 Columns	GE Healthcare	45-001-397

5.1.6 Software used

Table 5.6 Software

Software	Manufacture
Adobe Illustrator	Adobe System
GraphPad Prism	GraphPad Software
FlowJo V9.6.3	BD Life Science

Zeiss ZEN Imaging Software	Zeiss
ChemDraw	PerkinElmer
AptaNext	Inhouse program, Laura Lledo
AIDA Biopackage	Raytest
Microsoft office package	Microsoft
IDT oligo analyzer	(https://eu.idtdna.com/calc/analyzer)

5.1.7 Oligos

Table 5.7 Oligos

Split-combine cell SELEX	
Name	Sequence
M2 EdU library	CAC GAC GAC AGA GAC CAC AG -N42- CCA GCA GCC AGA GAC GAA CA (Library N= dA: dC: dG: EdU (1:1:1:0.7))
M2-forward primer-biotin	5'- Biotin- CACGACGACAGAGACCACAG -3'
M2-forward primer-Atto 647N	5'- ATTO 647N - CACGACGACAGAGACCACAG -3'
M2-forward primer	5'- CACGACGACAGAGACCACAG -3'
M2-reverse primer	5'- phosphate- TGTTCGTCTCTGGCTGCTGG -3'
FT2 library	CACGACGCAAGGGACCACAGG -N42- CAGCACGACACCGCAGAGGCA(N= dA:dC:dG:EdU = 1:1:1:1)
Clicked competitior	(N = 1:1:1:1 dA:dG:dC:EdU): 5′-N42-A-3
S1	CACGACGACAGAGACCACAGCGGAXXCGCGXGXAGCAAAAGGAAGAC-GCGGCGCGXXXAGCX CC AGC AGC CAG AGA CGA ACA
S1 SC	CACGACGACAGAGACCACAGGCAAACCGAG-GAGCCCGAXXCGXGXCXAXGXGCGGAAGAGGX CC AGC AGC CAG AGA CGA ACA
S1 DNA	CACGACGACAGAGACCAC AG CGGATTCGCGTGTAGCAAAAGGAAGAC-GCGGCGCGTTTAGCT CC AGC AGC CAG AGA CGA ACA
S2	CACGACGACAGAGACCACAGGGCAXGAGCCCGAACCGCGCGXGX-AGCGAGAGACGAACAXA CCA GCA GCC AGA GAC GAA CA
S2 SC	CAC GAC GAC AGA GAC CAC AG GXCGCCXGCG GXGGGAGCAAACGCGA-GACCGAGACAXAACA CCA GCA GCC AGA GAC GAA CA
X5T	CACGACGACAGAGACCACAGCGGA**T**XCGCGXGXAGCAAAAGGAAGAC-GCGGCGCGXXXAGCX CC AGC AGC CAG AGA CGA ACA

X6T	CACGACGACAGAGACCACAGCGGAX**T**CGCGXGXAGCAAAAGGAAGAC-GCGGCGCGXXXAGCX CC AGC AGC CAG AGA CGA ACA
X11T	CACGACGACAGAGACCACAGCGGAXXCGCG**T**GXAGCAAAAGGAAGAC-GCGGCGCGXXXAGCX CC AGC AGC CAG AGA CGA ACA
X13T	CACGACGACAGAGACCACAGCGGAXXCGCGXG**T**AGCAAAAGGAAGAC-GCGGCGCGXXXAGCX CC AGC AGC CAG AGA CGA ACA
X36T	CACGACGACAGAGACCACAGCGGAXXCGCGXGXAGCAAAAGGAAGAC-GCGGCGCG**T**XXAGCX CC AGC AGC CAG AGA CGA ACA
X37T	CACGACGACAGAGACCACAGCGGAXXCGCGXGXAGCAAAAGGAAGAC-GCGGCGCGX**T**XAGCX CC AGC AGC CAG AGA CGA ACA
X38T	CACGACGACAGAGACCACAGCGGAXXCGCGXGXAGCAAAAGGAAGAC-GCGGCGCGXX**T**AGCX CC AGC AGC CAG AGA CGA ACA
X42T	CACGACGACAGAGACCACAGCGGAXXCGCGXGXAGCAAAAGGAAGAC-GCGGCGCGXXXAGC**T** CC AGC AGC CAG AGA CGA ACA
S1.5	CACGACGACAGAGACCACAG CGGATTCGCG**X**G**X**AGCAAAAGGAAGAC-GCGGCGCG**X**T**X**AGC**X** CC AGC AGC CAG AGA CGA ACA
S1.4	CACGACGACAGAGACCACAG CGGATTCGCG**X**G**X**AGCAAAAGGAAGAC-GCGGCGCG**X**T**X**AGCT CC AGC AGC CAG AGA CGA ACA
S1.3	CACGACGACAGAGACCACAG CGGATTCGCGTG**X**AGCAAAAGGAAGAC-GCGGCGCGTT**X**AGC**X** CC AGC AGC CAG AGA CGA ACA
S1.2	CAC GACGACAGAGACCACAGCGGATTCGCGTG**X**AGCAAAAGGAAGAC-GCGGCGCGTT**X**AGCT CC AGC AGC CAG AGA CGA ACA
S1.42	CGGATTCGCG**X**G**X**AGCAAAAGGAAGACGCGGCGCG**X**T**X**AGCT
S1.36	CGCG**X**G**X**AGCAAAAGGAAGACGCGGCGCG**X**T**X**AGCT
S1.35	CGCG**X**G**X**AGCAAAAGGAAGACGCGGCGCG**X**TX**A**GC
S1.33	CG**X**G**X**AGCAAAAGGAAGACGCGGCGCG**X**T**X**AGC
DNA cell-SELEX	
M2 library	CAC GAC GAC AGA GAC CAC AG -N42- CCA GCA GCC AGA GAC GAA CA (Library N= dA: dC: dG: dT (1:1:1:1))
MD1	CACGACGACAGAGACCACAGTGATGGCGGTTTGACGGTCCGAGCCAA-GAGTGGTGAGTTCGACCAGCAGCCAGAGAC GAACA
MD2	CACGACGACAGAGACCACAGAAGCAGA-GATTAGGGCCATGTGCCCCAAGTCAAGGGATTAGCCAGCAGCC AGAGAC-GAACA
MD3	CAC GAC GAC AGA GAC CAC AG CCTGAGGACAAAACTCTACGAGCG-CAACGAGGTTAAAGAGGT CCA GCA GCC AGA GAC GAA CA
MD4	CAC GAC GAC AGA GAC CAC AG GAAGAAAAGGGAAGCAATGCTG-GACAGCCGGCCAGCTCCTGG CCA GCA GCC AGA GAC GAA CA
MD5	CACGACGACAGAGACCACAGAGGCACAGCGTAGAGCCAG GCAGCTG-CAAATCAAGACATGACCAGCAGCCAGAGAC GAACA

MD6	CACGACGACAGAGACCACAGAGGCAAAGACTGGAGTG CTGTGGCCA-TAAGCCAAGGAATGACCAGCAGCCAGAGACGAA CA
MD7	CACGACGACAGAGACCACAGCCATCCCCTCTCCCCATCCGCCCGAGAC-CACAGCCACTCCCCCAGCA GCC AGA GAC GAA CA
MD8	CAC GAC GAC AGA GAC CAC AG CAGCAAACGTGGCTATACTAAGAACAC-TGACAAGTCCGCAAA CCA GCA GCC AGA GAC GAA CA
MD9	CACGACGACAGAGACCACAGATCACCGTTTATTGGGCACCTACTCGACAC-GGTGCCTCCTGC CCA GCA GCC AGA GAC GAA CA
DC-12 & D-7 aptamer	
DC-12	GCTGTGTGACTCCTGCAACCAGGGTGGGATGGGTATTTTGAGGTG-GAGGTGGGGGTTGGTT GCAGCTGTATCTTGTCTCC
DC-12 SC1	GCT GTG TGA CTC CTG CAA GGATGGTGGCGGTGTTGTGGTGAGTT-GGTGAATTGGTAGGCGGGCAGC TGT ATC TTG TCT CC
DC-12 SC2	GCT GTG TGA CTC CTG CAA GATGTTGAAGTGGTGGTGCGGTTGTGGTG-GAGTGTCGGAGTGGGC AGC TGT ATC TTG TCT CC
Ctrl 2	GCTGTGTGACTCCTGCAAGTGGTGTTAAGAGGTGAGGTATAACGCGGAAT-GGTGCGAGGCGCA GCTGTATCTTGTCTCC
D-7	GCTGTGTGACTCCTGCAACGTGGGTGGGTTTATATT-CGGTGGTGGTGGGGGTGGTACTGTT GCAGCTGTATCTTGTCTCC
G24A	CTAACCCCGGGTGTGGTGGGTGGACAGGGGGGTTAG

5.2 Methods

5.2.1 Working with nucleic acid

The nucleic acids used in this study were obtained from ELLA-Biotech GmbH, Microsynth or IBA Lifesciences GmbH. According to the manufacturer the lyophilized DNA was reconstituted in ddH2O. All oligonucleotides were stored at -20 °C.

The size and quality of oligonucleotides were evaluated using agarose gel electrophoresis. The concentration of the labeled oligonucleotides was determined by using by Nanodrop 2000c microarray option. To determine labeling efficiency, gel electrophoresis was utilized, and fluorescence was measured using the Phosphorimager FLA-3000 (Fujifilm).

5.2.1.1 Agarose gel electrophoresis

PCR products or ssDNA were monitored on 4% agarose gels. A 4% (w/v) agarose gel was prepared by dissolving 4 g of agarose in 100 mL of 1X TBE buffer and boiling it in the microwave for several minutes. In subsequent steps, the ethidium bromide solution was diluted to 1:10000 in 40 mL of gel and poured after mixing. Electrophoresis was performed at 150 V for 13-15 minutes in a 1X TBE buffer. Samples were mixed with 6x DNA loading buffer at a ratio

of 1:6 before loading. A UV transilluminator (Genoplex, VWR) was used to visualize the separated oligonucleotides. The size of oligonucleotides was determined based on a comparison with the DNA ladder (Life Technologies).

5.2.1.2 Polyacrylamide gel electrophoresis

The labeling efficiency of radioactively labeled nucleic acids (^{32}P) was analyzed using urea polyacrylamide gels. **Table 5.2.1** describes the procedure for receiving the gel (10%) and pouring it between the two glass plates of the chamber. It was then allowed to polymerize for 45 to 60 minutes. Polymerizing the glass plates was followed by carefully adjusting the running chamber and filling it with 1 x TBE buffer. A 30-minute pre-run was conducted at 370 V. Using a syringe, the gel wells were rinsed with 1x TBE buffer after the pre-run. Using a PAA loading buffer, the nucleic acid samples were diluted and heated at 95°C for 3 minutes. This was followed by 1h of running the gel at 370V.

Table 5.2.1 Composition of 10% of PAGE-gel

Table 5.8 Composition of 10% of PAGE-gel

Reagent	**Volume for 1 gel**
8.3 M urea in 10X TBE	4 ml
Rotiphorese sequenziergel konzentrat	16 ml
8.3 M urea	20 ml
10% (w/v) APS	320 µl
TEMED	16 µl

5.2.1.3 PCR

5.2.1.3.1 Gradient PCR

Gradient PCR was used to select the optimal annealing temperature for the designed libraries, M1 and M2. Different annealing temperatures were used with a 5 °C difference starting from 70 °C to 45 °C. After the first PCR, another gradient PCR was performed for the designed libraries by narrowing the temperature range. The tested temperatures were; 65 °C, 62°C, 60°C, 58°C, 55°C and 52°C. The PCRs were carried out in a Veriti 96 well thermocycler (Applied Biosystems) using the following PCR program **(table 5.2.2)** and pipetting scheme **(table 5.2.3)**.

Table 5.9 PCR program for gradient PCR

Step	**Time (second)**	**Temperature (°C)**

Denaturation (only first cycle)	120	95°C
Denaturation	30	95°C
Annealing	30	70°C- 45 °C
Extension	30	72°C
Final extension	120	72°C
Soak	∞	4°C

Table 5.10 PCR pipetting scheme for gradient PCR

Components	**Stock concentration**	**Volume (µl)**	**Final concentration**
Fwd primer (M1or M2)	10 µM	2.5	1 µM
Rev primer (M1or M2)	10 µM	2.5	1 µM
dNTPs	25 mM	0.25	0.25 mM
Pwo-polymerase buffer	10 X	2.5	1 X
Pwo polymerase	2.5 U/ µl	0.25	0.025 U/ µl
templet (ssDNA)	5 nM	2.5	0.5 nM
dd H2O		14.5	
Total volume		25	

5.2.1.3.2 PCR

The PCR was used to test the amplification properties of the designed libraries; M1 and M2. Using the optimal annealing temperature (58°C) for the designed libraries. 5 PCRs were conducted by re-amplifying the previous PCR product until both libraries showed an effective amplification property using the abovementioned condition.

A Large-scale PCR was used to amplify S1 and S2 clickmer after identification from the split-combine cell SELEX procedure. Using the same PCR program mentioned above with an annealing temperature of 58°C, Atto 647 N labeled M2 forward primer and the pipetting scheme below in **table 5.2.4**.

Table 5.11 PCR pipetting scheme for large-scale PCR

Components	**Stock concentration**	**Volume (µl)**	**Final concentration**
Fwd primer (M1or M2)	100 µM	97	1 µM
Rev primer (M1or M2)	100 µM	97	1 µM
EdU mix (dATPs, dCTPs, dGTPs, and EdUTP)	25 mM	97	0.25 mM

Pwo-polymerase buffer	10 X	970	1 X
Pwo polymerase	2.5 U/ µl	97	0.025 U/ µl
templet (ssDNA)	5 nM	48	0.024 nM
dd H2O		8,342	
Total volume		9,700	

5.2.1.4 Emulsion PCR (ePCR)

5.2.1.4.1 ePCR optimization

In order to optimize the ePCR, two different formulas were used. In the first formula, the oil phase consists of span 80, tween 80, triton X-100, and mineral oil [53], as depicted in **table 5.2.5**. After mixing all the compoenets of the master mix (aqueous ohase). The oil/ aqueous ratio is 2:1(see **table 5.2.6)**. BSA was included in the aqueous phase at a final concentration of 10 mg/mL. During the vortexing of the oil phase, the master mix was gradually added to the oil phase over two minutes, and after the complete addition of the aqueous phase, the mixture remined vortexing for the next 5 min.

In the second formula, the oil phase consists of Tegosoft, mineral oil and ABIL WE [54]. (see **table 5.2.7**). After mixing all the oil phase components, short vortexing was performed for five seconds. The oil/aqueous ratio was 4:1. In 2 mL tubes, 150 µL of the aqueous (**Table 5.2.8**) with 600 µl of the oil was added containing one steel bead. Mixing was performed with a tissue lyzer by agitating at a rate of 15 Hz for 40 seconds. Mixing was then repeated for 15 seconds. This emulsion was then divided into aliquots and placed in PCR tubes, with a maximum volume of 150 µL for each tube, before starting the PCR cycler.

Table 5.12 Oil phase composition for the first formula

Component	**Amount (µl)**	**Final concentration**
Span 80	90	4.5% (vol/vol)
Tween 80	8	0.4% (vol/vol)
Triton X-100	1	0.05% (vol/vol)
Mineral oil	1901	----------

Table 5.13 Master mix (aqueous phase) for the first formula

Component	**Stock concentration**	**Volume**	**Final concentration**

Fwd primer (M1or M2)	100 µM	1.5	1 µM
Rev primer (M1or M2)	100 µM	1.5	1 µM
BSA	100 mg/ml	15	10 mg/ml
dNTPs	25 mM	1.5	0.25 mM
Pwo-polymerase buffer	10 X	15	1 X
Pwo polymerase	2.5 U/ µl	1.5	0.025 U/ µl
Templet (ssDNA)		----------	
dd H2O		----------	
Total volume		150	

Table 5.14 Oil phase component for the second formula

Component	**Amount (µl)**	**Final concentration**
TEGOSOFT DEC	438	73% (v/v)
ABIL WE 09	42	7% (v/v)
Mineral oil	120	20% (v/v)

Table 5.15 Master mix (aqueous phase) for the second formula

Component	**Stock concentration**	**Volume (µl)**	**Final concentration**
Fwd primer (M1or M2)	100 µM	1.5	1 µM
Rev primer (M1or M2)	100 µM	1.5	1 µM
BSA	100 mg/ml	1.5	1 mg/ml
dNTPs	25 mM	1.5	0.25 mM
Pwo-polymerase buffer	10 X	15	1 X
Pwo polymerase	2.5 U/ µl	1.5	0.025 U/ µl
Templet (ssDNA)	----------	----------	

dd H2O	----------	----------	----------
Total volume		150	

5.2.1.4.2 Quality control for the ePCR

The quality of the ePCR was determined in two ways. The first method encompassed the analysis of the PCR product on 4% agarose gel to determine if any by-products were produced during the process. the second method was to examine the droplets under a microscope. Thereby 5µL of the resultant emulsion was loaded on a microscopy slide, covered with a cover glass, and visualized by laser scanning microscopy.

5.2.1.4.3 Breaking the ePCR

the emulsion was transferred to a 2 ml tube and centrifuged at 12,000 g for 10 minutes. The top oily layer was separated from the lower milky layer containing the emulsion droplets with the PCR product. The oily layer was discarded without affecting the bottom layer. The emulsion was broken by adding an equal amount of phenol, chloroform, and isoamyl alcohol (25:24:1) and vertexing multiple times using the maximum speed. The vortexing was repeated several times until the bottom layer was completely dissolved. the samples were centrifuged at 16,000 g for 3 minutes, and the upper aqueous phase was collected. The collected phase was then mixed with an equal amount of chloroform and centrifuged at 16.000x g for 3 minutes. The upper phase was collected and transferred to another tube. the PCR product was validated by gel electrophoresis. the PCR product was then purified by using A PCR clean-up kit.

5.2.1.4.4 ePCR during SELEX

During the DNA SELEX and the split-combine cell SELEX, ePCR was performed to amplify the bound fraction of ssDNA. However, the same protocol was used with a much higher volume during the selections. The master mix or aqueous phase volume was 750 µL, and the oil phase volume was 3 mL. The emulsion was prepared and aliquoted into PCR tubes with a total volume of not more than 150 µL per PCR tube. In addition, the forward primer (M2-FW) was biotinylated, and the reverse primer (M2-RV) was 5'phosphorylated to facilitate single-strand displacement by λexonuclease enzyme digestion. After amplification using a thermocycler (Biometric), the emulsion was broken using the same protocol described previously, and the PCR product was analyzed on a 4% agarose gel. Afterwards, samples were purified using a NucleoSpin® Clean-Up kit (Macherey-Nagel).

5.2.2 Purification

5.2.2.1 Silica spin columns

For dsDNA purification, spin columns were used after each PCR and for ssDNA purification, after exonuclease enzyme digestion. After the click reaction, ssDNA was purified using NucleoSpin® Clean-Up kit (Macherey-Nagel). All purifications were performed according to the manufacturer's instructions. In summary, the NTI buffer was used in a ratio of 1:2 (sample: NTI) for dsDNA. The NTC buffer was used in the ratio of 1:4 (sample: NTC) for ssDNA. Following centrifugation with a silica column, the columns were washed twice with NT3 buffer, and the product was eluted three times with 25 µ ddH2O.

5.2.2.2 Phenol-chloroform extraction

After the SELEX rounds, phenol-chloroform extraction was used to isolate the bound fraction from the cell lysate. The phenol was added in a 1:1 ratio to the sample, followed by thorough vortexing and centrifugation at maximum speed for 3 minutes. The upper phase was transferred into another tube, and 2 volumes of chloroform was added, followed by vortexing and centrifugation for 3 minutes at maximum speed. Afterwards, the upper phase was transferred into another tube.

5.2.2.3 Agarose gel purification

Agarose gel purification was performed to purify the DNA fragments based on their size. Agarose gel purification was conducted following the second round of selection from a 4% agarose gel and after adapter ligation from a 2% agarose gel for NGS (next-generation sequencing) samples. A sample of DNA was cut out from the gel according to its size and then purified using NucleoSpin® Clean-Up kit (Macherey-Nagel). The gel piece was heated up in NTI buffer at 56°C until all the gel had dissolved. Subsequent purification was performed as described in **section 5.2.2.1**.

5.2.2.4 DNA Extraction from the cell lysate

Before performing selection, four different extraction methods were examined. 1000,000 PC-3 cells were collected into six 1.5 mL tubes. The cells were centrifuged at 200x g for 5 minutes. The cells were resuspended in 50 µL dd H2O, and 1 pmol of DNA library was added to five samples. After that, all the samples were heated at 95°C for 10 minutes. One sample was subsequently centrifuged at 15,000x g for 10 minutes. One sample was subjected to phenol-chloroform extraction, as explained in **section 5.2.2.2**. One sample was then purified using the G-25 (GE Healthcare) column, as described in the manufacturer's instructions. Another sample was purified using the NucleoSpin® Clean-Up kit (Macherey-Nagel), as described in **section 5.2.2.1**. Since it was feared that the purification methods would affect the yield of the bound fraction from the cells, the last sample was not purified. PCR reagents were added to each sample, as described in **table 5.2.4**. The PCR product was visualized on VWR Genoplex Gel Documentation System after running on a 4% agarose gel. Two

samples were included; positive control consists of 1 pmol of the DNA library with all PCR reagents but without cell lysates; negative control consists of cell lysates and all the PCR reagents.

5.2.3 λ-Exonucleases digestion

The single-stranded DNA (ssDNA) was generated using λ-exonuclease. The λ-exonuclease is a highly efficient enzyme, capable of digesting only phosphorylated 5'ends of double-stranded DNA (dsDNA). The exonuclease exhibits a low affinity for ssDNA and non-phosphorylated DNA [63]. ssDNA was generated by the end of each selection round using the amplicon from the ePCR. The concentration of amplicons was measured using Nanodrop, and digestion was initiated using 3 µl λ-exonuclease per 100 pmol dsDNA in 1x reaction buffer (Thermo Scientific). Incubation was conducted for 30 minutes at 37°C, 900 rpm. Agarose gel electrophoresis was performed to verify the reaction. Thereby the dsDNA was loaded as a control to monitor effective digestion. If the digestion was incomplete, the samples were incubated for 15 minutes and analyzed on an agarose gel for complete digestion. The samples were then purified using a PCR clean-up kit as described in **section**

5.2.4 Next-generation sequencing (NGS)

To perform NGS, the sample was prepared per the protocol by Tolle et al. {Tolle, 2016 #49 . Several samples were multiplexed using twelve different indexes introduced using PCR. These indices permit the loading of twelve samples into one sequencing run. Thus, PCR was conducted using 24 primers (12 FW-primers and 12 RV-primers) with twelve different index sequences. Listed below in **table 5.2.9**. Several SELEX cycles of enriched selections were amplified with these primers, and twelve samples were mixed and ligated to Illumina adapters.

This adaptation was performed using the TruSeq DNA PCR-Free Sample Preparation Kit LT (Ref. 15037063, Illumina). Afterward, the sample was purified via 2% agarose gel and NucleoSpin® Clean-Up kit (Macherey-Nagel) and was eluted in resuspension buffer. Using a KAPA library quantification kit (Sigma-Aldrich), the DNA is validated and quantified prior to sequencing. The sequencing was conducted by Prof. Joachim Schultze's group (LIMES, Bonn). Using an Illumina HiSeq 1500 instrument. Single-end sequencing of 75 bp was performed with the Illumina platform. AptaNext software was utilized to analyze the raw data (a program developed by Laura Lledo Byrant in-house).

Table 5.16 Sequence indexes used for NGS.

Index	**sequence**	**Index**	**sequence**	**Index**	**sequence**
Index 1	CGATGT	**Index 5**	CAGATC	**Index 9**	ACTTGA
Index 2	TGACCA	**Index 6**	CTTGTA	**Index 10**	GATCAG
Index 3	ACAGTG	**Index 7**	ATCACG	**Index 11**	TAGCTT
Index 4	GCCAAT	**Index 8**	TTAGGC	**Index 12**	GGCTAC

5.2.5 Click chemistry

Add 500 µl of water to 10 mg of sodium ascorbate powder to prepare a fresh 100 mM sodium ascorbate solution. Mix the solution vigorously until all the ascorbate has dissolved. 70 µl of water should be mixed with 4 µl of THPTA and 1 µl of CuSO4 at 100 mM each. Next, CuAAC catalyst solution is prepared by adding 25 µl of freshly prepared 100 mM sodium ascorbate solution, as shown in **Table 5.2.10**. Note: To ensure that the THPTA–CuI complex has formed, the catalyst solution must be left at room temperature for at least 10 - 15 minutes before adding it to the DNA and azide.

Table 5.17 Components of the catalyst solution

Components	Stock Conc.	Volume	Final Conc.
Water		70 µl	
THPTA	100 mM	4 µl	4 mM
$CuSO_4$	100 mM	1 µl	1 mM
Ascorbate	100 mM	25 µl	25 mM

In another tube, a total of 70 µl of the EdU DNA sample was mixed with 10 µl of 10 mM azide dissolved in DMSO and 10 µl of 0.1 M phosphate buffer. The click reaction was started by adding 10 µl of CuAAC catalyst solution to the mixture and incubating it for 45 minutes at 37 °C and 650 r.p.m, followed by purification of the modified DNA using a PCR clean-up kit**,** as described in **section 5.2.2.1**. Azides used within the selection include imidazole-azide (Im-dU), indole-azide (In-dU), ethanamine-azide (Ea-dU), isobutyl-azide (Ib-dU), and cyclic arginine-glycine-aspartic acid peptide (cRGD-dU) with a final concentration of 1 mM, except for isobutyl-azide, which had a final concentration of 30mM.

5.2.5.1 LC-MS

The strands of DNA were separated and analyzed by reversed-phase ion-pairing chromatography. A total of 100 pmol of test-oligo (5'- GCACTGTXCATTCGCG -3') was functionalized according to **section 5.2.4.** A reverse phase Agilent Zorbax 2.1x50mm, 5m (SB-C18) 2.1x100mm column was used to separate 15 pmol of DNA. The mobile phase was composed of 10 mM triethylammonium (TEA) and 100 mM hexafluoroisopropanol (HFIP). Gradients of 0-30% acetonitrile were applied over 20 minutes at 0.5 ml/min. The mass spectrometry was performed on an HTC Esquire (Brucker). For measurements with an Ultrascan in the negative mode, the settings were the following: 50 psi, dry gas: 10 l/min, dry temperature: 365°C, SPS: 1000 m/z, ICC: 70000, scan: 500-1500 m/z.

5.2.5.2 Nucleoside digestion

To perform the enzyme analysis of nucleosides, 100 pmol clicked DNA was incubated in 1x S1 nuclease reaction buffer and 50 U S1 nuclease for 60 min at 37°C and 800 rpm in 30 µl. A 3.5 µl alkaline phosphatase buffer and 0.5 U alkaline phosphatase (CIAP) (1 U/µl) were added, followed by 2.5 U snake venom phosphodiesterase I (5 U/Ml) and 125 U Benzonase® nuclease (250 U/µl). Incubation was performed at 37°C and 800 rpm for 120 min. After digestion, the samples were heated up to 95°C for 3 minutes and centrifuged for 3 minutes at 12000 rcf. A total of 20 µL of supernatant were used for HPLC analysis.

5.2.5.3 HPLC

Nucleoside samples were analyzed using an Agilent 1100 HPLC system coupled to a Bruker HTC Esquire mass spectrometer with a Phenomenex Synergi Fusion-RP column (2 x 50 mm, 4 mm). HPLC conditions were: 0.5 l/min flow; buffer A: 0.1% NH4OAc (pH 7); buffer B: Acetonitrile; gradient: 10 min 100 % A, then 20 min gradient to 30% B.

5.2.6 Working with cells

5.2.6.1 Cell culture

The cells were maintained under tissue culture standard conditions (37°C, 5% CO2, 95% humidity) for a maximum of two months. Trypsin was used to split the cells every 2-3 days for all cell lines. All cell lines were free of Mycoplasma contamination which was confirmed by Mycoplasma PCR (Minerva Biolabs) every three months

5.2.6.2 Cell lines

PC-3 cells (DSMZ, ACC 465) cells were cultured in 45% RPMI (Thermo Fischer) and 45% Ham's F-12 (Thermo Fischer) and 10% FCS (Sigma). LNCAP cells (DSMZ, ACC 256) were cultured in RPMI medium supplemented with 20% FCS. MCF-7 (ATCC, HTB-22), H460 (ATCC, HTB-177) Jurkat cells (TIB-152, ATCC), and Ramos cells (CRL-1596, ATCC) cells were cultured in RPMI medium supplemented with 10% FCS. HepG2 (ATCC, HB-8065), HEK293T (ATCC, CRL-3216) and Hela (ATCC, CCL-2), cells were cultured in DMEM (Thermo Fischer) supplemented with 10% FCS. J774A1 cells (mouse macrophages) were provided by Prof. Dr. Albert Hass (University of Bonn, German), Cultured in DMEM supplemented with 10% FCS, THP-1 cells (human monocytes) were provided by Prof. Dr. Albert Hass (University of Bonn, German), cultured in RPMI supplemented with 10% FCS. all the cell lines were cultured under tissue culture standard conditions.

5.2.7 Cell-SELEX

5.2.7.1 Split-combine cell SELEX

Various numbers of PC-3 cells were seeded in decreasing culture plate sizes based on the selection round, as shown in **Table 5.2.11**. The cells were incubated overnight at 37°C, 5% CO2, and 95%

humidity. In round 1, the M2 library (250 pmol for each) was clicked with the following azides independently: Indole (In-dU), Imidazole (Im-dU), cyclic RGD (cRGD-dU), ethanamine (Ea-dU), and Methylpropane (Mp-dU). The click reaction was performed as described in **section 5.2.4**. After that, the clicked library was purified using NucleoSpin®Clean-Up kit (Macherey-Nagel), as described in **section 5.2.2.1**. The concentration of clicked purified libraries was tested on Nanodrop 2000c, and 100 pmol of each functionalized library was combined to a total of 500 pmol. After combining the functionalized libraries, the libraries were heated at 80°C for 5 min and diluted directly in 4 mL selection buffer (RPMI medium supplemented with 10% FCS and 0.1 mg/ml ssDNA). The cells were washed twice with prewarmed DPBS, and RPMI containing 10% FCS before incubating with the clicked M2 library. The clicked M2 library was added to the cells for 45 minutes at 37ºC, 5% CO2, and 95% humidity, with agitation every five minutes. After the 45 min incubation, the supernatant was transferred to another 12 cm dish and incubated with PC-3 cells for 1.5 hour at 37ºC, 5% CO2, and 95% humidity, with agitation every five minutes. This way of incubation was named dual-incubation and the aim was to collect more binder sequences for the next round. The first and the second dish were washed with 4 mL RPMI medium supplemented with 10% FCS and incubated for 5 minutes. Afterward, 4 mL of RPMI medium was added to each plate, and the cells were scraped using a cell scraper. The cells were collected and transferred into a 15 mL conical tube. The cells were centrifuged for 5 min at 200x g. The supernatant was discarded, and 500 µl of dd H2O was added to the cells. The cells were transferred to a 2 ml tube, and the bound fraction was eluted by heating for 10 min at 95°C. to remove the cell debris, the cells were centrifuged for 10 min at 15,000 g. The supernatant was collected into another 2 ml tube. The nucleic acid was isolated using the phenol-chloroform protocol described in **section 5.2.2.2**. The upper phase was transferred to a 2 ml tube, and 3 µl of RNase A/T1 was added to digest RNA. For digestion, the tube was placed in a thermomixer at 37°C for 30 min. Followed by the NucleoSpin®Clean-Up kit (Macherey-Nagel), as described in **section 5.2.2.1**. The recovered ssDNA was amplified using ePCR with a total volume of 750 µl, as described in **section 5.2.1.4.4**. The amplification in round 1 was performed by using dNTPs. The EdUTP was not included in this particular amplification. After ePCR, the products were analyzed on 4% agarose gel, as described in **section 5.2.1.1**. The PCR product was purified using NucleoSpin®Clean-Up kit (Macherey-Nagel), as described in **section 5.2.2.1**. Subsequently, λ-exonuclease digestion was performed to digest the dsDNA, as described in **section 5.2.2.5**. Following digestion, the ssDNA was purified with NucleoSpin®Clean-Up kit (Macherey-Nagel), as described in **section 5.2.2.1**.

Round 2 was developed for this selection; this round aimed to remove most sequences that can bind to PC-3 without the clicked-in moieties. To achieve this, round 1 was amplified using dNTPs. The outcome is canonical ssDNA. The same steps were followed in round 1; however, the unbound fraction was isolated this time. After the dual-incubation, the unbound fraction was in a 4 ml RPMI

medium. the unbound fraction was purified using NucleoSpin®Clean-Up kit (Macherey-Nagel), as described in **section 5.2.2.1**. After purification, 3 µl of RNase A/T1 was added to digest RNA. For digestion, the tube was placed in a thermomixer at 37°C for 30 min. The amplification in round 2 was performed using an EdU mix (dATPs, dCTPs, dGTPs, and EdUTP). After amplification, the PCR product was analyzed on 4% agarose gel, followed by ethanol precipitation to decrease the volume. After ethanol precipitation, an agarose gel purification was performed to remove the genomic DNA obtained on the gel, as described in **section 5.2.2.3**. Another ePCR was conducted to increase the amount of PCR product for the next round.

Round 3 was performed as describe in round 1. The only difference was that only one incubation with PC-3 cells was performed for 45 min, and the ePCR was performed using an EdU mix.

LNCaP cells were included in the selection as a counter cell-line for the selection starting from round 4. 1 x10^6 of LNCap cells were seeded into 6 cm culture plates, and a dual incubation with LNCaP cells was performed, as shown in **Table 5.2.11**. the clicked rounds were incubated with LNCaP for 45 min in some rounds, and double incubation was performed to remove most of the sequences that can bind to all cell lines. Clicked competitors were included in the selection {Tolle, 2015 #5} to increase the selection stringency starting from round 4. The amount of clicked competitors was 200 pmol till the end of the selection. The clicked competitors were only applied during the incubation with PC-3 cells. More washing steps were applied to increase the stringency of the selection. The duration of the washing steps was always 3 min, but the number of washing steps increased with the selection round. After 9 rounds of selection, the enrichment was tested using the flow cytometer protocol described in section 3.

After initial enrichment, three more selection rounds were performed. These rounds are called the deconvolution step. The deconvolution step was performed to increase the copy number of the selected clickmers with a particular azide. In the deconvolution step, the enriched library from round 9 was clicked independently with the same azides, and after purification, there was no combining step. The selection round was performed using a single azide. The same protocol was followed as for round 9. In brief, the clicked library was incubated twice with LNCaP cells for 45 minutes each, followed by incubation with PC-3 cells for 45 minutes. Thereafter, heat elution, centrifugation, phenol-chloroform extraction, Macherey-Nagel purification, and ePCR were performed.

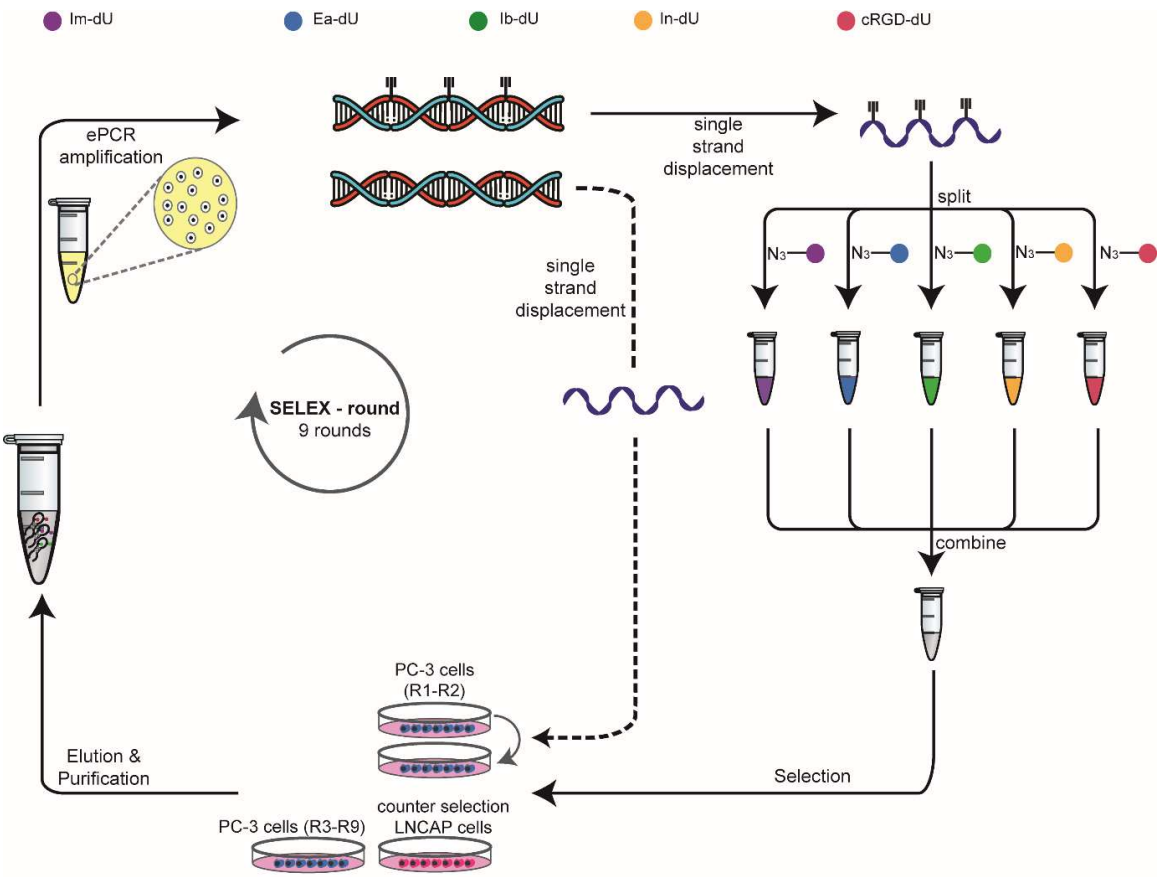

Figure 5.1 Schematic of split-combine cell SELEX
The ssDNA starting library was aliquoted into five parts. Each part was modified with one azide. The five aliquots were then combined after the click reaction. The selection was conducted on PC-3 cells. A dual-incubation was performed on PC-3 cells during the first round, the first incubation lasting 45 minutes and the second incubation lasting 1.5 hours. The bound sequences from both cells were recovered, and ePCR was performed on the bound fraction. Two different counter-selections were conducted. Round 2 was the first counter-selection, where the bound fraction from round 1 was amplified by ePCR utilizing thymidine instead of EdU. After λ-exonuclease digestion, the products were incubated with PC-3 cells to remove sequences binding to PC-3 cells without modifications. The exact incubation time was used in round 2 with dual-incubation to PC-3 cells. In Round 3, bound fractions from round 2 were amplified by ePCR with EdU, modified with the same azides used in round 1, then incubated with PC-3 cells once and eluted by ePCR. From round 4, LNCaP cells were included in the selection process as another counter-selection. In the selection process, stringency was increased by increasing the wash steps, adding more competitors (clicked competitors), increasing LNCaP cells, and decreasing PC-3 cells. Following nine rounds of selection, three rounds of deconvolution were performed to increase the number of copies of unique sequences that bind to PC-3 cells with a particular azide.

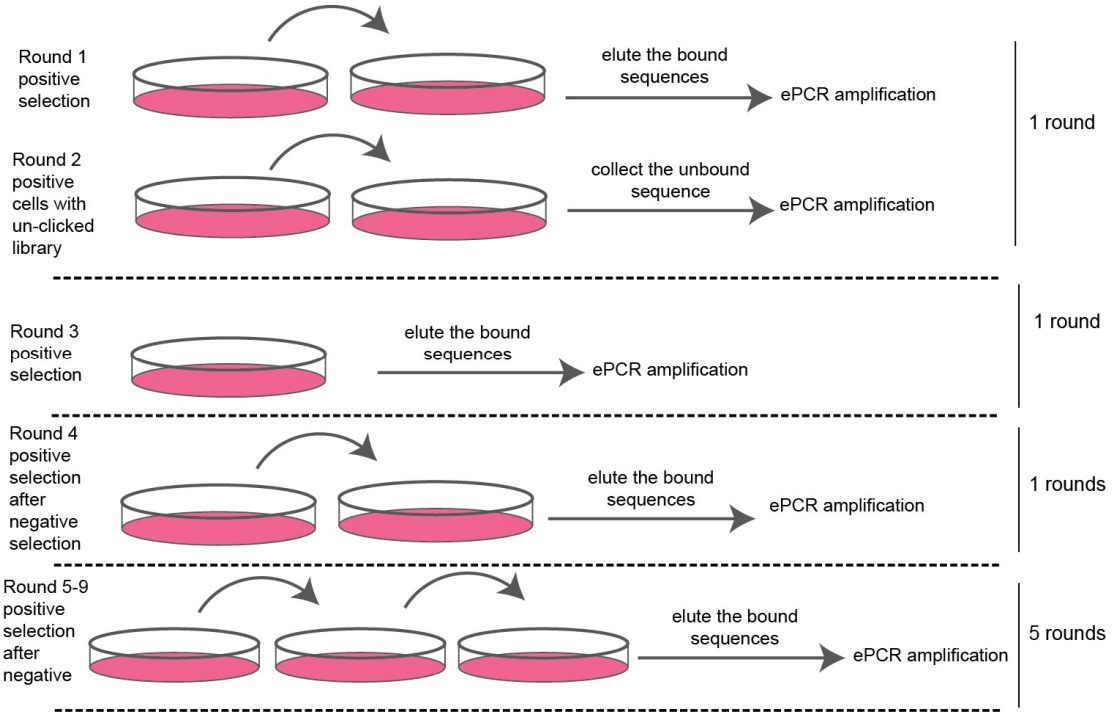

Figure 5.2 Split-combine cell SELEX procedure
This figure shows the concept of the dual incubation performed during the selection. In the first and second rounds, dual incubation was performed against PC-3 cells. In round 3, there was no dual incubation. Starting from round 4, dual incubation was performed against LNCaP cells (negative cells) to remove most sequences that can bind to all cell lines non-specifically.

Table 5.18 summary of split-combine cell SELEX conditions

Selection round	PC-3 cells count	Plate size (cm) PC-3 cells	LNCAP Cells count	Plate size (cm) LNCaP Cells	Dual-incubation	Incubation time (45 min)	Counter-selection incubation time (45 min)
1	$2X10^6$	12	No	No	With PC-3	2X PC-3	No
2	$2X10^6$	12	No	No	With PC-3	2X PC-3	No
3	$2X10^6$	12	No	No	No	1X PC-3	No
4	$1X10^6$	6	$1X10^6$	6	No	1X PC-3	1X LNCaP
5	$1X10^6$	6	$1X10^6$	6	With LNCaP	1X PC-3	2X LNCaP
6	$5X10^5$	6-well plates	$1X10^6$	6	With LNCaP	1X PC-3	2X LNCaP
7	$5X10^5$	6-well plates	$1X10^6$	6	With LNCaP	1X PC-3	2X LNCaP
8	$5X10^5$	6-well plates	$1X10^6$	6	With LNCaP	1X PC-3	2X LNCaP
9	$5X10^5$	6-well plates	$1X10^6$	6	With LNCaP	1X PC-3	2X LNCaP

10	$5X10^5$	6-well plates	$1X10^6$	6	With LNCaP	1X PC-3	2X LNCaP
11	$5X10^5$	6-well plates	$1X10^6$	6	With LNCaP	1X PC-3	2X LNCaP
12	$5X10^5$	6-well plates	$1X10^6$	6	With LNCaP	1X PC-3	2X LNCaP

Table 5.19 Summary of split-combine cell SELEX conditions

round	DNA (pmol)	Incubation volume	washes	Washes after centrifugation	Clicked com-petitors	ePCR	2nd ePCR
1	500	4 ml	2X/ 4 ml	No	No	22	No
2	20	4 ml	2X/ 4 ml	No	No	22	10
3	20	4 ml	2X/ 4 ml	1X/ 7 ml	No	22	5
4	20	2 ml	2X/ 4 ml	2X/ 7 ml	200 pmol	28	8
5	20	2 ml	2X/ 4 ml	2X/ 7 ml	200 pmol	29	6
6	20	2 ml	2X/ 4 ml 1X/ 7 ml	2X/ 7 ml	200 pmol	30	5
7	20	2 ml	2X/ 4 ml 1X/ 7 ml	2X/ 7 ml	200 pmol	30	4
8	15	2 ml	2X/ 4 ml 1X/ 7 ml	2X/ 7 ml	200 pmol	30	No
9	15	2 ml	2X/ 4 ml 1X/ 7 ml	2X/ 7 ml	200 pmol	30	No
10	15	2 ml	2X/ 4 ml 1X/ 7 ml	2X/ 7 ml	200 pmol	30	No
11	15	2 ml	2X/ 4 ml 1X/ 7 ml	2X/ 7 ml	200 pmol	29	No
12	15	2 ml	2X/ 4 ml 1X/ 7 ml	2X/ 7 ml	200 pmol	29	No

5.2.7.2 DNA cell-SELEX

The DNA cell SELEX was conducted using the split-combine cell protocol as described in **section 5.2.6.1**. Modifications were made in round 2 where LNCaP were used. Furthermore, no clicked competitors were used during the entire selection process. However, additional washing steps were applied in order to increase the selection stringency, as described in **table 5.2.13 and table 5.2.14**.

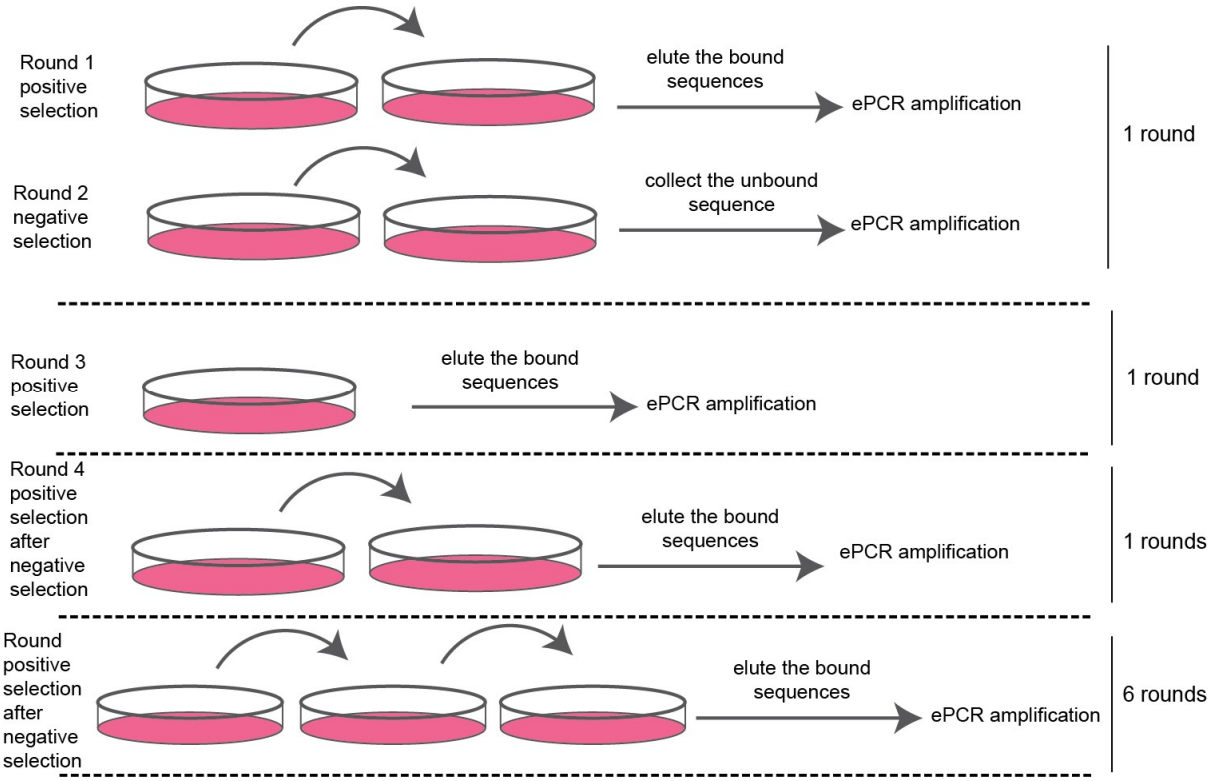

Figure 5.3 DNA cell SELEX procedure
The DNA cell SELEX was performed as described in the figure. The starting library was incubated with PC-3 cells, and after 45 min of incubation, the supernatant was transferred to another cell culture dish having PC-3 cells. the bound fraction from both dishes was eluted and amplified with ePCR for the next round. Round 2 is a counter selection, the enriched sequences from round 1 were incubated with LNCaP cells, and the unbound fraction was collected and amplified by ePCR. Afterwards, round 3 was performed by incubating the enriched sequences from round 2 with PC-3 cells. LNCAP was included in the selection rounds as a negative cell line.

Table 5.20 Summary of DNA cell SELEX conditions.

round	DNA (pmol)	Incubation volume	washes	Washes after centrifugation	ssDNA (mg/ml)	ePCR
1	500	4 ml	2X/ 4 ml	No	0.01	22
2	20	4 ml	2X/ 4 ml	No	0.01	22
3	20	4 ml	2X/ 4 ml	1X/ 7 ml	0.1	22
4	20	2 ml	2X/ 4 ml	1X/ 7 ml	0.1	22
5	20	2 ml	2X/ 4 ml	2X/ 7 ml	0.1	25
6	20	2 ml	2X/ 4 ml	2X/ 9 ml	0.1	25

			1X/ 7 ml			
7	20	2 ml	2X/ 4 ml 1X/ 7 ml	2X/ 9 ml	0.1	27
8	20	2 ml	2X/ 4 ml 1X/ 7 ml	2X/ 9 ml	0.1	27
9	15	2 ml	2X/ 4 ml 1X/ 7 ml	2X/ 9 ml	0.1	27
10	15	2 ml	2X/ 4 ml 1X/ 7 ml	2X/ 9 ml	0.1	30

Table 5.21 Summary of DNA cell SELEX conditions

Selection round	PC-3 cells count	Plate size (cm) PC-3 cells	LNCAP Cells count	Plate size (cm) LNCaP Cells	Dual-incubation	Incubation time (45 min)	Counter-selection incubation time (45 min)
1	$2x10^6$	12	No	No	With PC-3	2X PC-3	No
2	No	No	$2X10^6$	12	With LNCaP	No	2X LNCaP
3	$2x10^6$	12	No	No	No	1X PC-3	No
4	$1x10^6$	6	$1X10^6$	6	No	1X PC-3	1X LNCaP
5	$1x10^6$	6	$1X10^6$	6	With LNCaP	1X PC-3	2X LNCaP
6	$5x10^5$	6-well plates	$1X10^6$	6	With LNCaP	1X PC-3	2X LNCaP
7	$5x10^5$	6-well plates	$1X10^6$	6	With LNCaP	1X PC-3	2X LNCaP
8	$5x10^5$	6-well plates	$1X10^6$	6	With LNCaP	1X PC-3	2X LNCaP
9	$5x10^5$	6-well plates	$1X10^6$	6	With LNCaP	1X PC-3	2X LNCaP
10	$5x10^5$	6-well plates	$1X10^6$	6	With LNCaP	1X PC-3	2X LNCaP

5.2.8 Interaction analysis

5.2.8.1 ^{32}P labelling of ssDNA

For a radioactive binding assay, the ssDNA was labeled with ^{32}P at its 5' end using T4 polynucleotide kinase (PNK). The reagents (**Table 5.2.14**) were mixed and incubated at 37°C and 300 rpm for 1

hour. To remove the unreacted 32P-ATP, the labeled DNA was passed through a G25 spin column (GE Healthcare).

For background binding analysis, the starting library (EdU-M2 library) was clicked with the following azides: 3-(2-azidoethyl) benzofuran (BF-dU), 5-(azidomethyl) benzo[d][1,3] dioxole (Bd-dU), 4-(2-azidoethyl) morpholine (Mp-dU), 4-(2-azidoethyl) -1H-imidazole (Im-dU), cyclic RGD (cRGD), 1-azido-2-methylpropane (Ib-dU) , 2-azido-ethanamine (Ea-dU), 3-(2-azidoethyl)-1H-indole (In-dU), as described in **section 5.2.4**. After clicking in the azides. The clicked starting library was purified using NucleoSpin® Clean-Up kit (Macherey-Nagel).

Table 5.22 Pipetting scheme for one reaction of ^{32}P labeling of DNA

Reagent	Stock concentration	Final concentration	Volume (µl)
ssDNA	1µM	10 pmol	10
dd H2O	----------	----------	5
T4 PNK reaction buffer	10X	1 X	2
γ-^{32}P-ATP	10 UCi/µl	10 µCi	1
T4 PNK	10 U/µl	20 U	2

5.2.8.2 Cell binding assay using Cherenkov protocol

1.0 x 10^5 PC-3 cells were seeded into 24-well plates and cultivated for 24 hours. The cells were washed once with prewarmed DPBS and once with prewarmed RPMI medium. PC-3 cells were incubated with 1 pmol of ^{32}P-starting library M2 in 500 µl of DPBS, RPMI medium, RPMI medium supplemented with 10% FCS or RPMI medium containing different competitors (ssDNA, BSA, clicked competitors 1:1 or 1:10 ration (starting library: clicked competitors). The starting library was incubated with PC-3 cells for 45 min. After incubation, the incubation buffer was collected in 1.5 tubes as fraction 1. The cells were washed twice with 500 µl DPBS or RPMI medium. Both washes were collected as fractions 2 and 3. 500 µl trypsin was added for 5 min at 37 °C for cell detachment. the trypsin was collected as a fraction 4. The radioactivity for each fraction was measured using the liquid scintillation counter WinSpectral (Perkin Elmer). The percentage of the bound ^{32}P-starting library was calculated using the following formula:

$$\% \text{ Bound DNA} = \left\{\frac{fraction\ IV}{Fraction\ I + fraction\ II + fraction\ III + fractio\ \ IV}\right\} X\ 100$$

5.2.8.3 Flow cytometry

5.2.8.3.1 DNA cell SELEX and split-combine cell SELEX interaction study

5.2.8.3.1.1. Interaction study in 24-well plate

$1.0x10^5$ PC-3 cells were seeded into 24-well plates and cultivated for 24 hours. The cells were washed once with prewarmed DPBS and once with prewarmed RPMI medium with a total volume of 500 µl. PC-3 cells were incubated with 27 pmol of clicked labeled with ATTO 647N starting library, round9 and round 12 clicked with different azides in 290 µL of RPMI medium containing 10% FCS, 0.1 mg/mL ssDNA and 1:1 ratio of clicked competitors for 45 min. Then, cells were washed three times with (500 µL, 500 µL, and 1 mL) prewarmed RPMI medium. The cells were scraped and transferred into FACS tubes. The samples were centrifuged for 5 minutes at 200xg, and the supernatant was removed for volume reduction. 20,000 cells were analyzed using flow cytometry.. Testing the binding ability of the S1, S1 SC scramble sequence, S2, and S2 SC scramble sequence with different azides was performed with the protocol mentioned above.

For the DNA sequences obtained from the DNA cell-SELEX, the following protocol was used to evaluate the binding ability between the sequences (MD1, MD2, MD3, MD4, MD5, MD6, MD7, MD8, and MD9) and PC-3 cells. $1.0x10^5$ PC-3 cells were seeded into 24-well plates and cultivated for 24 hours. The cells were washed once with 200 µl prewarmed DPBS and once with 200 µl prewarmed RPMI medium. PC-3 cells were incubated with 250 nM ATTO 647N labeled aptamers in 290 µL RMPI medium containing 10% FCS, 0.5 mg/mL ssDNA for 45 min. cells were washed three times (500 µL, 500 µL, and 1 mL) with prewarmed RPMI medium. The cells were scraped and transferred into FACS tubes. The samples were centrifuged for 5 minutes at 200xg, and the supernatant was removed for volume reduction. 20,000 cells were analyzed using flow cytometry.

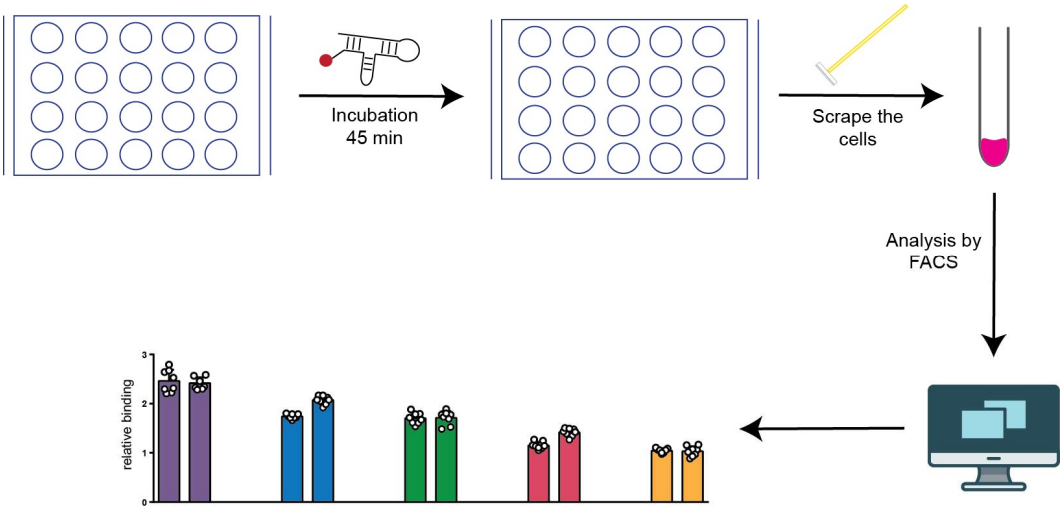

Figure 5.4 Illustrate the main points of the flow cytometer procedure
Starting from seeding the cells, incubating the labeled clickmer, scraping the cells and transfer into FACS tubes, and at the end, analyzing the fluorescence using a flow cytometer and plotting the data using a graph prism.

5.2.8.3.1.2. Interaction study in 48-well plate

30,000 PC-3 cells were seeded into 48 well-plate and cultivated for 24 hours. The cells were washed once with 100 µl prewarmed DPBS and once with 100 µl RPMI medium. The cells were incubated with 47.8 nM of ATTO 647N labeled S1 clicked with different azides or ATTO 647N labeled and clicked S1 SC in 45 µL of RPMI medium supplemented with 10%FCS, 2.87 mg/ml BSA, 0.287 mg/ml ssDNA and 1:1 ratio (aptamer: clicked competitors) for 45 min. Then, the cells were washed three times (200 µL, 200 µL, and 400 µL) with prewarmed RPMI medium. The cells were scraped and transferred into FACS tubes. The samples were centrifuged for 5 minutes at 200xg, and the supernatant was removed for volume reduction. 20,000 cells were analyzed using the BD FACS Canto II in mean fluorescence intensities (MFI) acquisition mode. This protocol was used during the EdU study (X5T, X6T, X11T, X13T, X36T, X37T, X38T, and X42T), testing different variants of S1 clickmer (S1.5, S1.4, S1.3, and S1.2) and the truncation study (S1.42, S.36, S1.35, S1.33).

5.2.8.3.1.3. Competition assay

For the competition assay, the protocol in **section 5.2.7.3.1.2** was used. The ratio between the labeled to unlabeled clickmer was (1:10). The labeled clickmer was 48.7 nM, and the concentration of unlabeled clickmer was 487.5 nM.

5.2.8.3.1.4. Concentration-dependent assay

For the concentration-dependent assay, the protocol in **section 5.2.7.3.1.2** was used, but different concentrations of the clicked and labeled S1 or clicked and labeled S1 SC were applied to PC-3 cells. Eight different concentrations were used (0.956 nM, 9.56 nM, 23.9 nM, 47.8 nM, 95.7 nM, 191.4 nM, 335 nM, and 478.5 nM). The ratio between the clickmer and the clicked competitor was (1:1). Different concentration of the clicked competitor was used depending on the concentration of the clickmer.

5.2.8.3.1.5. Specificity test

For testing the specificity, the cells were seeded at a different amount to have the next day 80% confluency. The cells were seeded into 48-well plates. 30,000PC-3 and H460 cells were seeded into a 48-well plate. 65,000 cells of HEK 293T, HELA, MCF-7, and 90,000 HEPG-2 cells were seeded into a 48-well plate. After seeding, the protocol in **section 5.2.7.3.1.2** was used.

The binding of S1 with Suspended PC-3 or LNCaP cells was also tested using the following protocol. The cells were detached using cold DPBS with 2 mM EDTA and centrifuged at 200xgg for 5 min.

The supernatant was replaced by RPMI medium supplemented with 10% FCS. The cells were counted, and 50,000 were incubated with 48.7 nM concentration of the clicked labeled clickmers in RPMI medium supplemented with 10% FCS 2.87 mg/ml BSA, 0.287 mg/ml ssDNA, and 1:1 ratio (clickmer: clicked competitors) for 45 min. After 45 min of incubation, the cells were washed twice with 2 mL RPMI medium with 10% FCS and centrifuged at 200xg for 5 min. 20,000 cells were analyzed in a flow cytometer. Mean fluorescence intensities (MFI) were acquired by BD FACS Canto II and analyzed by FlowJo software.

5.2.8.3.1.6. Binding at 4°C and 37°C

The binding at 37°C and 4°C was performed as described in **section 5.2.7.3.1.2**. Some steps in the protocol changed for the binding at 4°C. First, before the binding experiment, the cells were placed on ice for 10 min, and the cells were placed on the ice box during the whole procedure. Second, the cells were washed with cold DBPS and RPMI medium before the incubation and with cold RPMI after the incubation step. Finally, the cells were centrifuged at 4°C in a refrigerated centrifuge during the centrifugation.

5.2.8.3.1.7. Binding of biotinylated aptamer

The same protocol mentioned above was used for testing the binding of the biotinylated clickmer. Before the binding experiment, the biotinylated clickmers were coupled first with ATTO 647N streptavidin. The coupling was performed in dd H2O at a concretion of 2,5 µM for each. After that, we incubated them at room temperature in the dark for 30 min. after the coupling was completed, the labeled clickmers were incubated with the cells as mentioned in **section 5.2.7.3.1.2**

5.2.8.3.2 Interaction analysis of DC-12

THP-1 cells were counted using a hemacytometer, and then $4.0x10^5$ cells were resuspended in FACS tubes. THP-1 cells were incubated with 250 nM of the aptamers labeled with ATTO 647N for 10 minutes at 37 °C and 5% CO2 in 100 µl of culturing medium (RPMI 10%FCS). Then, the cells were washed with 2 mL of prewarmed washing buffer (DPBS, 1 mM MgCl2). the cells were centrifuged for 5 minutes at 200 x g. the supernatant was discharged, and the cells were rewashed with 1 mL of washing buffer. After that, the cells were centrifuged again, and the supernatant was discharged to reduce the volume. Fifty thousand cells were analyzed in the flow cytometer. Mean fluorescence intensities (MFI) were acquired by BD FACS Canto II and analyzed by FlowJo software (BD).

The binding assay at 4°C was also done using the same protocol mentioned above, but to test the binding at 4 °C the cells were resuspended in a cold medium, and the aptamers were incubated with cells in ice. The washing buffer was prepared before the experiment and incubated in ice for 30 min. the samples were centrifuged at 4 °C. after the washes, fifty thousand cells were analyzed in the flow cytometer. Mean fluorescence intensities (MFI) were acquired by BD FACS Canto II and analyzed by FlowJo software (BD).

5.2.8.3.2.1. Binding of the biotinylated DC-12 aptamer

The binding assay of biotinylated aptamers was done as the same protocol mentioned above. Still, the biotinylated aptamers were incubated with streptavidin 488 Alexa Flour for 30 min in the dark at room temperature. Then the coupled aptamers were incubated with the cells. The same protocol was used as before **section 5.2.7.3.2**.

5.2.8.3.2.2. test the specificity

the binding interaction between the DC-12 and THP-1, Jurkat, and Ramos cells was tested using the following protocol: 3'-biotinylated DC-12 was first coupled to streptavidin 488 Alexa flour for 30 min in the dark at room temperature. DC-12 SC1, DC-12 SC2 and G24A were used as negative controls. They were also coupled to streptavidin 488 Alexa flour.

For the attached cells (PC-3 and Hela cells). the following protocol was used to test the specificity of DC-12. 1 x 10^5 of PC-3 cells and Hella cells were seeded into a 24-well plate and cultivated for 24 hours. The cells were washed once with a prewarmed washing buffer. the cells were incubated with 250 nM of 3'- ATTO 647N labeled aptamers for 10 minutes at 37 °C and 5% CO2 in 200 µl Binding buffer (RPMI 10%FCS). Then, cells were washed once times with 2 mL prewarmed washing buffer. The cells were scraped and transferred into FACS tubes. The samples were centrifuged for 5 minutes at 200 x g and the supernatant and the washing step was repeated again but the cells were washed with 1 mL of washing buffer. After that, the supernatant discarded to reduce the volume. thirty thousand cells were analyzed in flow cytometer. Mean fluorescence intensities (MFI) were acquired by BD FACS Canto II and analyzed by FlowJo software.

5.2.8.3.3 working with D-7 aptamer

5.2.8.3.3.1. Binding of the biotinylated D-7

2 x 10^5 J774A1 cells were seeded into 24-well plates and cultivated for 24 hours. The biotinylated variants of D-7 were incubated with streptavidin 488 Alexa Flour for 30 min in the dark at room

temperature. The ratio between the biotinylated aptamer and streptavidin 488 Alexa Flour is (1:1). The cells were washed once with a prewarmed washing buffer. J774A1 cells were incubated with 250 nM of the coupled aptamers with streptavidin 488 Alexa for 10 minutes at 37 °C and 5% CO2 in 200 µl binding buffer (DMEM 10%FCS). Then, cells were washed once times with 2 mL pre-warmed washing buffer. The cells were scraped and transferred into FACS tubes. The samples were centrifuged for 5 minutes at 200 x g, the supernatant and the washing step were repeated, and the cells were washed with 1 mL of washing buffer. After that, the supernatant discarded to reduce the volume. fifty thousand cells were analyzed in a flow cytometer. Mean fluorescence intensities (MFI) were acquired by BD FACS Canto II and analyzed by FlowJo software (BD).

5.2.8.3.3.2. competition assay between D-7 and its variants

For the competition assay, the protocol in **section 5.2.7.3.3.1** was used with some changes. 2 x 10^5 J774A1 cells were seeded into 24-well plates and cultivated for 24 hours. J774A1 cells were incubated with 250 nM of 5'- ATTO 647N labeled D-7 for 10 minutes at 37 °C and 5% CO2 in 200 µl binding buffer (DMEM 10%FCS). The biotinylated variants (5'-biotinylated D-7, and 5'-Biotinylated C18 D-7, There is a C18 linker between the biotin and D-7. 3'-Biotinylted D-7) was added to the cells with the labeled D-7 aptamer at different ratio (1:2) (1:4) (1:8) (labeled: biotinylated). D-7 unlabeled was used as a positive control for this experiment. Unlabeled Ctrl2 was also included in the experiment as a negative control. Then, cells were washed once times with 2 mL prewarmed washing buffer. The cells were scraped and transferred into FACS tubes. The samples were centrifuged for 5 minutes at 200 x g, the supernatant and the washing step were repeated, and the cells were washed with 1 mL of washing buffer. After that, the supernatant discarded to reduce the volume. fifty thousand cells were analyzed in a flow cytometer. Mean fluorescence intensities (MFI) were acquired by BD FACS Canto II and analyzed by FlowJo software (BD).

5.2.8.4 Confocal microscopy

5.2.8.4.1 Internalization study for S1 clickmer

80 thousand PC-3 cells or 160 thousand MCF-7 cells were seeded on round coverslips. The round coverslips were washed with ethanol for 30 min, then washed again with DPBS and placed into a 4-well plate. The coverslips were rewashed with DPBS, and then the cells were seeded on the coverslips for 24 hours for attachment. After 24 hours, the cells were washed twice, once with prewarmed DPBS and once with prewarmed RPMI. The cells were incubated with 50nM of clicked labeled with ATTO 647N S1 or S1 SC with different azides in 290 µL of RPMI medium containing 10% FCS, 0.1 mg/mL ssDNA and 50nM of clicked competitors for 45 min. Then, cells were washed three times with

(500µL, 500 µL and 1 ml) prewarmed RPMI medium. The cells were fixed using 4% paraformaldehyde for 20 min at room temperature. After fixation, the cells were washed three times with DPBS, each time with 500 µL. The membrane was stained with WGA 488 (12.5 µg/mL) for 10 min. The cells were rewashed three times with DPBS. The nuclei were stained with (1 µg/mL) DAPI in DPBS for 5 min. The cells were washed three times with DPBS and then twice with ddH2O, the first time with 2 mL and the second time with 1 mL. The coverslips were mounted onto the slides with a flourogel mounting medium. After 24 hours, the coverslips were sealed, and analyze the slides were using LSM 710 confocal laser scanning microscopy.

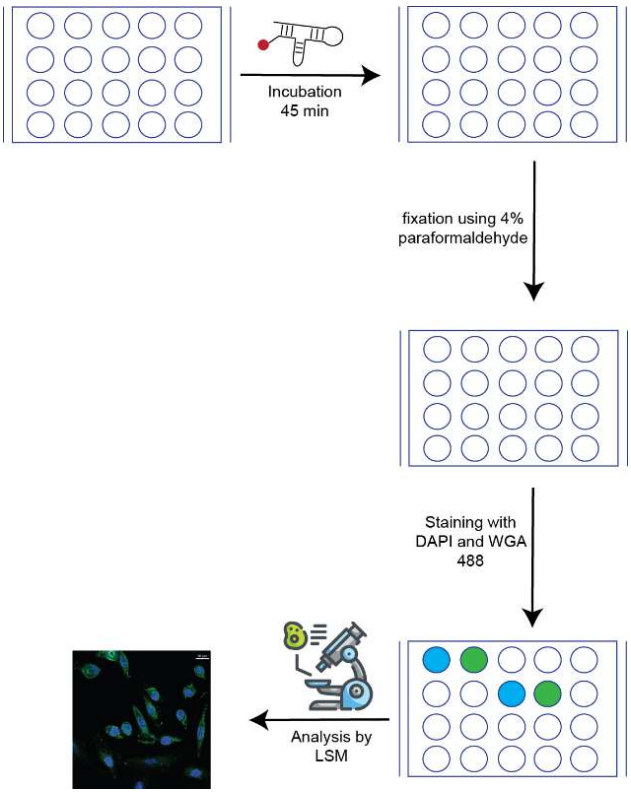

Figure 5.5 Shows the procedure of the internalization study.

5.2.8.4.2 Inhibit the internalization of D-7 aptamer

2 x 10^5 J774A1 cells were seeded into a 24-well plate covered before with round coverslips. The coverslips were cleaned with 80% ethanol for 15 min and washed twice with DPBS. The cells were cultivated for 24 hours. The next day, the cells were washed with 500mL of prewarmed or cooled washing buffer. The cells were treated with 100uM of Dynasore, 160uM Genistein or washing buffer for 30 min in ice or at 37 °C. the cells were washed with washing buffer, and the labeled aptamers with ATTO 647N were added at the concentration 250nM for 10 min at 37 °C or in ice. Then, the cells were washed trices with 0.5mL, 1 ml and 1 ml of washing buffer. The cells were fixed using 200uL of 4% paraformaldehyde for 15 min at room temperature. followed by the washing step with DPBS three times with 1 ml. The membrane was stained with WGA Alexa Flour 488 (200ug/mL in

300uL DPBS) for 10 min at room temperature. The cells were washed trices with 1 ml of DPBS. The nuclei were stained with1 µg/ml DAPI (0.5 µl 1 mg/ml DAPI in 500 µl DPBS) for 5 min at room temperature and washed trice with DPBS, once with 2 ml ddH2O. The coverslips were mounted onto the slides carefully with fluorogel mounting medium. The slides were placed in the dark overnight at RT, and on the next day microscopy data of the slides were acquired using LSM 710 confocal laser scanning microscope (Zeiss). Percentages of positive cells were estimated by manually counting, amounting between 150 to 200 cells in total.

5.2.9 Pull-down assay

5.2.9.1 DC-12 aptamer

5.2.9.1.1 THP-1 cell membrane protein extract

The method is based on the protocol [195]. THP-1 cells were counted using hemocytometry, and then the cells were washed with 10 mL cooled DPBS and centrifuged at 1000 x g for 3 min. The cell pellet was resuspended in 750 µL cooled homogenization buffer (300 mM Sucrose, 5 mM Tris-HCl pH 7.4, 0.1 mM EDTA and 1 mM PMSF). After that, the cells were transferred into a homogenizer, and approximately one hundred strokes were applied. The solution was collected into a 1.5 mL tube and centrifuged at 800 x g for 5 minutes at 4°C. The supernatant was transferred into a new 2 ml Eppendorf tube and centrifuged for two hours at 20,000 x g and 4 °C. yielding a pellet of membrane fraction. The pellet was washed carefully with cold DPBS and centrifuged again in the same condition for one hour. The supernatant containing the cytosolic fraction was discarded, and the pellet was resuspended in 100 µL of storage buffer (5 mM Tris-HCl, pH 7.4, 1 mM PMSF). The membrane fraction solution was stored at -20 and loaded into the SDS-PAGE in different volume.

5.2.9.1.2 Blue silver staining

The method is based on the protocol of Candiano et al [196]. After electrophoresis, the SDS-PAGE gel was incubated for 30 min in a fixing solution (50% (v/v) Ethanol 2% (v/v) Phosphoric acid), followed by two times washing steps with dd H2O for 20 min each. Then, the gel was stained with silver-impregnating solution (10% (v/v) Phosphoric acid, 10% (v/v) Ammonium sulfate, 0.12% (w/v) G-250 Coomassie, 20% (v/v) Methanol) overnight. The gel was washed with dd H2O for one hour the next day.

5.2.9.1.3 Glutaraldehde-Silver stain

The staining is based on the methodology of Heukeshoven and Dernick and modified after Jin et al. [197] [198]. First, the gel was incubated for 30 min in 125 mL fixing solution (40% (v/v) Ethanol, 10% (v/v) Acetic acid), followed by 30 min in 125 mL sensitizing solution (6.8% (v/v) Sodium acetate, 0.125% (v/v) Glutaraldehyde, 0.2% (w/v) Sodium thiosulfate). After this, the gel was washed three times with 125 mL double-distilled water for 5 min and then incubated for 20 min with 125 mL silver impregnating solution (0.015% (v/v) Formaldehyde, 0.25% (w/v) Silver nitrate). Next, the gel was washed twice with 125 mL double-distilled water for 1 min and 125 mL developing solution (3% (w/v) Sodium carbonate, 0.008% (v/v) Formaldehyde) was added for 8 min. The reaction was ended by adding 125 mL stopping solution (1.5% (w/v) EDTA)

5.2.9.1.4 Pull-down assay for DC-12

The method is based on the protocol of [199]. 100 µL of Dynabeads M-280 Streptavidin was washed three times with 500 µL, 600µL and 700µL of DPBS, and then 100 pmol of the biotinylated aptamers (DC-12, Ctrl2) were incubated with the beads at 21°C for 1 hour at 1000 rpm and pipetting up and down every 10 min for coupling. After that, the coupled beads were washed once with 500 mL of culturing medium (RPMI 10%FCS). The following steps were done in a cold room on the ice, 1.5 million THP-1 cells were added to the coupled beads and incubated for 30 minutes, and each sample was pipetted up and down every 5 min. After incubation, the samples were transferred to a 12-well plate, and the supernatant of unbound cells was removed by applying a strong magnetic force. Then, the beads were washed twice with 1 mL washing buffer (DPBS, 1 mM MgCl2). The ice-cold cell lysis buffer (DPBS, 1 mM MgCl2, 1% NP40, 0.1% protease inhibitor cocktail) was added and incubated for 30 minutes. Next, the supernatant of unbound cell lysate was discarded, and the remaining beads were washed trice with 1 mL washing buffer II (DPBS, 1mM MgCl2, 0.05% protease inhibitor cocktail, 1mM PMSF). Finally, the isolated protein complex was recovered with 15 µL dd H2O and 5 µL 4x Laemmli buffer by heat (10 min; 95 °C) or with 15 µL of 5M or 8M urea by heating to 37°C for 10 minutes Subsequently, the beads were removed. The supernatant was loaded on an SDS-PAGE or stored at -20 °C. After electrophoresis, the gel was stained with glutaraldehyde-silver. For the MagStrep Type 3 X beads, the same protocol was that mentioned above, but we used 25 µL of the beads, and the elution, was performed at 95°C for 10 min.

5.2.9.2 D-7 pull-down assay

The method is based on the protocol of [188]. One million of J774A1 cells were seeded in a 6-well plate and cultivated for 24 hours. The cells were washed with cooled DPBS. 100uM of Dynasore was incubated with cells for 30 min at ice and then the cells were washed with 1 ml of washing buffer has been done with. 200pmole of 5'- biotinylated D-7 or Control 2 was incubated with cells for 10

min in 1 mL of culturing medium (DMEM 10% FCS). After that, the cells were washed three times with 2 ml, 2 ml and 1 ml of washing buffer (DPBS, 1 mM MgCl2). The cells were scraped and centrifuged to reduce the volume to 500 µL and the samples were transferred to a 1.5 ml Eppendorf tube. All the steps after were done in the cold room, 1 mg of Dynabeads M-280 Streptavidin was added and incubated with cells for 30 min. the cells were mixed every 5 min with pipetting up and down. After incubation, the samples were transferred to a 12-well plate, and the supernatant of un-bound cells was removed by applying a strong magnetic force. Then, the beads were washed twice with 1 mL washing buffer (DPBS, 1 mM MgCl2). The ice-cold cell lysis buffer (DPBS, 1 mM MgCl2, 1% NP40, 0.1% protease inhibitor cocktail) was added and incubated for 30 minutes. Next, the supernatant of unbound cell lysate was discarded, and the remaining beads were washed trice with 1 mL washing buffer II (DPBS, 1mM MgCl2, 0.05% protease inhibitor cocktail). Finally, the isolated protein complex was recovered with 15 µL double-distilled water and 5 µL 4x Laemmli buffer by heat (10 min; 95 °C) the beads were removed, and the supernatant was loaded on an SDS-PAGE or stored at - 20 °C. After electrophoresis, the gel was stained with glutaraldehyde-silver.

5.2.9.3 S1 pull-down assay

The pull-down assay for S1 clickmer was performed first using the following protocol. 100 µl of Dynabeads M-280 Streptavidin beads were taken and placed in a 1,5 ml tube. The beads were washed with RPMI medium without FCS or phenol red three times with 100 µl, 120 µl, and 150 µl. 50 pmol of biotinylated S1 clicked with imidazole (im-dU) or cyclic RGD (cRGD-dU) was incubated with the 100 µl of streptavidin Dynabeads in a total volume of 200 µl of RPMI medium. The clickmer and the beads were incubated for 45 min at 37°C and 1400 rpm for coupling. Afterwards, the unbound clickmer was washed with RPMI medium without FCS or phenol red three times with 200 µl. 1 million PC-3 cells were added to the coupled clickmer in 1 ml RPMI medium without FCS or phenol red supplemented with 1 mg/ml ssDNA and 100 pmol of clicked competitors for 45 min at 37°C and 1400 rpm for binding. After binding the coupled aptamer with the cells, the beads were washed three times with 1 ml of cold RPMI medium without FCS or phenol red. Then the cell lysis buffer (RPMI medium without FCS or phenol red, 1%NP-40, 10 mg/ml PSMF) was added to lyse the cells for 30 min at 4°C. After cell lysis, the beads were washed four times with 1 ml cold RPMI medium without FCS or phenol red. Then the bound fraction was eluted using 8,3 M urea with 0.3% tri-acid. The eluted fraction was loaded on 10% SDS-PAGE gel.

During the optimization of the pull-down assay, different parameters were changed—first, the cell count. Initially, we used 1 million cells; later, we tried with 500,000 and 100,000 cells. Second, the incubation time between the coupled clickmer with cells changed from 45 min to 30, 20 and 10 min. Third different amounts of clickmer were used. Initially, we used 50 pmol, but later we tried 30, 20, and 10 pmol; during this change, the beads amount was also changed from 100 µl to 50 µl. The final parameters used for the pull-down assay were the following. 50 µl of Dynabeads M-280 Streptavidin

beads were incubated with 30 pmol of biotinylated S1 clickmer. After coupling and washing, 500,000 PC-3 cells or MCF-7 were incubated with the coupled clickmer for 20 min. The beads were washed three times, and the bound fraction was eluted using 8,3 M urea with 0.3% tri-acid. The eluted fraction was loaded on 10% SDS-PAGE gel.

6 SUPPORTING INFORMATION

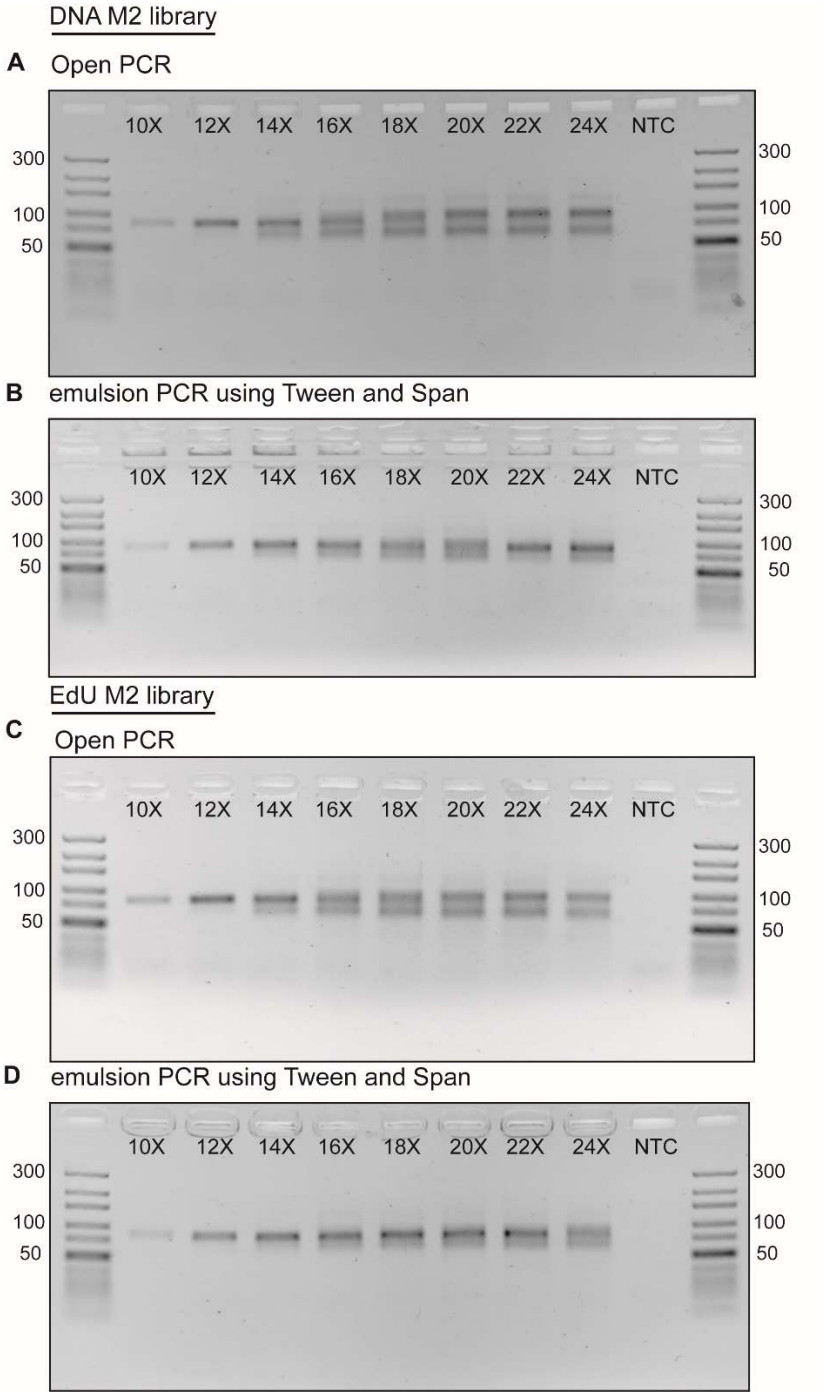

Figure 6.1 llustrates the comparison between emulsion PCR (ePCR) and conventional PCR.
Using DNA M2 library **(A)** and **(B)** The results of ePCR and conventional PCR were compared by running 4% agarose gels stained with ethidium bromide from 10 to 26 PCR cycles. Using EdU M2 library **(C)**and **(D)** The results of ePCR and conventional PCR were compared by running 4% agarose gels stained with ethidium bromide from 10 to 26 PCR cycles.

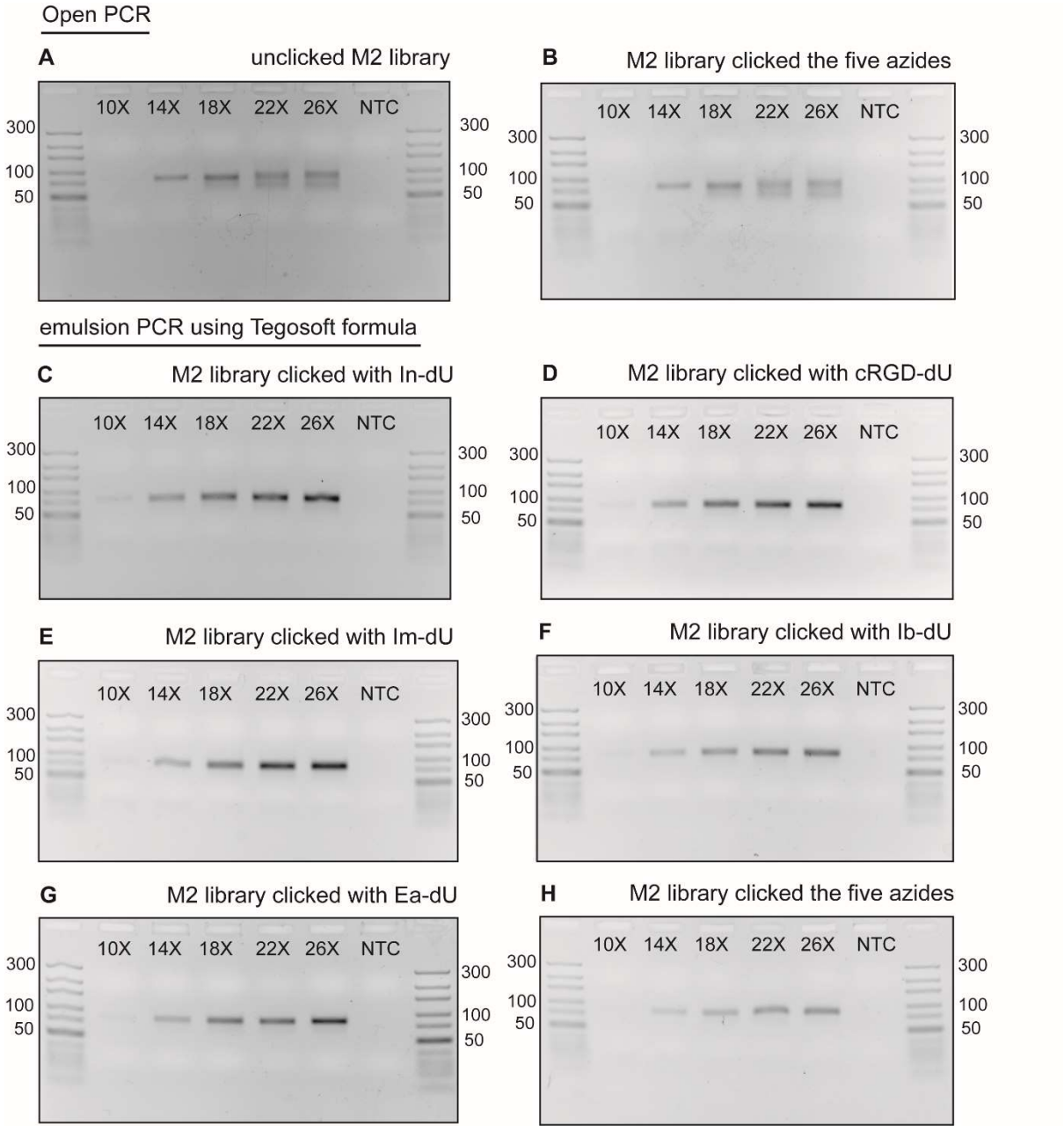

Figure 6.2 the comparison between emulsion PCR (ePCR) and conventional PCR
The results of conventional PCR amplification using **(A)** un-clicked M2 library **(B)** clicked M2 library with: imidazole, cyclic RGD, isobutyl, ethanamine, and indole after 10, 14, 18, 22, and 26 PCR cycles. Using emulsion PCR protocol. The amplification of clicked library were compared **(C)** M2 library clicked with indole (In-du) **(D)** M2 library clicked with cyclic RGD (cRGD-dU) **(E)** M2 library clicked with imidazole (Im-dU) **(F)** M2 library clicked with isobutyl (Ib-dU) **(G)** M2 library clicked with Ethanamine (Ea-dU) **(H)** M2 clicked with the five mentioned azides.

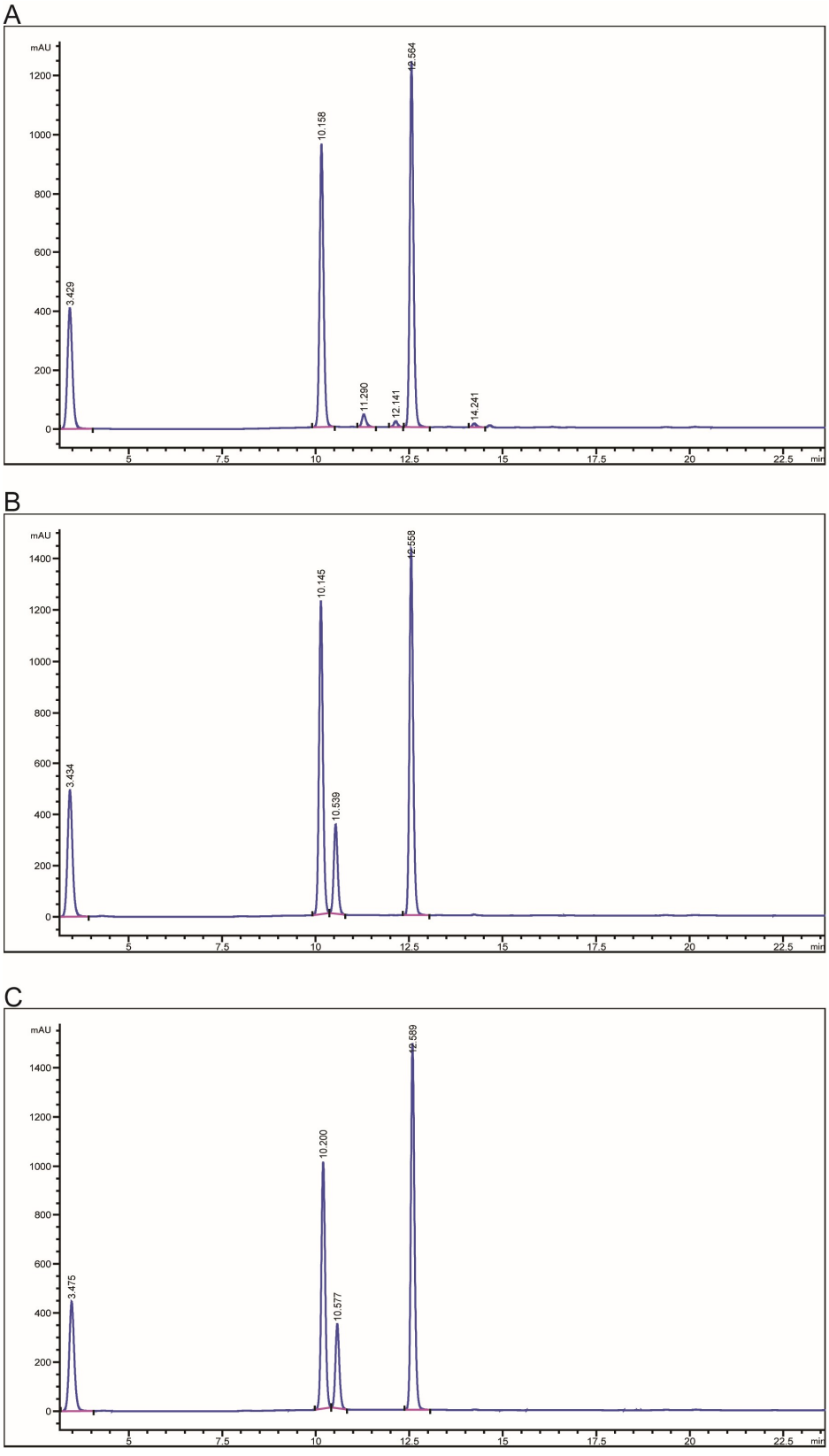

Figure 6.3 HPLC analysis.
Shows the HPLC analysis after nucleoside digestion **(A)** EdU FT2 library **(B)** DNA FT2 library **(C)** DNA M2 library.

Round 1

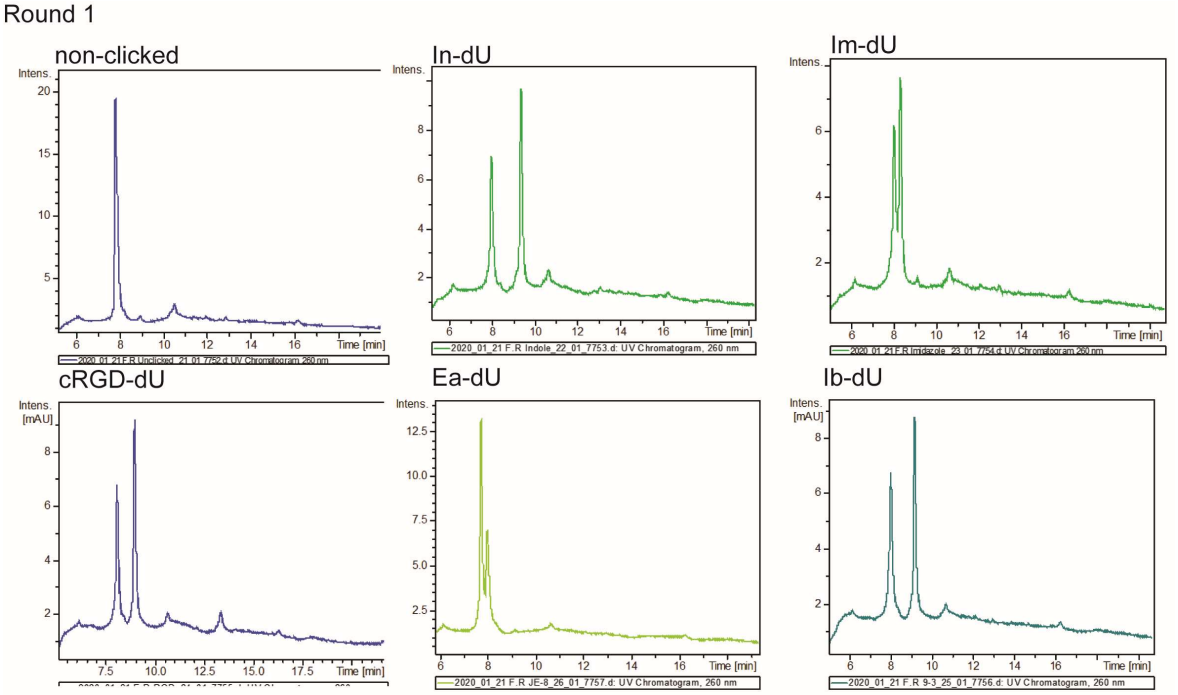

Round 3

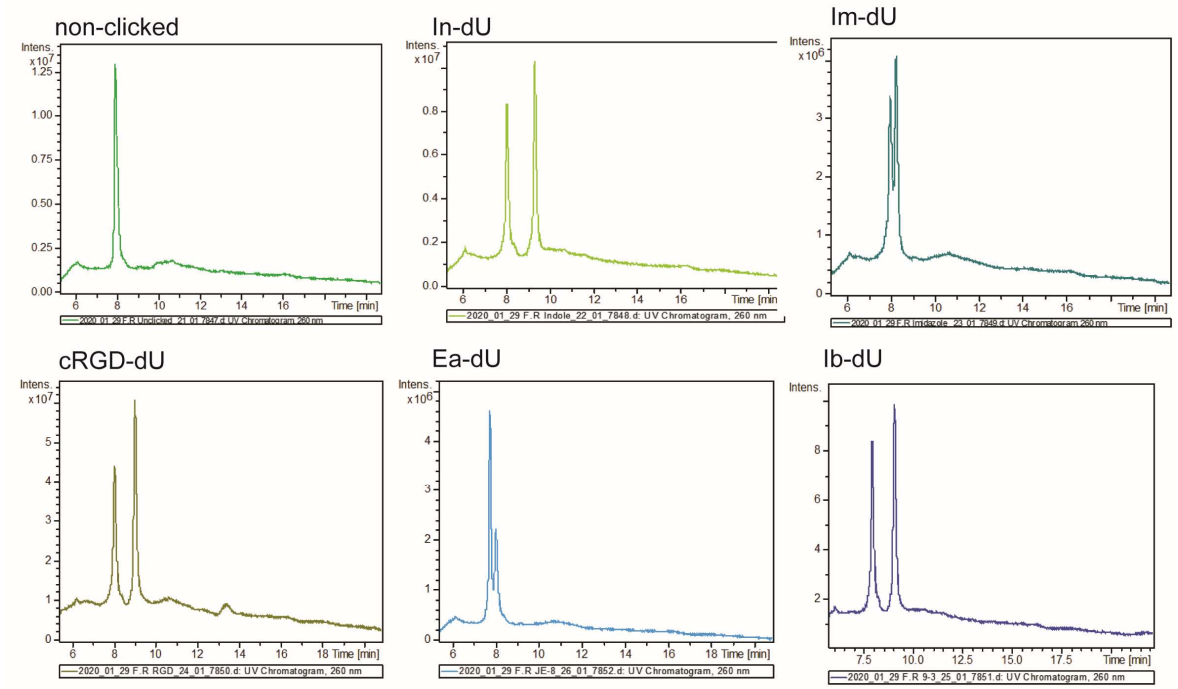

Round 4

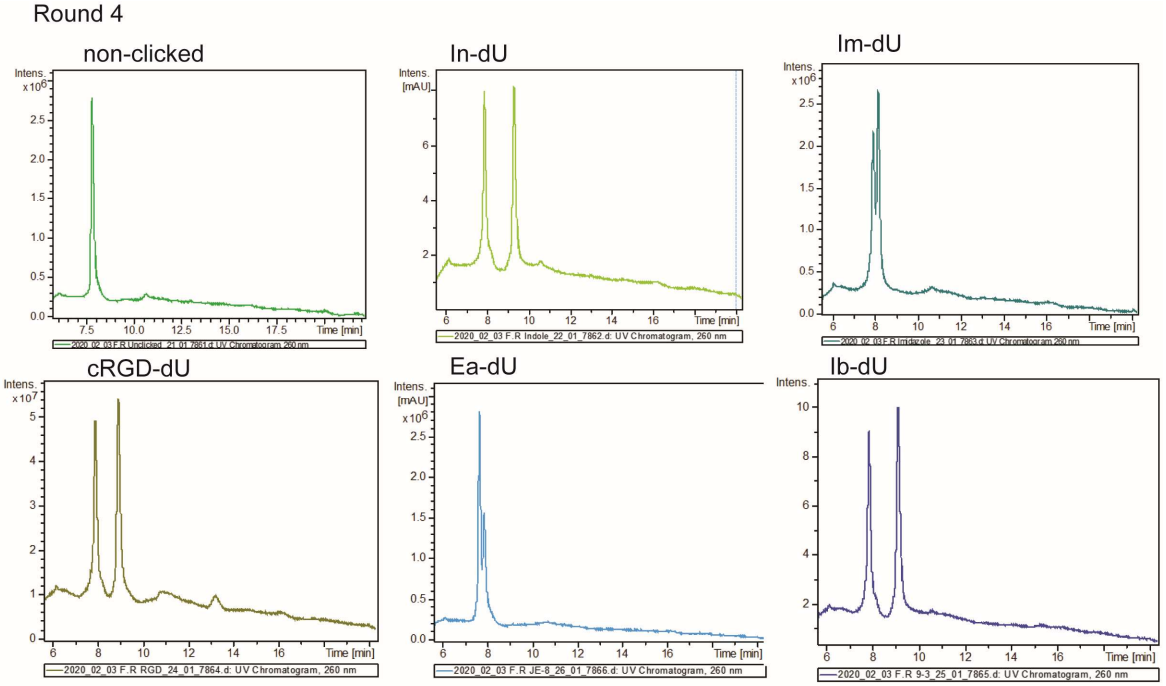

Round 5

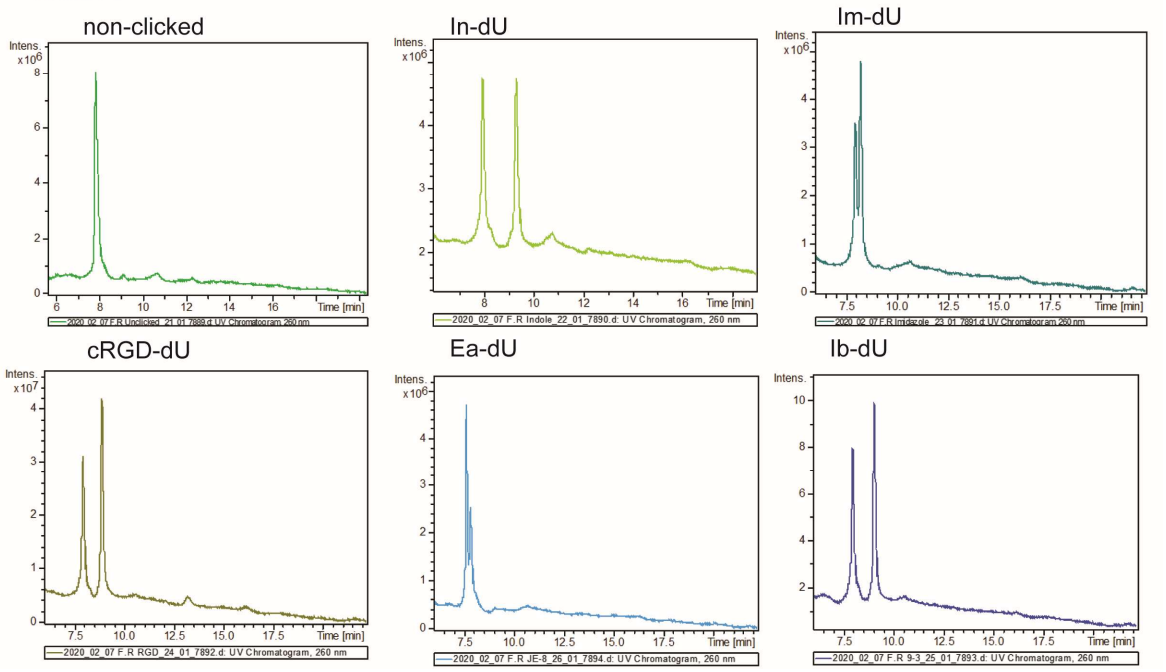

Round 6

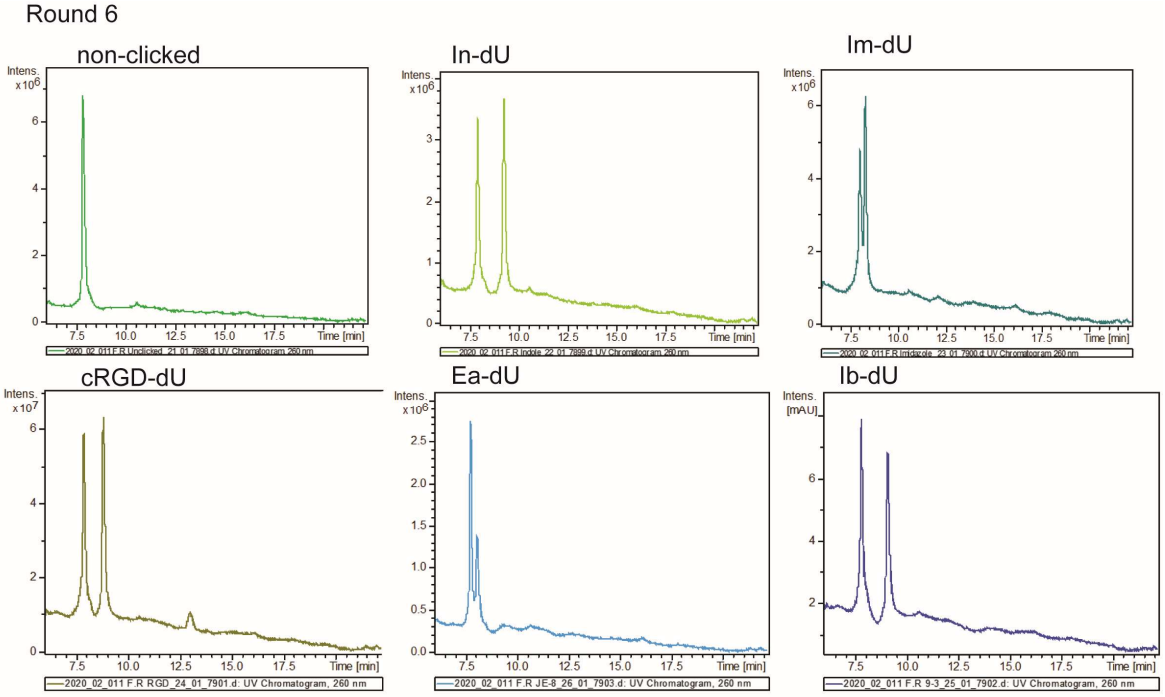

Round 7

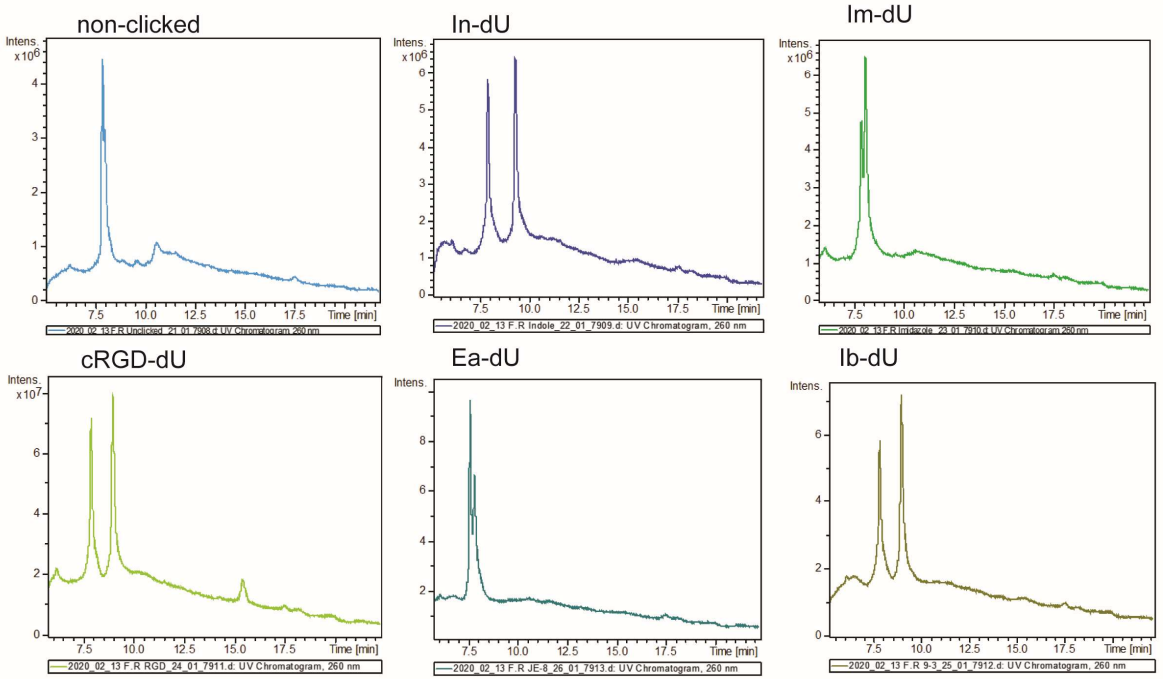

Round 8

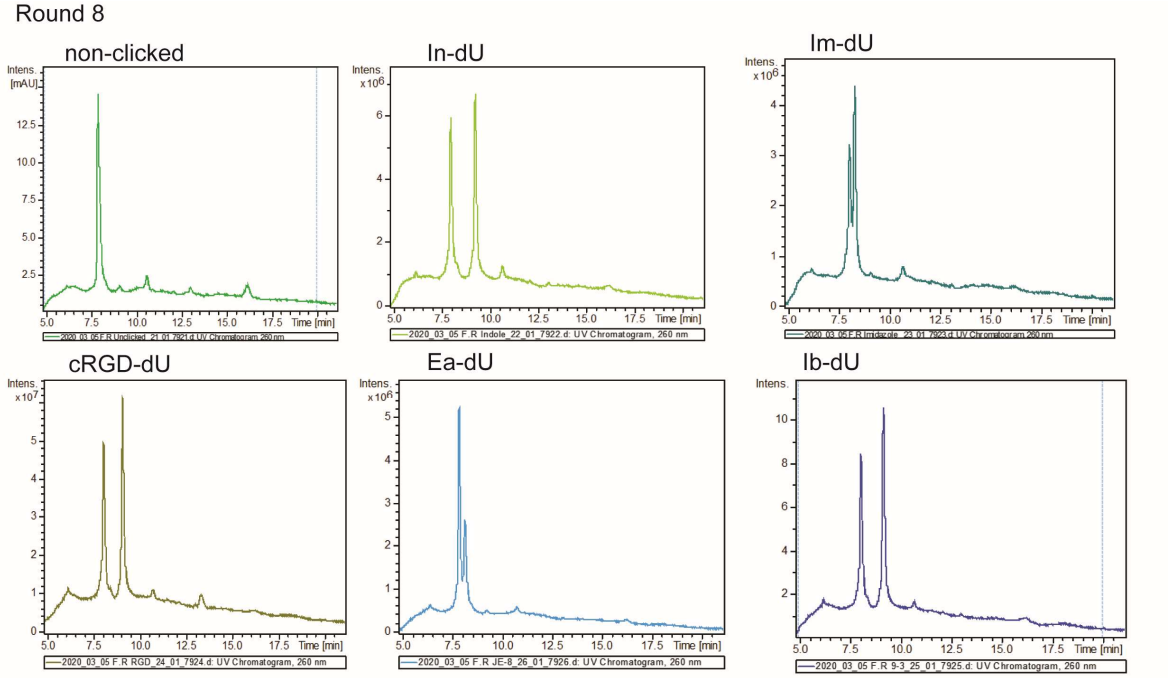

Round 9

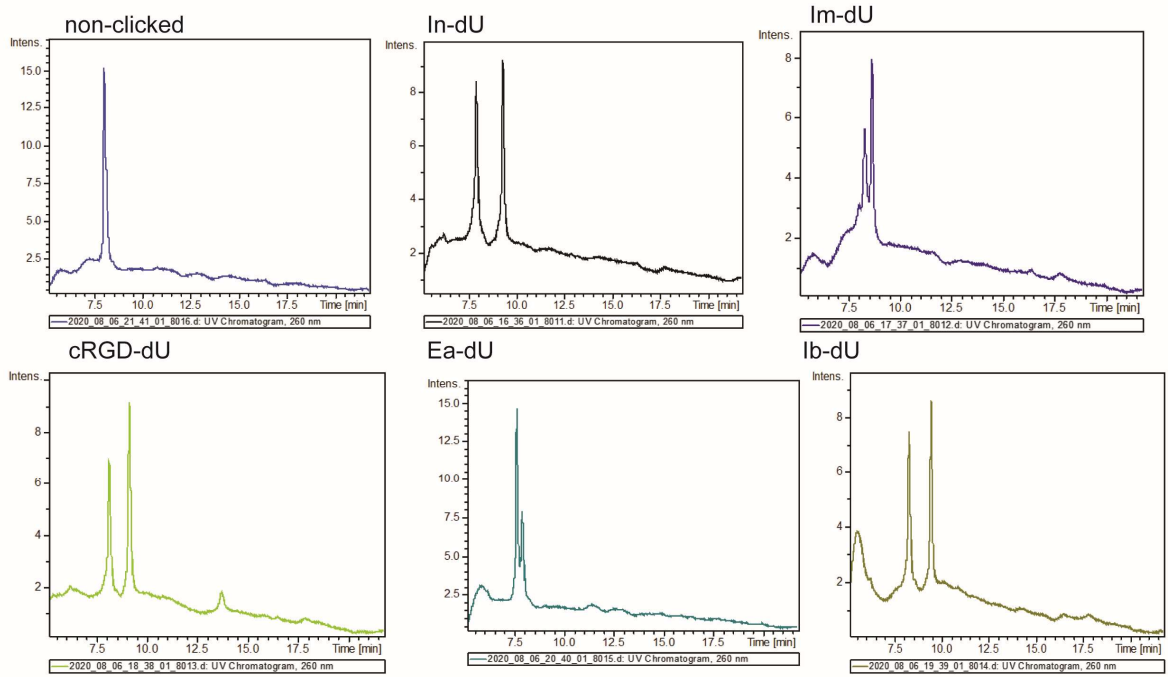

Round 10

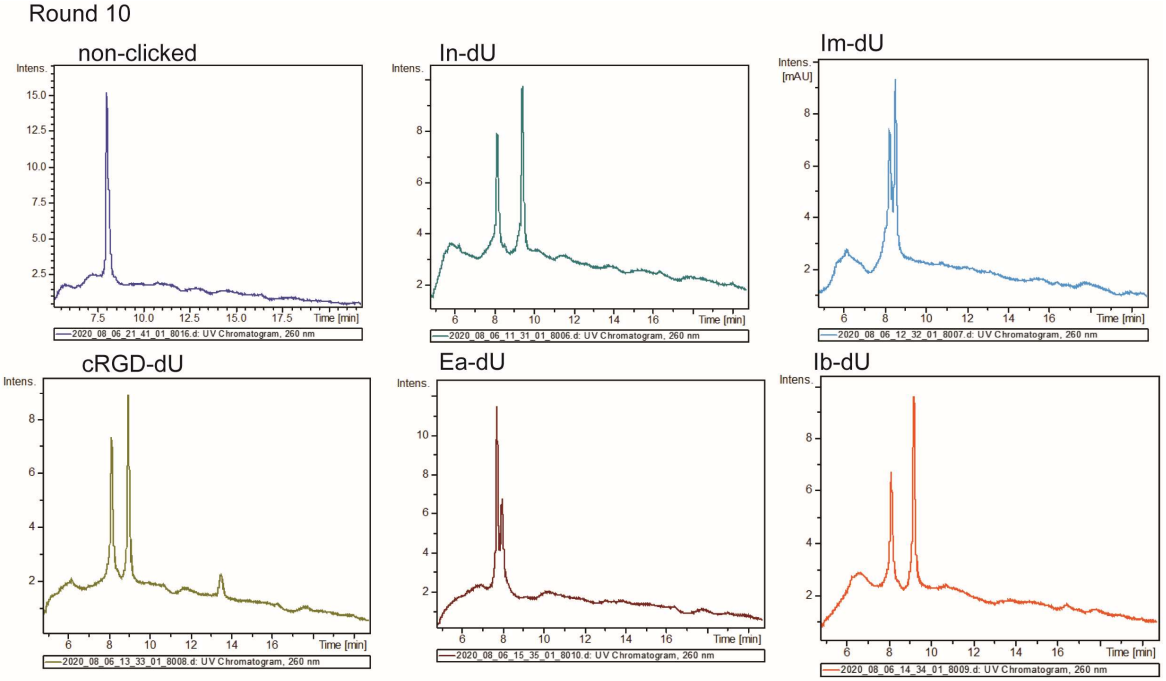

Round 11

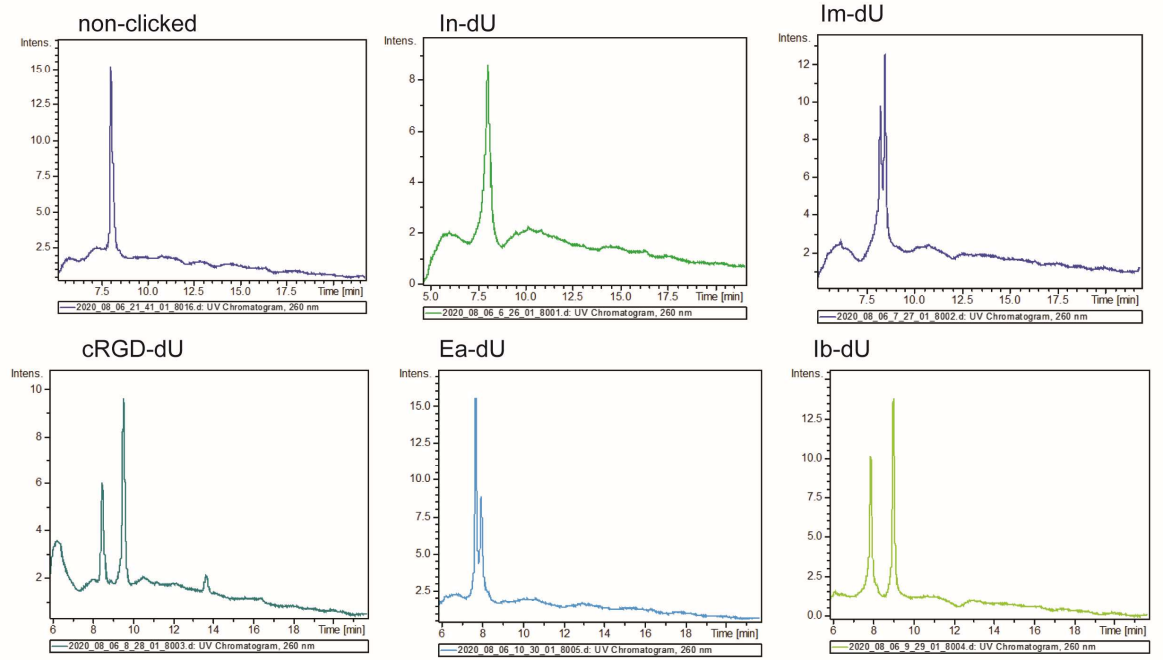

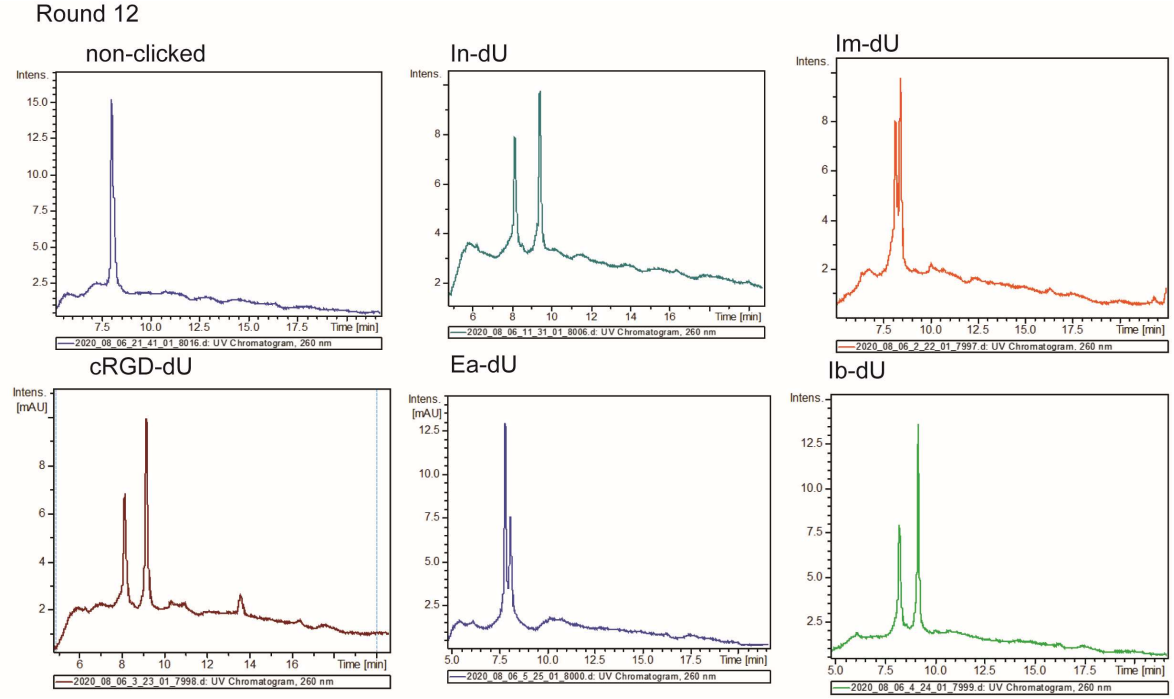

Figure 6.4 investigation of the click reaction with tester EdU during the split-combine cell SELEX.
Tester EdU was used to evaluate the click reaction during all the click reaction performed during the seleletion. Starting from round 1 till round 12.

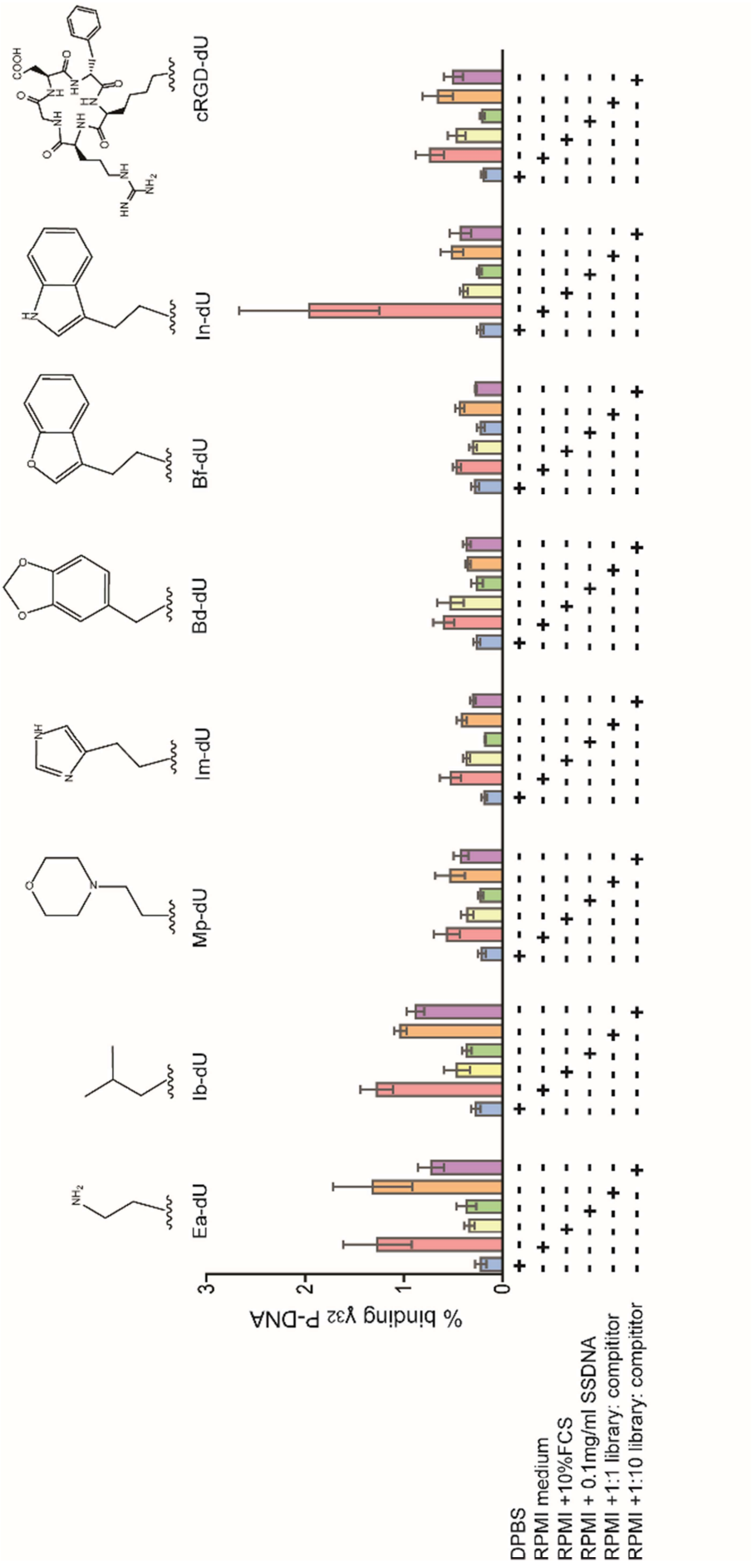
Ea-dU
Ib-dU
Mp-dU
Im-dU
Bd-dU
Bf-dU
In-dU
cRGD-dU
% binding γ32 P-DNA
0
1
2
3
DPBS
RPMI medium
RPMI +10%FCS
RPMI + 0.1mg/ml SSDNA
RPMI +1:1 library: compititor
RPMI +1:10 library: compittor

Figure 6.5 the background interaction between the clicked starting library and PC-3 cells.
The starting library was clicked with the following azides: 3-(2-azidoethyl) benzofuran (BF-dU), 5-(azidomethyl) benzo[d][1,3] dioxole (Bd-dU), 4-(2-azidoethyl) morpholine (Mp-dU), 4-(2-azidoethyl) -1H-imidazole (Im-dU), cyclic RGD (cRGD), 1-azido-2-methylpropane (Ib-dU), 2-azido-ethanamine (Ea-dU), and 3-(2-azidoethyl)-1H-indole (In-dU). different compititiors were used to decrease to the backgrounf binding, 0.1 mg/ ml ssDNA, clicked compitiors at different ratio to library 1:1 or 1:10.

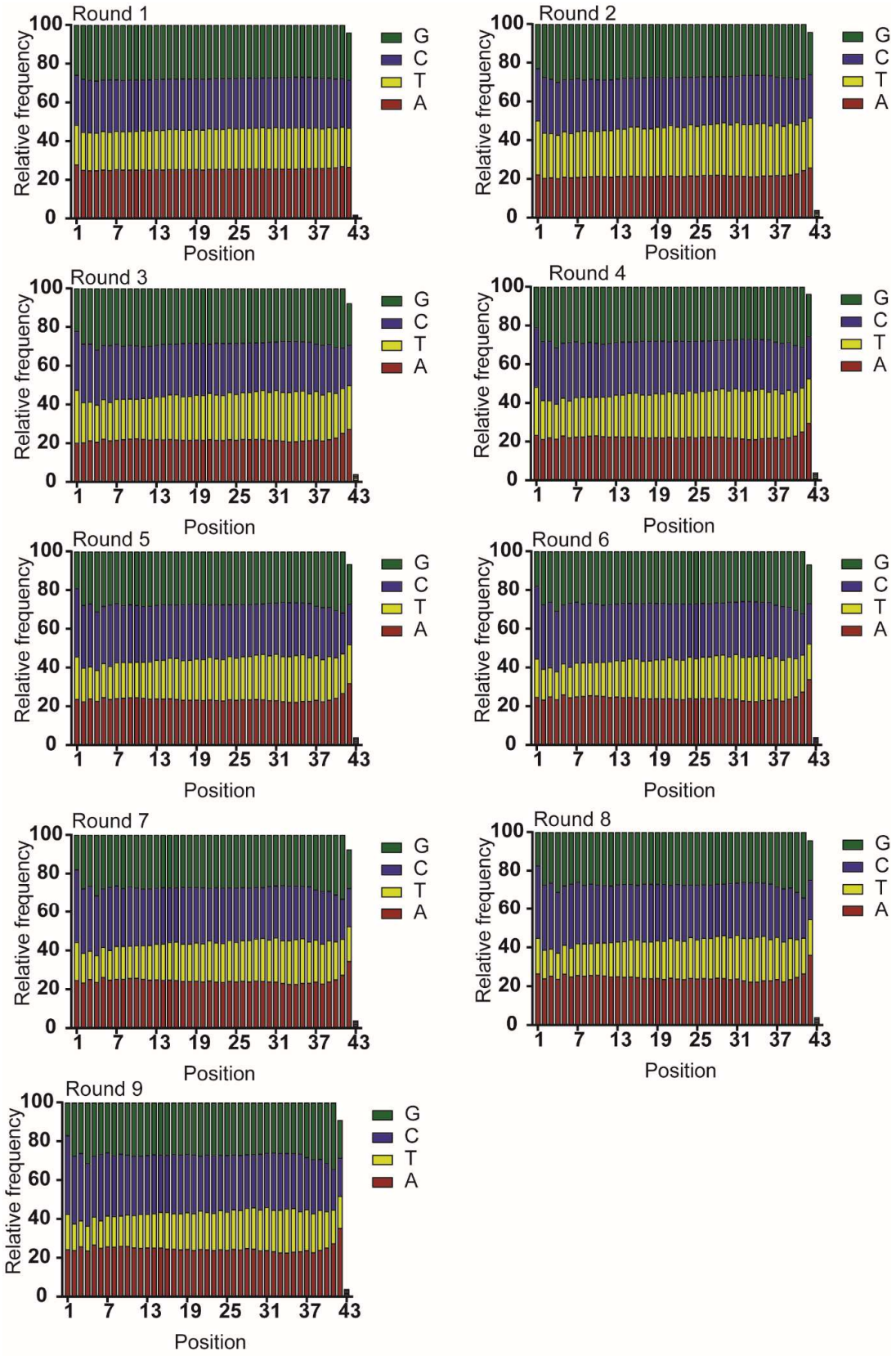

Figure 6.6 Nucleotide disrribution for the DNA cell SELEX. Starting from round 1 till roud 9.

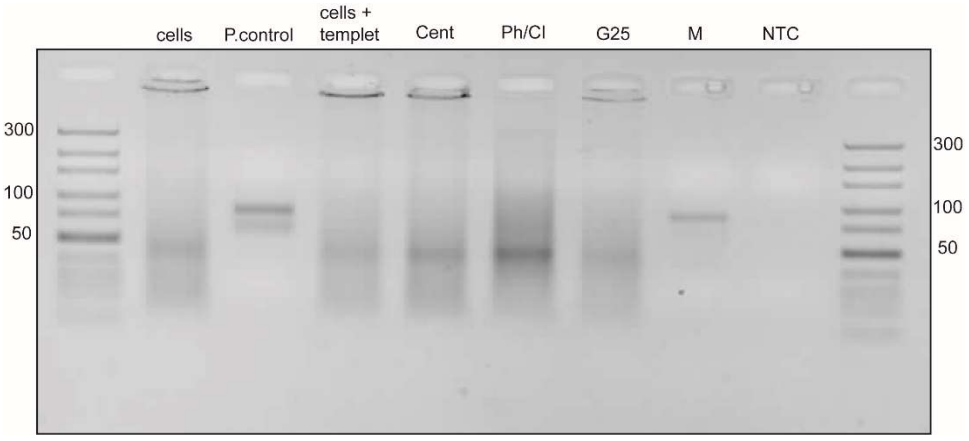

Figure 6.7 Extraction methods used to choose the optimum method for the selection.
1000,000 PC-3 cells were collected into six 1.5 mL tubes. The cells were centrifuged at 200x g for 5 minutes. The cells were resuspended in 50 µL dd H2O, and 1 pmol of DNA library was added to five samples and all the samples were heated to 95°C for 10 min. Afterwards, PCR was performed after several purification method, Lane (1) only the cells lysate without templet, Lane (2) the positive control (P.control) which refers to templet with master mix without cells. Lane (3) (cells + templet) which refers to cell lysate with the templet without purification. Lane (4) centrifugation (Cent) which refers to cells lysate + templet after centrifugation purification. Lane (5) phenol/chloroform extraction (Ph/Cl) PCR was performed after purification with phenol/chloroform extraction. Lane (6) G25, PCR was performed after purification with G25. Lane (7) PCR was performed after purification with Macherey-Nagel kit

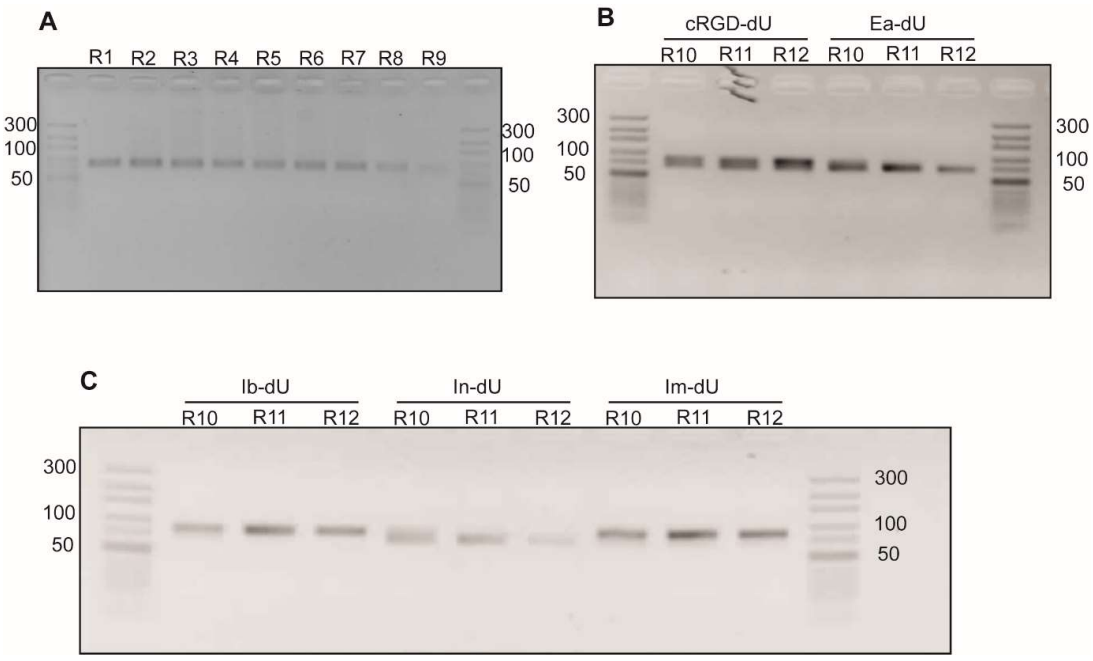

Figure 6.8 displays the PCR products of the split-combine cell SELEX.
(A) the first 9 round**. (B-C)** the deconvolution step for all zides imidazole (Im-dU), cRGD (cRGD-dU), ethanamine (Ea-dU), isobutyl (Ib-dU) and indole (In-dU)**.**

Table 6.1 Sequences found in the DNA cell SELEX; only the randome region, the frequency of he sequences related to the SELEX round.

		Frequency [%]									
FAMILY	SEQUENCE	Round 0	Round 1	Round 2	Round 3	Round 4	Round 5	Round 6	Round 7	Round 8	Round 9	Round 10
MD1	TGATGGCGGTTTGACGGTCCGAGCCAAGAGTGGTGAGTTCGA	0	0	0	0	0	0,0001	0,0007	0,0046	0,0196	0,1372	0,6174
MD2	AAGCAGAGATTAGGGCCATGTGCCCCAAGTCAAGGGATTAG	0	0	0	0,0036	0,0041	0,009	0,0089	0,0109	0,0081	0,0332	0,0398
MD3	CCTGAGGACAAAACTCTACGAGCGCAACGAGGTTAAAGAGGT	0	0	0	0	0	0,0001	0,0001	0,0015	0,0032	0,0147	0,0387
MD4	GAAGAAAAGGGAAGCAATGCTGGACAGCCGGCCAGCTCCTGG	0	0	0,0001	0,004	0,0031	0,0045	0,0038	0,0045	0,0047	0,0271	0,0304
MD5	AGGCACAGCGTAGAGCCAGGCAGCTGCAAATCAAGACATGA	0	0	0	0,0014	0,0016	0,0044	0,0058	0,0061	0,004	0,0199	0,0252
MD6	AGGCAAAGACTGGAGTGCTGTGGCCATAAGCCAAGGAATGA	0	0	0,0001	0,0029	0,0018	0,0056	0,0053	0,0042	0,0023	0,0172	0,0246
MD7	CCACTCCCCTCTCCCCATCCGCCCGAGACCACAGCCACTCCC	0	0	0	0,0017	0,0011	0,006	0,0102	0,0082	0,0097	0,0219	0,0199
MD7	CCACTCCCCTCTCCCCATCCACCCGAGACCACAGCCACTCCC	0	0	0	0,001	0,0008	0,0035	0,0078	0,0071	0,0081	0,0158	0,0158
MD7	CCACTCCCCTCTCCCCATCGGCCCGAGACCACAGCCACTCCC	0	0	0	0,0004	0,001	0,002	0,0054	0,0032	0,0039	0,0087	0,009
MD7	CCACTCCCCTCTCACCATCCGCCCGAGACCACAGCCACTCCC	0	0	0	0,0004	0,0005	0,0019	0,0041	0,0032	0,0039	0,0082	0,0087
MD7	CCACTCTCTTCTCCCCATCCGCCCGAGACCACAGCCACTCCC	0	0	0	0,0003	0,0003	0,0013	0,0031	0,0025	0,0025	0,0051	0,0062
MD7	CCACTCCCCTCTCACCATCCACCCGAGACCACAGCCACTCTC	0	0	0	0,0003	0,0005	0,0013	0,0028	0,0027	0,0024	0,0053	0,0058
MD7	CCACTCCCCTCTCCCCATCCACCCGAGACCACAGCCACACCC	0	0	0	0,0005	0,0005	0,001	0,0022	0,0014	0,0016	0,0033	0,0037
MD7	CCACTCCCCTCTCCCCATCCACCCGAGACCACAGCCACTCTC	0	0	0	0,0002	0,0001	0,0006	0,0017	0,0011	0,0013	0,0025	0,0035
MD7	CCACTCCCCTCTCACCATCCACCCGAGACCACAGCCACTCCC	0	0	0	0,0001	0,0002	0,0006	0,0016	0,0011	0,0013	0,0022	0,0033
MD7	CCACTCCCCTCTCACCATCCACCAGAGACCACAGCCACTCCC	0	0	0	0,0003	0,0001	0,001	0,0019	0,0015	0,0017	0,0035	0,0031
MD7	CCACTCCCCTCTCCCGATCCGCCCGAGACCACAGCCACTCCC	0	0	0	0,0001	0,0001	0,0014	0,0013	0,0011	0,0014	0,0025	0,0023
MD7	CCACTCCCTTCTCCCCATCCGCCCGAGACCACAGCCACTCCC	0	0	0	0	0,0003	0,0005	0,0007	0,001	0,0009	0,0019	0,0023
MD7	CCACTCCCTTCTCACCATCCGCCCGAGACCACAGCCACTCTC	0	0	0	0,0003	0,0003	0,0006	0,001	0,0006	0,0008	0,0019	0,0021
MD7	CCACTCTCTTCTCCCCATCCACCCGAGACCACAGCCACTCCC	0	0	0	0,0002	0	0,0006	0,0006	0,0005	0,0008	0,0011	0,0015
MD7	CCACTCCCCTCTCCCCATCAACCCGAGACCACAGCCACTCCC	0	0	0	0,0002	0,0001	0,0004	0,001	0,0006	0,0006	0,0015	0,0014
MD7	CCACTCCCTTCTCACCATCCACCCGAGACCACAGCCACTCCC	0	0	0	0	0,0001	0,0002	0,0004	0,0002	0,0005	0,0011	0,0014
MD7	CCACTCCCCTCTCACCATCCGCCAGAGACCACAGCCACTCTC	0	0	0	0,0001	0,0001	0,0004	0,0007	0,0005	0,0003	0,0014	0,001
MD7	CCACTCCCCTCTCCCCATCCGCCAGAGACCACAGCCACTCCC	0	0	0	0	0,0001	0,0002	0,0004	0,0004	0,0005	0,0006	0,0009
MD7	CCACTCCCTTCTCACCATCCGCCCGAGACCACAGCCACTCCC	0	0	0	0,0001	0,0001	0,0002	0,0009	0,0003	0,0005	0,0011	0,0009
MD7	CCACTCCCTTCTCCCCATCCACCCGAGACCACAGCCACTCCC	0	0	0	0,0001	0,0001	0,0003	0,0004	0,0007	0,0003	0,0013	0,0009
MD7	CCACTCCCCTCTCCCCATCCGCCCGAGACCACGCCACTCCC	0	0	0	0,0001	0,0001	0,0006	0,0003	0,0004	0,0006	0,001	0,0008
MD7	CCACTCCCTTCTCCCCATCCACCGGAGACCACAGCCACTCCC	0	0	0	0,0001	0,0001	0,0006	0,0003	0,0003	0,0005	0,0013	0,0008
MD7	CCACTCTCTTCTCACCATCCGCCCGAGACCACAGCCACTCCC	0	0	0	0,0001	0	0,0003	0,0005	0,0004	0,0003	0,0007	0,0008
MD7	CCACTCCCCTCTCCCCATCCACCCGAGACCACGCCACTCCC	0	0	0	0,0001	0,0001	0,0006	0,0002	0,0004	0,0005	0,0009	0,0007
MD7	CCACTCTCCTCTCCCCATCCGCCCGAGACCACAGCCACTCCC	0	0	0	0	0,0001	0,0004	0,0004	0,0002	0,0003	0,0012	0,0005
MD8	CAGCAAACGTGGCTATACTAAGAACACTGACAAGTCCGCAAA	0	0	0	0,0026	0,002	0,0035	0,0041	0,0026	0,003	0,0149	0,0177
MD9	CCACGGACACTCGTGCCTGAACTGAGTGCTTGGGGAGGGCCA	0	0	0	0,0006	0,0015	0,0029	0,0031	0,0038	0,0043	0,0111	0,0176
MD10	TCACCGTTTATTGGGCACCTACTCGACACGGTGCCTCCTGC	0	0	0	0,002	0,0013	0,0014	0,0016	0,0019	0,0023	0,0184	0,017
MD10	ATCACCGTTTATTGGGCACCTACTCGACACGGTGCCTCCTGC	0	0	0	0	0,0022	0,001	0,0013	0,0009	0,0026	0,0022	0,0107
MD11	AGAAAGCAGAGATTAGGGCCATGTGCCCCAAGTCAAGGGATT	0	0	0	0	0,0032	0,0044	0,0063	0,0044	0,0081	0,0069	0,016
MD12	CCACTCTCTTCTCCCCATCCACCAGAGACCACAGCCACTCCC	0	0	0	0,0003	0,0007	0,0018	0,0027	0,0035	0,0027	0,0078	0,0064
MD12	CCACTCCCCTCTCACCATCCACCAGAGACCACAGCCACTCTC	0	0	0	0,0003	0,0005	0,002	0,002	0,0026	0,0022	0,0058	0,0057
MD12	CCACTCTCTTCTCCCCATCCACCCGAGACCACAGCCACTCTC	0	0	0	0,0001	0	0,0004	0,0003	0,0008	0,0007	0,0008	0,0017
MD13	AGACAGAGATTGGAGTGATGTCCAGTCTCAAGGAATGAGAG	0	0	0	0,0019	0,002	0,0048	0,0035	0,0035	0,002	0,0122	0,0153
MD14	CACCCCAAACACACCCAGGCCATCAGTCTGGGGAAGTGGAAC	0	0	0	0	0,0027	0,0032	0,003	0,0031	0,0054	0,0043	0,0153
MD14	AGACCCAAACACACCCAGGCCATCAGTCTGGGGAAGTGGAAC	0	0	0	0	0,0002	0,0002	0,0005	0,0007	0,0012	0,001	0,0017
MD15	GGAACAGTACAAAACCTGCAGCCCTGGCCACACCAGCAAAAT	0	0	0	0,0025	0,0015	0,0028	0,0037	0,003	0,0033	0,0189	0,0148
MD16	CAGGCACAGACACAAGTGATTGAACATCAAGAGGAGCAGAGG	0	0	0	0,0008	0,001	0,0037	0,0052	0,007	0,005	0,0165	0,0145
MD17	GGAAGCAATGCTGGACAGCCGGCCAGCTCCTGGGCTGTGGGG	0	0	0	0	0,0028	0,0028	0,0029	0,0019	0,0032	0,0038	0,0127
MD18	CGAAGGCAATGTGACCATGGGCAGAGACTGGAGTTATATGGC	0	0	0	0,0014	0,0008	0,002	0,0024	0,0022	0,0017	0,0087	0,0115
MD19	CCCCCGACTCTCCCTGCCCTCAAAGCAGCCCCACAGAGAGA	0	0	0	0,0005	0,0004	0,0012	0,003	0,0037	0,005	0,0095	0,0112
MD20	GAAGGCACAGCGTAGAGCCAGGCAGCTGCAAATCAAGACATG	0	0	0	0	0,0013	0,0017	0,0029	0,0042	0,0052	0,0038	0,0107

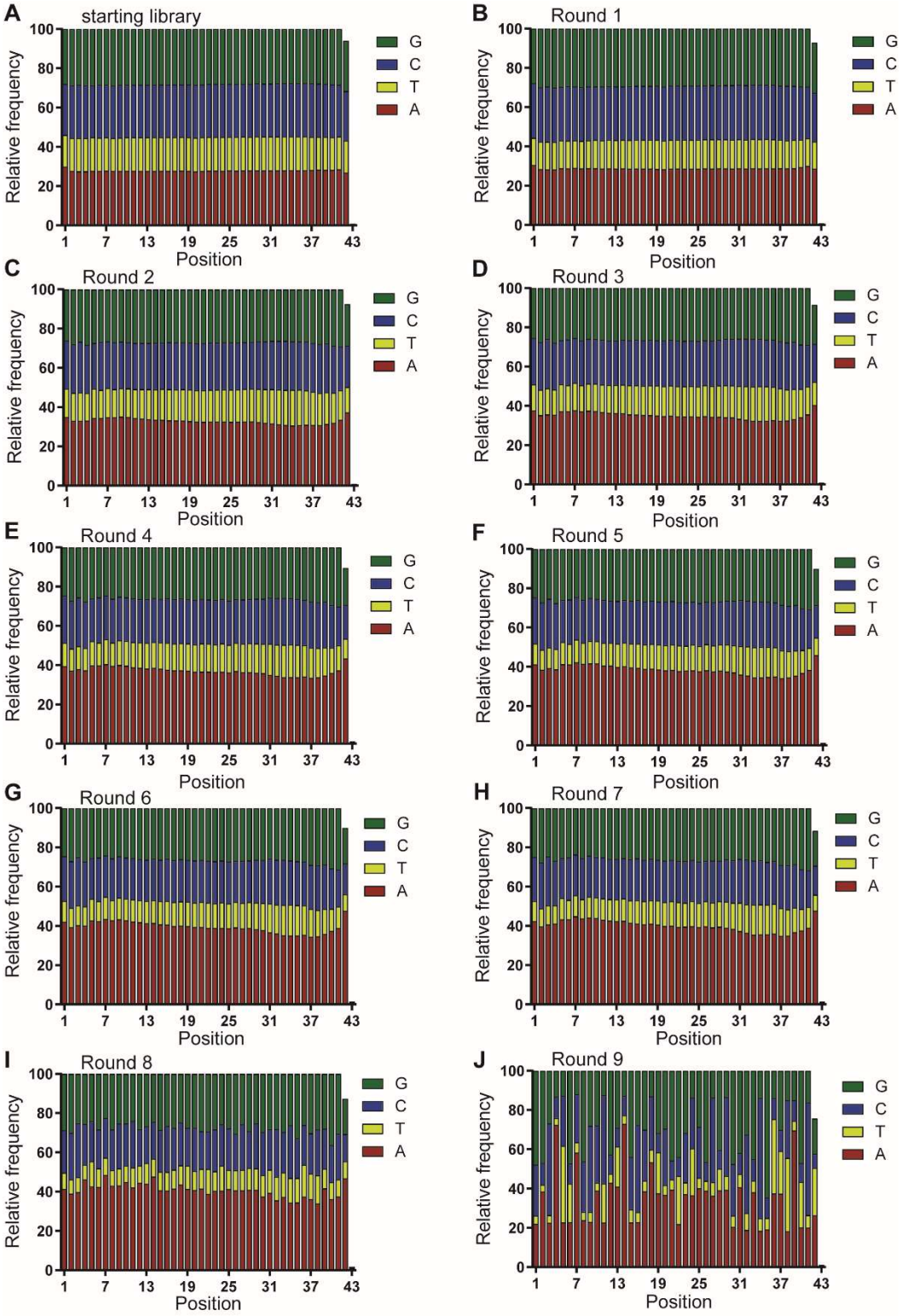

Figure 6.9 Nucleotide distribution for the split-combine cell SELEX during the first 9 rounds of the selection.

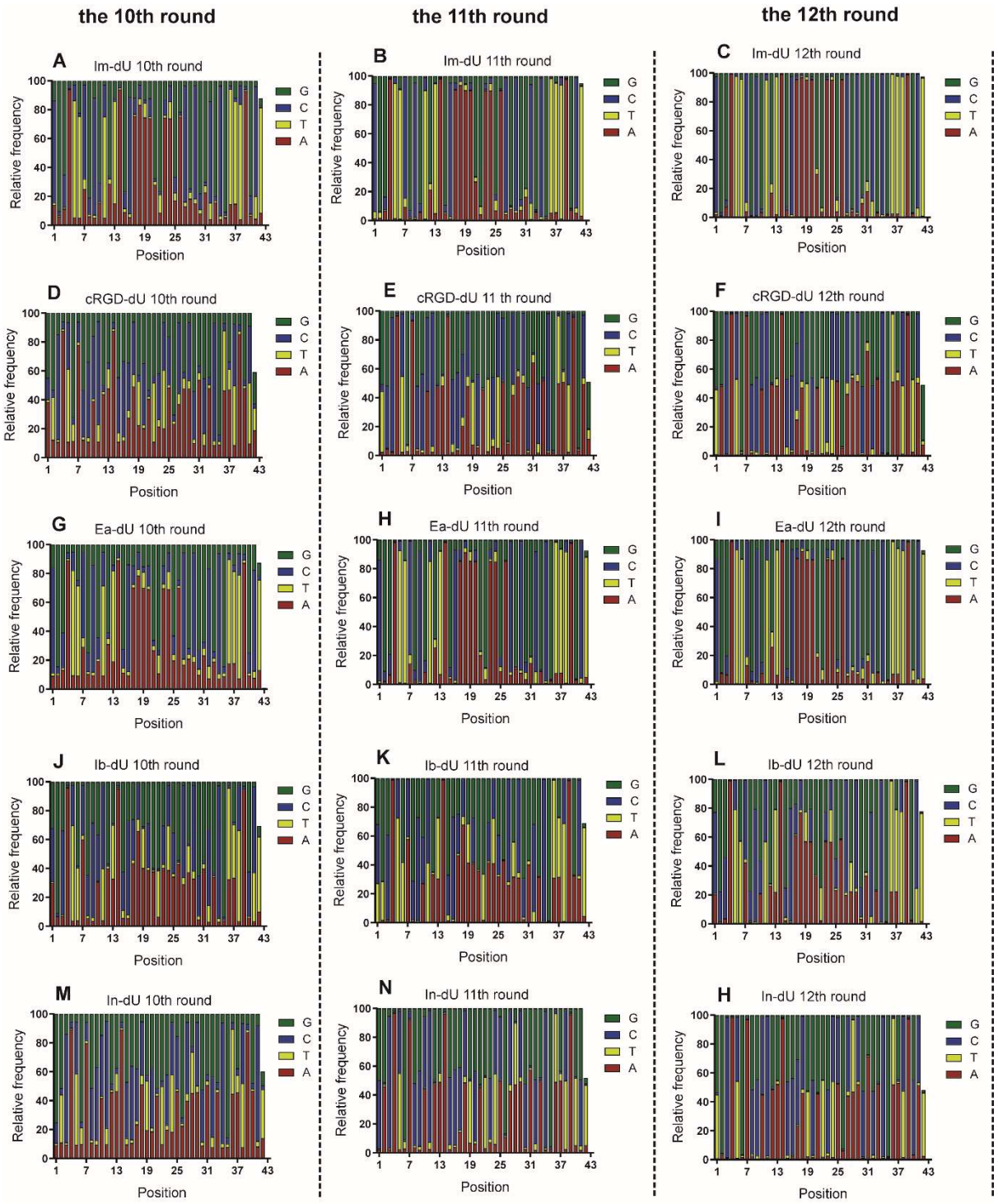

Figure 6.10 nucleotide distribution fort he split-combine cell SELEX during the deconvoulation step.

Table 6.2 Sequences found in the split-combine cell SELEX; only the randome region, the frequency of he sequences related to the SELEX round

		Frequency [%]									
FAMILY	SEQUENCE	Round 0	Round 1	Round 2	Round 3	Round 4	Round 5	Round 6	Round 7	Round 8	Round 9
S1	CGGATTCGCGTGTAGCAAAAGGAAGACGCGGCGCGTTTAGCT	0,0002	0,0015	0,0005	0,0005	0,0012	0,0016	0,0061	0,0391	0,5682	4,3925
S1	CGGATTCGCGTATAGCAAAAGGAAGACGCGGCGCGTTTAGCT	0	0,0007	0,0005	0,0002	0,0003	0,0009	0,0015	0,0067	0,1095	1,0548
S1	CGGATTCGCGTGTAGCAAAAAGAAGACGCGGCGCGTTTAGCT	0	0	0	0	0,0006	0,0004	0,0004	0,0052	0,0523	0,7445
S1	CGGATTCGCGTGTAGCAAAAGGAAGACGCGGTGCGTTTAGCT	0	0,0002	0	0	0	0	0,001	0,0046	0,0578	0,4937
S1	CGAATTCGCGTGTAGCAAAAGGAAGACGCGGCGCGTTTAGCT	0	0,0002	0	0,0001	0	0,0002	0,0004	0,0037	0,0442	0,393
S1	CGGATTTGCGTGTAGCAAAAGGAAGACGCGGCGCGTTTAGCT	0	0	0	0	0	0	0,0007	0,0055	0,0407	0,3574
S1	CGGATTCGCGTGTAACAAAAGGAAGACGCGGCGCGTTTAGCT	0	0	0	0	0	0	0,0006	0,0021	0,0327	0,3057
S1	CGGATTCGCGTGTAGCAAAAGGAAGACGCGACGCGTTTAGCT	0	0	0	0	0,0003	0	0,0006	0,0009	0,0206	0,2897
S1	CGGATTCGCGTGTAGCAAAAGGAATACGCGGCGCGTTTAGCT	0	0	0	0	0,0003	0,0002	0,0003	0,0015	0,0271	0,2398
S1	CGGATTCGCGTGTAGCAAAAGGAAGACGCGGCGCGTTTAGTT	0	0	0	0	0	0	0,0006	0,0031	0,0171	0,2114
S1	CGGATTCGCGTGTAGCAAAAGAAAGACGCGGCGCGTTTAGCT	0	0	0	0	0,0003	0,0002	0,001	0,0019	0,0191	0,1884
S1	CGGATTCGCGTATAGCAAAAAGAAGACGCGGCGCGTTTAGCT	0	0,0005	0	0	0,0003	0	0,0001	0,0006	0,0131	0,1826
S1	CGGATTCGCGTTTAGCAAAAGGAAGACGCGGCGCGTTTAGCT	0	0,0002	0	0,0001	0	0	0	0,0007	0,0146	0,1297
S1	CGGATTCGCGTGTAGCAAAAGGAAGACGCGTCGCGTTTAGCT	0	0	0	0	0,0003	0	0,0001	0,0003	0,0126	0,1233
S1	CGGATTCGCGTGTAGCAAAAGGAAGACGCAGCGCGTTTAGCT	0	0	0	0	0	0	0,0003	0,0003	0,0065	0,1229
S1	CGAATTCGCGTATAGCAAAAGGAAGACGCGGCGCGTTTAGCT	0	0	0	0	0	0,0002	0,0003	0,001	0,0106	0,1175
S1	CGGATTCGCGTGTAGTAAAAGGAAGACGCGGCGCGTTTAGCT	0	0	0	0	0	0	0	0,0009	0,01	0,0921
S1	CGGATTCGCGTGTAGCAAAAGGAAGACGCGGCGCATTTAGCT	0	0	0	0	0	0	0	0,001	0,01	0,091
S1	CGGATTCGCGTGTAGCAAAATGAAGACGCGGCGCGTTTAGCT	0	0,0002	0,0005	0	0	0,0002	0	0,0004	0,0085	0,0874
S1	CGGATTCGCGTGTAGCAAAAGGAAGACGCGGCGCGTTTAACT	0	0	0	0	0	0	0,0001	0,0004	0,0131	0,0817
S1	CGGATTCGCATGTAGCAAAAGGAAGACGCGGCGCGTTTAGCT	0	0	0	0	0	0	0,0001	0,0006	0,0116	0,0778
S1	CGGATTCGCGTGTAGCAAAAGGAAAACGCGGCGCGTTTAGCT	0	0,0005	0	0	0	0	0	0,0012	0,0055	0,0774
S1	CGGATTCGCGTGTAGCAAAAGGAAGACGCTGCGCGTTTAGCT	0	0	0	0	0	0	0	0,0003	0,004	0,0757
S1	CGGATTCGCGTATAGCAAAAGGAAGACGCGGTGCGTTTAGCT	0	0	0	0	0	0	0,0001	0,001	0,008	0,0737
S1	CGGATTCGCGTGTAGCAAAAGGAAGACGTGGCGCGTTTAGCT	0	0,0002	0	0,0001	0	0	0,0001	0,0007	0,0085	0,0726
S1	CGGATTTGCGTATAGCAAAAGGAAGACGCGGCGCGTTTAGCT	0	0	0	0	0	0	0	0,0007	0,0065	0,0699
S1	CGAATTCGCGTGTAGCAAAAAGAAGACGCGGCGCGTTTAGCT	0	0	0	0	0	0	0,0003	0,0006	0,006	0,0682
S1	CGGATTTGCGTGTAGCAAAAAGAAGACGCGGCGCGTTTAGCT	0	0,0002	0	0	0,0003	0	0	0,0004	0,008	0,0613
S1	CGGATTCGCGTGTAGCAAAAAGAAGACGCGTCGCGTTTAGCT	0	0	0	0	0	0	0,0001	0,0004	0,0055	0,0607
S1	TGGATTCGCGTGTAGCAAAAGGAAGACGCGGCGCGTTTAGCT	0	0	0	0	0	0,0002	0	0,0007	0,004	0,0589
S1	CGGATTCGCGTGTAGCAAAAGGAAGACACGGCGCGTTTAGCT	0	0	0	0	0	0	0	0,0003	0,01	0,0571
S1	CGGATTCGTGTGTAGCAAAAGGAAGACGCGGCGCGTTTAGCT	0	0	0	0,0001	0	0	0	0,0004	0,005	0,0544
S1	CGGATTCGCGTATAACAAAAGGAAGACGCGGCGCGTTTAGCT	0	0	0	0	0	0	0	0,0003	0,005	0,0518
S1	CGGATTCGCGTGTAACAAAAAGAAGACGCGGCGCGTTTAGCT	0	0	0	0	0	0	0	0,0001	0,0025	0,0504
S1	CGAATTCGCGTGTAGCAAAAGGAAGACGCGGTGCGTTTAGCT	0	0	0	0	0	0	0	0,0003	0,0055	0,0491
S1	CGGATTCGCGTATAGCAAAAGGAAGACGCGGCGCGTTTAGTT	0	0	0,0005	0	0	0	0	0,0003	0,0025	0,0491
S1	CGGATTCGCGTGTAGCAAAAGGAAGACGCGGCACGTTTAGCT	0	0,0002	0	0	0	0	0,0001	0,0006	0,0025	0,0466
S1	CGGATTCACGTGTAGCAAAAGGAAGACGCGGCGCGTTTAGCT	0	0	0	0	0,0003	0	0,0001	0,0001	0,0045	0,0449
S1	CGGATTCGCATATAGCAAAAGGAAGACGCGGCGCGTTTAGCT	0	0	0	0	0	0	0,0001	0,0004	0,0035	0,0436
S1	CGGATTCGCGTATAGCAAAAGAAAGACGCGGCGCGTTTAGCT	0	0,0002	0	0	0	0	0,0001	0,0001	0,0035	0,0435
S1	CGGATTTGCGTGTAGCAAAAGAAAGACGCGGCGCGTTTAGCT	0	0	0	0	0	0	0	0,0001	0,004	0,0406
S1	CGGATTCGCGTGTAGCAAAAGGAAGACGCGATGCGTTTAGCT	0	0	0	0	0	0	0	0,0004	0,0035	0,0374
S1	CGAATTTGCGTGTAGCAAAAGGAAGACGCGGCGCGTTTAGCT	0	0	0	0	0,0003	0	0	0,0001	0,005	0,0369
S1	CGGATTCGCGTGTAGCAAAAAGAAGACGCGGCGCGTTTAGTT	0	0	0	0	0	0,0002	0	0,0001	0,0025	0,0361
S1	CGGATTCGCGTGTAGCAAAAGGAAGACGCGGCGTGTTTAGCT	0	0	0	0	0	0	0	0,0001	0,005	0,0349
S1	CGGATTCGCGTGTAGCAAAAAAAAGACGCGGCGCGTTTAGCT	0	0	0	0	0	0	0,0001	0,0001	0,0035	0,0338
S1	CGGATTTGCGTGTAGCAAAAGGAAGACGCGGTGCGTTTAGCT	0	0	0	0	0	0	0,0001	0,0003	0,0035	0,0337
S1	CGGATTCGCGTGTAGCAAAAAGAATACGCGGCGCGTTTAGCT	0	0	0	0	0,0003	0	0,0001	0,0001	0,004	0,0313
S1	CGAATTCGCGTGTAACAAAAGGAAGACGCGGCGCGTTTAGCT	0	0	0	0	0	0	0,0001	0	0,0025	0,0312
S1	CGGATTCGCGTGTAACAAAAGGAAGACGCGGTGCGTTTAGCT	0	0	0	0	0	0	0	0,001	0,0035	0,0308
S1	CAGATTCGCGTGTAGCAAAAGGAAGACGCGGCGCGTTTAGCT	0	0	0	0	0	0	0,0001	0	0,003	0,0305
S1	CGGATTTGCGTGTAACAAAAGGAAGACGCGGCGCGTTTAGCT	0	0	0	0	0	0	0	0,0001	0,0025	0,0288
S1	CGGATTCGCGTGTAGCAAAAGGAAGACGCGTTGCGTTTAGCT	0	0	0	0	0	0	0	0	0,003	0,0285
S1	CGGATTTGCGTGTAGCAAAAGGAAGACGCGACGCGTTTAGCT	0	0	0	0	0	0	0	0,0001	0,0035	0,0283
S1	CGAATTCGCGTGTAGCAAAAGGAAGACGCGACGCGTTTAGCT	0	0	0	0,0002	0	0	0	0	0,005	0,0272
S1	CGGATTCGCGTATAGCAAAATGAAGACGCGGCGCGTTTAGCT	0	0	0	0	0,0003	0,0002	0	0	0,0025	0,0242
S1	CGGATTCGCGTGTAGCAAAAGGAAGACGCGGTGCGTTTAGTT	0	0	0	0	0	0	0	0,0004	0,003	0,0235
S1	CGGATTCGCGTGTATCAAAAGGAAGACGCGGCGCGTTTAGCT	0	0	0	0	0	0	0,0001	0	0,004	0,0229
S1	CGGATTCGCGTGTAGCAAAAGAAAGACGCGGTGCGTTTAGCT	0	0,0002	0	0	0	0	0	0	0,003	0,0222
S1	CGGATTCTCGTGTAGCAAAAGGAAGACGCGGCGCGTTTAGCT	0	0	0	0	0	0	0,0001	0	0,0025	0,022
S1	CGAATTCGCGTGTAGCAAAAGGAAGACGCGGCGCGTTTAGTT	0	0	0	0	0,0003	0	0	0,0003	0,004	0,0213
S1	CGTATTCGCGTGTAGCAAAAGGAAGACGCGGCGCGTTTAGCT	0	0	0	0	0	0	0	0	0,006	0,019
S1	CGGATTTGCGTGTAGCAAAAGGAATACGCGGCGCGTTTAGCT	0	0	0	0	0	0	0	0,0001	0,003	0,0167
S1	CGGATTCGCGTGTAGCAAAAGGAAGACGCGGCGTGTTTAACT	0	0	0	0	0	0	0,0001	0,0001	0,003	0,0156
S1	CGGATTCGCGTTTAGCAAAAGGAAGACGCAGCGCGTTTAGCT	0	0	0	0	0	0	0	0	0,003	0,0147
S1	CGAATTCGCGTGTAGCAAAAGGAAGACGCAGCGCGTTTAGCT	0	0	0	0	0	0	0	0	0,003	0,0121
S1	CGGATTTGCGTTTAGCAAAAGGAAGACGCGGCGCGTTTAGCT	0	0	0	0	0	0	0	0,0001	0,003	0,0119
S2	GGCATGAGCCCGAACCGCGCGTGTAGCGAGAGACGAACATA	0	0	0	0	0	0	0,0077	0	0	0,0338
S2	GGCATGAGCCCGAACCGCGCGTGTAGCTAGAGACGAACATA	0	0	0	0	0	0	0,0035	0	0	0,0211
S2	GGCATGAGCCCGAACCGCGCGTGTAGCGAGAGACGAACAAG	0	0	0	0	0	0	0,0003	0	0,006	0,0142
S2	GGCATGAGCCCGAACCGCGCGTGTAGCGAGAGACGAACAGA	0	0	0	0	0	0,0016	0	0	0,003	0,0014
S3	AACAGAAGGGAAACAGAGAGTGAGGGAAGGTGAGATGGAGGG	0	0,0002	0,0005	0,0034	0,0087	0,0189	0,0244	0,02	0,0382	0,0172
S3	AACAGAAGGGAAACAGAGAGTGAGGGAAGGTGAAATGGAGGG	0	0	0	0,0004	0,0012	0,0018	0,0058	0,0067	0,009	0,0062
S3	AACAAAAGGGAAACAGAGAGTGAGGGAAGGTGAGATGGAGGG	0	0	0	0,0004	0,0017	0,0029	0,0041	0,0044	0,007	0,0058
S3	AACAGAAGGGAAACAGAGAGTGAGGGAAGGTGAGATGGAGGA	0	0	0,0005	0,0001	0,0026	0,0024	0,0029	0,003	0,006	0,0046
S3	AACAGAAGGGAAACAGAGAGTGAGGAAAGGTGAGATGGAGGG	0	0	0	0	0,0006	0,0024	0,0032	0,0039	0,006	0,0033
S3	AACAGAAGGAAAACAGAGAGTGAGGGAAGGTGAGATGGAGGG	0	0	0	0	0,0015	0,0022	0,0036	0,0028	0,0035	0,002
S3	AACAGAAGGGAAACAGAAAGTGAGGGAAGGTGAGATGGAGGG	0	0	0	0	0	0,0016	0,0016	0,0024	0,002	0,0014
S3	AACAGAAGGGAAACAGAGAGTGAGGGAAGGTGAGATGAAGGG	0	0	0	0	0,0003	0,0004	0,0012	0,0015	0,0025	0,0013
S4	AGACAGAGATTGGAGTGATGTCCAGTCTCAAGGAATGAGAG	0	0,0012	0,0005	0,0321	0,047	0,0482	0,0328	0,0482	0,0211	0,0117
S4	AGACAGAGATTGGAGTGATGTCCAGTCTCAAGAAATGAGAG	0	0	0	0,0009	0,0049	0,0029	0,0033	0,004	0,0035	0,0012
S4	AGACAGAGATTGGAGTAATGTCCAGTCTCAAGGAATGAGAG	0	0	0	0,001	0,0038	0,0029	0,0036	0,0052	0,003	0,0011
S4	AGACAGAGATTGGAGTGATGTCCAGTTTCAAGGAATGAGAG	0	0	0	0,0005	0,0009	0,0004	0,0019	0,0033	0,001	0,0005
S4	AGACAGAGATTGGAGTGATGTTCAGTCTCAAGGAATGAGAG	0	0	0	0,0011	0,0029	0,0024	0,0019	0,0034	0,002	0,0005
S4	AGACAGAGATTGGAGTGATGTCCAGTCTCAAGGAATAAGAG	0	0	0	0,0004	0,0015	0,002	0,0012	0,0022	0,0015	0,0004
S4	AAACAGAGATTGGAGTGATGTCCAGTCTCAAGGAATGAGAG	0	0	0	0,0002	0,0023	0,0011	0,0019	0,0018	0,0005	0,0003
S4	AGACAGAAATTGGAGTGATGTCCAGTCTCAAGGAATGAGAG	0	0	0	0,0015	0,002	0,0042	0,0048	0,0059	0,0035	0,0003
S4	AAGCAGAGATTAGGGCCATGTGCCCCAAGTCAAGGGATTAG	0	0,0017	0,0036	0,0266	0,0392	0,0304	0,0178	0,0233	0,01	0,0086
S4	AAGCAGAGATTAGGGCCATGTGTCCCAAGTCAAGGGATTAG	0	0	0	0,0009	0,002	0,0018	0,0017	0,0025	0,0005	0,0009
S4	AAGCAGAAATTAGGGCCATGTGCCCCAAGTCAAGGGATTAG	0	0	0	0,0015	0,0049	0,0024	0,0023	0,0047	0,0025	0,0007
S4	AAACAGAGATTAGGGCCATGTGCCCCAAGTCAAGGGATTAG	0	0	0	0,0014	0,0009	0,0022	0,0012	0,0025	0,002	0,0005
S4	AAGCAGAGATTAGGACCATGTGCCCCAAGTCAAGGGATTAG	0	0	0	0,0014	0,0015	0,0029	0,0013	0,0021	0,002	0,0005
S4	AAGCAGAGATTAGGGCCATGTGCCCCAAGTCAAGGAATTAG	0	0	0	0,0012	0,002	0,0027	0,0023	0,0025	0,003	0,0005

Table 6.3 Sequences found the last rounds of the split-combine cell SELEX and three round of deconvoulation step with imidazole (Im-dU); only the randome region, the frequency of he sequences related to the SELEX round.

		Frequency [%]					
FAMILY	SEQUENCE	Round 7	Round 8	Round 9	Round 10	Round 11	Round 12
S1	CGGATTCGCGTGTAGCAAAAGGAAGACGCGGCGCGTTTAGCT	0,0391	0,5683	4,3925	12,7037	17,8882	13,5061
S1	CGGATTCGCGTGTAGCAAAAAGAAGACGCGGCGCGTTTAGCT	0,0052	0,0523	0,7445	3,6104	7,0764	7,497
S1	CGGATTCGCGTATAGCAAAAGGAAGACGCGGCGCGTTTAGCT	0,0067	0,1095	1,0548	4,0464	5,4086	3,667
S1	CGGATTCGCGTGTAGCAAAAGGAAGACGCGACGCGTTTAGCT	0,0009	0,0206	0,2897	1,4468	2,5662	2,8808
S1	CGGATTCGCGTATAGCAAAAAGAAGACGCGGCGCGTTTAGCT	0,0006	0,0131	0,1826	1,285	2,5684	2,8161
S1	CGGATTCGCGTGTAGCAAAAGGAATACGCGGCGCGTTTAGCT	0,0015	0,0271	0,2398	1,1872	2,0953	1,9132
S1	CGGATTCGCGTGTAGCAAAAGGAAGACGCAGCGCGTTTAGCT	0,0003	0,0065	0,1229	0,7334	1,3911	1,7997
S1	CGGATTCGCGTGTAGCAAAAGGAAGACGCGATGCGTTTAGCT	0,0004	0,0035	0,0374	0,3443	0,8877	1,5043
S1	CGGATTCGCGTTTAGCAAAAGGAAGACGCGGCGCGTTTAGCT	0,0007	0,0146	0,1297	0,6431	1,1944	1,4582
S1	CGGATTCGCGTGTAGCAAAAAGAAGACGCGACGCGTTTAGCT	0	0,002	0,0408	0,322	0,7313	1,1241
S1	CGGATTCGCGTGTAGCAAAAGGAAGACGCGGTGCGTTTAGCT	0,0046	0,0578	0,4937	1,6678	1,8773	1,1169
S1	CGGATTCGCGTGTAGCAAAAGGAAGACGCGTCGCGTTTAGCT	0,0003	0,0126	0,1233	0,553	1,0188	1,0843
S1	CGAATTCGCGTGTAGCAAAAGGAAGACGCGGCGCGTTTAGCT	0,0037	0,0442	0,3931	1,2421	1,1784	1,0768
S1	CGGATTCGCGTGTAGCAAAATGAAGACGCGGCGCGTTTAGCT	0,0004	0,0085	0,0874	0,476	0,887	0,9997
S1	CGGATTTGCGTGTAGCAAAAGGAAGACGCGGCGCGTTTAGCT	0,0055	0,0407	0,3574	1,2406	1,182	0,9359
S1	CGGATTCGCGTGTAGCAAAAGGAAGACGCTGCGCGTTTAGCT	0,0003	0,004	0,0757	0,3735	0,8118	0,9339
S1	CGGATTCGCGTGTAACAAAAGGAAGACGCGGCGCGTTTAGCT	0,0021	0,0327	0,3057	0,8777	0,8795	0,8729
S1	CGGATTCGCGTGTAGCAAAAAGAAGACGCGTCGCGTTTAGCT	0,0004	0,0055	0,0607	0,3344	0,6572	0,7637
S1	CGGATTCGCGTGTAGCAAAAGGAAGACGCGGCGCGTTTAGTT	0,0031	0,0171	0,2114	0,669	0,6547	0,6503
S1	CGGATTCGCGTGTAGCAAAAGGAAGACGCGTTGCGTTTAGCT	0	0,003	0,0285	0,2056	0,4228	0,5958
S1	CGGATTCGCGTGTAGCAAAAAGAAGACGCAGCGCGTTTAGCT	0	0,0005	0,0144	0,1403	0,3452	0,5917
S1	CGAATTCGCGTGTAGCAAAAAGAAGACGCGGCGCGTTTAGCT	0,0006	0,006	0,0682	0,3555	0,4681	0,5835
S1	CGGATTCGCGTGTAGCAAAAAGAATACGCGGCGCGTTTAGCT	0,0001	0,004	0,0313	0,2005	0,4734	0,5426
S1	CGGATTCGCGTGTAGCAAAAGGAATACGCGACGCGTTTAGCT	0,0003	0,001	0,021	0,2029	0,4577	0,5377
S1	CGGATTCGCGTTTAGCAAAAGGAAGACGCAGCGCGTTTAGCT	0	0,003	0,0147	0,1284	0,3174	0,5363
S1	CGGATTCGCGTGTAGCAAAAGGAAGACGCAATGCGTTTAGCT	0	0	0,0068	0,0951	0,2686	0,5283
S1	CGGATTTGCGTGTAGCAAAAAGAAGACGCGGCGCGTTTAGCT	0,0004	0,008	0,0613	0,35	0,4506	0,4902
S1	CGGATTCGCGTGTAGCAAAAGAAAGACGCGGCGCGTTTAGCT	0,0019	0,0191	0,1884	0,6157	0,5582	0,4842
S1	CGGATTCGCGTTTAGCAAAAAGAAGACGCGGCGCGTTTAGCT	0	0,0005	0,0145	0,1293	0,29	0,4447
S1	CGGATTCGCGTGTAGCAAAAAGAAGACGCGGTGCGTTTAGCT	0,0001	0,002	0,0615	0,3528	0,4859	0,4443
S1	CGGATTCGCGTGTAGCAAAAGGAAGACGCAACGCGTTTAGCT	0,0001	0,002	0,0225	0,1789	0,3188	0,429
S1	CGGATTCGCGTGTAACAAAAAGAAGACGCGGCGCGTTTAGCT	0,0001	0,0025	0,0504	0,2348	0,3049	0,4234
S1	CGGATTCGCGTATAGCAAAAGGAAGACGCAGCGCGTTTAGCT	0,0001	0,0015	0,0264	0,1986	0,3655	0,3662
S1	CGGATTCGCGTGTAGCAAAAAGAAGACGCGTTGCGTTTAGCT	0	0,0005	0,0093	0,0906	0,2187	0,3309
S1	CGGATTCGCGTGTAGCAAAAAGAAGACGCGGCGCGTTTAGTT	0,0001	0,0025	0,0361	0,1818	0,238	0,3224
S1	CGAATTCGCGTATAGCAAAAGGAAGACGCGGCGCGTTTAGCT	0,001	0,0106	0,1175	0,5102	0,436	0,3158
S1	CGGATTCGCGTATAGCAAAATGAAGACGCGGCGCGTTTAGCT	0	0,0025	0,0242	0,179	0,3117	0,3063
S1	CGGATTCGCGTATAGCAAAAGGAAGACGCGACGCGTTTAGCT	0	0,0015	0,0394	0,224	0,3071	0,2728
S1	CGGATTCGCGTGTAGTAAAAGGAAGACGCGGCGCGTTTAGCT	0,0009	0,01	0,0921	0,3409	0,2686	0,2717
S1	CGGATTCGCGTGTAGCAAAAGGAAGACGCGGCGCGTTTAACT	0,0004	0,0131	0,0817	0,2577	0,2248	0,2684
S1	CGGATTCGCGTGTAGCAAAAGGAAGACGCGGCGCATTTAGCT	0,001	0,01	0,091	0,2783	0,2504	0,2532
S1	CGGATTCGCGTGTAGCAAAAGGAAAACGCGGCGCGTTTAGCT	0,0012	0,0055	0,0774	0,2914	0,233	0,245
S1	CGGATTTGCGTGTAGCAAAAGGAAGACGCGACGCGTTTAGCT	0,0001	0,0035	0,0283	0,1714	0,234	0,2437
S1	CGGATTCGCGTGTAGCAAAAGGAAGACGCGGCGTGTTTAACT	0,0001	0,003	0,0156	0,1087	0,2155	0,2431
S1	CGGATTCGCGTGTAGCAAAAAGAAGACGCGATGCGTTTAGCT	0	0	0,0033	0,0404	0,1279	0,2402
S1	CGAATTCGCGTATAGCAAAAAGAAGACGCGGCGCGTTTAGCT	0	0,001	0,0202	0,1499	0,1988	0,2303
S1	CGAATTCGCGTGTAGCAAAAGGAAGACGCGACGCGTTTAGCT	0	0,005	0,0272	0,1486	0,1575	0,2183
S1	CGGATTCGCGTGTAGCAAAAAAAAGACGCGGCGCGTTTAGCT	0,0001	0,0035	0,0338	0,1455	0,1664	0,2139

Table 6.4Sequences found the last rounds of the split-combine cell SELEX and three round of deconvoulation step with cyclic RGD (cRGD-dU); only the randome region, the frequency of he sequences related to the SELEX round.

		Frequency [%]					
FAMILY	SEQUENCE	Round 7	Round 8	Round 9	Round 10	Round 11	Round 12
S2	GGCATGAGCCCGAACCGCGCGTGTAGCGAGAGACGAACATA	0	0	0,0338	0,001	0,0024	5,6105
S2	GGCATGAGCCCGAACCGCGCGTGTAGCTAGAGACGAACATA	0	0	0,0211	0,0004	0,0005	0,5053
S2	GGCATGAGCCCGAACCACGCGTGTAGCGAGAGACGAACAAG	0	0,0005	0,0016	0,0197	0,0443	0,0948
S2	GGCATGAGCCCGAACCGCGCGTGTAGCGAGAGACGAACAAG	0	0,006	0,0142	0,0433	0,05	0,0526
S2	GGCATGAGCCCGAACCTCGCGTGTAGCGAGAGACGAACAAG	0	0	0,0018	0,0107	0,0175	0,0285
S2	GGCATGAGCCCGAACCGCGCGTGTAGCGAGAGACGAACAGA	0	0,003	0,0014	0,0057	7,168	0,0052
S1	CGGATTCGCGTGTAGCAAAAGGAAGACGCGGCGCGTTTAGCT	0,0391	0,5682	4,3924	2,7642	0,8241	0,1672
S1	CGGATTCGCGTATAGCAAAAGGAAGACGCGGCGCGTTTAGCT	0,0067	0,1095	1,0547	0,6485	0,1926	0,0448
S1	CGGATTCGCGTGTAGCAAAAAGAAGACGCGGCGCGTTTAGCT	0,0052	0,0523	0,7445	0,5667	0,1832	0,0425
S1	CGGATTCGCGTGTAGCAAAAGGAAGACGCGACGCGTTTAGCT	0,0009	0,0206	0,2897	0,2953	0,1732	0,04
S1	CGAATTCGCGTGTAGCAAAAGGAAGACGCGGCGCGTTTAGCT	0,0037	0,0442	0,393	0,2372	0,0625	0,0171
S1	CGGATTTGCGTGTAGCAAAAGGAAGACGCGGCGCGTTTAGCT	0,0055	0,0407	0,3574	0,1718	0,0453	0,0161
S1	CGGATTCGCGTGTAGCAAAAGGAAGACGCAGCGCGTTTAGCT	0,0003	0,0065	0,1229	0,1313	0,062	0,0143
S1	CGGATTCGCGTATAGCAAAAAGAAGACGCGGCGCGTTTAGCT	0,0006	0,0131	0,1826	0,1277	0,0401	0,0142
S1	CGGATTCGCGTGTAGCAAAAGGAAGACGCGGTGCGTTTAGCT	0,0046	0,0578	0,4937	0,1809	0,048	0,0129
S1	CGGATTCGCGTTTAGCAAAAGGAAGACGCGGCGCGTTTAGCT	0,0007	0,0146	0,1297	0,095	0,0348	0,011
S1	CGGATTCGCGTGTAGCAAAAGGAAGACGCGGCGCGTTTAGCA	0,0003	0,002	0,0185	0,0408	0,0335	0,0103
S1	CGGATTCGCGTGTAGCAAAAGGAAGACGCGGCGCGTTTAGTT	0,0031	0,0171	0,2114	0,1177	0,0336	0,0096
S1	CGGATTCGCGTGTAACAAAAGGAAGACGCGGCGCGTTTAGCT	0,0021	0,0327	0,3057	0,1304	0,0377	0,0095
S1	CGGATTCGCGTGTAGCAAAAGAAAGACGCGGCGCGTTTAGCT	0,0019	0,0191	0,1884	0,0977	0,0227	0,0075
S1	CGGATTCGCGTGTAGCAAAAGGAATACGCGGCGCGTTTAGCT	0,0015	0,0271	0,2398	0,0917	0,0254	0,0075
S1	CGGATTCGCGTGTAGCAAAAAGAAGACGCGACGCGTTTAGCT	0	0,002	0,0408	0,0483	0,0278	0,0073
S1	CGAATTCGCGTATAGCAAAAGGAAGACGCGGCGCGTTTAGCT	0,001	0,0106	0,1175	0,0671	0,0171	0,0067
S1	CGGATTCGCGTGTAGCAAAAGGAAGACGCTGCGCGTTTAGCT	0,0003	0,004	0,0757	0,0398	0,0154	0,0061
S1	CGGATTCGCGTGTAGCAAAAGGAAGACGCGTCGCGTTTAGCT	0,0003	0,0126	0,1233	0,0804	0,0275	0,0059
S1	CGGATTCGCGTATAGCAAAAGGAAGACGCGACGCGTTTAGCT	0	0,0015	0,0394	0,0354	0,0195	0,0056
S1	CGAATTCGCGTGTAGCAAAAAGAAGACGCGGCGCGTTTAGCT	0,0006	0,006	0,0682	0,0504	0,0142	0,0048
S1	CGGATTCGCGTGTAGCAAAATGAAGACGCGGCGCGTTTAGCT	0,0004	0,0085	0,0874	0,0426	0,0131	0,0048
S1	CGGATTCGCGTGTAGCAAAAGGAAGACGCGGCGCATTTAGCT	0,001	0,01	0,091	0,054	0,0125	0,0045
S1	CGGATTCGCGTGTAGCAAAAGGAAGACGCGGCGCGTTTAACT	0,0004	0,0131	0,0817	0,0393	0,0101	0,0042
S1	CGGATTCGCGTGTAGCAAAAGGAAGACGCGATGCGTTTAGCT	0,0004	0,0035	0,0374	0,0432	0,0173	0,004
S1	CGGATTCGCGTGTAGCAAAAGGAAGACGTGGCGCGTTTAGCT	0,0007	0,0085	0,0726	0,0449	0,0125	0,004
S1	CGGATTTGCGTGTAGCAAAAAGAAGACGCGGCGCGTTTAGCT	0,0004	0,008	0,0613	0,035	0,0101	0,0039
S1	CGGATTTGCGTATAGCAAAAGGAAGACGCGGCGCGTTTAGCT	0,0007	0,0065	0,0699	0,0398	0,0099	0,0038
S1	CGAATTCGCGTGTAGCAAAAGGAAGACGCGACGCGTTTAGCT	0	0,005	0,0272	0,0255	0,0116	0,0037
S1	CGGATTCGCGTATAGCAAAAGGAAGACGCAGCGCGTTTAGCT	0,0001	0,0015	0,0264	0,0308	0,0157	0,0037
S1	TGGATTCGCGTGTAGCAAAAGGAAGACGCGGCGCGTTTAGCT	0,0007	0,004	0,0589	0,0462	0,0109	0,0034
S1	CGGATTCGCGTGTAGCAAAAAGAAGACGCGTCGCGTTTAGCT	0,0004	0,0055	0,0607	0,0441	0,0126	0,0033
S1	CGGATTCGCGTGTAGCAAAAGGAAGACGCAACGCGTTTAGCT	0,0001	0,002	0,0225	0,0252	0,0133	0,0033
S1	CGGATTCGCGTGTAGCAAAAGGAAAACGCGGCGCGTTTAGCT	0,0012	0,0055	0,0774	0,0446	0,0097	0,0032
S1	CGGATTCGCGTGTAGCAAAAAGAAGACGCAGCGCGTTTAGCT	0	0,0005	0,0144	0,0212	0,0089	0,0029
S1	CGGATTCGCGTGTAGCAAAAAGAAGACGCGGTGCGTTTAGCT	0,0001	0,002	0,0615	0,0291	0,009	0,0029
S1	CGGATTCGCGTGTAGTAAAAGGAAGACGCGGCGCGTTTAGCT	0,0009	0,01	0,0921	0,0439	0,0089	0,0029
S1	CGGATTCGCATGTAGCAAAAGGAAGACGCGGCGCGTTTAGCT	0,0006	0,0116	0,0778	0,0421	0,0098	0,0028
S1	CGGATTCGCGTATAGCAAAAGGAAGACGCGGTGCGTTTAGCT	0,001	0,008	0,0737	0,0292	0,0082	0,0028
S1	CGGATTCACGTGTAGCAAAAGGAAGACGCGGCGCGTTTAGCT	0,0001	0,0045	0,0449	0,0267	0,0056	0,0027
S1	CGGATTCGCGTGTAACAAAAAGAAGACGCGGCGCGTTTAGCT	0,0001	0,0025	0,0504	0,0268	0,0079	0,0027
S1	CGGATTCGCGTGTAGCAAAAGGAAGACGCGGCACGTTTAGCT	0,0006	0,0025	0,0466	0,0328	0,0076	0,0026

Table 6.5 Sequences found in three round of deconvoulation step with ethanamine (Ea-dU); only the randome region, the frequency of he sequences related to the SELEX round.

		Frequency [%]		
FAMILY	SEQUENCE	Round 10	Round 11	Round 12
S1	CGGATTCGCGTGTAGCAAAAGGAAGACGCGGCGCGTTTAGCT	16,4414	22,8028	19,1675
S1	CGGATTCGCGTATAGCAAAAGGAAGACGCGGCGCGTTTAGCT	4,4842	6,8186	6,6283
S1	CGGATTCGCGTTTAGCAAAAGGAAGACGCGGCGCGTTTAGCT	0,9044	2,1461	3,8818
S1	CGGATTCGCGTGTAGCAAAAAGAAGACGCGGCGCGTTTAGCT	2,8554	4,0145	3,1603
S1	CGGATTCGCGTGTAGCAAAAGGAAGACGCTGCGCGTTTAGCT	0,5564	1,5909	2,3937
S1	CGGATTCGCGTGTAGCAAAAGGAAGACGCGACGCGTTTAGCT	1,1464	1,701	1,8118
S1	CGGATTCGCGTATAGCAAAAAGAAGACGCGGCGCGTTTAGCT	0,9882	1,668	1,7153
S1	CGAATTCGCGTGTAGCAAAAGGAAGACGCGGCGCGTTTAGCT	1,3336	1,5536	1,3925
S1	CGGATTTGCGTGTAGCAAAAGGAAGACGCGGCGCGTTTAGCT	1,3693	1,5953	1,2599
S1	CGGATTCGCGTGTAGCAAAAGGAATACGCGGCGCGTTTAGCT	0,7952	1,0124	0,7704
S1	CGGATTCGCGTGTAACAAAAGGAAGACGCGGCGCGTTTAGCT	0,6712	0,8198	0,749
S1	CGGATTCGCGTGTAGCAAAAGGAAGACGCGTCGCGTTTAGCT	0,57	0,8528	0,7403
S1	CGGATTCGCGTGTAGCAAAAGGAAGACGCGGTGCGTTTAGCT	0,9561	0,8933	0,6712
S1	CGGATTCGCGTGTAGCAAAAGGAAGACGCGGCGCGTTTAGTT	0,6175	0,7277	0,6611
S1	CGGATTCGCGTGTAGCAAAATGAAGACGCGGCGCGTTTAGCT	0,4131	0,6715	0,6081
S1	CGGATTCGCGTGTAGCAAAAGGAAGACGCGATGCGTTTAGCT	0,2569	0,4623	0,6038
S1	CGGATTCGCGTGTAGCAAAAGGAAGACGCGTTGCGTTTAGCT	0,2232	0,459	0,6017
S1	CGGATTCGCGTGTAGCAAAAGGAAGACGCGGCGCGTTTAGCA	0,1429	0,3759	0,5538
S1	CGGATTCGCGTTTAGCAAAAAGAAGACGCGGCGCGTTTAGCT	0,1282	0,3211	0,5439
S1	CGGATTCGCGTATAGCAAAAGGAAGACGCGACGCGTTTAGCT	0,234	0,4123	0,5021
S1	CGAATTCGCGTATAGCAAAAGGAAGACGCGGCGCGTTTAGCT	0,3961	0,4941	0,498
S1	CGGATTCGCGTGTAGCAAAAGGAAGACGCAGCGCGTTTAGCT	0,4471	0,5266	0,4833
S1	CGGATTCGCGTGTAGCAAAAGGAAGACGCGGCGCATTTAGCT	0,4303	0,5001	0,4778
S1	CGGATTCGCGTGTAGCAAAAGAAAGACGCGGCGCGTTTAGCT	0,4918	0,5152	0,4541
S1	CGGATTCGCGTATAGCAAAAGGAAGACGCTGCGCGTTTAGCT	0,0947	0,2671	0,4327
S1	CGGATTCGCGTTTAGCAAAAGGAAGACGCAGCGCGTTTAGCT	0,0974	0,2141	0,4209
S1	CGGATTTGCGTATAGCAAAAGGAAGACGCGGCGCGTTTAGCT	0,3191	0,3996	0,3647
S1	CGGATTCGCGTGTAGCAAAAAGAAGACGCGACGCGTTTAGCT	0,186	0,3248	0,3415
S1	CGGATTCGCGTATAGCAAAAGGAAGACGCAGCGCGTTTAGCT	0,1442	0,2472	0,3144
S1	CGGATTCGCGTATAGCAAAATGAAGACGCGGCGCGTTTAGCT	0,1562	0,2965	0,3102
S1	CGGATTCGCGTGTAGCAAAAGGAAGACGCGGCGCGTTTAACT	0,2605	0,303	0,2979
S1	CGGATTCGCGTTTAGCAAAAGGAAGACGCTGCGCGTTTAGCT	0,0251	0,0958	0,2819
S1	CGGATTCGCATGTAGCAAAAGGAAGACGCGGCGCGTTTAGCT	0,2573	0,279	0,2595
S1	TGGATTCGCGTGTAGCAAAAGGAAGACGCGGCGCGTTTAGCT	0,2484	0,2837	0,2586
S1	CGAATTCGCGTTTAGCAAAAGGAAGACGCGGCGCGTTTAGCT	0,0722	0,1359	0,2581
S1	CGGATTTGCGTTTAGCAAAAGGAAGACGCGGCGCGTTTAGCT	0,0794	0,1548	0,2514
S1	CGGATTCGCGTGTAGCAAAAGGAAGACGTGGCGCGTTTAGCT	0,2411	0,2656	0,2495
S1	CGGATTTGCGTGTAGCAAAAAGAAGACGCGGCGCGTTTAGCT	0,2723	0,3279	0,2457
S1	CGGATTCACGTGTAGTAAAAGGAAGACGCGGCGCGTTTAGCT	0,0565	0,1627	0,2403
S1	CGGATTCGCGTGTAGTAAAAGGAAGACGCGGCGCGTTTAGCT	0,248	0,2587	0,2352
S1	CGGATTCGCGTGTAGCAAAAGGAAGACGCGGCGTGTTTAACT	0,1204	0,2149	0,2335
S1	CGGATTCGCATATAGCAAAAGGAAGACGCGGCGCGTTTAGCT	0,1829	0,2197	0,2308
S1	CGAATTCGCGTGTAGCAAAAAGAAGACGCGGCGCGTTTAGCT	0,245	0,2715	0,2258
S1	CGGATTCGCGTGTAGCAAAAGGAAGACGCTACGCGTTTAGCT	0,0783	0,1504	0,2219
S1	CGGATTCGCGTATAGCAAAAGGAAGACGCGGCGCGTTTAGTT	0,1615	0,2088	0,2213
S1	CGGATTCGCGTGTAGCAAAAGGAAAACGCGGCGCGTTTAGCT	0,2118	0,2166	0,2185
S1	CGGATTCGCGTATAACAAAAGGAAGACGCGGCGCGTTTAGCT	0,1569	0,2054	0,2152
S1	CGGATTCGCGTGTAGCAAAAGGAAGACGCGGCACGTTTAGCT	0,1914	0,2154	0,2116

Table 6.6 Sequences found the last rounds of the split-combine cell SELEX and three round of deconvoulation step with isobutyl (Ib-dU); only the randome region, the frequency of he sequences related to the SELEX round.

		Frequency [%]					
FAMILY	SEQUENCE	Round 7	Round 8	Round 9	Round 10	Round 11	Round 12
S1	CGGATTCGCGTGTAGCAAAAGGAAGACGCGGCGCGTTTAGCT	0,0391	0,5682	4,3924	7,0936	14,1202	19,432
S1	CGGATTCGCGTGTAGCAAAAAGAAGACGCGGCGCGTTTAGCT	0,0052	0,0523	0,7445	2,1307	4,2848	5,9536
S1	CGGATTCGCGTGTAGCAAAAGGAAGACGCGACGCGTTTAGCT	0,0009	0,0206	0,2897	0,6287	1,4119	2,2996
S1	CGGATTCGCGTATAGCAAAAGGAAGACGCGGCGCGTTTAGCT	0,0067	0,1095	1,0547	2,0831	2,4543	1,9293
S1	CGAATTCGCGTGTAGCAAAAGGAAGACGCGGCGCGTTTAGCT	0,0037	0,0442	0,393	0,7498	0,6604	1,1323
S1	CGGATTCGCGTGTAGCAAAAGGAAGACGCAGCGCGTTTAGCT	0,0003	0,0065	0,1229	0,299	0,6121	0,9367
S1	CGGATTTGCGTGTAGCAAAAGGAAGACGCGGCGCGTTTAGCT	0,0055	0,0407	0,3574	0,4882	0,4751	0,767
S1	CGGATTCGCGTGTAGCAAAAGGAAGACGCGGTGCGTTTAGCT	0,0046	0,0578	0,4937	0,9813	0,763	0,6629
S1	CGGATTCGCGTGTAGCAAAAGGAATACGCGGCGCGTTTAGCT	0,0015	0,0271	0,2398	0,5252	0,665	0,6607
S1	CGGATTCGCGTGTAGCAAAAGGAAGACGCGGCGCGTTTAGTT	0,0031	0,0171	0,2114	0,3874	0,3482	0,6053
S1	CGGATTCGCGTGTAGCAAAAAGAAGACGCGACGCGTTTAGCT	0	0,002	0,0408	0,1445	0,3423	0,6015
S1	CGGATTCGCGTGTAACAAAAGGAAGACGCGGCGCGTTTAGCT	0,0021	0,0327	0,3057	0,4423	0,3483	0,5995
S1	CGGATTCGCGTATAGCAAAAAGAAGACGCGGCGCGTTTAGCT	0,0006	0,0131	0,1826	0,5412	0,6519	0,5437
S1	CGGATTCGCGTGTAGCAAAAGGAAGACGCGATGCGTTTAGCT	0,0004	0,0035	0,0374	0,1655	0,3249	0,5328
S1	CGGATTCGCGTGTAGCAAAAGGAAGACGCGTCGCGTTTAGCT	0,0003	0,0126	0,1233	0,2872	0,4563	0,4936
S1	CGGATTCGCGTGTAGCAAAAGGAAGACGCTGCGCGTTTAGCT	0,0003	0,004	0,0757	0,1884	0,3521	0,4533
S1	CGGATTCGCGTGTAGCAAAAGAAAGACGCGGCGCGTTTAGCT	0,0019	0,0191	0,1884	0,4107	0,306	0,4465
S1	CGGATTCGCGTGTAGCAAAATGAAGACGCGGCGCGTTTAGCT	0,0004	0,0085	0,0874	0,1926	0,3179	0,3805
S1	CGGATTCGCGTTTAGCAAAAGGAAGACGCGGCGCGTTTAGCT	0,0007	0,0146	0,1297	0,2393	0,338	0,367
S1	CGAATTCGCGTGTAGCAAAAAGAAGACGCGGCGCGTTTAGCT	0,0006	0,006	0,0682	0,2303	0,2084	0,3519
S1	CGGATTCGCGTGTAGCAAAAAGAAGACGCGTCGCGTTTAGCT	0,0004	0,0055	0,0607	0,1738	0,2758	0,2685
S1	CGGATTCGCGTGTAGCAAAAGGAAGACGCGGCGCATTTAGCT	0,001	0,01	0,091	0,1559	0,1205	0,2527
S1	CGGATTTGCGTGTAGCAAAAAGAAGACGCGGCGCGTTTAGCT	0,0004	0,008	0,0613	0,1445	0,151	0,2446
S1	TGGATTCGCGTGTAGCAAAAGGAAGACGCGGCGCGTTTAGCT	0,0007	0,004	0,0589	0,109	0,1226	0,2337
S1	CGGATTCGCGTGTAGCAAAAAGAAGACGCAGCGCGTTTAGCT	0	0,0005	0,0144	0,0668	0,1294	0,2187
S1	CGGATTCGCGTGTAGCAAAAGGAAGACGTGGCGCGTTTAGCT	0,0007	0,0085	0,0726	0,1329	0,1079	0,2073
S1	CGGATTCGCGTGTAGCAAAAGGAAGACGCGGCGCGTTTAACT	0,0004	0,0131	0,0817	0,1471	0,0906	0,1996
S1	CGGATTCGCGTGTAGCAAAAGGAAGACGCAACGCGTTTAGCT	0,0001	0,002	0,0225	0,0806	0,1298	0,1931
S1	CGGATTCGCGTGTAACAAAAAGAAGACGCGGCGCGTTTAGCT	0,0001	0,0025	0,0504	0,1305	0,1101	0,1926
S1	CGGATTCGCGTGTAGCAAAAGGAAAACGCGGCGCGTTTAGCT	0,0012	0,0055	0,0774	0,1772	0,1077	0,1907
S1	CGGATTCGCATGTAGCAAAAGGAAGACGCGGCGCGTTTAGCT	0,0006	0,0116	0,0778	0,154	0,115	0,1859
S1	CGGATTCGCGTGTAGTAAAAGGAAGACGCGGCGCGTTTAGCT	0,0009	0,01	0,0921	0,1852	0,1002	0,1843
S1	CGGATTCGCGTGTAGCAAAAAGAAGACGCGGCGCGTTTAGTT	0,0001	0,0025	0,0361	0,1133	0,1015	0,18
S1	CGGATTCGCGTGTAGCAAAAAGAAGACGCGGTGCGTTTAGCT	0,0001	0,002	0,0615	0,2037	0,1532	0,17
S1	CGGATTCGCGTGTAGCAAAAGGAAGACACGGCGCGTTTAGCT	0,0003	0,01	0,0571	0,1216	0,0788	0,1679
S1	CGGATTCGCGTGTAGCAAAAGGAAGACGCGGCACGTTTAGCT	0,0006	0,0025	0,0466	0,099	0,0741	0,161
S1	CGGATTCGCGTATAGCAAAAGGAAGACGCGACGCGTTTAGCT	0	0,0015	0,0394	0,1108	0,1488	0,1563
S1	CGGATTCGTGTGTAGCAAAAGGAAGACGCGGCGCGTTTAGCT	0,0004	0,005	0,0544	0,0939	0,0772	0,1435
S1	CGGATTCGCGTGTAGCAAAAGGAAGACGCTACGCGTTTAGCT	0	0,0005	0,0121	0,048	0,0891	0,143
S1	CGAATTCGCGTGTAGCAAAAGGAAGACGCGACGCGTTTAGCT	0	0,005	0,0272	0,0688	0,0717	0,1375
S1	CGGATTCGCGTGTAGCAAAAAGAATACGCGGCGCGTTTAGCT	0,0001	0,004	0,0313	0,1003	0,1249	0,135
S1	CGGATTCGCGTGTAGCAAAAGGAAGATGCGGCGCGTTTAGCT	0,0004	0,002	0,032	0,0736	0,0649	0,1328
S1	CGGATTCGCGTGTAGCAAAAAAAAGACGCGGCGCGTTTAGCT	0,0001	0,0035	0,0338	0,1138	0,0906	0,1281
S1	CGAATTCGCGTATAGCAAAAGGAAGACGCGGCGCGTTTAGCT	0,001	0,0106	0,1175	0,2752	0,151	0,1266
S1	CGGATTCGCGTATAGCAAAAGGAAGACGCAGCGCGTTTAGCT	0,0001	0,0015	0,0264	0,0751	0,1166	0,1255
S1	CGGATTCGCGTGTAGCAAAAGGAAGACGCGGCGTGTTTAGCT	0,0001	0,005	0,0349	0,0839	0,0508	0,1197
S1	CGGATTCGCGTGTAGCAAAAGGAAGACGCGTTGCGTTTAGCT	0	0,003	0,0285	0,086	0,1096	0,1141
S1	CAGATTCGCGTGTAGCAAAAGGAAGACGCGGCGCGTTTAGCT	0	0,003	0,0305	0,0728	0,0505	0,112

Table 6.7 Sequences found the last rounds of the split-combine cell SELEX and three round of deconvoulation step with indole (In-dU); only the randome region, the frequency of he sequences related to the SELEX round.

		Frequency [%]					
FAMILY	SEQUENCE	Round 7	Round 8	Round 9	Round 10	Round 11	Round 12
S1	CGGATTCGCGTGTAGCAAAAGGAAGACGCGGCGCGTTTAGCT	0,0391	0,5682	4,3924	2,7705	1,0661	0,1539
S1	CGGATTCGCGTGTAGCAAAAAGAAGACGCGGCGCGTTTAGCT	0,0052	0,0523	0,7445	0,7394	0,3914	0,0559
S1	CGGATTCGCGTATAGCAAAAGGAAGACGCGGCGCGTTTAGCT	0,0067	0,1095	1,0547	0,4168	0,1219	0,0287
S1	CGGATTCGCGTGTAGCAAAAGGAAGACGCAGCGCGTTTAGCT	0,0003	0,0065	0,1229	0,189	0,1404	0,0189
S1	CGGATTCGCGTGTAGCAAAAGGAAGACGCGACGCGTTTAGCT	0,0009	0,0206	0,2897	0,2247	0,1092	0,0162
S1	CGAATTCGCGTGTAGCAAAAGGAAGACGCGGCGCGTTTAGCT	0,0037	0,0442	0,393	0,23	0,085	0,0158
S1	CGGATTTGCGTGTAGCAAAAGGAAGACGCGGCGCGTTTAGCT	0,0055	0,0407	0,3574	0,1732	0,0607	0,0129
S1	CGGATTCGCGTGTAGCAAAAGGAAGACGCGGTGCGTTTAGCT	0,0046	0,0578	0,4937	0,2555	0,0855	0,0127
S1	CGGATTCGCGTATAGCAAAAAGAAGACGCGGCGCGTTTAGCT	0,0006	0,0131	0,1826	0,1034	0,0352	0,009
S1	CGGATTCGCGTGTAACAAAAGGAAGACGCGGCGCGTTTAGCT	0,0021	0,0327	0,3057	0,1321	0,0498	0,0088
S1	CGGATTCGCGTGTAGCAAAAGGAAGACGCGGCGCGTTTAGTT	0,0031	0,0171	0,2114	0,1204	0,0521	0,0084
S1	CGGATTCGCGTGTAGCAAAAGGAAGACGCGTCGCGTTTAGCT	0,0003	0,0126	0,1233	0,1109	0,0545	0,0066
S1	CGGATTCGCGTTTAGCAAAAGGAAGACGCGGCGCGTTTAGCT	0,0007	0,0146	0,1297	0,0299	0,0115	0,0061
S1	CGGATTCGCGTGTAGCAAAAGGAAGACGCTGCGCGTTTAGCT	0,0003	0,004	0,0757	0,0571	0,023	0,0057
S1	CGAATTCGCGTGTAGCAAAAAGAAGACGCGGCGCGTTTAGCT	0,0006	0,006	0,0682	0,0602	0,0287	0,0055
S1	CGGATTCGCGTGTAGCAAAAAGAAGACGCAGCGCGTTTAGCT	0	0,0005	0,0144	0,0327	0,0312	0,0052
S1	CGGATTCGCGTGTAGCAAAAGAAAGACGCGGCGCGTTTAGCT	0,0019	0,0191	0,1884	0,0962	0,0318	0,0052
S1	CGGATTCGCGTGTAGCAAAAAGAAGACGCGACGCGTTTAGCT	0	0,002	0,0408	0,0549	0,034	0,0051
S1	CGGATTCGCGTGTAGCAAAAGGAATACGCGGCGCGTTTAGCT	0,0015	0,0271	0,2398	0,038	0,0139	0,005
S1	CGGATTCGCGTGTAGCAAAAAGAAGACGCGTCGCGTTTAGCT	0,0004	0,0055	0,0607	0,0717	0,0412	0,0047
S1	CGGATTTGCGTGTAGCAAAAAGAAGACGCGGCGCGTTTAGCT	0,0004	0,008	0,0613	0,0469	0,0209	0,0046
S1	CGAATTCGCGTATAGCAAAAGGAAGACGCGGCGCGTTTAGCT	0,001	0,0106	0,1175	0,0416	0,0123	0,0044
S1	CGGATTCGCGTGTAGCAAAAGGAAGACGCGGCGCATTTAGCT	0,001	0,01	0,091	0,0548	0,0203	0,0044
S1	CGGATTCGCGTGTAGCAAAAAGAAGACGCGGTGCGTTTAGCT	0,0001	0,002	0,0615	0,0563	0,0232	0,0039
S1	CGGATTCGCGTGTAGCAAAAGGAAGACGCGATGCGTTTAGCT	0,0004	0,0035	0,0374	0,0481	0,0305	0,0038
S1	CGGATTCGCGTGTAGCAAAAGGAAGACGTGGCGCGTTTAGCT	0,0007	0,0085	0,0726	0,0438	0,016	0,0033
S1	TGGATTCGCGTGTAGCAAAAGGAAGACGCGGCGCGTTTAGCT	0,0007	0,004	0,0589	0,0448	0,0182	0,0032
S1	CGGATTCGCGTGTAGCAAAATGAAGACGCGGCGCGTTTAGCT	0,0004	0,0085	0,0874	0,0594	0,0141	0,0031
S1	CGGATTCGCGTGTAGCAAAAGGAAGACGCGGCGCGTTTAACT	0,0004	0,0131	0,0817	0,0403	0,0135	0,003
S1	CGGATTCGCGTGTAGTAAAAGGAAGACGCGGCGCGTTTAGCT	0,0009	0,01	0,0921	0,0439	0,016	0,0028
S1	CGGATTCGCGTGTAGCAAAAGGAAGACGCAACGCGTTTAGCT	0,0001	0,002	0,0225	0,0354	0,0234	0,0027
S1	CGGATTTGCGTATAGCAAAAGGAAGACGCGGCGCGTTTAGCT	0,0007	0,0065	0,0699	0,0256	0,0084	0,0027
S1	CGGATTCGCATGTAGCAAAAGGAAGACGCGGCGCGTTTAGCT	0,0006	0,0116	0,0778	0,0447	0,0166	0,0026
S1	CGGATTCGCGTGTAGCAAAAAGAAGACGCGGCGCGTTTAGTT	0,0001	0,0025	0,0361	0,0324	0,0174	0,0024
S1	CGGATTCGCGTGTAGCAAAAGGAAGACGCGGCACGTTTAGCT	0,0006	0,0025	0,0466	0,0385	0,0129	0,0024
S1	CGGATTCGCGTGTAGCAAAAGGAAGACACGGCGCGTTTAGCT	0,0003	0,01	0,0571	0,0426	0,0139	0,0023
S1	CGGATTCGCATATAGCAAAAGGAAGACGCGGCGCGTTTAGCT	0,0004	0,0035	0,0436	0,0197	0,0049	0,0022
S1	CGGATTCGCGTATAGCAAAAGGAAGACGCGACGCGTTTAGCT	0	0,0015	0,0394	0,022	0,01	0,0022
S1	CGGATTCGCGTATAGCAAAAGGAAGACGCGGTGCGTTTAGCT	0,001	0,008	0,0737	0,0281	0,0109	0,0022
S1	CGGATTCGCGTGTAGCAAAAGGAAAACGCGGCGCGTTTAGCT	0,0012	0,0055	0,0774	0,0432	0,0129	0,0022
S1	CGGATTCGCGTATAGCAAAAGGAAGACGCAGCGCGTTTAGCT	0,0001	0,0015	0,0264	0,029	0,016	0,0021
S1	CGGATTCACGTGTAGCAAAAGGAAGACGCGGCGCGTTTAGCT	0,0001	0,0045	0,0449	0,0251	0,0084	0,002
S1	CGGATTCGCGTGTAACAAAAAGAAGACGCGGCGCGTTTAGCT	0,0001	0,0025	0,0504	0,0365	0,0166	0,0019
S1	CGGATTCGCGTGTAGCAAAAGGAAGATGCGGCGCGTTTAGCT	0,0004	0,002	0,032	0,03	0,0078	0,0019
S1	CGGATTCGCGTATAACAAAAGGAAGACGCGGCGCGTTTAGCT	0,0003	0,005	0,0518	0,0172	0,0055	0,0018
S1	CGGATTCGCGTATAGCAAAAGAAAGACGCGGCGCGTTTAGCT	0,0001	0,0035	0,0435	0,0157	0,0037	0,0017
S1	CGGATTCGCGTGTAGCAAAAAAAAGACGCGGCGCGTTTAGCT	0,0001	0,0035	0,0338	0,0243	0,0131	0,0017
S1	CGGATTCGCGTGTAGCAAAAGGAAGACGCAATGCGTTTAGCT	0	0	0,0068	0,0162	0,0129	0,0017

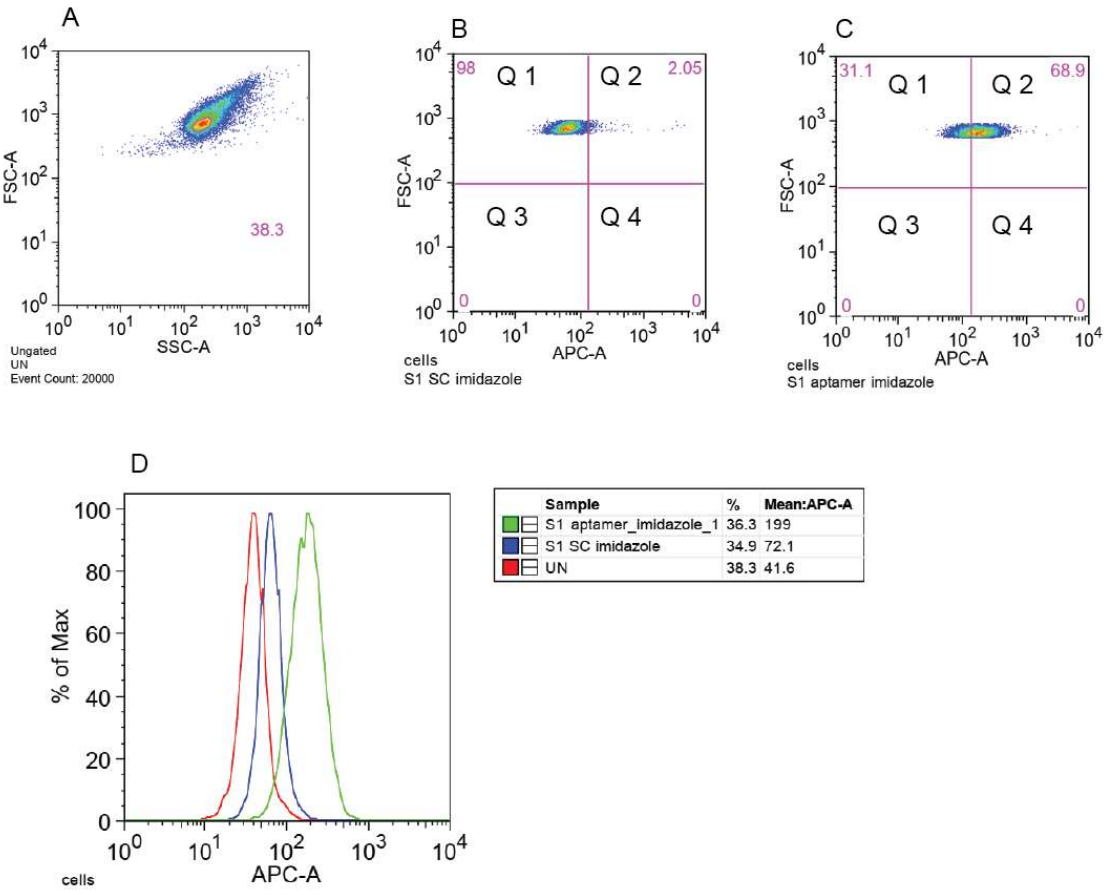

E

SC	S1	Ratio of binding
72,1	192	2,81471
70,7	199	2,76006
		2,7157
		2,66297
Plot these values		

Figure 6.11 Flow cytometer data analysis. (A) gating strategy (B) the quadra (Q1,Q2, Q3, Q4) for the scramble sequence and (C) for the S1 imidazole (D) showing the shifting in the fluorescence of the S1 imidazole.

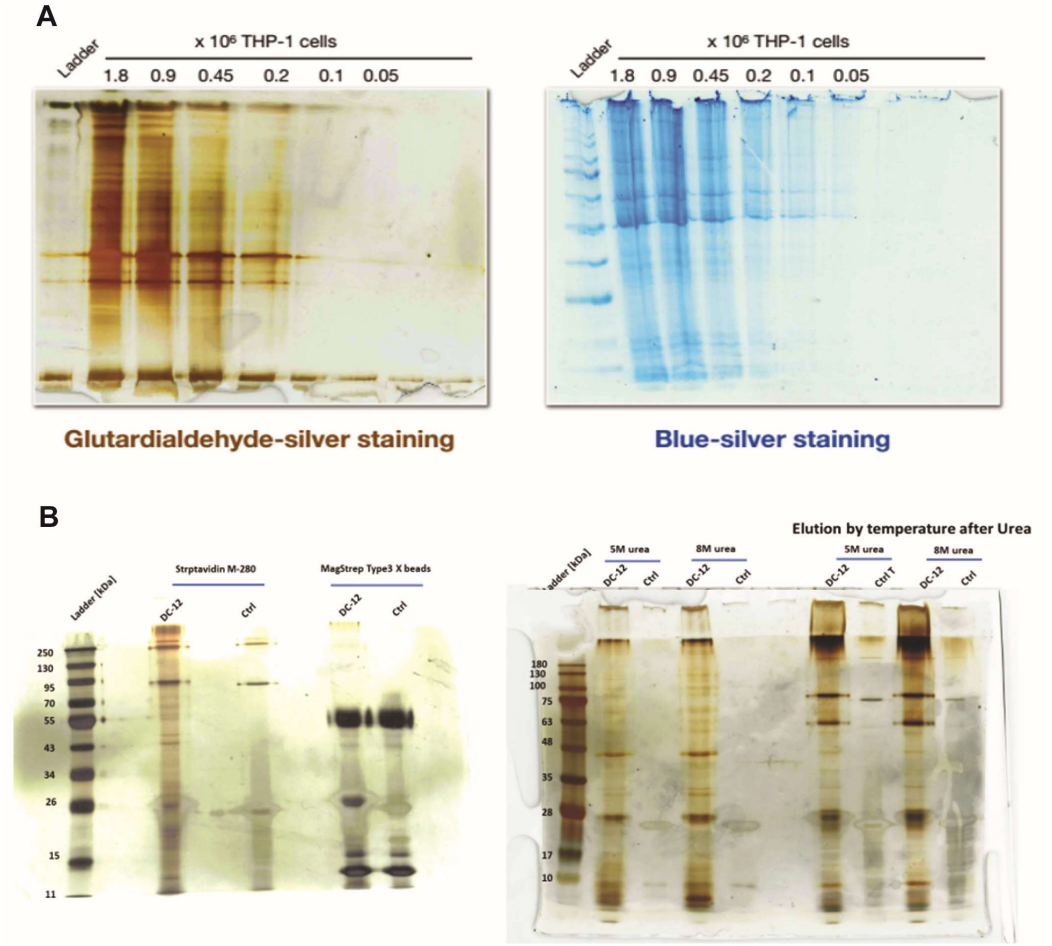

Figure 6.12 Pull down assay optimization
(A) The membrane protein fraction from THP-1 cells were isolaled and stained with Glutardialdeyde-silver staining or with blue-silver staining. **(B) (left)** The pull-down assay was performed using two different types of beads: Dynabeads M-280 Streptavidin and MagStep Type 3 X beads. Biotinylated DC-12 coupled with the different beads was incubated with 1.5 million THP-1 cells, and after washing and cell lysis, the protein complex was recovered with temperature. The experiment was repeated twice, independent experiments. **(B) (right)** Pull-down assay, 100 Pmol of DC-12 or control 2 was coupled with Dynabeads M-280 Streptavidin, and then the coupled aptamer was incubated with 1.5 million of THP-1 cells after washing and cell lysis. The protein complex was recovered with 5 M or 8 M urea at 37°C. followed by another elution with temperature (10 min at 95°C) (n = 2 independent experiments).

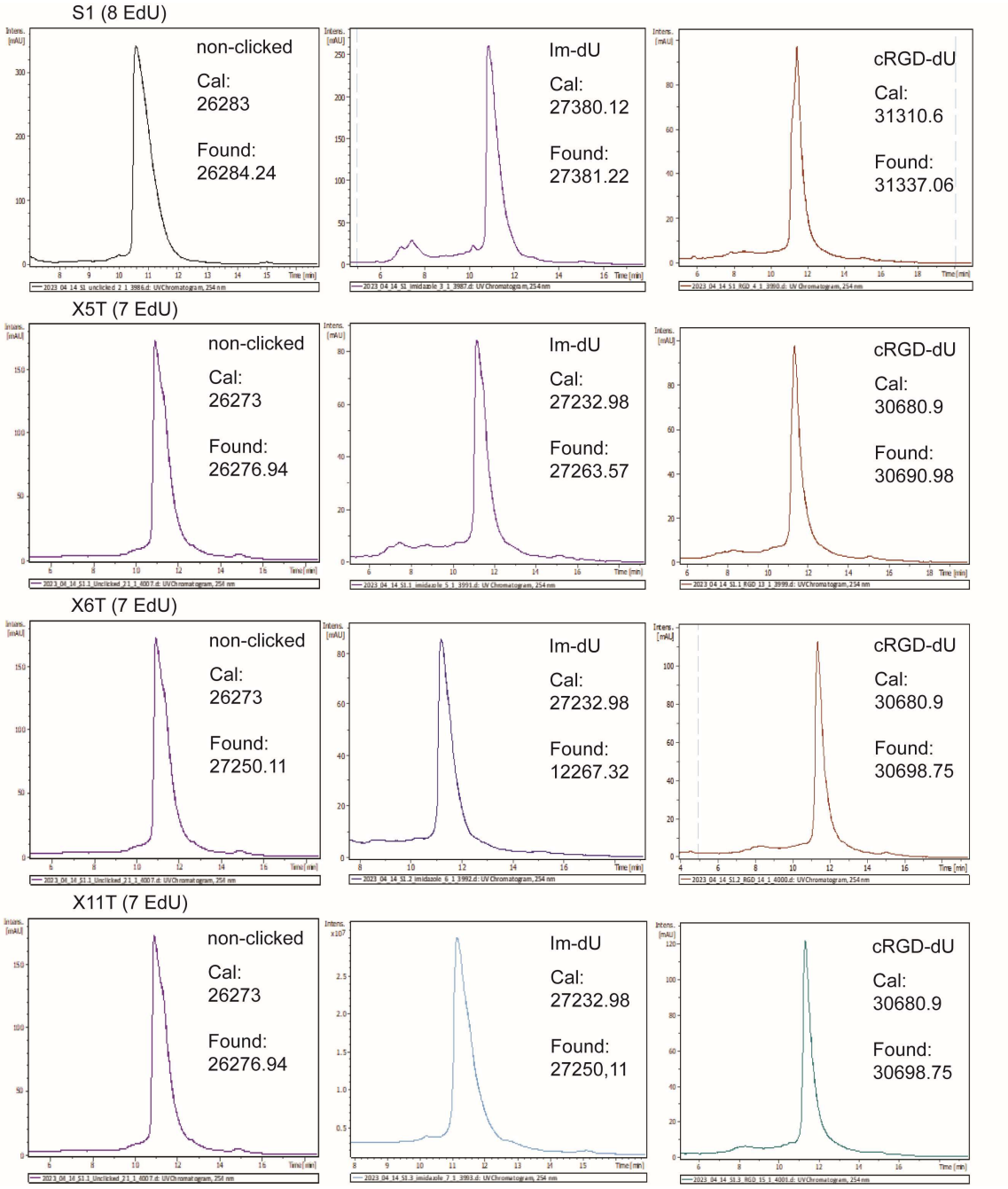
S1 (8 EdU)
non-clicked
Cal:
26283
Found:
26284.24
Im-dU
Cal:
27380.12
Found:
27381.22
cRGD-dU
Cal:
31310.6
Found:
31337.06
X5T (7 EdU)
non-clicked
Cal:
26273
Found:
26276.94
Im-dU
Cal:
27232.98
Found:
27263.57
cRGD-dU
Cal:
30680.9
Found:
30690.98
X6T (7 EdU)
non-clicked
Cal:
26273
Found:
27250.11
Im-dU
Cal:
27232.98
Found:
12267.32
cRGD-dU
Cal:
30680.9
Found:
30698.75
X11T (7 EdU)
non-clicked
Cal:
26273
Found:
26276.94
Im-dU
Cal:
27232.98
Found:
27250,11
cRGD-dU
Cal:
30680.9
Found:
30698.75

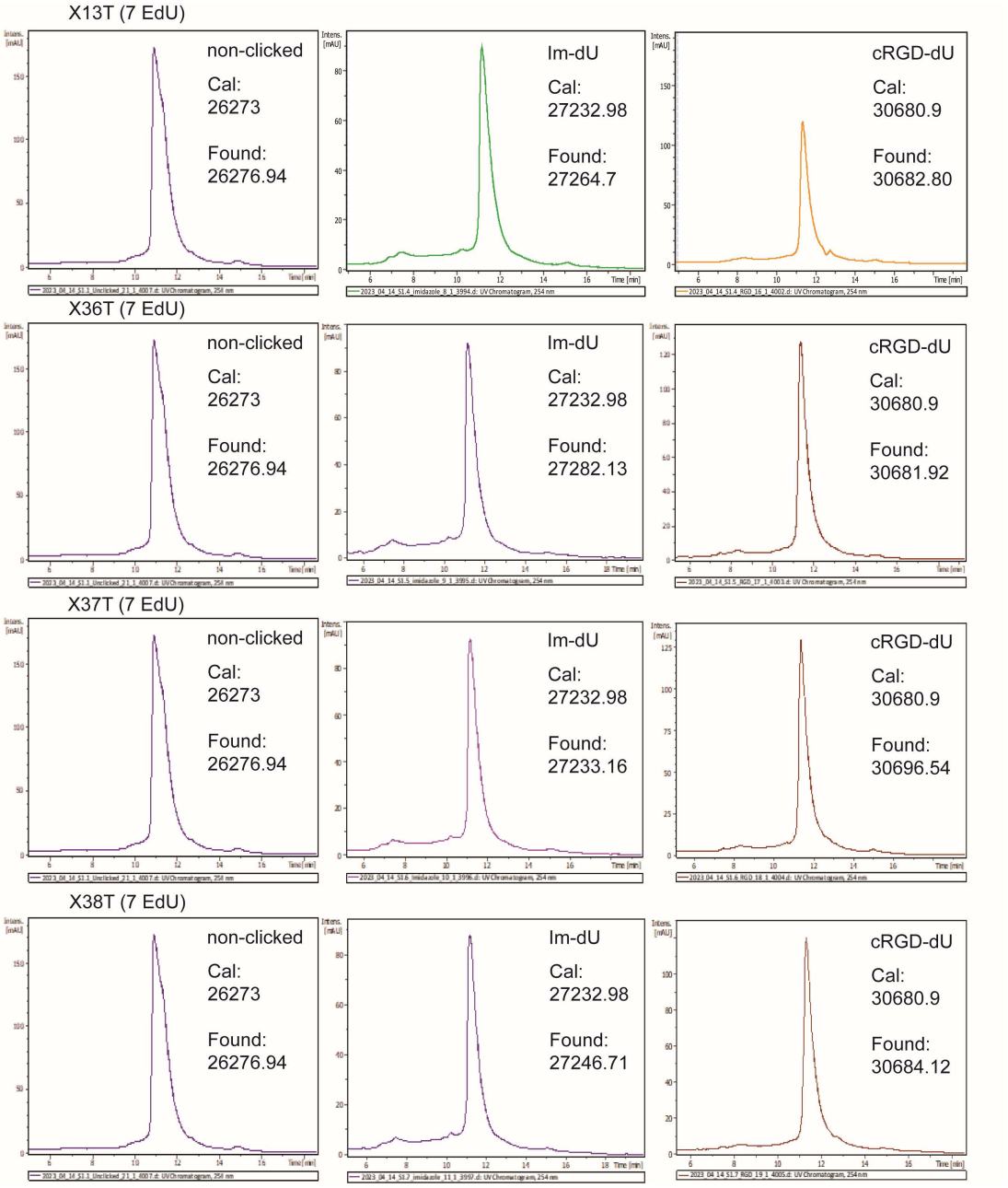
X13T (7 EdU)
non-clicked
Cal:
26273
Found:
26276.94
Im-dU
Cal:
27232.98
Found:
27264.7
cRGD-dU
Cal:
30680.9
Found:
30682.80
X36T (7 EdU)
non-clicked
Cal:
26273
Found:
26276.94
Im-dU
Cal:
27232.98
Found:
27282.13
cRGD-dU
Cal:
30680.9
Found:
30681.92
X37T (7 EdU)
non-clicked
Cal:
26273
Found:
26276.94
Im-dU
Cal:
27232.98
Found:
27233.16
cRGD-dU
Cal:
30680.9
Found:
30696.54
X38T (7 EdU)
non-clicked
Cal:
26273
Found:
26276.94
Im-dU
Cal:
27232.98
Found:
27246.71
cRGD-dU
Cal:
30680.9
Found:
30684.12

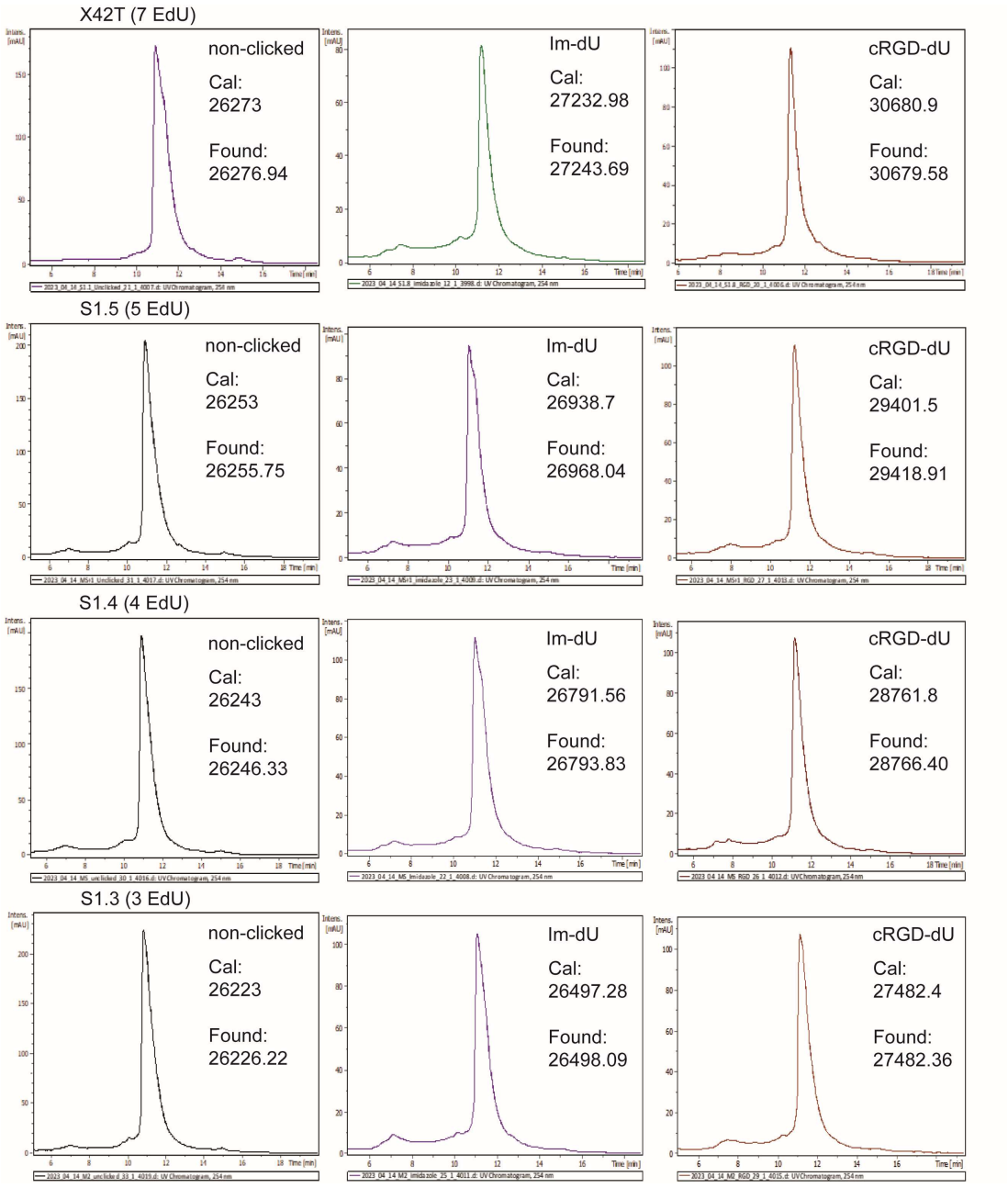
X42T (7 EdU)
non-clicked
Cal:
26273
Found:
26276.94
Im-dU
Cal:
27232.98
Found:
27243.69
cRGD-dU
Cal:
30680.9
Found:
30679.58
S1.5 (5 EdU)
non-clicked
Cal:
26253
Found:
26255.75
Im-dU
Cal:
26938.7
Found:
26968.04
cRGD-dU
Cal:
29401.5
Found:
29418.91
S1.4 (4 EdU)
non-clicked
Cal:
26243
Found:
26246.33
Im-dU
Cal:
26791.56
Found:
26793.83
cRGD-dU
Cal:
28761.8
Found:
28766.40
S1.3 (3 EdU)
non-clicked
Cal:
26223
Found:
26226.22
Im-dU
Cal:
26497.28
Found:
26498.09
cRGD-dU
Cal:
27482.4
Found:
27482.36

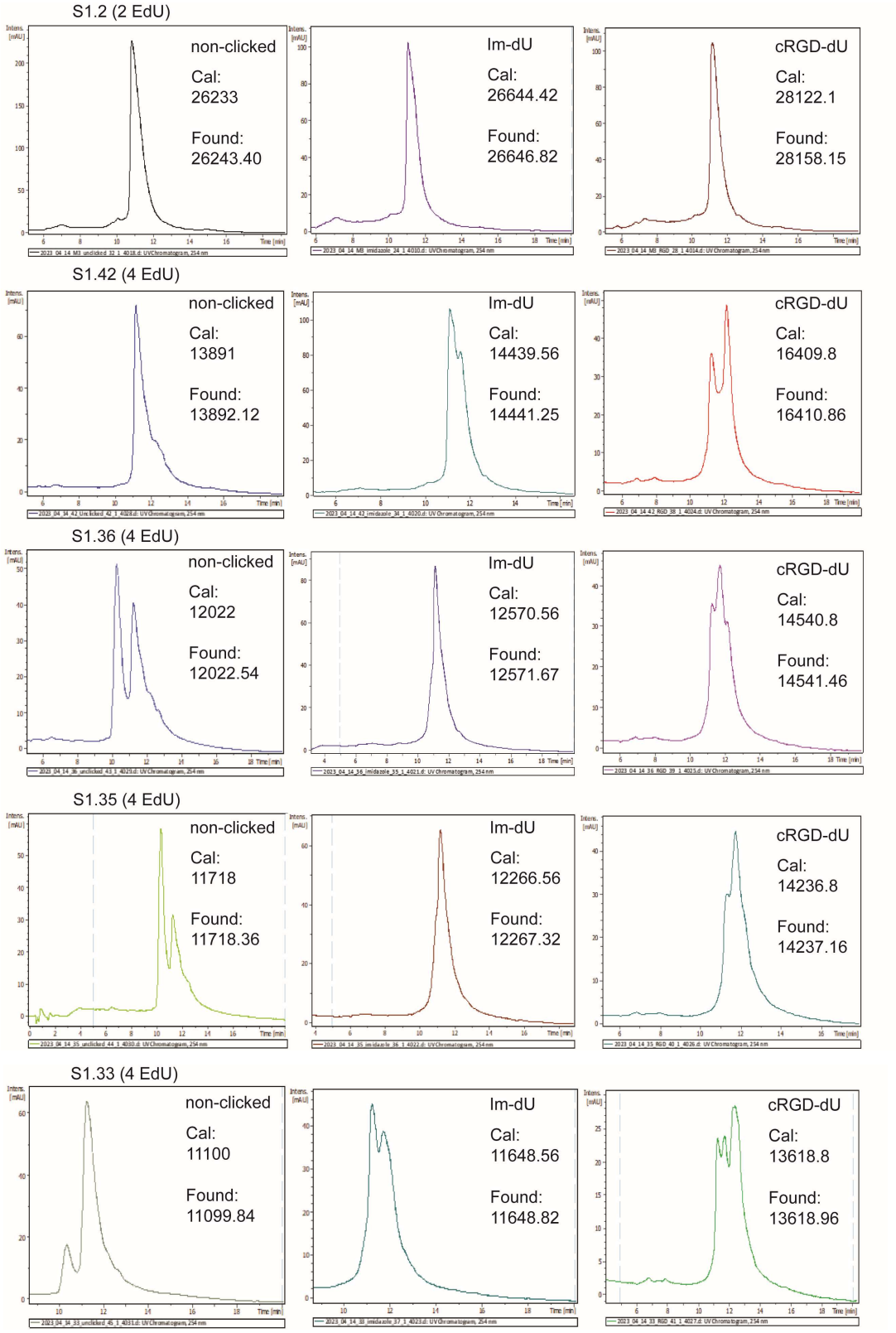

Figure 6.13 Detected masses. the detected Masses of the S1 clickmer, point mutants, S1 with less EdU content, and truncated version of S1 clickmer.

7 REFERENCES

1. Wang, T., et al., *Three decades of nucleic acid aptamer technologies: Lessons learned, progress and opportunities on aptamer development.* 2019. **37**(1): p. 28-50.
2. Ellington, A.D. and J.W.J.n. Szostak, *In vitro selection of RNA molecules that bind specific ligands.* 1990. **346**(6287): p. 818-822.
3. Tuerk, C. and L.J.s. Gold, *Systematic evolution of ligands by exponential enrichment: RNA ligands to bacteriophage T4 DNA polymerase.* 1990. **249**(4968): p. 505-510.
4. Robertson, D.L. and G.F.J.N. Joyce, *Selection in vitro of an RNA enzyme that specifically cleaves single-stranded DNA.* 1990. **344**(6265): p. 467-468.
5. AlShamaileh, H., et al., *Aptamer-mediated survivin RNAi enables 5-fluorouracil to eliminate colorectal cancer stem cells.* 2017. **7**(1): p. 5898.
6. Tan, L., et al., *PEGylated anti‐MUC1 aptamer‐doxorubicin complex for targeted drug delivery to MCF7 breast cancer cells.* 2011. **11**(10): p. 1331-1335.
7. Ruiz Ciancio, D., et al., *Aptamers as diagnostic tools in cancer.* 2018. **11**(3): p. 86.
8. Song, K.-M., S. Lee, and C.J.S. Ban, *Aptamers and their biological applications.* 2012. **12**(1): p. 612-631.
9. Otte, D.-M., et al., *Nucleic Acid Aptamers: From Basic Research to Clinical Applications*, in *Handbook of Chemical Biology of Nucleic Acids*, N. Sugimoto, Editor. 2022, Springer Nature Singapore: Singapore. p. 1-25.
10. Zhou, J. and J.J.N.r.D.d. Rossi, *Aptamers as targeted therapeutics: current potential and challenges.* 2017. **16**(3): p. 181-202.
11. Kaur, H., et al., *Aptamers in the therapeutics and diagnostics pipelines.* 2018. **8**(15): p. 4016.
12. Hoellenriegel, J., et al., *The Spiegelmer NOX-A12, a novel CXCL12 inhibitor, interferes with chronic lymphocytic leukemia cell motility and causes chemosensitization.* 2014. **123**(7): p. 1032-1039.
13. Marasca, R. and R.J.B. Maffei, The Journal of the American Society of Hematology, *NOX-A12: mobilizing CLL away from home.* 2014. **123**(7): p. 952-953.
14. Ninichuk, V., et al., *Late onset of Ccl2 blockade with the Spiegelmer mNOX-E36‐3′ PEG prevents glomerulosclerosis and improves glomerular filtration rate in db/db mice.* 2008. **172**(3): p. 628-637.
15. Kulkarni, O., et al., *Spiegelmer inhibition of CCL2/MCP-1 ameliorates lupus nephritis in MRL-(Fas) lpr mice.* 2007. **18**(8): p. 2350-2358.
16. Schwoebel, F., et al., *The effects of the anti-hepcidin Spiegelmer NOX-H94 on inflammation-induced anemia in cynomolgus monkeys.* 2013. **121**(12): p. 2311-2315.
17. Ruscito, A. and M.C.J.F.i.c. DeRosa, *Small-molecule binding aptamers: Selection strategies, characterization, and applications.* 2016. **4**: p. 14.
18. Bock, L.C., et al., *Selection of single-stranded DNA molecules that bind and inhibit human thrombin.* 1992. **355**(6360): p. 564-566.
19. Cheng, C., et al., *Potent inhibition of human influenza H5N1 virus by oligonucleotides derived by SELEX.* 2008. **366**(3): p. 670-674.
20. Davydova, A., et al., *Aptamers against pathogenic microorganisms.* 2016. **42**(6): p. 847-865.
21. Graziani, A.C., et al., *High efficiency binding aptamers for a wide range of bacterial sepsis agents.* 2017. **27**(4): p. 838-843.
22. Cerchia, L. and V.J.T.i.b. De Franciscis, *Targeting cancer cells with nucleic acid aptamers.* 2010. **28**(10): p. 517-525.
23. Domenyuk, V., et al., *Poly-ligand profiling differentiates trastuzumab-treated breast cancer patients according to their outcomes.* 2018. **9**(1): p. 1219.
24. Gopinath, S.C.B.J.A. and b. chemistry, *Methods developed for SELEX.* 2007. **387**: p. 171-182.

25. Chen, M., et al., *Development of cell-SELEX technology and its application in cancer diagnosis and therapy.* 2016. **17**(12): p. 2079.
26. Cerchia, L., et al., *Neutralizing aptamers from whole-cell SELEX inhibit the RET receptor tyrosine kinase.* 2005. **3**(4): p. e123.
27. Sefah, K., et al., *Development of DNA aptamers using Cell-SELEX.* 2010. **5**(6): p. 1169-1185.
28. Morris, K.N., et al., *High affinity ligands from in vitro selection: complex targets.* 1998. **95**(6): p. 2902-2907.
29. Mayer, G.J.A.C.I.E., *The chemical biology of aptamers.* 2009. **48**(15): p. 2672-2689.
30. Fang, X. and W.J.A.o.c.r. Tan, *Aptamers generated from cell-SELEX for molecular medicine: a chemical biology approach.* 2010. **43**(1): p. 48-57.
31. Mallikaratchy, P., et al., *Aptamer directly evolved from live cells recognizes membrane bound immunoglobin heavy mu chain in Burkitt's lymphoma cells.* 2007. **6**(12): p. 2230-2238.
32. Shangguan, D., et al., *Cell-specific aptamer probes for membrane protein elucidation in cancer cells.* 2008. **7**(5): p. 2133-2139.
33. Ye, M., et al., *Generating aptamers by cell-SELEX for applications in molecular medicine.* 2012. **13**(3): p. 3341-3353.
34. Ma, H., et al., *Nucleic acid aptamers in cancer research, diagnosis and therapy.* 2015. **44**(5): p. 1240-1256.
35. Shangguan, D., et al., *Aptamers evolved from live cells as effective molecular probes for cancer study.* 2006. **103**(32): p. 11838-11843.
36. Guo, K.-T., et al., *CELL-SELEX: Novel perspectives of aptamer-based therapeutics.* 2008. **9**(4): p. 668-678.
37. Raddatz, M.S.L., et al., *Enrichment of cell‐targeting and population‐specific aptamers by fluorescence‐activated cell sorting.* 2008. **47**(28): p. 5190-5193.
38. Sun, H., et al., *Oligonucleotide aptamers: new tools for targeted cancer therapy.* 2014. **3**: p. e182.
39. Avci-Adali, M., et al., *Pitfalls of cell-systematic evolution of ligands by exponential enrichment (SELEX): existing dead cells during in vitro selection anticipate the enrichment of specific aptamers.* 2010. **20**(6): p. 317-323.
40. Mayer, G., et al., *Fluorescence-activated cell sorting for aptamer SELEX with cell mixtures.* 2010. **5**(12): p. 1993-2004.
41. Souza, A.G., et al., *3D Cell-SELEX: Development of RNA aptamers as molecular probes for PC-3 tumor cell line.* 2016. **341**(2): p. 147-156.
42. Vorobyeva, M.A., et al., *Key aspects of nucleic acid library design for in vitro selection.* 2018. **19**(2): p. 470.
43. Bowser, M.T.J.A., *SELEX: just another separation?* 2005. **130**(2): p. 128-130.
44. Komarova, N. and A.J.M. Kuznetsov, *Inside the black box: what makes SELEX better?* 2019. **24**(19): p. 3598.
45. Kuwahara, M., S.J.A.D.P. Obika, and XNA, *In vitro selection of BNA (LNA) aptamers.* 2013. **4**(2): p. 39-48.
46. Kohlberger, M., G.J.B. Gadermaier, and A. Biochemistry, *SELEX: Critical factors and optimization strategies for successful aptamer selection.* 2022. **69**(5): p. 1771-1792.
47. Shao, K., et al., *Emulsion PCR: a high efficient way of PCR amplification of random DNA libraries in aptamer selection.* 2011. **6**(9): p. e24910.
48. Musheev, M.U. and S.N.J.A.c.a. Krylov, *Selection of aptamers by systematic evolution of ligands by exponential enrichment: addressing the polymerase chain reaction issue.* 2006. **564**(1): p. 91-96.
49. Blind, M. and M.J.M.T.-N.A. Blank, *Aptamer selection technology and recent advances.* 2015. **4**: p. e223.
50. Witt, M., et al., *Comparing two conventional methods of emulsion PCR and optimizing of Tegosoft‐based emulsion PCR.* 2017. **17**(8): p. 953-958.

51. Yufa, R., et al., *Emulsion PCR significantly improves nonequilibrium capillary electrophoresis of equilibrium mixtures-based aptamer selection: allowing for efficient and rapid selection of aptamer to unmodified ABH2 protein.* 2015. **87**(2): p. 1411-1419.
52. Levay, A., et al., *Identifying high-affinity aptamer ligands with defined cross-reactivity using high-throughput guided systematic evolution of ligands by exponential enrichment.* 2015. **43**(12): p. e82-e82.
53. Williams, R., et al., *Amplification of complex gene libraries by emulsion PCR.* 2006. **3**(7): p. 545-550.
54. Diehl, F., K.W. Kinzler, and B. Vogelstein, *Single-molecule PCR on microparticles in water-in-oil emulsions*. 2014, Google Patents.
55. Tsuji, S., et al., *Effective isolation of RNA aptamer through suppression of PCR bias.* 2009. **386**(1): p. 223-226.
56. Gao, H., et al., *Comparison of different methods for preparing single stranded DNA for oligonucleotide microarray.* 2003. **36**(13): p. 2849-2863.
57. Liang, C., et al., *Comparison of the methods for generating single-stranded DNA in SELEX.* 2015. **140**(10): p. 3439-3444.
58. Amano, R., et al., *Kinetic and thermodynamic analyses of interaction between a high-affinity RNA aptamer and its target protein.* 2016. **55**(45): p. 6221-6229.
59. Dickman, M. and D.P.J.A.B. Hornby, *Isolation of single-stranded DNA using denaturing DNA chromatography.* 2000. **284**(1): p. 164-167.
60. Higuchi, R.G. and H.J.N.a.r. Ochman, *Production of single-stranded DNA templates by exonuclease digestion following the polymerase chain reaction.* 1989. **17**(14): p. 5865-5865.
61. Nehdi, A., et al., *Novel strategies to optimize the amplification of single-stranded DNA.* 2020. **8**: p. 401.
62. Sharma, T.K., J.G. Bruno, and A.J.B.a. Dhiman, *ABCs of DNA aptamer and related assay development.* 2017. **35**(2): p. 275-301.
63. Avci-Adali, M., et al., *Upgrading SELEX technology by using lambda exonuclease digestion for single-stranded DNA generation.* 2009. **15**(1): p. 1-11.
64. Dastjerdi, K., et al., *Generation of an enriched pool of DNA aptamers for an HER2‐overexpressing cell line selected by Cell SELEX.* 2011. **58**(4): p. 226-230.
65. Takahashi, M., E. Sakota, and Y.J.B. Nakamura, *The efficient cell-SELEX strategy, Icell-SELEX, using isogenic cell lines for selection and counter-selection to generate RNA aptamers to cell surface proteins.* 2016. **131**: p. 77-84.
66. Sanger, F., S. Nicklen, and A.R.J.P.o.t.n.a.o.s. Coulson, *DNA sequencing with chain-terminating inhibitors.* 1977. **74**(12): p. 5463-5467.
67. Stoltenburg, R., C. Reinemann, and B.J.B.e. Strehlitz, *SELEX—A (r) evolutionary method to generate high-affinity nucleic acid ligands.* 2007. **24**(4): p. 381-403.
68. Schütze, T., et al., *Probing the SELEX process with next-generation sequencing.* 2011. **6**(12): p. e29604.
69. Zimmermann, B., et al., *Monitoring genomic sequences during SELEX using high-throughput sequencing: neutral SELEX.* 2010. **5**(2): p. e9169.
70. Beier, R., E. Boschke, and D.J.B.r.i. Labudde, *New strategies for evaluation and analysis of SELEX experiments.* 2014. **2014**.
71. Tolle, F., G.J.N.A.A.S. Mayer, Characterization,, and Application, *Preparation of SELEX samples for next-generation sequencing.* 2016: p. 77-84.
72. Cho, M., et al., *Quantitative selection of DNA aptamers through microfluidic selection and high-throughput sequencing.* 2010. **107**(35): p. 15373-15378.
73. Hoinka, J. and T.J.M. Przytycka, *AptaPLEX–A dedicated, multithreaded demultiplexer for HT-SELEX data.* 2016. **106**: p. 82-85.
74. Blank, M.J.N.A.A.S., Characterization, and Application, *Next-generation analysis of deep sequencing data: bringing light into the black box of SELEX experiments.* 2016: p. 85-95.

75. Hoinka, J., R. Backofen, and T.M.J.M.T.-N.A. Przytycka, *AptaSUITE: a full-featured bioinformatics framework for the comprehensive analysis of aptamers from HT-SELEX experiments.* 2018. **11**: p. 515-517.
76. Ruan, S., S.J. Swamidass, and G.D.J.B. Stormo, *BEESEM: estimation of binding energy models using HT-SELEX data.* 2017. **33**(15): p. 2288-2295.
77. Thiel, W.H. and P.H.J.M. Giangrande, *Analyzing HT-SELEX data with the Galaxy Project tools–A web based bioinformatics platform for biomedical research.* 2016. **97**: p. 3-10.
78. Rohloff, J.C., et al., *Nucleic acid ligands with protein-like side chains: modified aptamers and their use as diagnostic and therapeutic agents.* 2014. **3**: p. e201.
79. Gold, L., et al., *Aptamer-based multiplexed proteomic technology for biomarker discovery.* 2010: p. 1-1.
80. Davies, D.R., et al., *Unique motifs and hydrophobic interactions shape the binding of modified DNA ligands to protein targets.* 2012. **109**(49): p. 19971-19976.
81. Ramaraj, T., et al., *Antigen–antibody interface properties: Composition, residue interactions, and features of 53 non-redundant structures.* 2012. **1824**(3): p. 520-532.
82. Young, L., R. Jernigan, and D.J.P.S. Covell, *A role for surface hydrophobicity in protein‐protein recognition.* 1994. **3**(5): p. 717-729.
83. Pagano, B., et al., *Stability and binding properties of a modified thrombin binding aptamer.* 2008. **94**(2): p. 562-569.
84. Joshi, A. and M.J.C. Mayr, *In aptamers they trust: caveats of the SOMAscan biomarker discovery platform from SomaLogic*. 2018, Am Heart Assoc. p. 2482-2485.
85. Candia, J., et al., *Assessment of variability in the SOMAscan assay.* 2017. **7**(1): p. 14248.
86. Ashley, S.L., et al., *Six-SOMAmer index relating to immune, protease and angiogenic functions predicts progression in IPF.* 2016. **11**(8): p. e0159878.
87. Webber, J., et al., *Proteomics analysis of cancer exosomes using a novel modified aptamer-based array (SOMAscanTM) platform.* 2014. **13**(4): p. 1050-1064.
88. Albaba, D., S. Soomro, and C.J.M. Mohan, *Aptamer-based screens of human body fluids for biomarkers.* 2015. **4**(3): p. 424-431.
89. Kraemer, S., et al., *From SOMAmer-based biomarker discovery to diagnostic and clinical applications: a SOMAmer-based, streamlined multiplex proteomic assay.* 2011. **6**(10): p. e26332.
90. Tanaka, K., et al., *Base-modified aptamers obtained by cell-internalization SELEX facilitate cellular uptake of an antisense oligonucleotide.* 2021. **23**: p. 440-449.
91. Uemachi, H., et al., *Discovery of cell-internalizing artificial nucleic acid aptamers for lung fibroblasts and targeted drug delivery.* 2020. **105**: p. 104321.
92. Rostovtsev, V.V., et al., *A stepwise huisgen cycloaddition process: copper (I)‐catalyzed regioselective "ligation" of azides and terminal alkynes.* 2002. **114**(14): p. 2708-2711.
93. Tornøe, C.W., C. Christensen, and M.J.T.J.o.o.c. Meldal, *Peptidotriazoles on solid phase:[1, 2, 3]-triazoles by regiospecific copper (I)-catalyzed 1, 3-dipolar cycloadditions of terminal alkynes to azides.* 2002. **67**(9): p. 3057-3064.
94. Kolb, H.C., M. Finn, and K.B.J.A.C.I.E. Sharpless, *Click chemistry: diverse chemical function from a few good reactions.* 2001. **40**(11): p. 2004-2021.
95. Pfeiffer, F., et al., *Identification and characterization of nucleobase-modified aptamers by click-SELEX.* 2018. **13**(5): p. 1153-1180.
96. Tolle, F., et al., *A versatile approach towards nucleobase‐modified aptamers.* 2015. **54**(37): p. 10971-10974.
97. Rosenthal, M., F. Pfeiffer, and G.J.A.C.I.E. Mayer, *A Receptor‐Guided Design Strategy for Ligand Identification.* 2019. **58**(31): p. 10752-10755.

98. Shim, J.-Y., A.C. Bertalovitz, and D.A.J.J.o.b.c. Kendall, *Identification of essential cannabinoid-binding domains: structural insights into early dynamic events in receptor activation.* 2011. **286**(38): p. 33422-33435.
99. Plückthun, O., et al., *Dynamic changes in DNA populations revealed by split–combine selection.* 2020. **11**(35): p. 9577-9583.
100. Siegl, J., et al., *Split–Combine Click-SELEX Reveals Ligands Recognizing the Transplant Rejection Biomarker CXCL9.* 2022. **17**(1): p. 129-137.
101. Betz, K., et al., *KlenTaq polymerase replicates unnatural base pairs by inducing a Watson-Crick geometry.* 2012. **8**(7): p. 612-614.
102. Piccirilli, J.A., et al., *Enzymatic incorporation of a new base pair into DNA and RNA extends the genetic alphabet.* 1990. **343**(6253): p. 33-37.
103. Malyshev, D.A. and F.E.J.A.C.I.E. Romesberg, *The expanded genetic alphabet.* 2015. **54**(41): p. 11930-11944.
104. Futami, K., et al., *Genetic alphabet expansion provides versatile specificities and activities of unnatural-base DNA aptamers targeting cancer cells.* 2019. **14**: p. 158-170.
105. Kimoto, M., et al., *Generation of high-affinity DNA aptamers using an expanded genetic alphabet.* 2013. **31**(5): p. 453-457.
106. Biondi, E., et al., *Laboratory evolution of artificially expanded DNA gives redesignable aptamers that target the toxic form of anthrax protective antigen.* 2016. **44**(20): p. 9565-9577.
107. Sefah, K., et al., *In vitro selection with artificial expanded genetic information systems.* 2014. **111**(4): p. 1449-1454.
108. Kaur, H.J.B.e.B.A.-G.S., *Recent developments in cell-SELEX technology for aptamer selection.* 2018. **1862**(10): p. 2323-2329.
109. Pranay, K., et al., *Challenges of aptamers as targeting ligands for anticancer therapies*, in *Aptamers Engineered Nanocarriers for Cancer Therapy*. 2023, Elsevier. p. 455-480.
110. Alshaer, W., H. Hillaireau, and E.J.A.d.d.r. Fattal, *Aptamer-guided nanomedicines for anticancer drug delivery.* 2018. **134**: p. 122-137.
111. Pang, X., et al., *Bioapplications of cell-SELEX-generated aptamers in cancer diagnostics, therapeutics, theranostics and biomarker discovery: a comprehensive review.* 2018. **10**(2): p. 47.
112. Rahimizadeh, K., et al., *Development of cell-specific aptamers: recent advances and insight into the selection procedures.* 2017. **22**(12): p. 2070.
113. Maimaitiyiming, Y., et al., *Novel insights into the role of aptamers in the fight against cancer.* 2019. **145**: p. 797-810.
114. Yoon, S. and J.J.J.C.o.i.o. Rossi, *Emerging cancer-specific therapeutic aptamers.* 2017. **29**(5): p. 366.
115. Blank, M., et al., *Systematic evolution of a DNA aptamer binding to rat brain tumor microvessels: selective targeting of endothelial regulatory protein pigpen.* 2001. **276**(19): p. 16464-16468.
116. Daniels, D.A., et al., *A tenascin-C aptamer identified by tumor cell SELEX: systematic evolution of ligands by exponential enrichment.* 2003. **100**(26): p. 15416-15421.
117. Tolle, F. and G.J.C.S. Mayer, *Dressed for success–applying chemistry to modulate aptamer functionality.* 2013. **4**(1): p. 60-67.
118. Van Simaeys, D., et al., *Identification of cell membrane protein stress-induced phosphoprotein 1 as a potential ovarian cancer biomarker using aptamers selected by cell systematic evolution of ligands by exponential enrichment.* 2014. **86**(9): p. 4521-4527.
119. Cazap, E., et al., *Structural barriers to diagnosis and treatment of cancer in low-and middle-income countries: the urgent need for scaling up.* 2016. **34**(1): p. 14.
120. Hori, S.-i., et al., *Current advances in aptamers for cancer diagnosis and therapy.* 2018. **10**(1): p. 9.

121. Henschke, C.I.J.C., *Early lung cancer action project: overall design and findings from baseline screening.* 2000. **89**(S11): p. 2474-2482.
122. Li, K., et al., *Screening of specific nucleic acid aptamers binding tumor markers in the serum of the lung cancer patients and identification of their activities.* 2017. **39**(7): p. 1010428317717123.
123. Funston, G., et al., *Recognizing gynecological cancer in primary care: risk factors, red flags, and referrals.* 2018. **35**: p. 577-589.
124. Tsai, S.-C., L.-Y. Hung, and G.-B.J.B. Lee, *An integrated microfluidic system for the isolation and detection of ovarian circulating tumor cells using cell selection and enrichment methods.* 2017. **11**(3): p. 034122.
125. Farokhzad, O.C., et al., *Nanoparticle-aptamer bioconjugates: a new approach for targeting prostate cancer cells.* 2004. **64**(21): p. 7668-7672.
126. Farokhzad, O.C., et al., *Targeted nanoparticle-aptamer bioconjugates for cancer chemotherapy in vivo.* 2006. **103**(16): p. 6315-6320.
127. Taghdisi, S.M., et al., *Targeted delivery of Epirubicin to cancer cells by PEGylated A10 aptamer.* 2013. **21**(8): p. 739-744.
128. Bates, P.J., et al., *Discovery and development of the G-rich oligonucleotide AS1411 as a novel treatment for cancer.* 2009. **86**(3): p. 151-164.
129. Rosenberg, J.E., et al., *A phase II trial of AS1411 (a novel nucleolin-targeted DNA aptamer) in metastatic renal cell carcinoma.* 2014. **32**: p. 178-187.
130. Wu, X., et al., *Aptamers: active targeting ligands for cancer diagnosis and therapy.* 2015. **5**(4): p. 322.
131. Adams, J.J.L., *The case of scirrhous of the prostate gland with corresponding affliction of the lymphatic glands in the lumbar region and in the pelvis.* 1853. **1**(1): p. 393-393.
132. Denmeade, S.R. and J.T.J.N.R.C. Isaacs, *A history of prostate cancer treatment.* 2002. **2**(5): p. 389-396.
133. Wang, X., et al., *Insights into Aptamer–Drug Delivery Systems against Prostate Cancer.* 2022. **27**(11): p. 3446.
134. Greenlee, R.T., et al., *Cancer statistics, 2001.* 2001. **51**(1): p. 15-36.
135. Ross, R., *Cancer Epidemiology and Prevention. 2. Schottenfeld, D.; Searle, JG.; Fraumeni, JF., editors*. 1997, Oxford Univ. Press New York:.
136. Huggins, C., R. Stevens, and C.V.J.A.o.s. Hodges, *Studies on prostatic cancer: II. The effects of castration on advanced carcinoma of the prostate gland.* 1941. **43**(2): p. 209-223.
137. Turco, F., et al., *How to Improve the Quality of Life of Patients with Prostate Cancer Treated with Hormone Therapy?* 2023: p. 9-26.
138. Powell Gray, B., et al., *Tunable cytotoxic aptamer–drug conjugates for the treatment of prostate cancer.* 2018. **115**(18): p. 4761-4766.
139. van Winden, L.J. and H.H.J.A.i.c.c. van Rossum, *Testosterone analysis in prostate cancer patients.* 2022. **108**: p. 73-104.
140. Potocki, P.M. and P.J.J.O.i.C.P. Wysocki, *Evolution of prostate cancer therapy. Part 1.* 2022. **18**(3): p. 177-188.
141. Westaby, D., et al., *A new old target: androgen receptor signaling and advanced prostate cancer.* 2022. **62**: p. 131-153.
142. Medicine, L.S.G.J.N.E.J.o., *Leuprolide versus diethylstilbestrol for metastatic prostate cancer.* 1984. **311**(20): p. 1281-1286.
143. Seidenfeld, J., et al., *Single-therapy androgen suppression in men with advanced prostate cancer: a systematic review and meta-analysis.* 2000. **132**(7): p. 566-577.
144. Barani, M., et al., *Nanotreatment and nanodiagnosis of prostate cancer: recent updates.* 2020. **10**(9): p. 1696.
145. Pienta, K.J. and D.C.J.C.a.c.j.f.c. Smith, *Advances in Prostate Cancer Chemotherapy: A New Era Begins 1.* 2005. **55**(5): p. 300-318.
146. Komura, K., et al., *Current treatment strategies for advanced prostate cancer.* 2018. **25**(3): p. 220-231.

147. Zhu, L., et al., *Aptamers entirely built from therapeutic nucleoside analogues for targeted cancer therapy.* 2022. **144**(4): p. 1493-1497.
148. Germer, K., et al., *RNA aptamers and their therapeutic and diagnostic applications.* 2013. **4**(1): p. 27.
149. Chu, T.C., et al., *Aptamer: toxin conjugates that specifically target prostate tumor cells.* 2006. **66**(12): p. 5989-5992.
150. Chen, J., et al., *Constructing artificial nucleobase compilation to enable precise molecular medicine.*
151. Plückthun, O., *Simultaneous identification of nucleotide-modified aptamers with different properties by multiplexed click-SELEX*. 2020, Universitäts-und Landesbibliothek Bonn.
152. Tolle, F., *Click-SELEX*. 2016, Universitäts-und Landesbibliothek Bonn.
153. De Jong, L.A., et al., *Receptor–ligand binding assays: technologies and applications.* 2005. **829**(1-2): p. 1-25.
154. Pleiko, K., et al., *Differential binding cell-SELEX method to identify cell-specific aptamers using high-throughput sequencing.* 2019. **9**(1): p. 1-12.
155. Shraim, A.a.S., et al., *Developing and characterization of chemically modified RNA aptamers for targeting wild type and mutated c-KIT receptor tyrosine kinases.* 2019. **63**(5): p. 2209-2228.
156. Que-Gewirth, N.S. and B.J.G.t. Sullenger, *Gene therapy progress and prospects: RNA aptamers.* 2007. **14**(4): p. 283-291.
157. Huang, Y.F., et al., *Molecular assembly of an aptamer–drug conjugate for targeted drug delivery to tumor cells.* 2009. **10**(5): p. 862-868.
158. Haßel, S.K., *Aptamers for targeted activation of T cell-mediated immunity*. 2016, Universitäts-und Landesbibliothek Bonn.
159. Akhtar, U., *Pharmacological reprogramming of macrophages through aptamiRs*. 2020, Universitäts-und Landesbibliothek Bonn.
160. Lomenick, B., et al., *Target identification using drug affinity responsive target stability (DARTS).* 2011. **3**(4): p. 163-180.
161. Preta, G., et al., *Dynasore-not just a dynamin inhibitor.* 2015. **13**(1): p. 1-7.
162. Fernando, L.P., et al., *Mechanism of cellular uptake of highly fluorescent conjugated polymer nanoparticles.* 2010. **11**(10): p. 2675-2682.
163. Hall, B., et al., *Design, synthesis, and amplification of DNA pools for in vitro selection.* 2009. **39**(1): p. 9.2. 1-9.2. 28.
164. Famulok, M. and A.J.C.o.i.c.b. Jenne, *Oligonucleotide libraries-variatio delectat.* 1998. **2**(3): p. 320-327.
165. Martínez-Roque, M.A., et al., *DNA aptamer selection for SARS-CoV-2 spike glycoprotein detection.* 2022. **645**: p. 114633.
166. Siegl, J., O. Plückthun, and G.J.R.C.B. Mayer, *Dependence of click-SELEX performance on the nature and average number of modified nucleotides.* 2022. **3**(3): p. 288-294.
167. Sun, F., D. Galas, and M.S.J.J.o.m.b. Waterman, *A Mathematical Analysis ofin VitroMolecular Selection–Amplification.* 1996. **258**(4): p. 650-660.
168. Wang, Y., et al., *DNA aptamer evolved by cell-SELEX for recognition of prostate cancer.* 2014. **9**(6): p. e100243.
169. Shi, J., F. Wang, and S.J.B.r. Liu, *Radiolabeled cyclic RGD peptides as radiotracers for tumor imaging.* 2016. **2**: p. 1-20.
170. Buyst, D., et al., *Identification of a pKa-regulating motif stabilizing imidazole-modified double-stranded DNA.* 2015. **43**(1): p. 51-62.
171. Hulme, E.C. and M.A.J.B.j.o.p. Trevethick, *Ligand binding assays at equilibrium: validation and interpretation.* 2010. **161**(6): p. 1219-1237.
172. Mayor, S. and R.E.J.N.r.M.c.b. Pagano, *Pathways of clathrin-independent endocytosis.* 2007. **8**(8): p. 603-612.
173. McMahon, H.T. and E.J.N.r.M.c.b. Boucrot, *Molecular mechanism and physiological functions of clathrin-mediated endocytosis.* 2011. **12**(8): p. 517-533.

174. Gomes de Castro, M.A., C. Höbartner, and F.J.P.O. Opazo, *Aptamers provide superior stainings of cellular receptors studied under super-resolution microscopy.* 2017. **12**(2): p. e0173050.
175. Liu, A.P., et al., *Local clustering of transferrin receptors promotes clathrin-coated pit initiation.* 2010. **191**(7): p. 1381-1393.
176. Opazo, F., et al., *Modular assembly of cell-targeting devices based on an uncommon G-quadruplex aptamer.* 2015. **4**: p. e251.
177. Wang, S., et al., *Elucidating the cellular uptake mechanism of aptamer-functionalized graphene-isolated-Au-nanocrystals with dual-modal imaging.* 2016. **141**(11): p. 3337-3342.
178. Xu, X., et al., *Inhibition of DNA replication and induction of S phase cell cycle arrest by G-rich oligonucleotides.* 2001. **276**(46): p. 43221-43230.
179. Soundararajan, S., et al., *Plasma membrane nucleolin is a receptor for the anticancer aptamer AS1411 in MV4-11 leukemia cells.* 2009. **76**(5): p. 984-991.
180. Reyes-Reyes, E.M., Y. Teng, and P.J.J.C.r. Bates, *A new paradigm for aptamer therapeutic AS1411 action: uptake by macropinocytosis and its stimulation by a nucleolin-dependent mechanism.* 2010. **70**(21): p. 8617-8629.
181. Kotula, J.W., et al., *Aptamer-mediated delivery of splice-switching oligonucleotides to the nuclei of cancer cells.* 2012. **22**(3): p. 187-195.
182. Bing, T., N. Zhang, and D.J.A.b. Shangguan, *Cell‐SELEX, an effective way to the discovery of biomarkers and unexpected molecular events.* 2019. **3**(12): p. 1900193.
183. Cowperthwaite, M.C. and A.D.J.J.o.m.e. Ellington, *Bioinformatic analysis of the contribution of primer sequences to aptamer structures.* 2008. **67**: p. 95-102.
184. Coleman, T.M. and F.J.R.b. Huang, *Optimal random libraries for the isolation of catalytic RNA.* 2005. **2**(4): p. 129-136.
185. Gawande, B.N., et al., *Selection of DNA aptamers with two modified bases.* 2017. **114**(11): p. 2898-2903.
186. Gao, S., et al., *Post-SELEX optimization of aptamers.* 2016. **408**: p. 4567-4573.
187. Vu, C.Q., et al., *Oligonucleotide hybridization combined with competitive antibody binding for the truncation of a high-affinity aptamer.* 2017. **19**(10): p. 609-617.
188. Tonapi, S.S., et al., *Translocation of a cell surface spliceosomal complex induces alternative splicing events and lymphoma cell necrosis.* 2019. **26**(5): p. 756-764. e6.
189. Bing, T., et al., *Aptameric probe specifically binding protein heterodimer rather than monomers.* 2019. **6**(11): p. 1900143.
190. Bing, T., et al., *Facile discovery of cell-surface protein targets of cancer cell aptamers.* 2015. **14**(10): p. 2692-2700.
191. Odeh, F., et al., *Aptamers chemistry: Chemical modifications and conjugation strategies.* 2019. **25**(1): p. 3.
192. Jutras, B.L., A. Verma, and B.J.C.p.i.m. Stevenson, *Identification of novel DNA‐binding proteins using DNA‐affinity chromatography/pull down.* 2012. **24**(1): p. 1F. 1.1-1F. 1.13.
193. Jiang, Y., et al., *Specific aptamer− protein interaction studied by atomic force microscopy.* 2003. **75**(9): p. 2112-2116.
194. Elskens, J.P., J.M. Elskens, and A.J.I.j.o.m.s. Madder, *Chemical modification of aptamers for increased binding affinity in diagnostic applications: Current status and future prospects.* 2020. **21**(12): p. 4522.
195. Suski, J.M., et al., *Isolation of plasma membrane–associated membranes from rat liver.* 2014. **9**(2): p. 312-322.
196. Candiano, G., et al., *Blue silver: a very sensitive colloidal Coomassie G‐250 staining for proteome analysis.* 2004. **25**(9): p. 1327-1333.
197. Heukeshoven, J. and R.J.E. Dernick, *Simplified method for silver staining of proteins in polyacrylamide gels and the mechanism of silver staining.* 1985. **6**(3): p. 103-112.
198. Jin, L.T., et al., *Sensitive silver staining of protein in sodium dodecyl sulfate‐polyacrylamide gels using an azo dye, calconcarboxylic acid, as a silver‐ion sensitizer.* 2004. **25**(15): p. 2494-2500.

199. Cibiel, A., et al., *From ugly duckling to swan: unexpected identification from cell-SELEX of an anti-Annexin A2 aptamer targeting tumors.* 2014. **9**(1): p. e87002.

200. Moradzadeh Esmaeili,N, Split-combine Click-SELEX of DNA library targeting SARS-CoV-2 Spike protein (master thesis), 2021, Universitäts-und Landesbibliothek Bonn.

8 ACKNOWLEDGEMENT

I would like to express my deepest gratitude to my advisor, Prof. Mayer, for his unwavering support, guidance, and encouragement throughout my doctoral studies. His guidance and constructive feedback helped me improve my presentation skills significantly, and I am now confident in my ability to deliver a clear and effective scientific talk. I learned so much from him about the scientific process, including how to think critically about my work and how to engage in scientific discussions with others. His mentorship has made a significant impact on my life.

I also want to extend my thanks to PD. Dr. van Echten-Deckert who generously supported me during my journey and especially at the end of my PhD journey. She gave me a space in her lab to write my thesis, she encouraged me to finish my thesis. It wasn't an easy time for me, but with her encouragement, I could finish the writing. I would like to express my heartfelt gratitude to her, without whom completing my thesis would not have been possible.

I am deeply grateful to Prof. Menche for accepting my request to serve as a referee for my thesis. I would also like to express my sincerest appreciation to Prof. Kirfel for kindly agreeing to participate as a referee for the thesis dissertation.

I'm grateful to Shah Alam and Sumiya Afsar for their constant support and encouragement during the final months of my doctoral journey. Their kindness and friendship were a great source of strength and motivation for me. I'm thankful for the moments of joy and laughter we shared during this challenging time. Their unwavering belief in me and my abilities gave me the confidence to complete my thesis. I consider them like siblings and feel blessed to have them in my life. Their support and friendship have positively impacted my life and thinking, and I'm honored to have them as my friends. Also, I am grateful to my colleagues, Tjasa, Anna, Nima, Mehrenaze, Minh, Tejal, Laura lledo, and Ankuna who have been an essential part of my academic journey. Their support, encouragement, and camaraderie have made the long hours in the lab more bearable, and I will always cherish the memories we shared.

I would like to express my sincere gratitude to my friends: Georg Pietruschka and Ignazio Geraci, who have been a constant source of support and encouragement throughout my doctoral journey. Your unwavering belief in me and my abilities, and your willingness to listen and provide advice, have been instrumental in helping me overcome the challenges and obstacles that I encountered along the way. Your willingness to proofread my drafts, brainstorm ideas, and provide feedback has been invaluable, and I am grateful for your time and effort. Your words of encouragement, whether in person or through a quick message, helped me stay motivated and focused when I needed it the most.

Finally, to my friends and my family:

تحية الى اصدقائي المخلصين الذين كان دعمهم وتشجيعهم وسيلتي لانهاء هذا المشوار الذي كان طويلا وكان محفوف بالمشقات لقد سهلو علي هذا الطريق الطويل من الصعب ان اذكر اسماأهم ولكن اخص بالشكر اصدقاء السكن في الاردن وبالاخص صديقي المقرب جدا معتز تنبكجي واصدقائي الذين كانو سندا لي في اشهري الأخيرة وبالاخص نايف عليط ومحمد زريق الاشهر الأخيرة كانت صعبة جدا ولكن بتشجيعهم انجزت الرسالة.

أخيرا اشكر اهلي بالاخص امي وابي اللذان دعموني على طول المسيرة من أول المشوار الى نهايته توجيهاتهم وحبهم لي اعطاني الدعم في اصعب اللحظات ما كنت لاكتب هذه الكلمات واصل لهذه الدرجة العلمية بدون دعمهم المالي والمعنوي. دعائهم لي وفقني وسهل علي مهمتي لانجاز المستحيل. اخي العزيز عبد العزيز أيضا اشكره من داخل قلبي دعمني ماليا ومعنويا لولا وجوده في حياتي ما كنت لاسافر الى ألمانيا واكمل دراستي. اخواتي رحاب وهبة صديقتان الدرب.

الشكر الأول والاخير لربي فالله خير حافظ وهو ارحم الرحمين. هذه الابيات كان معي على طول طريقي وكنت اردها طوال يومي.

فليتك تحلو والحياة مريرة وليتك ترضى والانام غضاب

وليت الذي بيني وبينك عامر وبيني وبين العالمين خراب

إذا صح منك الوصل فالكل هين وكل الذي فوق التراب تراب

Thank you all for being a part of my journey